Investigating the Cell Population of the Adult Human Nucleus Pulposus

A thesis submitted to the University of Manchester for the degree of Doctor of Philosophy
in the Faculty of Medical and Human Sciences

2014

Francesca Ludwinski

School of Medicine

Table of Contents

CHAPTER 2: GENERAL MATERIALS AND METHODS

CHAPTER 7: REFERENCES

Word Count: 75,374

List of Tables

List of Figures

Abstract

Low back and neck pain are prevalent conditions in developed societies, and are linked to degeneration of the intervertebral disc (IVD), where aberrant cell biology, particularly in cells of the nucleus pulposus (NP) is thought to drive these degenerative changes. Recent microarray investigations have shed some light as to the phenotype of NP cells; an area of IVD research previously undefined, but the unique gene markers identified have yet to be investigated in a cohort of specimens representative of a range of ages and stages of degeneration, as well as localised to cells of the disc. Additionally, evidence regarding the expression of novel marker genes at the protein level is to date, largely unaddressed, but is imperative in order to fully characterise the adult human NP cell phenotype, as it is not understood whether all NP cells will express these proteins, or just a subset of cells. Similarly, few studies have assessed variations in the novel gene and protein expression profile of adult NP cells with ageing and degeneration, and it is therefore essential to determine this and identify whether the phenotype of NP cells alters as a consequence of such variables. Furthermore, the cervical NP cell phenotype is at present poorly characterised and it is therefore assumed that it is comparable to that of lumbar NP cells, with regards to chondrogenic and catabolic gene expression. Elucidation of whether NP cells derived from the two spinal regions are comparable with regards to phenotype may allow for the interchangeable use of cervical and lumbar IVD specimens for *in vitro* purposes.

This study aimed to investigate the adult human NP cell phenotype, through comparison of gene expression levels determined by quantitative real-time PCR in specimens obtained from a range of adult human disc levels of varying ages and degenerative grades, and to assess the expression of novel NP and notochordal (NC) cell marker proteins by immunohistochemistry, in order to ascertain whether expression is ubiquitous, or whether discrete NP cell sub-populations exist *in vivo*, particularly with regards to NC cell marker expression using flow cytometry techniques. It has been postulated that the phenotype of NP cells is influenced by microenvironmental factors akin to those observed *in vivo*, and therefore an *ex vivo* model system for studying the effects of microenvironmental factors on the gene expression and histological profiles of cells within the NP was developed.

Analysis of the cervical NP cell gene expression profile, and comparison to lumbar specimens confirmed that specimens from the two spinal regions were phenotypically similar and could therefore be used interchangeably. Following this, investigation of novel NP and NC cell marker expression in a cohort of degenerate human IVD samples identified differential expression of a range of markers, indicative of cell sub-populations existing within the tissue. It was subsequently demonstrated that discrete NC cell-like and NP cell-like cellular sub-populations exist, but crucially, provided support against the loss of NC cells from the NP with ageing, and intimate either that they differentiate into chondrocyte-like NP cells or that the subsets of NP cells are discrete with regards to ontogeny. The mechanisms underlying this required elucidation, and a novel *ex vivo* model system has been developed here, allowing for the assessment of NC cell phenotypic response to microenvironmental factors. Preliminary testing has indicated that hypoxic culture of porcine IVD explants results in alterations in the NP ECM and cellularity as compared to normoxic cultures, suggesting that microenvironment may influence alterations to NC cell phenotype.

Taken together, these findings suggest that adult human NP tissues are comprised of heterogeneous cell populations, with differential expression of both NP and NC cell markers. Future work to investigate whether the functions of these phenotypically distinct cells differs may elucidate an optimal cell type for recapitulation in novel cell-based regenerative therapies for repair of the degenerate IVD.

Declaration

No portion of the work referred to in the thesis has been submitted in support of an application for another degree or qualification of this or any other university or other institute of learning.

Copyright Statement

Abbreviations

°C	Degrees Celsius
ΔCt	Delta cycle threshold
µg	Microgram
µl	Microlitre
µm	Micrometer
3D	Three-dimensional
A2M	Alpha-2-macroglobulin
ABC	Avidin-biotin complex
AC	Articular chondrocyte
ACAN	Aggrecan
ADAMTS	A disintegrin and metalloproteinase with thrombospondin motif
AF	Annulus fibrosus
AJ	Apophyseal joint
ANXA3	Annexin A3
β2-M	Beta-2-microglobulin
BASP1	Brain acid soluble protein 1
BCP	1-bromo-3-chloropentane
BDNF	Brain-derived neurotrophic factor
BHQ1	Black hole quencher
BMP	Bone morphogenic protein
bp	Base pair
BSA	Bovine serum albumin
CAXII	Carbonic anhydrase-12
CDH2	Cadherin-2
cDNA	Complimentary deoxyribonucleic acid
CEP	Cartilaginous endplate
CHRD	Chordin
cm	Centimetre
CLEC2B	C-type lectin domain family 2 member B
CO_2	Carbon dioxide
$CoCl_2$	Cobalt chloride
COL2A1	Collagen, type II, alpha 1
COMP	Cartilage oligomeric protein
CS	Chondroitin sulphate
Ct	Cycle threshold
CTGF	Connective tissue growth factor
DAB	3,3'-diaminobenzidine tetrahydrochloride
DEPC	Diethylpyrocarbonate
DIG-11-UTP	Digoxigennin-11-uridine-5'-triphosphate
DMEM	Dulbecco's modified eagles medium
dNTP	Deoxyribonucleotide triphosphate
dTTP	Thymidine triphosphate
ECM	Extracellular matrix
EDTA	Ethylenediaminetetraacetic acid
EIF2B1	Eukaryotic translation initiation factor 2B
ELISA	Enzyme-linked immunosorbant assay
FACS	Fluorescence-activated cell sorting

FBLN1	Fibulin 1
FBS	Foetal bovine serum
FGF	Fibroblastic growth factor
FOXA2	Forkhead box A2
FOXF1	Forkhead box F1
GAG	Glycosaminoglycan
GAP	Growth-associated protein
GAPDH	Glyceraldehyde-3-phosphate dehydrogenase
GPC3	Glypican 3
H_2O_2	Hydrogen peroxide
HA	Hyaluronic acid
HBB	Haemoglobin, beta
HBSS	Hank's balanced salt solution
HCl	Hydrochloric acid
H&E	Haematoxylin and eosin
HS-PG	Heparin sulphate proteoglycan
HSPS	High salt precipitation solution
IBSP	Integrin-binding sialoprotein
IL-1	Interleukin-1
IL-1R	Interleukin-1 receptor
IL-1RA	Interleukin-1 receptor antagonist
IMS	Industrial methylated spirits
ISH	*In situ* hybridisation
IVD	Intervertebral disc
kN	Kilonewtons
KRT8	Cytokeratin8
KRT18	Cytokeratin-18
KRT19	Cytokeratin-19
KS	Keratin sulphate
L	Litre
LBP	Low back pain
LGALS3	Galectin-3
M	Molar
MAT	Matrillin
MCT	Microcentrifuge tube
ml	Millilitre
mm	Millimetre
mM	Millimolar
MMP	Matrix metalloproteinase
MPa	Megapascal
MRI	Magnetic resonance imaging
mRNA	Message ribonucleic acid
MRPL19	Mitochondrial ribosomal protein L19
MSC	Mesenchymal stem cell
NaCl	Sodium chloride
NC	Notochordal
NCAM1	Neural cell adhesion molecule 1
NFQ	Non-fluorescent quencher
ng	Nanogram
NGF	Neural growth factor

nm	Nanometre
nM	Nanomolar
Nm	Newton metres
NO	Nitric oxide
NP	Nucleus pulposus
NR	Nerve root
O_2	Oxygen
OVOS2	Ovostatin 2
Pax	Paired box protein
PBS	Phosphate buffered saline
PDAR	Pre-developed assay reagents
PG	Proteoglycan
PRELP	Proline arginine-rich end leucine-rich repeat protein
PTHrP	Parathyroid hormone-related protein
PTN	Pleiotrophin
qPCR	Quantitative polymerase chain reaction
RNA	Ribonucleic acid
ROS	Reactive oxygen species
RPLP0	Ribosomal protein, large, P0
RT-PCR	Reverse transcription polymerase chain reaction
SA β-galactosidase	Senescence-associated β-galactosidase
SC	Spinal cord
SE	Standard error of the mean
SGCG	Sarcoglycan, gamma
Shh	Sonic hedgehog
SIPS	Stress-induced premature senescence
Sox	Sry-related high mobility group box
SSC	Saline sodium citrate
T	Brachyury (gene notation)
TGF-β	Transforming growth factor-β
TIMP	Tissue inhibitor of metalloproteinase
Tm	Melting temperature
TNF-α	Tumour necrosis factor-α
TNFR1A	Tumour necrosis factor receptor type 1A
TNFR1B	Tumour necrosis factor receptor type 1B
TYRO3	Protein tyrosine kinase
UK	United Kingdom
US	United States
UV	Ultraviolet
VB	Vertebral body
VCAN	Versican
VEGF	Vascular endothelial growth factor
VIM	Vimentin
v/v	volume/volume
w/v	weight/volume

Acknowledgement

Firstly I wish to thank my supervisors Professor Hoyland, Dr. Richardson and Mr. Gnanalingham for their support and advice during the three years and beyond. Your talents as exceptional scientists and clinicians has better equipped me to succeed in my endeavour than I could ever have possibly hoped for, and your encouraging words when things were not always going to plan kept me motivated to keep on trying. There are a number of individuals, whose technical knowledge has contributed greatly to the completion of this thesis, including Pauline, Andy, Sonal, Daman, John, and Mike. Your expertise in helping to design and troubleshoot these experiments is hugely valued, and for this I must sincerely thank you all. I also wish to recognise Dr. Ross Atkinson for providing me with my surgical specimens and Professor Freemont for sacrificing many early mornings to histologically grade my specimens; this was no small undertaking, so thank you very much. Additionally, to all of my colleagues, Hamish, Matt, Shahnaz, Jude, Kim, Chris, Ricardo, Louise and Nicola, thank you not only for your help, but mostly for the laughs we shared and I wish you all the greatest of luck in your future career pursuits. My early morning breakfasts with Kim and lunches with Sonal provided some much appreciated time away from the project, as well as some memorable moments, so thank you both! Regarding memorable moments, thanks to Nicola for spending many hours dissecting pigs with me; I could never have done it all on my own!

On a personal note, there are many who have inspired me to chase my dream of a PhD, but the most important of these are my parents and grandparents. You have sacrificed so much so that I may take every opportunity available to me, and for this I will forever be indebted to you. Thanks also to my brother and sister for being supportive and interested in my work, even if you didn't particularly understand or care. To Joe, Katie, Marianne, Alice and Joanna who were always on the end of a phone when I needed a chat or glass of wine, thank you so much. It's nice to know that nothing changes if you relocate to another city for four years. Finally, thank you to Neal from the very bottom of my heart. Your unfaltering support over the last four years gave me such motivation to continue and strive to succeed and I hope I too can enable you to achieve all that you want so selflessly. Thank you to you all, I could not have done this without you.

Chapter 1:

General Introduction

1.1 Investigation Overview

The high prevalence of low back pain (LBP) in Western populations and the association with intervertebral disc (IVD) degeneration has become a focal point for scientific and clinical research, with the ultimate aims being to better understand the aberrant cell biology (particularly in the nucleus pulposus (NP) region of the IVD), which drives this degeneration and to develop novel cell-based therapies which will restore normal function to the tissue. Imperative to fulfilling both of these aims is the comprehensive elucidation of the NP cell phenotype. If a better understanding of the phenotypic profile of human NP cells were to be gained, this would in turn shed some light as to the developmental origins of cells of the tissue, as currently, the evidence presented for this is conflicting and limited to a handful of studies. Additionally, as cells of the IVD synthesise the tissue matrix in which they reside (a function demonstrated to alter with progressing tissue degeneration), an insight as to the genes expressed by these cells may uncover the cellular mechanisms underlying this atypical matrix production. It has also been demonstrated that age-related changes occur within the IVD, particularly with regards to cell population and extracellular matrix (ECM) homeostasis. An understanding of the genes that govern NP cell function and a description of their expression levels with progressing age may therefore provide an explanation for these differences. The final area of IVD biology which would be better understood if the implicated cell phenotype could be fully characterised is the degeneration of the disc. It is postulated that IVD degeneration is a cell-driven process, and therefore, the phenotype of these cells may influence these degenerative changes. Taken together, an understanding of the optimal cell phenotype with regards to tissue development, homeostasis, ageing and degeneration would enable the better design of novel regenerative therapies for clinical use. However, whilst the current literature is comprised of novel descriptions of the NP cell phenotype, these have yet to be investigated in a cohort of human specimens where a range of ages and degenerative scores are represented, and their protein expression has not been localised to cells of the tissue. Thus, this study focussed on the characterisation of the adult human NP cell phenotype across a range of disc levels, ages and degenerative scores at both the gene and protein level, and the development of a novel *ex vivo* model to test the effect of microenvironment on this expression profile.

1.2 Low Back and Neck Pain

The human vertebrae are divided into four regions: cervical, thoracic, lumbar and sacral. LBP is related directly to the lumbar spine segment, and is estimated to affect 60-80% of individuals in developed societies at some point in their lives (Kelsey *et al.*, 1992), whilst 10% of these suffer with the chronic LBP (Waddell, 1996). LBP poses a huge socioeconomic burden in the UK, with approximately £12 billion in costs arising annually through lost work days, social benefit payments and costs to the healthcare system attributed to 17 million LBP sufferers (Maniadakis and Gray, 2000, N.I.C.E., 2009). In the US LBP is thought to cost the economy approximately $85billion annually (Martin *et al.*, 2008), and is the third most common cause of surgical procedures (Andersson, 1999). Like LBP, chronic neck pain associated with the cervical portion of the spine is a highly common condition in developed societies, with a lifetime prevalence of approximately 70% (Makela *et al.*, 1991), and as such is one of the most commonly reported musculoskeletal disorders (Webb *et al.*, 2003). The precise aetiologies of LBP and neck pain are poorly understood; however, it has been demonstrated that degeneration of the lumbar IVD and LBP (Benneker *et al.*, 2005, Cheung *et al.*, 2009) and cervical IVD degeneration and neck pain (Matsumoto *et al.*, 1998) are directly correlated, whilst a correlation between pain and the severity of IVD degeneration has also been noted (Cheung *et al.*, 2009).

1.3 Intervertebral Disc Structure

Intervertebral discs are highly specialised tissues that separate the 24 vertebrae of the human spine and approximately 25% of the length of the human spine can be attributed to IVDs (Raj, 2008). These discs function not only to support both the upper and lower extremities, but also to withstand load applied to the spine through movement, and allow for deformation under such loads. The IVD itself is best described as comprising three distinct regions: the cartilaginous endplate (CEP), the annulus fibrosus (AF) and the nucleus pulposus (NP) (Figure 1.1).

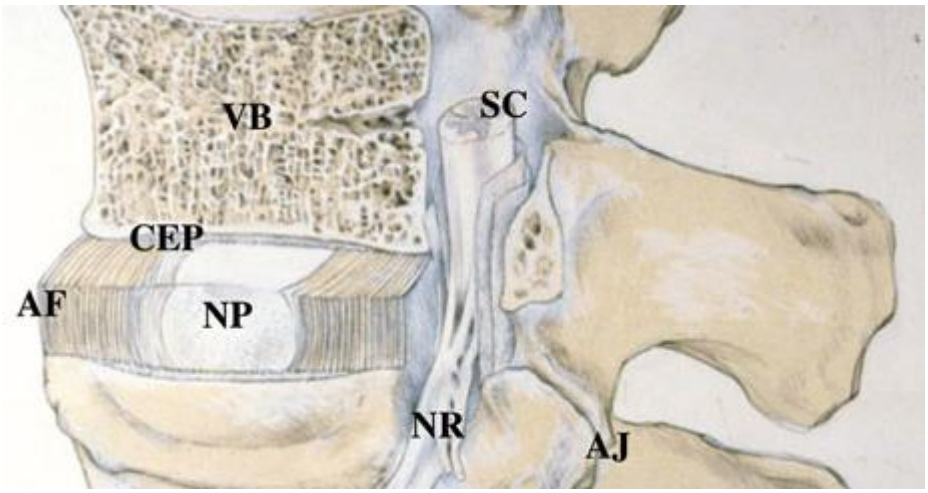

Figure 1.1 The intervertebral disc and spinal segment. The lamellae of the annulus fibrosus (AF) surrounds the nucleus pulposus (NP), with the disc separated from the vertebral body (VB) by cartilaginous endplates (CEP). Also demonstrated is the proximity of the disc to the spinal cord (SC), nerve root (NR) and apophyseal joint (AJ). Adapted from (Urban and Roberts, 2003).

1.3.1 Structure of the Adult Human IVD Tissues

1.3.1.1. The Cartilaginous Endplate

CEPs are comprised of thin layers of hyaline cartilage and are located on the superior and inferior vertebral surface and separate the vertebrae from the IVD (Roberts *et al.*, 1989). The CEP function is threefold: to absorb some of the pressure from load application thus protecting the vertebral column from pressure atrophy; to provide a physical barrier confining annulus and nucleus tissues to their anatomical location; and to act as a semi-permeable barrier across which nutrients and metabolites can be exchanged via diffusion between the NP, AF and VB (Humzah and Soames, 1988, Roberts *et al.*, 1989).

1.3.1.2. The Annulus Fibrosus

The AF is comprised primarily of collagen fibres arranged in concentric lamellae numbering between 10 and 25 (Marchand and Ahmed, 1990), and surrounds the nucleus pulposus. The AF is attached to the NP and CEPs, as well as longitudinal ligaments. The collagen fibres of the AF demonstrate an alternating orientation and are angled at approximately 70° to the vertical axis (Bogduk and Twomey, 1987). The AF functions to protect the NP from loading forces, and being comprised of collagen lamellae allows for both flexibility and rigidity (Pooni *et al.*, 1986). The

posterior region of the disc contains more densely packed collagen fibres, thereby preventing deformation of the disc under application of a variety of loads.

1.3.1.3. The Nucleus Pulposus

The centrally-located NP is gelatinous in appearance, and the fluid-like nature of the disc permits compression of the tissue under load. The hydrostatic pressure of the disc is maintained by the high proteoglycan (PG) content, and this allows for the NP to flatten and expand when a load is applied (Bibby *et al.*, 2001, Colombini *et al.*, 2008).

1.3.2 Variations in IVD Structure According to Spinal Region

Both the size and shape of the IVD change according to spinal level. Compared to lumbar discs, cervical IVDs are much smaller in size, with a disc radius of <1cm, compared to >2cm in the lumbar region (Pooni *et al.*, 1986), (Figure 1.2). The proportion of NP tissue in the cervical IVD at birth is only half that observed in the lumbar IVD (Taylor, 1975), and the cross sectional area of the NP increases linearly from the cervical to the lumbar region of the spine, with the L5-S1 disc NP occupying a much larger proportion of the cross-sectional area than that of C2-C3 (Pooni *et al.*, 1986). In terms of AF structure within the cervical disc, AF fibres are more numerous and thick in the anterior portion of the disc, whilst the posterior part comprises only a thin layer of collagen fibres, resulting in a crescentric appearance of the annulus, thought to enable control of movements in flexion/extension and contributing to the natural curvature of the cervical spine (Mercer and Bogduk, 1999), (Figure 1.3). Additionally, unlike the lumbar AF, the cervical annulus does not consist of concentric collagen lamellae surrounding the NP, but are orientated in alternating angles (Mercer and Bogduk, 1999). The angle of fibre orientation is 5° less in the cervical AF (65°) as compared to lumbar (70°), although the reasons for this distinction remain unexplained (Pooni *et al.*, 1986).

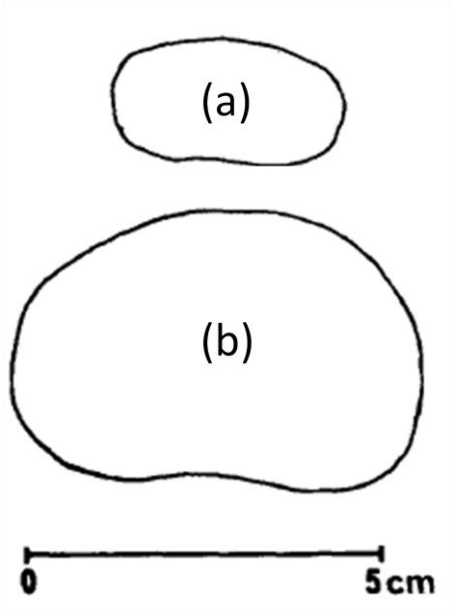

Figure 1.2 Distinctions in the cross-sectional shapes of cervical and lumbar IVDs. Discs obtained from the cervical C7-T1 (a) and lumbar L4-L5 (b) regions were assessed for their cross-sectional area. Adapted from (Pooni *et al*., 1986).

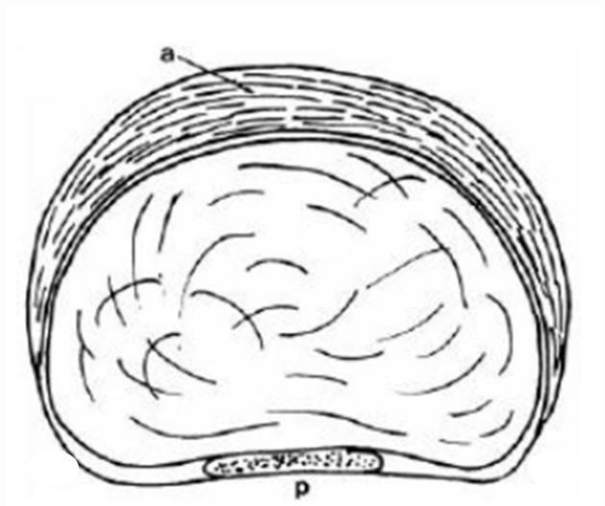

Figure 1.3 The cervical intervertebral disc. An illustration of a human cervical intervertebral disc. The anterior (a) annulus is crescentric in shape, and fibres are thickest in this part. The posterior (p) AF is limited to paramedian longitudinal fibres. Adapted from (Mercer and Bogduk, 1999).

1.3.3 Load-Bearing Properties of the Intervertebral Disc

A variety of loads are imparted on the IVD tissues, and it is the structure of the various tissues that permits this load application. Intradiscal pressures vary largely during daily activities, with walking, lifting, jogging and climbing stairs raising intradiscal pressure as much as 1.2MPa compared to lying prone, where the pressure is approximately 0.1MPa (Wilke *et al.*, 1999). Humans are a bipedal species, and

thus axial loading is applied to the spine continuously through upright posture and pressure from the body musculature. Pressures exerted on the human spine when sitting unsupported or standing are approximately 0.5MPa (Wilke *et al.*, 1999); however, atypical loads may be forced upon the tissues as a result of manual work or loss of tissue integrity through degeneration.

1.4 Intervertebral Disc Development

1.4.1 IVD Embryogenesis

The distinct structures of the NP, AF and CEP tissues of the IVD are thought to arise as a consequence of their different developmental origins (Urban and Roberts, 1995). The AF and CEPs have been demonstrated as mesenchymal in origin, whilst the embryonic NP derives from the notochord (Walmsley, 1953). Figure 1.4 illustrates the development of the IVD tissues. The notochord is located between two paraxial somites during early development, which are comprised of an epithelium and mesenchymal somitocoele that undergoes mesenchymal to epithelial transition and forms the sclerotome. Sclerotomal cells migrate medially from the somites to surround and condense around the notochord at approximately 30 days foetal gestation (Hunter *et al.*, 2003a, Peacock, 1951). This cellular condensation produces layers of condensed and less-condensed cells that subsequently form the AF and CEP/VB respectively (Aszodi *et al.*, 1998). The cells of the more condensed regions adopt a fibroblastic morphology, characteristic of AF cells, and form an orientation and alignment that will permit formation of the lamellar structures (Rufai *et al.*, 1995). Rapid cellular proliferation in the annular regions is noted (Taylor and Twomey, 1988), and both stress fibres and adherens junctions form within and between these cells in order to align them prior to the development of the mature AF collagen network (Hayes *et al.*, 1999). Extracellular matrix deposition is controlled via junctional complexes involving integrins and vinculin (Hayes *et al.*, 1999).

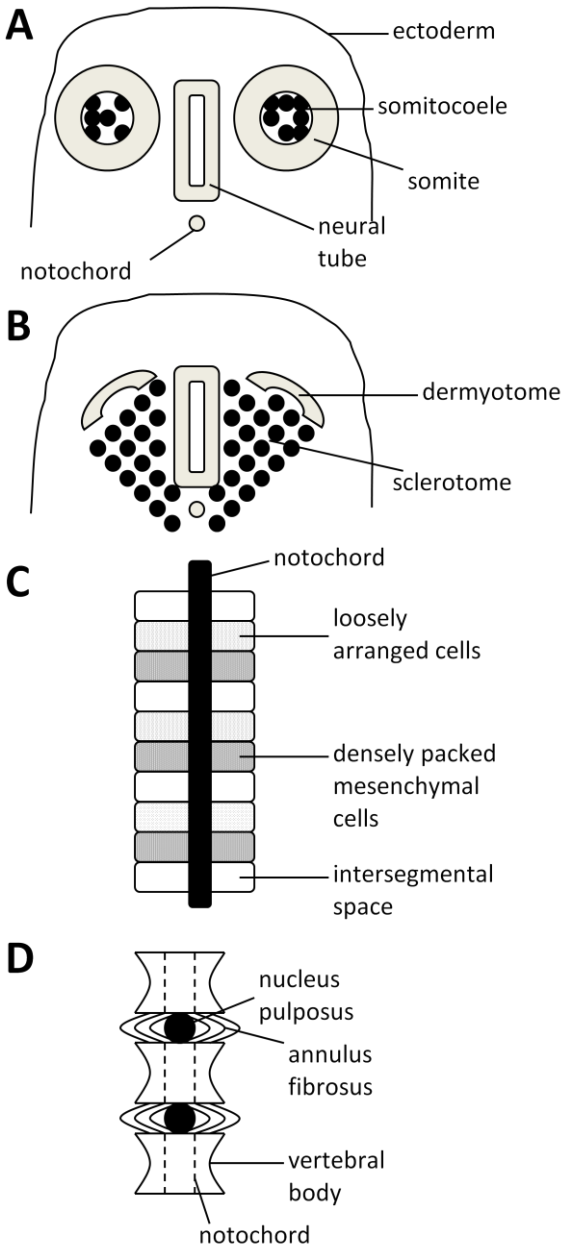

Figure 1.4 The development of the intervertebral disc. Somites are comprised of a somitocoele (A) that undergoes mesenchymal to epithelial transition, and forms the sclerotome which migrates towards the notochord (NC) and neural tube (B). Separation of the sclerotomal cells into areas of condensed and less-condensed cells is noted (C). NC involution occurs concurrently, resulting in the formation of the NP within the intersegmental/intervertebral space (D). Note, the orientation of A and B differs from that of C and D, by a 90° rotation about the x-axis. Reproduced from (Kaplan *et al.*, 2005, Rawls and Fisher, 2010).

Development of the nucleus pulposus regions occurs concurrently with annular morphogenesis. Notochordal contraction within the developing vertebral bodies is observed, whilst the tissue simultaneously expands within the intervertebral space to

form the NP (Aszodi *et al.*, 1998, Pazzaglia *et al.*, 1989, Peacock, 1951). When an embryo has grown to 17mm in size (8-9 weeks post conception), proliferation of the notochord is noted, and an ECM distinct to that of the surrounding AF is formed by these cells (Walmsley, 1953). The stages of notochordal transformation are outlined in Figure 1.5. At E12.5 in mice, the notochord is visible throughout the length of the embryo and is not segmented at this stage, whilst the layers of condensed and less-condensed cells are seen. At E13.5, notochordal involution has begun, with contraction in the VB regions and some expansion in the future intervertebral regions noted. The NC is fully retracted in the VB tissues at E14.5, and is further expanded in the disc space. In neonatal tissue, the notochord has expanded laterally and ossification of the VB is noted in primary ossification centres (Smith *et al.*, 2011). It has been suggested that mechanical forces exerted on the notochord underlies the involution of this tissue. Swelling of the tissue condensates that go on to form the VBs is hypothesised to constrict the notochord, thereby forcing migration of the tissue to the intervertebral space, as demonstrated in mice deficient in type II collagen. In such mice, VB formation is retarded and the involution of the NC is not observed, with the tissue remaining as a rod-like structure throughout the embryo, lacking the subsequent formation of NP tissue (Aszodi *et al.*, 1998). Incorrect formation of the notochord during development gives rise to vertebral defects, characterised by alterations in muscular arrangement, connective tissue disorganisation and notochordal collagen abnormalities (Santamaria *et al.*, 1994). Additionally, disruption to the zebrafish notochord by laser ablation resulted in the formation of embryos lacking centrum development, therefore inhibiting vertebral formation (Fleming *et al.*, 2004).

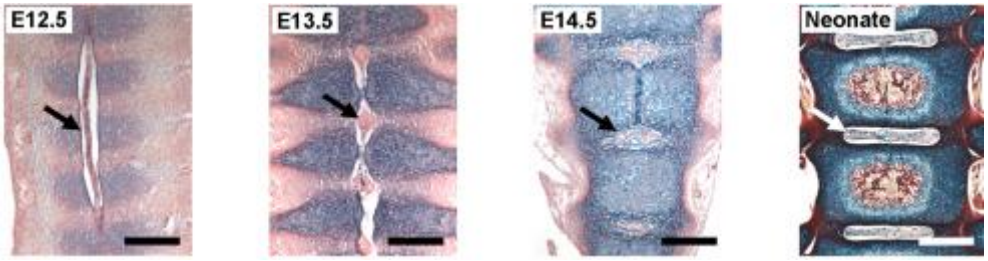

Figure 1.5 Notochordal transformation in the mouse embryo. Picrosirius red and alcian blue staining at E12.5 shows that the notochord (arrow) runs the length of the vertebral column and sclerotomal cell condensation is noted. At E13.5 the notochord contracts within the VB and expands within the disc region (arrow). At E14.5 the notochord is absent from within the VB and persists only in the intervertebral space (arrow). In neonates, the NP has expanded (arrow). Adapted from (Smith *et al.*, 2011).

1.4.2 Cellular Alterations with Skeletal Maturity of the NP

During human development, the NP is comprised of morphologically-distinct NC cells (Taylor, 1975), but it has been demonstrated that alterations to the cellular population of the NP occur with ageing and subsequent maturity of the tissue. NC cells are larger than the NP cells which populate the adult IVD (approximately 25µm as compared to 8µm in diameter (Hunter *et al.*, 2003b)), and are characterised by the abundance of vacuoles contained within the cells (approximately 80% of the cell volume (Hunter, 2005)), as well as their formation of large and dense cellular networks; features absent in the adult human NP tissue. The foetal NP is populated by an abundance of NC cells (Boos *et al.*, 2002), whereas the infant NP contains NC cell clusters and strands (Trout *et al.*, 1982a) which gradually disappear by age 8, and are replaced with smaller, rounded chondrocyte-like cells, that populate the NP throughout adulthood (Louman-Gardiner *et al.*, 2011). The developmental origin of adult human NP cells is controversial as it is not clear whether they derive from NC cells, or the surrounding AF/CEP cells, and is reviewed in section 4.1. Increased cell density of chondrocyte-like NP cells is noted in neonatal IVDs, and the number of chondrocyte-like NP cells populating the nucleus pulposus increases during early childhood (Boos *et al.*, 2002). However, decreased proliferation of NP cells is noted following adolescence, where the NP tissue itself becomes softer and relatively hypocellular (Boos *et al.*, 2002, Taylor, 1975). Of note, the loss of notochordal cells from the human NP is thought to precede the onset of IVD degeneration, as it is at the point of NC cell loss that the first signs of disc degeneration are observed

(Nerlich *et al.*, 1997). The precise mechanisms underlying the loss of these distinct cells from NP tissue is however currently unknown, although biomechanical alterations and an insufficient nutrient supply have been postulated to contribute (Louman-Gardiner *et al.*, 2011).

1.4.3 Molecular Processes in IVD Development

A range of molecular signals are responsible for the co-ordination of IVD development, and are summarised in Figure 1.6. Sonic hedgehog (Shh) is multifunctional in IVD embryogenesis; in addition to Wnt it mediates somite patterning, whilst also enabling definition of the sclerotome (Ehlen *et al.*, 2006). PTHrP, a known Shh target, is expressed only during IVD growth and specifically in the CEP region (Dahia *et al.*, 2009). Additionally, synergism between Shh and noggin occurs during sclerotomal formation (Mcmahon *et al.*, 1998). Noggin is a bone morphogenic protein (BMP) antagonist, and is initially expressed by all NC cells, before localisation to the AF where it is postulated to block BMP signalling from the adjacent vertebral bodies (Dipaola *et al.*, 2005, Mcmahon *et al.*, 1998). BMP signalling is imperative to the development and growth of the disc, and following this, expression of these proteins ceases (Dahia *et al.*, 2009). Transforming growth factor-β (TGF-β) localisation is isoform-dependent. TGF-β3 is expressed in the condensed sclerotomal cells that form the AF and VBs, and with progressing development, is localised to cells in the intervertebral space, with no expression noted in the adjacent VB (Pelton *et al.*, 1990). TGF is thought to control development of the AF, preventing chondrogenic differentiation of the future annular region, and through promotion of AF differentiation (Sohn *et al.*, 2010). Deletion of TGF-β receptor 2 in type II collagen-expressing cells results in aberrant NP and AF formation, with AF cells phenotypically resembling chondrocytes (Baffi *et al.*, 2004). Differential TGF-β signalling has also been noted post-natally, with low levels noted in the AF as compared to the NP and CEP (Dahia *et al.*, 2009). Finally, fibroblastic growth factor (FGF) signalling is not noted in the developing or growing NP, but is noted in the early developmental stages of the AF, and latter stages of development of the CEP (Dahia *et al.*, 2009).

Sry-related high-mobility-group box (Sox) gene family members are also essential in the development of the IVD, particularly Sox5, Sox6 and Sox9. Sox5 and Sox6 expression is detected in both sclerotomal and notochordal cells, and lacking expression of this transcription factor results in the absence of the normal ECM sheath surrounding the NC, cellular apoptosis, impaired inner AF differentiation and improper involution of the notochord, with subsequent aberrant NP formation noted (Smits and Lefebvre, 2003). Sox9 expression is noted in all developing cartilaginous tissues, and has been described previously in the notochord and sclerotome (Barrionuevo *et al.*, 2006). Like that described for Sox5 and Sox6, a deficiency in Sox9 results in atypical NC sheath formation, which prevents the proper development of the notochord and sclerotome (Barrionuevo *et al.*, 2006). In addition to Sox genes, NC development is also controlled by Brachyury, which has been demonstrated as crucial to the differentiation and survival of the NC in the stages prior to control by Sox markers (Hermann and Kispert, 1994).

Pax genes regulate a number of transcription factors, and it is thought that Pax1 and Pax9 are crucial for the development of the IVD, as Pax-1/Pax-9-deficient mice lack formation of a sclerotome, notochord and the resultant tissues (Peters *et al.*, 1999). There is interplay between the various signalling cascades that control the development of the IVD, with Pax-1 signalling controlled by Shh/noggin signalling originating in the NC, (Fan and Tessier-Lavigne, 1994, Mcmahon *et al.*, 1998). Expression patterns of Pax-1 varies with progressing development, with expression initially noted in all sclerotomal cells, but following disc formation this is limited to AF precursor cells (Dipaola *et al.*, 2005).

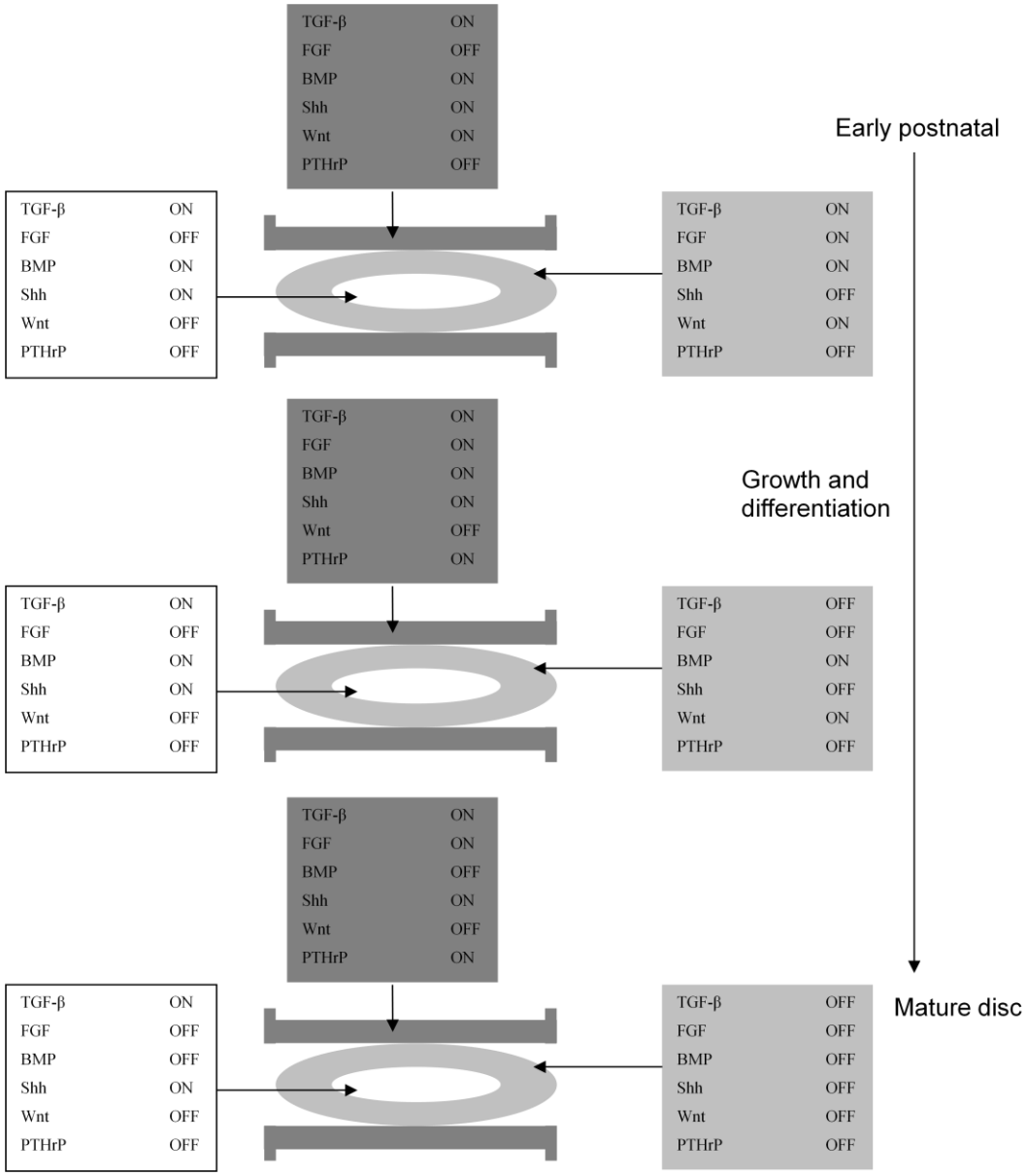

Figure 1.6 Alterations in molecular expression with growth. A map of signalling pathways in the differentiation, growth, and ageing of the IVD. Signalling in the NP is indicated in white, the AF in light grey and the CEP in dark grey. Adapted from (Dahia *et al.*, 2009).

1.5 The Mature Intervertebral Disc

Cells of the different adult human IVD regions have distinct cell morphologies and synthesise the ECM in which they reside. Cells of the CEP resemble those found in other cartilaginous tissues, whereby they are rounded in their morphology, and have a cell density of approximately $15x10^6$cells/mm^3 (Maroudas *et al.*, 1975). Cells of the AF are elongated and fibroblastic in appearance (Figure 1.7A) (Comper, 1996)

and the tissue is relatively densely populated when compared to that of the neighbouring NP, containing approximately $9x10^6$cells/mm^3 (Maroudas *et al.*, 1975). Adult NP cells (Figure 1.7B) resemble articular chondrocyte (AC) cells (Figure 1.7C) in that they are small and rounded in morphology, but only provide a cell density of $4x10^6$cells/mm^3 (Maroudas *et al.*, 1975), and thus the tissue is sparse in cellular content.

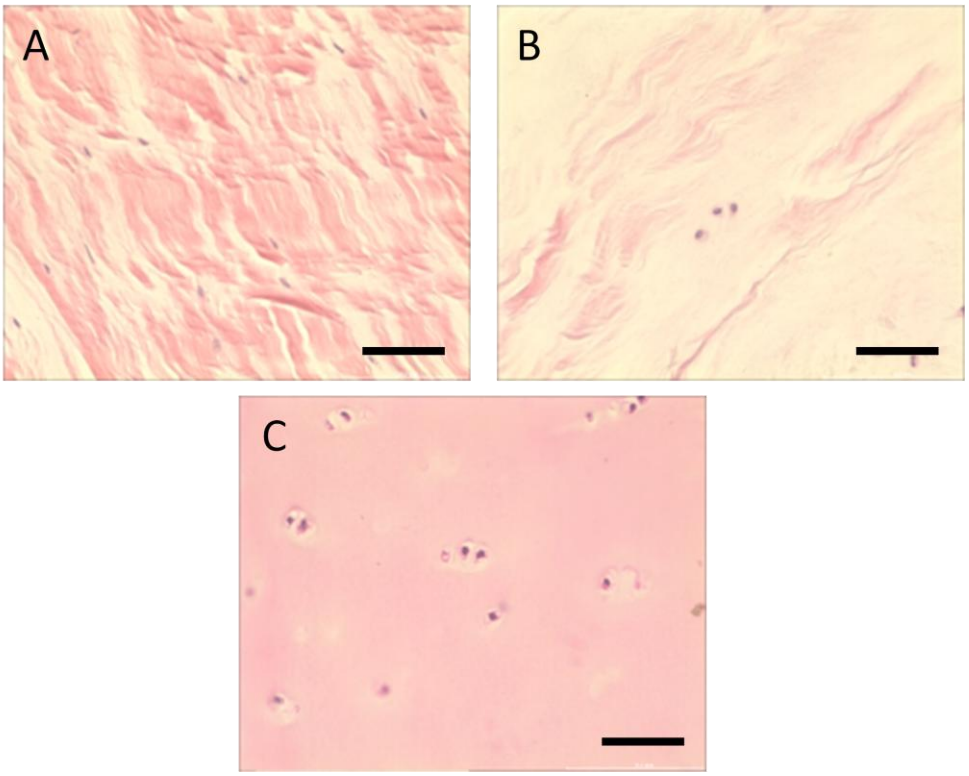

Figure 1.7 Histological analysis of AF, NP and AC cell morphology. Human IVD and articular cartilage cells stained with haematoxylin and eosin. The highly organised structure of the AF (A), with its concentric lamellae and fibroblast-like cells differs greatly from that of the hydrated NP (B), which contains fewer cells and a higher proportion of ECM, but NP cells resemble that observed in articular cartilage (C). Scale bars= 50µm.

The ECM within the IVD is highly complex, and comprised of a number of collagen and proteoglycan (PG) isoforms, in addition to a number other less abundant ECM proteins. Key ECM molecules within the IVD and the interactions they form with other ECM proteins are illustrated in Figure 1.8. The matrix synthesised by CEP cells is predominantly comprised of PGs reinforced by collagen (particularly type X collagen) fibrils (Lammi *et al.*, 1998, Rodriguez *et al.*, 2012); however, the CEP has varying composition depending on its location within the disc; the portion nearest

the AF has increased collagen content than that alongside the NP, where water and PG content is higher (Roberts *et al.*, 1989). The AF ECM is predominantly formed of type I collagen fibres, accounting for 50-60% of its dry weight (Bogduk and Twomey, 1987), but also contains interlamaellar PGs (Ortolani *et al.*, 1988) and elastin fibres that are anchored to the CEP; their role being to restore the disc to its original shape after movement and bind the lamellae together (Yu *et al.*, 2002).

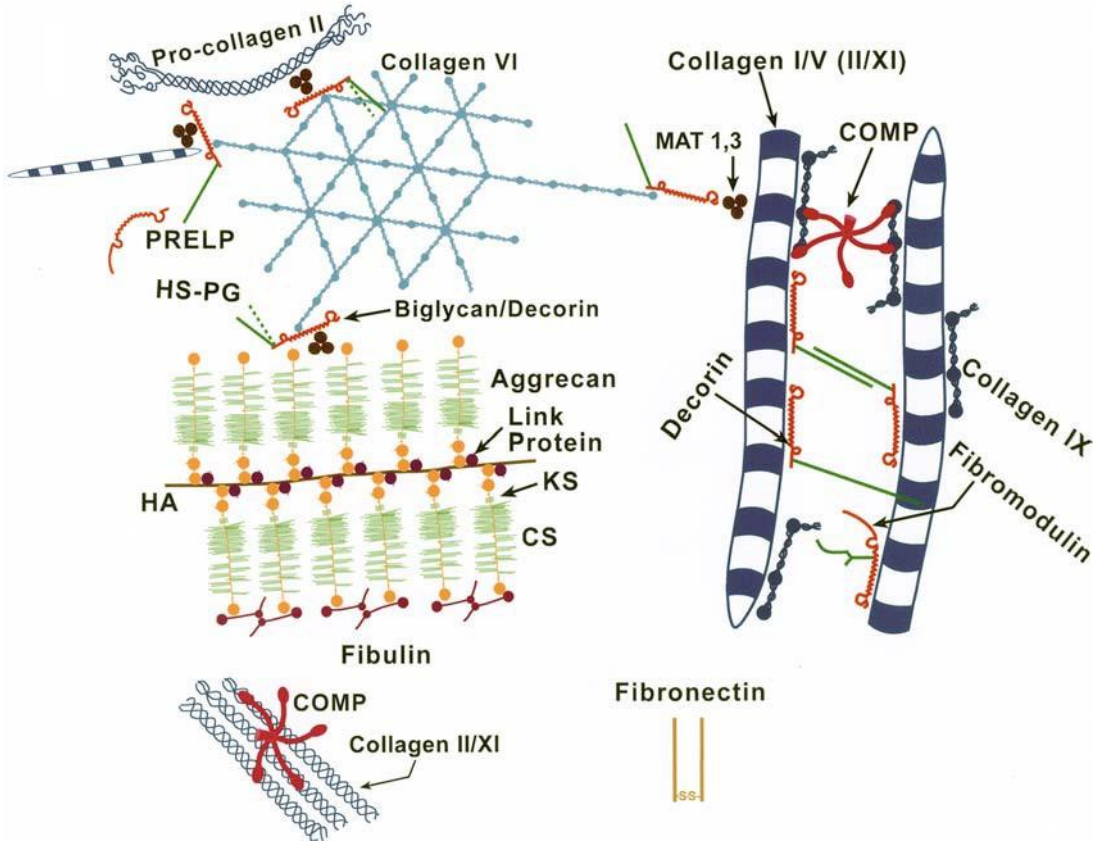

Figure 1.8 Assemblies of matrix proteins within the IVD. COMP = cartilage oligomeric protein; CS = chondroitin sulphate; KS = keratin sulphate; HA = hyaluronic acid; HS-PG = heparin sulphate proteoglycan; MAT = matrillin; PRELP = proline arginine-rich end leucine-rich repeat protein. (Feng *et al.*, 2006).

The NP tissue is comprised of 70-90% water, and this highly hydrated appearance is attributed to the high PG content, accounting for 65% of the dry weight of the tissue (Bogduk and Twomey, 1987). Aggrecan is the predominant PG found within the NP, and is responsible for water being drawn into the tissue by increasing its osmotic potential (Bogduk and Twomey, 1987). PGs comprise of a central core protein bound via covalent bonds to numerous negatively charged glycosaminoglycans

(GAGs). In the case of aggrecan, these GAG chains are sulphated – normally chondroitin or keratin sulphate, and bind to hyaluronic acid via link proteins (Melrose *et al.*, 2001). The NP ECM also contains type II collagen; the fibres of which are arranged irregularly, and comprise 15-20% of the weight of the dry NP (Le Maitre *et al.*, 2007c). Additionally, elastin fibres are noted within the NP and provide a loose structure to the NP, holding the gelatinous portion of the tissue together (Adams and Roughley, 2006). Other collagen isoforms can be found within the IVD, including types V, VI, IX and XI. Type VI collagen has been localised to the pericellular region of cells within the AF/NP transition zone, and is thought to be involved in signal transduction (Melrose *et al.*, 2008), whilst types V, IX, X and XI are localised throughout the disc, and interact with collagen isoforms I and II, thereby providing stability to both the tissue as a whole and the collagen network (Feng *et al.*, 2006).

Other ECM molecules have been described as present in the IVD. Versican is a PG whose structure is partially homologous with aggrecan, but unlike aggrecan, versican contains only chondroitin sulphate GAG chains (compared to both keratin sulphate and chondroitin sulphate GAG chains in aggrecan), and these are far fewer in number than the GAG chains in aggrecan, resulting in a lower charge on the versican molecules and the potential to bind less water (Wu *et al.*, 2005). Like aggrecan, versican also binds hyaluronic acid (Wu *et al.*, 2005), and has been localised within translamellar cross bridges of the AF (Melrose *et al.*, 2008), as well as the adult human NP (Sztrolovics *et al.*, 2002). Cartilage oligomeric protein (COMP) is essential in the organisation of collagen fibres within the AF collagen network by ensuring that they are closely spaced and parallel, but also binds to each of the globular domains of type IX collagen providing network stability (Feng *et al.*, 2006, Ishii *et al.*, 2006). Several other PGs play a role in collagen fibre assembly including biglycan and decorin, which predominantly bind to type VI collagen (Wiberg *et al.*, 2002), and fibromodulin and lumican which bind to other collagen isoforms (Feng *et al.*, 2006). Expression of these PGs is greater in AF tissues than the NP (Inkinen *et al.*, 1998, Singh *et al.*, 2009). Finally, fibronectin and cartilage intermediate layer protein (CILP) have been localised within the IVD and linked to increased incidence of IVD degeneration (Feng *et al.*, 2006, Seki *et al.*, 2005).

Crucially, a clear omission from the current literature exists with regard to a comparison of cervical and lumbar ECM molecule expression levels. A limited amount of literature exists which suggests that type II collagen expression is comparable between cervical and lumbar NP specimens at the protein level (Longo *et al.*, 2006, Park *et al.*, 2013); however, a model of human IVD degeneration where degeneration has been induced by exposure to cytokines demonstrated higher expression of types I and II collagen in cervical as compared to lumbar specimens (Park *et al.*, 2013). The expression of other matrix molecules in the cervical NP is however, yet to be investigated. Given that distinctions exist between discs from the two spinal regions with regards to gross structure, it is possible that such differences be linked to the levels of ECM molecules synthesised, and thus, this requires further investigation.

1.6 Alterations to the Human Intervertebral Disc

1.6.1 Age-Associated Changes in the Human IVD

A number of alterations to the morphology and molecular composition of the human IVD have been noted as associated with increasing age, although the close correlation between IVD degeneration and age complicates the separation of these two factors in the literature. In terms of cellularity, a change is noted with regards to the NP cell population from birth through to adolescence, with a loss of NC cells and increased localisation of small chondrocyte-like NP cells (described in 1.4.2). This has been well described in studies of the lumbar IVD (Louman-Gardiner *et al.*, 2011, Trout *et al.*, 1982a), but interestingly, there is a limited amount of data that suggests that this process applies to the cervical disc also (Oda *et al.*, 1988). The cell density of human NP cells has been shown to decrease with ageing, with the cell density in the elderly adult population only 10% of that of the newborn (Liebscher *et al.*, 2011). A similar decrease in AF cell density has also been demonstrated, whilst CEP cell density is only noted as decreasing until late adolescence (Liebscher *et al.*, 2011). Additionally, evidence also exists which suggests that the percentage of necrotic NP cells also increases with age in humans; from 2% in the foetal spine, to >50% in adult specimens (Trout *et al.*, 1982a).

Regarding the gross structure of the IVD, although the adult human IVD is generally considered avascular, maturity of the human lumbar IVD is associated with a loss of the vascularity present within the developing and infant IVD, particularly within the CEP, thereby altering both the oxygen and nutritional state of the disc (Grunhagen *et al.*, 2006). This is also briefly described within the cervical IVD, where it has been noted that blood vessels present in the CEP of neonates is replaced by cartilaginous tissue by adolescence (Oda *et al.*, 1988), but overall, alterations in tissue morphology and organisation with ageing are not as well characterised in the cervical region as for the lumbar IVD. Alterations to the tissue ECM of the IVD with ageing is thought to underlie gross morphological changes within the disc, including loss of disc height and dehydration of the tissue. Decreases in both collagen and total PG content has been observed as a function of age (Singh *et al.*, 2009). Decreased PG levels mean a reduced ability to retain water content within the NP ECM, and it is thought that this precedes the loss of disc height observed by MRI in degenerate specimens as compared to healthy (Frobin *et al.*, 2001). Levels of denatured type II collagen is significantly lower in younger IVDs (Antoniou *et al.*, 1996), suggesting that expression of matrix degrading enzymes is also lower in discs of the same age, although this is not elucidated. Interestingly the expression of a number of small PGs has been shown to increase with progressing age. Alterations to the PG composition of the disc tissues with ageing may therefore be linked to differences in load-bearing potential, as different PGs vary in their ability to hydrate a tissue. Biglycan expression increases in the NP and inner AF with ageing, whilst fibromodulin levels increase significantly in the outer AF region (Singh *et al.*, 2009). Also, increased type X collagen has been noted with ageing in the human IVD, although it is unclear from this study whether the increase is related specifically to age or degeneration (Boos *et al.*, 1997). Type X collagen is a marker of tissue hypertrophy (a feature not normally noted in the healthy IVD, with the exception of the CEP), and thus increased expression in the ageing IVD may be linked to ossification of a normally gelatinous tissue. Linked to the loss of total PG content within the NP with ageing, a loss of NP water content has also been demonstrated (Antoniou *et al.*, 1996). These variations in ECM composition with ageing have been well described within the lumbar IVD, although there is little information regarding this in the cervical region, and thus, this requires investigation. Finally, changes to the ECM of the IVD with ageing influences the mechanical properties of the tissue. Compressive stress testing

of lumbar IVDs has shown that load distribution within the disc is altered, with load shifted to the AF from the NP (Adams *et al.*, 1996). This effect is more severe in the lower lumbar discs as compared to the upper, but the loading profile of cervical discs was not described.

1.6.2 Degenerative Changes to the Human IVD

Numerous morphological alterations occur in the IVD through the process of disc degeneration. Notably, the boundary between the gelatinous NP and fibrous AF loses its distinction, with the NP becoming increasingly dehydrated and more fibrotic (Buckwalter, 1995). This results in a decrease in NP size, with decompression of the tissue arising also, thereby forcing more of the load-bearing onto the adjacent AF (Adams *et al.*, 1996). Additionally, irregularities in the AF lamellae have been noted, and disorganisation of the collagen and elastin networks is apparent (Urban and Roberts, 2003). A loss of AF integrity reduces the ability of the AF to constrain the NP, and as is frequently observed in disc degeneration, bulging or herniation of the NP tissue results. Herniation of the IVD results in pressure being applied to the nerves located in close proximity to the disc, and nociceptive pain is suffered as a consequence. Also, the NP is prone to tearing and large fissures originating in the NP penetrate the annulus; a feature increasingly common after childhood (Boos *et al.*, 2002). Fissures also develop in the CEP, resulting in a more fibrotic and calcified tissue, and normal diffusion of nutrients and metabolites into and thus out of the disc is impaired, as the CEP is the primary location of disc vasculature, where diffusion of nutrients must occur to provide nutrition for the disc (Trout *et al.*, 1982b). Interestingly, modic changes in magnetic resonance images of degenerate IVDs has been shown to be significantly correlated with LBP, and highlights alterations to the vertebral endplates and sub-chondral bone through changes in signal intensity (Zhang *et al.*, 2008). Endplate alterations are also noted in older individuals, with increased incidence of nuclear bulging into the tissue noted (Twomey and Taylor, 1985). A loss of endplate integrity results in NP decompression, thereby altering the load-bearing capabilities of the tissue, described previously. Morphological alterations to the disc as observed during degeneration are illustrated in Figure 1.9.

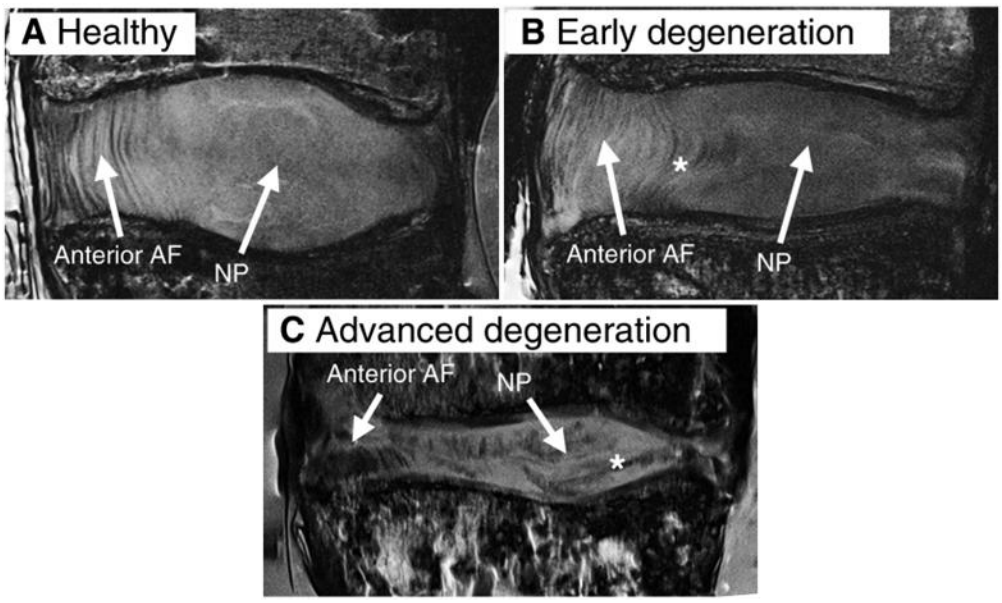

Figure 1.9 Progressive changes to the IVD with degeneration. A healthy disc exhibits distinct AF lamellae and gelatinous NP with good signal intensity (A). Discs undergoing early degeneration display a loss of disc height, decreased signal intensity in the NP and inward bulging of the AF (*) (B). Severely degenerate IVDs contain fissures penetrating deep into the AF from the NP (*), further decreases in disc height and a general loss of structural integrity (C). Adapted from (Smith *et al.*, 2011).

1.7 Intervertebral Disc Degeneration

1.7.1 Risk Factors for IVD Degeneration

A number of factors have been identified that may predispose an individual to developing IVD degeneration. Firstly, occupation is thought to influence the development of IVD abnormalities, with those workers whose occupation involves heavy lifting, twisting or repeated bending found to induce alterations to the disc that exceed those whose work was more sedentary (Battie *et al.*, 1995b, Videman *et al.*, 1990). Additionally, jobs which expose workers to vibrations have been proposed to induce degeneration by altering peripheral circulation in the CEP and outer AF of the IVD (vessels responsible for the nutrition of the largely avascular IVD), where regression of vascular growth has been reported, thereby compromising the nutrition of the disc (Elfering *et al.*, 2002, Kumar *et al.*, 1999). Smoking has been proposed by a number of studies to be a risk factor for the development of IVD degeneration (Deyo and Bass, 1989, Heliovaara *et al.*, 1991, Kelsey *et al.*, 1984, Pye *et al.*, 2007), and it is suggested that smoking too detrimentally alters the nutritional state of the disc through vessel wall changes and changes in blood flow (Ernst, 1993, Miller *et al.*, 2000). IVD cells exposed to nicotine demonstrate reduced cell proliferation,

disrupted ECM (including a shift from type II to type I collagen expression within the NP), and an atypical cell architecture, and the authors conclude that these changes may precede the onset of disc degeneration (Akmal *et al.*, 2004). Other lifestyle factors thought to influence the development of IVD degeneration include lack of exercise and obesity (Deyo and Bass, 1989, Elfering *et al.*, 2002), and the choice of automobile model (Kelsey *et al.*, 1984).

1.7.2 Genetic Association with Disc Degeneration

Genetic influences on the development of disc degeneration have been well-documented. Incidence of LBP has been significantly correlated with reports of discogenic pain in relatives (Bijkerk *et al.*, 1999, Postacchini *et al.*, 1988), whilst radiographic markers of degeneration have been shown to increase in severity when the patient had a first order relative who had undergone surgery for lumbar disc herniation (Matsui *et al.*, 1998). Additionally, studies in twins have demonstrated hereditary associations with alterations in the IVD that are more significant than the effects associated with environmental influences (Battie *et al.*, 1995a, Battie *et al.*, 1995b, Battie *et al.*, 2009).

A number of genes have been identified that may play a role in the development of IVD degeneration (summarised in Table 1.1). Firstly, mutations in the type IX collagen isoforms COL9A2 and COL9A3 have been associated with disc degeneration in the Finnish (Annunen *et al.*, 1999, Paassilta *et al.*, 2001, Videman *et al.*, 2009) and Chinese (Jim *et al.*, 2005) populations. Type I collagen polymorphisms alter the transcription factor binding sites and are thought to change the ratios of type I collagen subtypes, thereby affecting the strength of the IVD collagen network. Polymorphisms of the SP1 allele of COL1A1 have been associated with IVD degeneration in Dutch (Pluijm *et al.*, 2004), Finnish (Videman *et al.*, 2009), and Greek (Tilkeridis *et al.*, 2005) populations.

Polymorphisms in the CS1 subunit of aggrecan is associated with disc degeneration in Japanese (Kawaguchi *et al.*, 1999), Iranian (Mashayekhi *et al.*, 2010) and Turkish (Eser *et al.*, 2010) ethnicities, and it is hypothesised that these changes alter the ability of the subunit to bind GAGs (Doege *et al.*, 1997). Linked to this, variant alleles of vitamin D receptor have been implicated in disc degeneration, as

demonstrated in a Finnish study (Videman *et al.*, 1998), as well as Chinese (Cheung *et al.*, 2006) and Japanese (Kawaguchi *et al.*, 2002) populations. It is thought that alterations in the vitamin D receptor gene affect the integrity of the IVD ECM as it changes GAG sulphation (Kepler *et al.*, 2013).

Finally, a link between matrix metalloproteinase-3 (MMP3) allele 5A and lumbar disc degeneration has been demonstrated in a study conducted in Japan, but only in the oldest of patients (Takahashi *et al.*, 2001), and it is thought that the polymorphism with greater expression of 5A influences disc degeneration by increasing the amount of MMP3 protein expressed through increased transcription, and as detailed in section 1.7.4, MMPs are associated with IVD matrix degeneration (Ye *et al.*, 1995).

Table 1.1 Genes Associated with IVD Degeneration Studied in Human Populations

Protein	Likely IVD Function	Alleles with Variants
Type IX collagen	ECM support	COL9A2 COL9A3
Vitamin D receptor	GAG structure alteration	Taq1 Apa
Type I collagen	AF support	COL1A1
Aggrecan	NP osmotic gradient	CS1
MMP3	ECM degradation	5A 6A

Adapted from (Kepler et al., 2013)

1.7.3 Cellular Alterations Associated with Disc Degeneration

In terms of the cell population, IVD degeneration is associated with a transient loss of NP cells (Urban *et al.*, 2001). Given that the detrimental alterations to disc nutrient supply are linked to the degenerative processes, the observed loss in NP cell number may be consequence of this change. Also, degenerate discs have been shown to have increased levels of cell death via apoptosis (Johnson and Roberts, 2007), whilst up to 50% of adult IVD cells display necrotic properties (Trout *et al.*, 1982b). The apoptosis noted in the degenerate IVD may be unsurprising given that polymorphisms in the promoter region of Caspase-9 – an initiator caspase in apoptosis – is associated with increased risk of development of discogenic LBP (Guo

et al., 2011). However, methodologies used for identification of apoptotic cells involves either quantification of TUNEL-positive cells, or distinction of cells with a necrotic morphology (Johnson and Roberts, 2007, Trout *et al.*, 1982b), but not a combination of the two, which may be preferable (Alvarez and Ortiz, 1999), thereby raising the question of whether cell death in the IVD actually occurs. Moreover, IVD degeneration is also associated with increases in cell density, thought to follow the decrease reported by (Urban *et al.*, 2001). This is reportedly due to increased cell cluster formation and cellular proliferation (Boos *et al.*, 2002).

Healthy IVDs are generally aneural, but with the onset of degeneration, neural ingrowth into the tissue has been noted, particularly in the outer AF. The expression of substance P by these cells is considered indicative of a nociceptive nerve phenotype (Freemont *et al.*, 1997), and the expression of neurotrophins (including neural growth factor (NGF) and its appropriate receptors) by invading blood vessels is linked to the development of such features (Freemont *et al.*, 2002). It is postulated that aggrecan inhibits neural ingrowth in healthy IVDs. When the inhibitory effects of aggrecan isolated from AF and NP tissues on neurite growth and migration was assessed, it was noted that aggrecan isoforms pre-digested by enzymes inhibited neural growth to a lesser degree than intact isoforms (Johnson *et al.*, 2002). Enzymatic digestion deglycosylates aggrecan molecules in order that they more closely resemble aggrecan forms isolated from degenerate discs, and the ameliorated inhibitory effects of these molecules suggest that ECM degradation is implicated in the aetiology of neural ingrowth in the degenerate disc. Brain-derived neurotrophic factor (BDNF; also known as brain-derived growth factor, BDGF) is also thought to enhance neural ingrowth in the degenerate IVD, and its production by IVD cells is thought to be linked to IVD degenerative processes (Purmessur *et al.*, 2008). Additionally, semaphorin 3A expression has been demonstrated in the healthy adult IVD but not in degenerate specimens, whilst expression of PGP9.5 (a deubiquitnating enzyme involved in determination of neuronal cell fate and axonal pathfinding) was only detected in neuronal cells of the IVD in 8% of healthy and 39% of degenerative samples (Tolofari *et al.*, 2010). Semaphorin 3A is inhibitory to nerve growth at high concentrations, and decreased expression of this protein in disc degeneration is postulated to contribute to neural in growth in the degenerate IVD

(Tolofari *et al.*, 2010). A summary of factors considered inhibitory and stimulatory to neural growth in the IVD is illustrated in Figure 1.10.

Neovascularisation is a feature common to degenerate IVDs (Freemont *et al.*, 1997, Freemont *et al.*, 2002), and is noted as present in herniated tissues portions of the disc, and as increasing with patient age (Yasuma *et al.*, 1993). Factors expressed by IVD cells thought to influence the development of new blood vessels include vascular endothelial growth factor (VEGF) (Kokubo *et al.*, 2008), IL-1β (Lee *et al.*, 2011), and connective tissue growth factor (CTGF) (Ali *et al.*, 2008). Factors involved in the promotion of neoangiogenesis are also described in Figure 1.10.

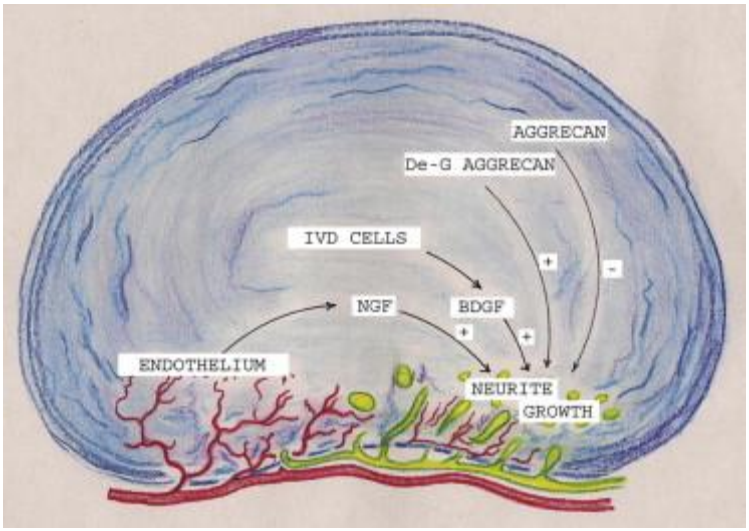

Figure 1.10 Diagrammatic representation of stimulatory or inhibitory factors for neural ingrowth in the IVD. Stimulatory factors are indicated with a (+) and inhibitory with a (-). De-G Aggrecan = degylcosylated aggrecan; NGF = neural growth factor; BDGF = brain-derived growth factor. New blood vessel growth is indicated in red, whilst new nerve growth is indicated in green (Kepler *et al.*, 2013).

Finally, cellular alterations are noted in terms of induction of cell senescence during IVD degeneration. It has been demonstrated that mean telomere length decreases with the progression of disc degeneration, whilst expression of the senescence markers $P16^{INK4A}$ and senescence-associated β-galactosidase have been reported as increased within the degenerate IVD as compared to normal specimens (Le Maitre *et al.*, 2007a). Interestingly, Caveolin-1 expression has also been demonstrated within the degenerate IVD (Heathfield *et al.*, 2008), and the presence of this proposed marker of stress-induced premature senescence (SIPS) during degeneration may suggest that, given the harsh microenvironment in the degenerate IVD, SIPS is likely

responsible for the accelerated cellular senescence observed, as opposed to replicative senescence (Kepler *et al.*, 2013).

1.7.4 Molecular Alterations Associated with Disc Degeneration

The morphological alterations previously described are postulated to result from aberrant cell biology, with cells secreting factors that are detrimental to the maintenance of tissue ECM, thus leading to the appearance of such degenerative features. In healthy discs, the balance between tissue anabolism and catabolism is sustained, but with advancing disc degeneration the balance shifts towards ECM breakdown, resulting in matrix loss. Several degradative enzymes have been implicated in the pathogenesis of IVD degeneration. MMPs are extracellular proteinases secreted in an inactive form prior to activation, whereby a cysteine residue in the pro-peptide domain is cleaved, allowing for the active site to interact with target proteins. MMP activation may occur at the cell surface via the cascade responsible for plasmin generation, utilising the uPA/uPAR/plasminogen cascade, and subsequent plasmin-mediated cleavage of the pro-peptide (Murphy *et al.*, 1999). This is particularly well investigated for the MMP isoform MMP-9 (Ramos-Desimone *et al.*, 1999). Alternatively, inactive MMP isoforms may be activated by other active MMPs. For example, active MMP-7 is known to activate MMPs -1, -2, -3, -9 and -10, whilst MMPs -1, -2, -7, -8, -9 and -13 are activated by MMP-3 (Imai *et al.*, 1995, Knauper *et al.*, 1996, Okada *et al.*, 1990, Reinemer *et al.*, 1994). Finally, MMPs may be activated in the intracellular compartment by furin, whereby this serine-protease present in the Golgi-network activates the enzyme prior to secretion. This has been demonstrated for MMPs -3 and -28 (Illman *et al.*, 2003, Kang *et al.*, 2002). A number of MMP isoforms have been implicated in IVD degeneration, including MMPs -1, -8, and -13 which degrade collagens; MMPs -2 and -9 which degrade partially denatured collagens, MMPs -3 and -10 which degrade other matrix proteins, and MMP-7 which is known to degrade both collagens and PGs (Bachmeier *et al.*, 2009, Gruber *et al.*, 2009, Le Maitre *et al.*, 2004a, Le Maitre *et al.*, 2006, Le Maitre *et al.*, 2007c, Millward-Sadler *et al.*, 2009, Richardson *et al.*, 2009, Rutges *et al.*, 2008, Zigouris *et al.*, 2011). Interestingly, certain MMP isoforms appear in fact to be downregulated in degenerate IVDs as compared to non-degenerate. For instance, MMP-19 is known to breakdown aggrecan, COMP and various collagen isoforms present in the IVD, but assessment of its expression

demonstrated a decrease with increasing degenerative status (Gruber *et al.*, 2005), suggestive of differing roles of MMP isoforms within the IVD. A distintegrin and metalloproteinase with thrombospondin motifs (ADAMTS) family members are also involved in the pathogenesis of the degenerate IVD. Detection of these enzymes in the healthy IVD is postulated to maintain normal tissue turnover, but increased expression in the degenerate IVD facilitates degradation of the disc matrix (Le Maitre *et al.*, 2004a, Pockert *et al.*, 2009). ADAMTS isoforms differ with regards to function. ADAMTS isoforms -1, -4, -5, -8, -9 and -15 are aggrecanases and are responsible for the proteolytic cleavage of aggrecan molecules. Residues Glu^{373}-Ala^{374} represent an aggrecanase cleavage site where ADAMTSs act that is separate from the Asn^{341}-Phe^{342} residues where all MMPs present in the IVD act (Sugimoto *et al.*, 1999, Tortorella *et al.*, 2000). Additionally, isoforms -1 and -8 also function as anti-angiogenic factors (Vazquez *et al.*, 1999), whilst isoforms -2 and -3 are involved in processing of procollagens to collagens (Fernandes *et al.*, 2001, Wang *et al.*, 2003). ADAMTSs -1, -4, -5, -9 and -15 have been demonstrated as increased in their expression in degenerate human specimens (Le Maitre *et al.*, 2004a, Pockert *et al.*, 2009), whilst ADAMTSs -7 and -12 have been demonstrated as upregulated in a rodent model of degeneration under load (Yu and Zhu, 2011).

In healthy IVDs, tissue inhibitors of metalloproteinases (TIMPs) moderate the expression of MMPs and ADAMTSs through competitive inhibition, maintaining the balance between matrix synthesis and breakdown. TIMPs -1, -2 and -3 have been described as expressed in the human IVD (Le Maitre *et al.*, 2004a, Pockert *et al.*, 2009). During degeneration, it is thought that an imbalance exists between the levels of MMPs/ADAMTSs and their TIMP inhibitors, which is thought to result in tissue degradation (Vo *et al.*, 2013). Given that expression of various MMP and ADAMTS isoforms are reportedly increased in degenerative discs, and that TIMPs act to inhibit such molecules in a 1:1 ratio (Visse and Nagase, 2003), an equivalent increase in TIMP expression would be required to ensure that the balance between matrix metabolism and catabolism is maintained. Another group of proteinases thought to play a role in degeneration of the IVD are cathepsins, with cathepsins D, G, K and L reported as increased in degenerate IVD (Ariga *et al.*, 2001, Gruber *et al.*, 2011, Konttinen *et al.*, 1999).

In addition to the increased disc catabolism, disc anabolism is decreased during IVD degeneration. Degenerate NP cells synthesise reduced levels of proteoglycan as compared to healthy disc cells, whilst collagen expression in the NP switches from that of type II to type I, resulting in a more fibrous tissue (Adams and Roughley, 2006). Expression of type III and X collagen has also been demonstrated in the degenerate NP. The presence of type X collagen is thought to indicate the transition to a hypertrophic phenotype (Boos *et al.*, 1997), whilst type III collagen is associated with type I collagen, and therefore its presence in the degenerate disc is unsurprising given the increased expression of type I collagen in degeneration (Nerlich *et al.*, 1997). Degenerate IVD cells not only demonstrate atypical expression of the predominant PG aggrecan, but also increased expression of other PGs including decorin and biglycan (Inkinen *et al.*, 1998). Thus, aberrant expression of IVD ECM components during degeneration combined with increased expression of catabolic factors, results in altered ECM integrity and mechanical properties characteristic of NP degeneration.

Cells of the degenerate IVD have been demonstrated to produce atypical levels of pro-inflammatory cytokines which further exacerbate tissue breakdown, and this is suggestive of alterations to the mechanisms controlling their normal expression as a consequence of degeneration. Healthy IVDs manage the deleterious effects of IL-1 through production of its antagonist IL-1RA (Le Maitre *et al.*, 2005). However, elevated levels of IL-1 have been reported during disc degeneration, with no corresponding increase in antagonist levels, thereby driving cells towards a more catabolic phenotype. IL-1 has been implicated in several degenerative processes including altered matrix synthesis (Le Maitre *et al.*, 2007c), increased matrix degeneration (Le Maitre *et al.*, 2005), and apoptotic cell death in annular cells (Zhao *et al.*, 2007). IL-1, particularly IL-1β, induces the expression of matrix degrading enzymes including MMPs and ADAMTSs (Le Maitre *et al.*, 2005, Shen *et al.*, 2003), whilst also providing a positive feedback loop for the production of further pro-inflammatory cytokines (Jimbo *et al.*, 2005). TNF-α is another inflammatory cytokine identified as expressed in the degenerate IVD (Le Maitre *et al.*, 2007b), where it has been linked to induction of MMP expression (Seguin *et al.*, 2005), induction of IL-1β expression (Millward-Sadler *et al.*, 2009), and neural ingrowth into the disc (Hayashi *et al.*, 2008). A number of other pro-inflammatory cytokines

have also been linked to degeneration of the IVD. IL-6 has been identified as expressed in herniated lumbar IVDs (Kang *et al.*, 1996), and has been demonstrated to amplify cellular responses to other pro-inflammatory cytokines (Studer *et al.*, 2011). Also, interleukins -8 and -17 have been identified within the IVD, but are not necessarily upregulated in degenerate specimens as compared to healthy (Burke *et al.*, 2002, Gruber *et al.*, 2013). Finally, although not a pro-inflammatory cytokine, endothelin-1 has been implicated in the degeneration of the CEP. Its expression is significantly increased in degenerate CEP cells as compared to normal, and has been shown to increase the expression of matrix degrading enzymes, whilst simultaneously decreasing the expression of TIMP inhibitors (Yuan *et al.*, 2013). Additionally, the same study has identified that expression of endothelin-1 is modulated by TNF-α, highlighting further crossover between the activities of these degeneration-inducing molecules. A summary of the molecules whose expression is altered during IVD degeneration is illustrated in Table 1.2.

Table 1.2 A Summary of Molecules with Altered Expression During IVD Degeneration

Molecule	↑ or ↓	Proposed Role	Reference
Substance P	↑	Neurotransmitter of nociceptive pain	(Freemont *et al.*, 1997) (Richardson *et al.*, 2009)
NGF	↑	Innervation of the IVD	(Freemont *et al.*, 2002)
BDNF	↑	Innervation of the IVD	(Purmessur *et al.*, 2008)
PGP9.5	↑	Innervation of the IVD	(Tolofari *et al.*, 2010)
VEGF	↑	Neovascularisation	(Kokubo *et al.*, 2008)
CTGF	↑	Neovascularisation	(Ali *et al.*, 2008)
$P16^{INK4A}$	↑	Marker of cellular senescence	(Le Maitre *et al.*, 2007a)
SA β-galactosidase	↑	Marker of cellular senescence	(Le Maitre *et al.*, 2007a)
Caveolin-1	↑	Marker of stress-induced premature senescence	(Heathfield *et al.*, 2008)
MMPs 1, 8, 10, 13	↑	Collagen degradation	(Le Maitre *et al.*, 2004a) (Bachmeier *et al.*, 2009) (Richardson *et al.*, 2009)
MMPs 2, 9	↑	Degradation of denatured collagens	(Rutges *et al.*, 2008) (Millward-Sadler *et al.*, 2009)
MMPs 3, 28	↑	Degeneration of non-collagen ECM molecules	(Le Maitre *et al.*, 2004a) (Gruber *et al.*, 2009)
ADAMTS 1, 4, 5, 7, 9, 12, 15	↑	ECM molecule degradation	(Le Maitre *et al.*, 2004a) (Pockert *et al.*, 2009) (Yu and Zhu, 2011)
Cathepsins D, G, K, L	↑	Matrix molecule degradation	(Ariga *et al.*, 2001) (Gruber *et al.*, 2011) (Konttinen *et al.*, 1999)
IL-1α	↑	Promotion of disc inflammation and catabolism	(Le Maitre *et al.*, 2005)
IL-1β	↑	Promotion of disc inflammation and catabolism	(Le Maitre *et al.*, 2005)
IL-6	↑	Amplification of cellular response to cytokines	(Kang *et al.*, 1996)
TNF-α	↑	Promotion of disc inflammation and catabolism	(Le Maitre *et al.*, 2007b)
Endothelin-1	↑	Promotion of disc catabolism	(Yuan *et al.*, 2013)
Decorin	↑	Hydration of disc tissue	(Inkinen *et al.*, 1998)
Biglycan	↑	Hydration of disc tissue	(Inkinen *et al.*, 1998)
Type I collagen	↑	Formation of fibrous NP	(Adams and Roughley, 2006)
Type III collagen	↑	Association with type I collagen	(Nerlich *et al.*, 1997)
Type X collagen	↑	Tissue hypertrophy	(Boos *et al.*, 1997)
Semaphorin 3A	↓	Inhibition of IVD innervation	(Tolofari *et al.*, 2010)
MMP19	↓	COMP and collagen degradation + protective?	(Gruber *et al.*, 2005)
Type II collagen	↓	Providing normal NP ECM structure	(Adams and Roughley, 2006)
Aggrecan	↓	Hydration of disc tissue	(Sive *et al.*, 2002)
IL-1RA	-	Antagonist to IL-1α and –β	(Le Maitre *et al.*, 2005)

↑ = increased expression in degeneration; ↓= decreased expression in degeneration.

1.7.5 Degeneration in the Cervical IVD

Few studies have investigated the pathogenesis of disc degeneration in the cervical spine, and thus it is presumed that the degenerative process is similar to that occurring in the lumbar IVD. A number of morphological changes have been identified that mirror those in the lumbar IVD, including loss of NP PG content resulting in a loss of disc height and space, and metamorphosis of the NP to a more fibrous tissue (Liang *et al.*, 2011, Oda *et al.*, 1988). However, alterations to disc height were only characterised in a rodent model of degeneration, and the distinctions between human and rodent NP size, load and cellularity may make this

an unsuitable model from which to draw conclusions. Calcification of the CEP is observed, as well as the formation of new blood vessels in the previously avascular disc, although the utilisation of specimens solely obtained from herniated disc portions in these investigations does not consider alterations to the disc in earlier stages of degeneration, and a more comprehensive analysis of changes across the degenerative process is required (Baba *et al.*, 1997, Furusawa *et al.*, 2001, Kokubo *et al.*, 2008). Herniation of the disc is commonly observed, as well as the formation of both horizontal and vertical clefts and separation of the endplate (Furusawa *et al.*, 2001, Kokubun *et al.*, 1996). Fissures have also been demonstrated to develop within the annulus, in addition to increased cellular proliferation and osteophyte formation (Hayashi *et al.*, 1997). Laminar structure within the AF becomes less distinct, with some fragmentation (Wang *et al.*, 2006), whilst nutritional impairment is thought to result from calcification and mineralisation of the CEP. Degenerative changes in the cervical spine in the absence of clinical symptoms have been noted also, with 60% of subject aged over 40 years demonstrating narrowing of the disc space or degenerative changes including disc bulging, herniation or foraminal stenosis (Boden *et al.*, 1990). There is also evidence to suggest that degenerative changes occur in tandem in the cervical and lumbar IVD of asymptomatic individuals (Matsumoto *et al.*, 2012). A glaring omission of the data discussed here is the assessment of variation in cervical NP cell phenotype with ageing and degeneration. Generally, the literature presents findings with regards to gross morphological alterations, but little consideration is given to gene expression alterations. Given that NP cells synthesise the ECM in which they are localised, and that this ECM appears disrupted in terms of histological appearance, it should be expected that the gene expression of these components will alter with progressing degeneration. This would match with data previously reported in the lumbar IVD (Sive *et al.*, 2002).

In addition to these findings at the morphological level, a handful of studies have investigated molecular changes occurring in the cervical spine during degeneration. Areas of granulation tissue within the disc demonstrated increased MMP3 expression, as well as positivity for iNOS (Furusawa *et al.*, 2001). MMP3 has previously been demonstrated to be involved in breakdown of lumbar disc tissue (Bishop and Pearce, 1993), and decreased levels of its inhibitor TIMP1 is thought to aid the degenerative process (Kanemoto *et al.*, 1996). IL-1-induced inhibition of PG

synthesis involves induction of NO synthesis in articular cartilage (Furusawa *et al.*, 2001) and its upregulation in cervical disc degeneration could indicate its crucial role in the pathogenesis of the disease. As observed in lumbar disc degeneration, pro-inflammatory mediators have also been identified in degenerate cervical IVDs, including IL-6, IL-1β, TNF-α and interferon-γ (Demircan *et al.*, 2007, Kokubo *et al.*, 2008, Wang *et al.*, 2006), although comparisons to expression levels in lumbar specimens was not made. Additionally, with the exception of Kokubo *et al.*, variations with degeneration were not investigated in these studies, and where specimens were graded for their level of tissue degeneration, MRI-based methodologies were utilised which fail to detect minor alterations to the NP matrix noted in earlier stages of degeneration that would otherwise be identified using histological methods. A number of growth factors have also been identified in degenerate cervical discs, including VEGF, nerve growth factor (NGF), neurofilament-68 and growth-associated protein (GAP)-43 (Kokubo *et al.*, 2008). In one rat model, levels of the pro-inflammatory mediator prostaglandin-E2 were upregulated, whilst levels of the anti-apoptotic molecule Bcl-2 were downregulated, which may serve to explain the increased cell death via apoptosis observed during disc degeneration (Wang *et al.*, 2006). Forced upright posture in a rat model of IVD degeneration highlighted decreased type II collagen and aggrecan expression, whilst gene expression of MMPs -3 and -13 and ADAMTS5 were increased significantly compared to normal controls (Liang *et al.*, 2011). However, as previously discussed, the suitability of a rodent system for modelling degeneration in the human IVD suggests that full characterisation of MMP, ADAMTS, TIMP and cytokine expression is needed using human cervical specimens rather than animal IVDs. Finally, Col10α1 gene expression was also increased slightly indicating potential matrix calcification and terminal stage degeneration (Boos *et al.*, 1997). Thus, like lumbar disc degeneration, the process of degeneration in the cervical spine appears to also be a cell-driven process, with alterations to the ECM and increased expression of inflammatory mediators driving these changes.

Thus, previous investigations have failed to fully characterise cervical NP cells in terms of phenotype during degeneration, with regards to both the expression of ECM molecules and the expression of markers known to be upregulated in degenerate lumbar discs (matrix-degrading enzymes and catabolic cytokines). Therefore, the

assumption that the pathological processes occurring in the lumbar spine are mirrored in the cervical region has not yet been proven and further investigation is thus required.

1.8 The Adult Human NP Cell Phenotype

1.8.1 Classic Concept of the NP Phenotype

Classically, cells of the adult human NP were considered 'chondrocyte-like', in terms of both morphology and phenotype. This is due to the fact that they are small and rounded, and express chondrocyte markers Sox9, type II collagen and aggrecan (Sive *et al.*, 2002). However, the ECM produced by NP and hyaline cartilage cells is distinctly different, in terms of the ratio of PG to collagen (Mwale *et al.*, 2004). NP cells produce a matrix that has a PG:collagen ratio of 27:1, whilst the ratio in cartilage is only 2:1, and this therefore has implications for the hydration state and stiffness of the tissue. This therefore prompted detailed investigation into the phenotype of NP cells, with a view to identifying markers that will allow for accurate demarcation of NP and AC cells.

1.8.2 Elucidation of Novel Markers of the NP Phenotype

A number of microarray studies have been performed over recent years, all aiming to identify a panel of marker genes that will distinguish NP from AC cells (Lee *et al.*, 2007, Minogue *et al.*, 2010a, Minogue *et al.*, 2010b, Power *et al.*, 2012, Sakai *et al.*, 2009). cDNA microarray methodologies boast the advantages of allowing for determination of the expression levels of thousands of genes simultaneously and therefore also the possibility of identifying marker gene panels in a single experiment. A microarray investigation was undertaken using adult human AC and NP cells, and a number of differentially expressed genes were identified (Minogue *et al.*, 2010a) (Figure 1.11). Crucially, the genes identified in this investigation confirmed the findings of previous bovine analyses (Minogue *et al.*, 2010b), in that several of the novel markers were highly differentially expressed in both models, including FOXF1 and KRT18. Subsequent analysis of the human NP phenotype by Power *et al.*, further confirmed the expression of CAXII, previously described as an adult human NP marker, whilst also identifying cell-surface markers uniquely

expressed by NP cells as compared to AC, which ultimately may enable direct isolation of human NP cells. However, the search for novel NP markers is further complicated by the finding of conflicting evidence regarding the expression of some of the novel markers. Degenerate human NP and AF specimens were not shown to differentially express KRT18 (Rutges *et al.*, 2010), whilst KRT8 expression (previously demonstrated in bovine and human NP cells at the gene level) has not been fully described at the protein level, with expression to date only elucidated in a subset of bovine NP cells (Gilson *et al.*, 2010). This raises the possibility that the NP is comprised of NP cell sub-populations with differing cell phenotypes, but this requires further investigation using cohort of specimens spanning a range of ages and levels of tissue degeneration before such conclusions can be made.

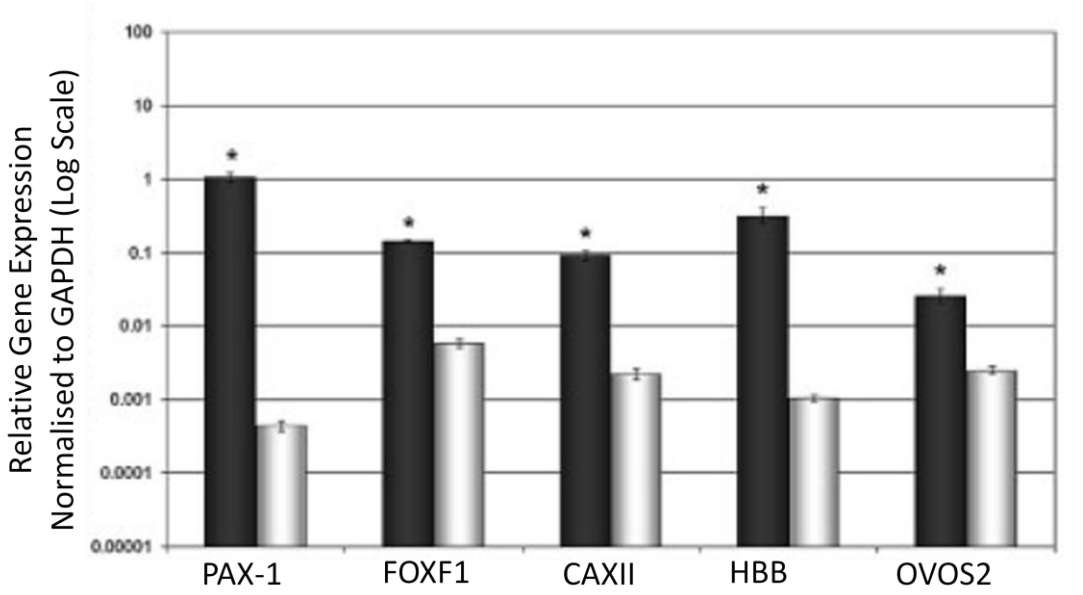

Figure 1.11 Differential expression of novel NP marker genes between human NP and AC cells. Expression levels of PAX-1, FOXF1, CAXII, HBB and OVOS2 were compared between human NP (black) and AC (grey) cells. *$p < 0.05$. Adapted from (Minogue *et al.*, 2010b).

A number of animal models were the initial model of choice for investigation, including dog (Sakai *et al.*, 2009) and rat (Lee *et al.*, 2007), although it should be noted that the canine model only compared phenotypic profiles of NP and AF cells, with distinctions between NP and AC cells made by RT-PCR analysis rather than microarray. Further study in a rabbit model analysing expression profiles of NP, AC and AF cells also highlighted genes that could be utilised in distinguishing the cell

types (Clouet *et al.*, 2009). In each, a panel of markers was identified that were differentially expressed between NP and AC/AF cells, confirming previous conclusions that although morphologically similar, NP and AC cells are distinct in terms of the genes expressed by each cell type (Mwale *et al.*, 2004, Poiraudeau *et al.*, 1999). A list of the novel NP markers identified by each microarray study is detailed in Table 1.3.

Table 1.3 The most differentially expressed NP genes as identified by microarray analysis in rodent, canine, bovine and human models.

Species Investigated	Gene Abbreviation	Confirmed in other models?	Gene or protein expression data?	Reference
Rat	KRT19	Bovine, human	Gene + protein	Lee *et al*., 2007 Minogue *et al*., 2010b
	ANXA3	-	Gene	Lee *et al*., 2007
	GPC3	-	Gene + protein	Lee *et al*., 2007
	PTN	-	Gene	Lee *et al*., 2007
	VIM	Human	Gene	Lee *et al*., 2007
Canine	KRT18	Bovine, human	Gene + protein	Sakai *et al*., 2009 Minogue *et al*., 2010b
	A2M	Human	Gene + protein	Sakai *et al*., 2009
	NCAM1/CD56	Bovine	Gene + protein	Sakai *et al*., 2009 Minogue *et al*., 2010b
	DSC2	Human	Gene + protein	Sakai *et al*., 2009
Bovine	KRT8	Human	Gene	Minogue *et al*., 2010b
	SNAP25	-	Gene	Minogue *et al*., 2010b
	CDH2	Human	Gene	Minogue *et al*., 2010b
	FOXF1	Human	Gene	Minogue *et al*., 2010b Minogue *et al*., 2010a
	BASP1	Human	Gene	Minogue *et al*., 2010b
Human	HBB	-	Gene	Minogue *et al*., 2010a
	OVOS2	-	Gene	Minogue *et al*., 2010a
	PAX1	-	Gene	Minogue *et al*., 2010a
	CAXII	-	Gene + protein	Minogue *et al*., 2010a Power *et al*., 2012
	CLEC2B	-	Gene	Power *et al*., 2012
	SGCG	-	Gene	Power *et al*., 2012
	TYRO3	-	Gene	Power *et al*., 2012

Adapted from (Ludwinski et al., 2013).

Inter-species variation was noted between the microarray investigations as the top differentially expressed markers identified in each study differed, and this implied that the identification of novel NP markers applicable to human cells would be

difficult. The use of animal models for investigations such as this is not necessarily appropriate because the NP of rodent, rabbit and some canine species are populated by NC cells, which appear to be lost from the tissue during infancy in humans, although it is unclear whether they are in fact lost, or have an altered morphology and persist in adult tissues. Thus, the differences between the animal and human microarray analyses may be attributed to the fact that NP microarray analysis was actually performed on tissues rich in NC cells rather than tissues resembling the adult human NP, which is primarily populated by smaller chondrocyte-like cells. In the canine microarray of Sakai *et al.*, Beagle breeds were utilised. These are a chondrodystrophic breed in which NC cells are lost and replaced by smaller chondrocyte-like cells, mirroring human development (unlike non-chondrodystrophic dogs which retain NC cells throughout life). No comparison of the two breed types was made, and thus it is not clear whether the data can be applied to all canine breeds. Additionally, although chondrodystrophic breeds such as beagles are considered more human-like in terms of NP cellularity, it is apparent from the immunohistochemical analysis of this investigation that the tissue was particularly NC cell-rich, and the markers identified may therefore be more applicable to NC cells rather than the smaller adult human NP-like cells. It is possible therefore that the NC cells employed in these investigations may also have distinct gene profiles as well as morphology as compared to that of the chondrocyte-like NP cells of the adult human IVD (Cappello *et al.*, 2006, Chen *et al.*, 2006, Choi *et al.*, 2008). An additional limitation of the previous animal investigations is that the majority of markers identified in the rodent microarray investigation were not subsequently confirmed in human specimens, and thus, the validity of these genes to mark adult human NP cells was not confirmed. Of the animal models investigated, the findings of the bovine microarray investigation appear to show the most overlap with markers of human NP/AF and AC cells. The similarities in expression profiles between the two models is unsurprising as unlike canine and rat, bovine discs provide a model where the structure, load and microenvironment is similar to that observed in the human spine (Miyazaki *et al.*, 2009, Showalter *et al.*, 2012). Additionally, a bovine model is advantageous over other animal models used in the study of the IVD, as it generally contains few morphologically distinct NC cells, with the cells populating the NP resembling those observed in the adult human NP, although it is yet to be investigated whether these smaller chondrocyte-like cells that

are thought to have derived from NC cells, still resemble NC cells with regards to phenotype.

1.8.3 The Influence of Ontogeny on NP Cell Phenotype

One of the most interesting findings of these investigations has been the expression of NC cell markers in cells of the adult human NP. KRT8, KRT18, KRT19 and T are genes expressed in the developing notochord which is considered to be the developmental origin of the mature NP (Gotz *et al.*, 1995, Gotz *et al.*, 1997b, Naka *et al.*, 1997, Vujovic *et al.*, 2006). These genes were shown to be highly expressed in NP cells when compared to AC/AF cells in a number of animal models (Lee *et al.*, 2007, Minogue *et al.*, 2010a, Minogue *et al.*, 2010b, Sakai *et al.*, 2009). Additionally, isolation of bovine NP and NC cells by size filtration and the subsequent analysis of cell expression profiles identified similarities in the genes expressed by the two cell types (Minogue *et al.*, 2010b). This is important for a number of reasons. Firstly, it suggests that the NC and NP cells share a common ontogeny, but may also be indicative of the persistence of a subset of NP cells within the adult NP cell population that resemble NC cells in terms of phenotype, but not morphology. Additionally, whether these cells are differentiated NC cells that have lost their morphology but retained an NC phenotype is unclear and therefore requires investigation.

1.8.4 The Possibility of a Resident Progenitor Cell Population in the Adult Human IVD

A number of studies have postulated that a resident progenitor/stem cell-like cell population exists within the intervertebral disc which may contribute to repair and regeneration of the tissue. A population of skeletal progenitor cells has been identified within both NP and AF tissues, which express stem cell markers including CD90, CD105 and CD166, and are able to differentiate into the classic mesenchymal stem cell lineages (Risbud *et al.*, 2007). Similarly, degenerate human NP specimens have been shown to contain a population of mesenchymal stem cells (MSCs), although the inability of these cells to differentiate down the adipogenic lineage raises the question of how MSC-like they are (Blanco *et al.*, 2010). Interestingly, it has been suggested that a stem cell niche exists at the boundary of the outer AF and adjoining ligaments of rabbit IVDs (Henriksson *et al.*, 2009, Yasen *et al.*, 2013).

Expression of progenitor markers Notch1, Stro-1, Jagged1 and Delta-4 has been localised to human degenerate tissue cells, although the potential of these to act as NP progenitor cells was not investigated (Henriksson *et al.*, 2009). The progenitor cell population identified at the outer AF/ligamentous boundary has since been described as a migrating cell population, intimating that the cells may possess an ability to respond to tissue damage and migrate to the site of injury (Henriksson *et al.*, 2012). The human CEP has also been shown to contain an MSC-like cell population that expresses MSC markers, although to a lesser degree than MSCs isolated from bone marrow (Liu *et al.*, 2011). The presence of a CEP progenitor cell population has since been confirmed by a second study (Huang *et al.*, 2012). More specific to the NP, a progenitor cell population has recently been identified as present within the human and murine NP (Sakai *et al.*, 2012); however, the numbers of these cells was also noted as markedly decreased with age in human specimens. Finally, a progenitor cell population has been identified within the canine NP, comprising just 1% of the total NP cell population, and expressing several markers of stemness, including Sox2, Oct3/4 and Nanog (Erwin *et al.*, 2013). Taken together, these findings indicate that a percentage of cells from each of the human IVD regions are stem cell-like with regards to phenotype and may therefore confer some regenerative capacity, which is likely diminished or ineffective with progressing tissue degeneration. Isolation of this cell population may identify a resident source of cells capable of regenerating the degenerate disc, although this first requires extensive validation. Additionally, these studies confirm previous investigations which suggest that the NP cell population is heterogeneous with regards to phenotype (Gilson *et al.*, 2010, Rutges *et al.*, 2010), although a more comprehensive analysis of NP cell populations and the possibility of NP cell sub-populations is required in order to ascertain whether human NP specimens spanning a range of ages and levels of tissue degeneration contain cell sub-populations which may act as a progenitor cell source within adult tissues.

1.9 Aims of the Project

The high prevalence of LBP and its association with degeneration of the IVD has prompted investigation into the development of novel cell-based therapies that aim to not only relieve the symptoms of LBP/degenerative disc disease, but also repair the aberrant cell biology and matrix loss that precedes the onset of such conditions. However, in order that the outcome of these approaches is most optimal, it is imperative that the cells intended for regeneration and/or replacement are fully characterised, both in terms of phenotype and behaviour. Recent years have seen an increased understanding of NP cell phenotype with regards to demarcation from articular chondrocyte cells; however, the data presented generally provides a phenotypic profile in terms of gene expression alone, and assessment only in small cohorts of human or animal specimens. Therefore, in order to obtain a detailed insight as to the NP cell phenotype across the general population, it is essential that such analyses are performed with specimens of a wide range of ages and severities of tissue degeneration. Furthermore, a limited amount of data exists that suggests that not only does the adult NP derive from the embryonic notochord, but that expression of NC cell markers in mature disc specimens is suggestive of NC cells persisting within the IVD past adolescence. However, the loss of morphologically distinct NC cells with ageing is not clear cut, and it is currently unknown whether these cells are indeed lost from the tissue, or whether they differentiate into smaller NP-like cells during infancy. If the cells do in fact differentiate, the mechanisms underlying this alteration require elucidation.

Given this, the present study was undertaken with a view to fully characterising cells of the adult human NP from both the cervical and lumbar region at the gene and protein level, and to provide an understanding of alterations to phenotype with age and degeneration, and to develop a model system that will allow for definition of the mechanisms underlying such changes. Evidence presented by previous studies is indicative of the existence of NP cell subpopulations within NP tissues, and it is therefore hypothesised that although all novel markers will be detected at the gene level, expression of these markers will be variable within the NP tissue when localised at the protein level. Additionally, the limited evidence highlighting the expression of NC cell markers within a subset of NP cells results in the hypothesis that a sub-population of NP cells will be identified within the NP that is discrete with

regards to their specific expression of NC cell markers as compared to other NP cells.

Therefore, the aims of this project were threefold:

1) To investigate the phenotype of the previously poorly defined cervical NP cell, in order to ascertain whether it would be a suitable tissue source for research purposes, thereby increasing the range of specimens available for analysis.
    a. To identify whether markers expressed by lumbar NP cells (chondrogenic and catabolic) are expressed by cells cervical in origin also, and to assess expression across ageing and increasing severity of degeneration.
    b. To compare the phenotype of lumbar and cervical NP cells in order to assess whether the gene expression profile is comparable.
2) To characterise the adult human NP cell with regards to gene and protein expression, in order to both validate previously described novel NP cell markers and to assess the expression of NC cell markers in adult specimens, with a view to determining whether NP cell sub-populations (including NC cell-like populations) exist.
    a. To assess the expression of novel NP and NC cell marker genes in adult human specimens, and to correlate expression with age and degeneration of the sample.
    b. To localise expression of a range of NP and NC cell marker proteins to adult human NP cells, and to correlate expression with age and degeneration of the sample.
    c. To assess co-expression of novel NP and NC cell marker proteins in NP cell sub-populations and identify whether discrete cell types exists in a heterogeneous population.
3) To establish an *in vitro* model system utilising animal cells suitable for the study of the hypothesised NC cell loss or differentiation during infancy in humans, with a view to elucidating the mechanisms underlying this.

a. To assess the suitability of NC cell-containing animal disc tissue for *in vitro* testing of the NC cell phenotype and morphological change.
b. To investigate the influence of microenvironmental factors on NC cell phenotypic and morphological maintenance.

Chapter 2:

General Materials and Methods

2.1 General Human Cell Culture

2.1.1 Equipment, Materials, Solutions and Supplements for Cell Culture

2.1.1.1 Equipment

Centrifuge for 50ml tubes; Universal 320	Hettich
Neubauer haemocytometer	Weber Scientific Int. Ltd.
Rotating Incubator	Hybaid

2.1.1.2 Materials

Cell culture flasks (T25, T75, T150)	Falcon
Cell sieves (40µm)	Fisher Scientific
Pipette tips (10µl, 200µl, 1ml)	Deckworks
Stripettes (5ml, 10ml, 25ml)	Costar
Tubes (15ml, 50ml)	BD Biosciences
24-blade scalpel blades	Swann Morton Ltd.

2.1.1.3 Solutions and Supplements

Antibiotic/antimycotic	Sigma Aldrich
Collagenase type II	Sigma Aldrich
Dulbecco's Modified Eagles Medium (DMEM)	Sigma Aldrich
Dulbecco's phosphate buffered saline (PBS)	Sigma Aldrich
Foetal bovine serum (FBS)	Gibco
Hyaluronidase	Sigma Aldrich
Sodium Pyruvate	Sigma Aldrich
Trypsin EDTA	Sigma Aldrich
Ascorbic acid sodium salts	Sigma Aldrich

2.1.2 IVD Sample Acquisition

An Intervertebral Disc Tissue Bank is in place at the University of Manchester, acquiring samples as surgical specimens from patients undergoing disc surgery for treatment of either disc herniation or IVD degeneration. Samples were obtained after informed consent was given by patients or relatives and in accordance with local ethical committee approval (08/H1010/36). After tissue was removed from the patient, it was placed in a 50ml centrifuge tube containing DMEM (containing 4500mg/L glucose, L-alanyl-L-glutamine, $NaHCO_3$ and pyridoxine HCl) supplemented with antibiotic and antimycotic (10,000U/ml penicillin, 10mg/ml streptomycin, 25µg/ml amphotericin B), 1mM sodium pyruvate and 1mM ascorbate (0.25g ascorbic acid sodium salts dissolved in 100ml dH_2O), stored at 4°C and transferred for use in the laboratory within 24 hours.

2.1.3 IVD Cell Isolation and Culture

2.1.3.1 Enzymatic Tissue Digestion

All aseptic cell culture techniques were practiced in a class II microbiological cabinet, ensuring sterility. NP cells were isolated from surgical specimens using enzymatic digestion. NP tissue was macroscopically dissected from AF tissue and mascerated into 1mm^3 pieces using a sterile 24-blade scalpel. The dissected tissue was then placed into a tube containing 25ml 0.1% (w/v) collagenase type II (125CDU/mg) and 0.1% (w/v) hyaluronidase (400U/mg) in serum-free DMEM (supplemented with antibiotic/antimycotic (10,000U/ml penicillin, 10mg/ml streptomycin, 25µg/ml amphotericin) and digested overnight at 37°C with agitation. The digestion solution was subsequently filtered through a 40µm cell sieve to remove undigested tissue, and cells centrifuged at 400g for 5 minutes at 4°C to pellet cells.

2.1.3.2 Cell Expansion and Maintenance

Pelleted cells were seeded into a T25 culture flask containing 5ml DMEM including Glutamax and 4500mg/L D-glucose (supplemented with 10% (v/v) FBS, 1mM sodium pyruvate, antibiotic/antimycotic (50,000U penicillin, 50mg streptomycin, 125µg amphotericin) and 1mM ascorbate) at a cell density of 20,000 cells/cm^2. Cells were then incubated at 37°C, 21% O_2, 5% CO_2 overnight to allow cells to adhere to the culture plastic. Culture media was then removed and replaced with fresh media to ensure the removal of non-adherent (dead) cells remaining in the flask. Following this, media was changed every 2-3 days until cells were 80% confluent. Cells were then removed from culture plastic through the application of 2ml Trypsin EDTA and incubation at 37°C for 5 minutes. Trypsin was neutralised with equal volumes of culture media, and cells centrifuged at 400g for 5 minutes to pellet cells for RNA extraction.

2.1.4 IVD Sample Details

2.1.4.1 Cervical NP Cohort

Table 2.1 Cervical NP Cohort Sample Details

Sample ID	Disc Level	Patient Age	Patient Sex	Degenerative Score
HH0069	C5/6 & C6/7	60	F	7
HH0102	C6/7	34	M	5
HH0109	C6/7	34	F	5
HH0111	C5/6	59	M	7
HH0139	C3/4	45	M	3
HH0140	C5/6	34	M	6
HH0156	C5/6	48	M	5
HH0217	C6/7	33	M	9
HH0236	C5/6	38	F	9
HH0250	C5/6	46	F	5
HH0262	C5/6	47	M	6
HH0265	C5/6	39	M	4
HH0271	C6/7	46	F	9
HH0315	C5/6	48	F	4
HH0318	C4/5	50	F	8
HH0347	C6/7	45	F	5
HH0351	C6/7	43	M	5
HH0353	C3/4	72	F	6
HH0354	C4/5	72	F	7
HH0362	C5/6	43	F	4
HH0364	C5/6	48	M	10
HH0388	C6/7	50	F	8
HH0402	C6/7	49	M	0
HH0410	C5/6	50	F	6
HH0420	C4/5	55	F	6
HH0421	C4/5	55	F	9
HH0427	C5/6	63	M	6
HH0448	C4/5	48	M	6

2.1.4.2 Lumbar NP Cohort

Table 2.2 Lumbar NP Cohort Sample Details

Sample ID	Disc Level	Patient Age	Patient Sex	Degenerative Score
HH0117	L4/5	23	M	6
HH0215	L4/5	58	M	10
HH0267	L4/5	48	F	5
HH0268	L5/S1	22	M	4
HH0272	L5/S1	27	F	8
HH0273	L5/S1	60	M	10
HH0281	L4/5	80	F	8
HH0283	L3/4	51	M	10
HH0285	L4/5	68	F	7
HH0291	L4/5	36	F	9
HH0292	L5/S1	26	M	6
HH0301	L4/5	65	F	6
HH0332	L4/5	75	F	9
HH0349	L4/5	41	M	8
HH0355	L5/S1	60	F	8
HH0359	L4/5	44	M	8
HH0360	L5/S1	26	F	6
HH0361	L4/5	44	F	8
HH0363	L5/S1	35	F	7
HH0386	L5/S1	38	F	11
HH0389	L5/S1	46	F	7
HH0395	L4/5	42	M	7
HH0404	L3/4	42	M	7
HH0416	L5/S1	46	M	8
HH0418	L4/5	25	M	7
HH0422	L4/5	25	M	6
HH0428	L5/S1	37	M	8
HH0430	L5/S1	40	F	10
HH0439	L5/S1	37	F	9
HH0440	L4/5	31	M	9
HH0442	L3/4	57	M	10
HH0445	L5/S1	37	F	7
HH0446	L4/5	31	M	7
HH0447	L5/S1	41	F	7

2.2 General Molecular Biology

2.2.1 Equipment, Materials, Reagents and Solutions for Molecular Biology

2.2.1.1 Equipment

Thermal Cycler	MJ Research
Nanodrop ND-1000	NanoDrop
Refridgerated centrifuge	Thermo Electron Corporation
StepOnePlus Real-Time PCR machine	Applied Biosystems
Vortex	Grant-Bio

2.2.1.2 Materials

Optical adhesive film for 96-well plates	Starlab
Positive displacement pipette tips (10µl)	Gilson
RNase-free tubes (0.5ml, 1.5ml, 2ml)	Axygen
RNase-free pipette tips (10µl, 200µl, 1ml)	Deckworks
96-well qPCR plates	Starlab

2.2.1.3 Reagents and Solutions

Ammonium acetate	Sigma Aldrich
DNase I buffer	Invitrogen
DNase I enzyme	Ambion
FAM-BHQ1 primers/probes	Sigma Aldrich
Glycoblue	Ambion
High-capacity reverse transcription kit	Applied Biosystems
Molecular biology-grade ethanol	Sigma Aldrich
Molecular biology-grade water	VWR
Phenol:Chloroform:IAA (25:24:1)	Sigma Aldrich
Pre-designed Assay Reagents for Internal Reference Gene Optimisation (PDAR)	Applied Biosystems
Propanol-2	Sigma Aldrich
Sodium chloride	Fisher Scientific
Sodium citrate	Sigma Aldrich
Total Human RNA	Clontech
Tri-Reagent	Ambion
Tris-EDTA buffer	Fluka
Whole Foetus RNA	Clontech
1-bromo-3-chloropentane	Sigma Aldrich
100x ROX	Sigma Aldrich
Lumino Ct qPCR Readymix	Sigma Aldrich

2.2.2 Total RNA Extraction

Cells were isolated from surgical specimens and expanded as detailed in 2.1.3. Cells were lysed upon the addition of 1ml Tri-Reagent to the pellet, which was pipetted up and down. The suspension was incubated at room temperature for 10 minutes, transferred to a 1.5ml microcentrifuge tube (MCT) and stored at -80°C prior to RNA

extraction. Following this, all work was performed under RNase-free conditions. After defrosting, cells were vortexed for 20 seconds, and then centrifuged at 12,000g for 15 minutes at 4°C to remove cell debris. The supernatant was transferred to a clean 1.5ml MCT and 100µl 1-bromo-3-chloropentane (BCP) added. An emulsion was formed by vortexing tubes for 20 seconds, and incubating at room temperature for 3 minutes. Samples were centrifuged at 12,000g for 15 minutes at 4°C to separate the RNA-containing aqueous phase from the phenol and protein in the interface and bottom layer. The upper aqueous phase was transferred to a fresh 1.5ml MCT, and 250µl high salt precipitation solution (HSPS) (0.8M sodium citrate, 1.2M NaCl), 250µl propanol-2 and 2µl glycoblue added, followed by incubation at room temperature for 10 minutes. Specimens were centrifuged at 12,000g for 20 minutes at 4°C to precipitate RNA and a visible blue RNA pellet formed. This pellet was washed in 1ml ice-cold 75% (v/v) ethanol and centrifuged for a further 5 minutes at 12,000g and 4°C. The ethanol was removed using a pipette and the pellet air-dried for approximately 10 minutes to allow evaporation of excess ethanol. Finally, RNA pellets were resuspended in 21.2µl Tris-EDTA buffer and stored at -80°C. Extracted RNA was quantified using a nanodrop ND-100 and ND-100 software v3.8.1, and specimens with an A260/280 ratio of 1.8 or higher were considered suitable for downstream gene expression analysis.

2.2.3 Removal of Genomic DNA Contamination from Extracted RNA

Quantified RNA was treated with DNase to ensure removal of genomic DNA contamination. One microlitre DNase I enzyme and 2µl DNase I reaction buffer was added to 20µl RNA and the reaction incubated at 37°C for 30 minutes. Samples were diluted to a total volume of 100µl upon addition of 77µl RNase-free water. RNA was extracted (and DNase I removed) by adding 100µl Phenol:Chloroform:IAA and vortexing to an emulsion. The samples were then centrifuged at 12,000g for 5 minutes at 4°C. The RNA-containing upper aqueous phase was transferred to a clean 1.5ml MCT and RNA was precipitated by adding 1µl glycoblue, 10µl ammonium acetate and 330µl 100% ethanol. MCTs were inverted to mix, incubated for 30 minutes on ice, and then centrifuged at 12,000g for 20 minutes at 4°C. A pellet was formed and supernatant removed, before washing the pellet in 1ml ice-cold 75% ethanol. MCTs were centrifuged at 12,000g for 5 minutes at 4°C and the supernatant

removed. MCTs were pulse-spun to draw down remaining ethanol, which was removed by pipette, and pellets left to air-dry for approximately 10 minutes. RNA pellets were then resuspended in 21.2µl Tris-EDTA buffer. RNA was quantified as detailed in 2.2.2 and stored at -80°C.

2.2.4 cDNA Synthesis from Extracted RNA

Samples with RNA concentrations above 200ng/µl were diluted to 200ng/µl. An assay mastermix was prepared on ice, containing 2µl 10x RT buffer, 0.8µl 25x 100mM dNTP mix, 2µl 10x random primers, 1µl Multiscribe^{TM} Reverse Transcriptase, 1µl RNase inhibitor and 3.2µl molecular biology-grade water per reaction. Ten microlitres of assay mastermix was added to 10µl extracted RNA in 0.5ml MCTs, and vortexed for 20 seconds to mix. Tubes were placed into the thermal cycler, and incubated at 25°C for 10 minutes, followed by 120 minutes at 37°C and 85°C for 5 seconds. Specimens were then incubated at 4°C until removed from the machine. cDNA was subsequently diluted to a concentration of 5ng/µl through the addition of molecular biology-grade water, and stored at -20°C.

2.2.5 qPCR Primer Design

Primers were designed against human gene sequences identified using PubMed Nucleotide. Where multiple transcript variants were identified, primers and probes were targeted to homologous regions across variants. Assays were designed to be intron-spanning, with either a primer or the probe sequences spanning the exon-exon boundary. A number of parameters were set in order to ensure optimal primer and probe efficiency:

1. Melting Temperature (Tm) – the Tm of primers was designed to be equal and fall within the 58-62°C range, whilst that of the probe was 10°C higher.

2. GC Content – GC-content was set between 30-80% for both primers and probes, and primers designed to contain more C bases than G.

3. Amplicon length – a maximum of 150 base pairs (bp) was used in the assay designs.

4. Primer lengths – primers were designed to be 15-30bp long.

5. GC Content at the 3' end – the 3' end of primers was designed to contain no more than 2 G or C bases in a total of 5.

6. Probe design parameters – probes were designed to be 13-25bp long, with no more than 3 repeating G bases, and no G base at the 5' end.

FAM-MGB probes contain a FAM-dye at the 5' end and a non-fluorescent quencher (NFQ) coupled with a minor groove binder (MGB) at the 3'. FAM-BHQ1 probes also contained a FAM-dye at the 5', but instead comprise of a black hole quencher (BHQ1) molecule located at the 3'. Both probe types are compatible with the TaqMan qPCR assay system. Once designed, all primer and probe sequences were analysed using PubMed BLAST software to ensure specificity to the mRNA of interest only.

2.2.6 Quantitative Real-Time Polymerase Chain Reaction

Gene expression analysis was performed using the TaqMan qPCR system. Either FAM-MGB or FAM-BHQ1 probes were utilised and optimal primer concentration determined empirically. Firstly, an assay mastermix was prepared, containing 5µl Lumino Ct qPCR Readymix, 1µl forward primer, 1µl reverse primer and 0.5µl probe, and 0.5µl water per well. Mastermix was vortexed to mix and 8µl pipetted into each well of the 96-well plate. Each biological sample was tested in triplicate (i.e. 3 wells) and 2µl of cDNA at a concentration of 5ng/µl pipetted into each well using a positive displacement pipette. For each gene tested, two wells of the plate served as negative controls, with cDNA replaced by 2µl molecular biology-grade water. Additionally, two wells were used as positive controls, where sample cDNA was replaced with 2µl of Total Human or Whole Foetus cDNA at 5ng/µl. Optical adhesive film was applied to seal the plate, and plates were centrifuged at 2000g for 60 seconds to ensure all reagents were drawn to the bottom of the well. The plate was analysed using the StepOnePlus Real Time PCR machine and StepOnePlus v2.1 software, and tested using the following parameters: 95°C for 20 seconds followed by 40 cycles of 95°C for 1 second and 60°C for 20 seconds. Optimised primer concentrations and primer/probe sequences are detailed in Table 2.3.

Table 2.3 Specific Details for qPCR Assays

Gene Name	Accession Number	Forward Primer Sequence 5'-3'	Reverse Primer Sequence 5'-3'	Probe Sequence 5'-3'	Optimal Primer Concentration
MRPL19	NM_014763	CACCGCCCCGTGGAA	TCCCCTTCGAGGAATGAATTC	AACGCAGGTTCTTGAGTC	900nM
EIF2B1	NM_001414	TCATCAAAGATGGAGCGACAATA	CCAGGACTCTCAGGACCACTCT	TGACTCACGCCTACTC	300nM
SOX9	NM_000346	CAGTACCCGCACTTGCACAAC	ACTTGTAATCCGGGTGGTCCTT	AGCTCTGGAGACTTCTGAA	900nM
COL2A1	NM_033150	GGAAGAGTGGAGACTACTGGATTGAC	TCCATGTTGCAGAAAACCTTCA	AGGCTGCACCTTGGA	900nM
ACAN	NM_001135	TCCGGAATGGAAACGTGAAT	CGGGAAGTGGCGGTAACAGT	AACTGCTGCAGACCAGG	900nM
VCAN	NM_004385	TGTGAGCAAGATACCGAGACATGT	ATTTGTAGCACTGCCCTTGGA	ACTATGGCTGGCACAAA	900nM
FOXF1	NM_001451	GCCGTATCTGCACCAGAACA	CGTTGAAAGAGAAGACAAACTCCTT	CTGCAAGGCATCCCG	900nM
PAX-1	NM_006192	ACCCCCGCAGTGAATGG	GGCCGACTGAGTGTATTTAATGTCT	CTAGAGAAACCTGCCTTAGA	900nM
KRT8	NM_002273	TGACCGACGAGATCAACTTCCT	TGGACAGCACCACAGATGTGT	CAGCTATATGAAGAGGAGATC	900nM
KRT18	NM_199187	GCGAGGACTTTAATCTTGGTGATG	TGGTCTTTTGGATGGTTTGCA	CAGCAGCAACTCC	900nM
KRT19	NM_002276	GGTCATGGCCGAGCAGAA	TTCAGTCCGGCTGGTGAAC	CGGAAGGATGCTGAAG	900nM
CAXII	NM_001218	CGTGCTCCTGCTGGTGATCT	AGTCCACTTGGAACCGTTCACT	AAAGGAACAGCCTTCCAG	900nM
IBSP	NM_004967	CCAGAGGAAGCAATCACCAAA	GCACAGGCCATTCCCAAA	AAGACTGCTTTAATTTTGCT	900nM
FBLN1	NM_006487	CCTTCGAGTGCCCTGAGAACTA	ACCGATGGCCTCATGCA	CAGCCACATGATCGTAG	900nM
NOTO	NM_001134462	AGTTGGAGAAAGTGTTTG	CTGCTTCTGATACTTGAC	AGACTCTCACGTGGTTCTCTGT	900nM
FOXJ1	NM_001454	GAGCAACTTCTTCCAGAA	CCTCCTCCGAATAAGTATG	CTGCGCTCTGAGCCAGGCAC	900nM
FOXA2	NM_021784	AGCAGCTACTATGCAGAG	GCTCATGTACGTGTTCAT	AGGGCTACTCCTCCGTGAGC	900nM
T	NM_003181	TTCTCCAACCTATTCTGACAACTCA	ATTCCAAGGCTGGACCAATTG	TTTATCCATGCTGCAATC	300nM
CHRD	NM_003741	CCGCTTCTCTATCTCCTA	GAGTGAGTGTCACAAGTG	CTAAGGAGCCGCAGAGACAACC	900nM
NOGGIN	NM_005450	AGCTATAGAGTTCAATGTTAT	GCACTTCTTTCTCATTTAC	ATAGAGAACAAATGGAATGACTAATCA	900nM
LGALS3	NM_001177388	CAGACAATTTTTCGCTCCATGA	GGCCATCCTTGAGGGTTTG	CGTTATCTGGGTCTGGAAA	900nM
CD24	NM_0013230	GCTCCTACCCACGCAGATTTAT	CCTTGGTGGTGGCATTAGTTG	CCAGTGAAACAACAAC	900nM
ADAMTS1	NM_006988	GCTCATCTGCCAAGCCAAAG	ATCTACAACCTTGGGCTGCAA	CATTGGCTACTTCTTC	900nM
ADAMTS4	NM_005099	ACTGGTGGTGGCAGATGACA	TCACTGTTAGCAGGTAGCGCTTT	ATGGCCGCATTCC	900nM
ADAMTS5	NM_007038	CAGCTGGGAGATGACCATGAG	CCCAACGTCTGCCATTCC	TTACTCGGGAGGATTTAT	900nM
ADAMTS8	NM_007037	TCCTGCTCACCAGACAGAACTTC	TCGATCACGGAGCAGCTTT	ATCGGGACCATTTGTGA	900nM
ADAMTS9	NM_182920	GCATTAACTCTGCCACTGACC	ATAGAAACTGCTGGCCGAAGG	TCCTCTTCCTCCTCTACCT	900nM
ADAMTS15	NM_139055	GAGTGACAAGCACCCCGAGTA	GTCACACATGGTACCCACATCAG	TCACCAGGCAGGACC	900nM
MMP1	NM_002421	GGAAAAGCAGCTCAAGAACAC	GAAGAGTTATCCCTTGCCTATCCA	CAGTCACTGGTGTCACC	900nM
MMP2	NM_004530	GCCCAAGAATAGATGCTGACTGT	GAGGGTTGGTGGGATTGGA	CCAGGCGCCCCTT	900nM
MMP3	NM_002422	ACAAAGGATACAACAGGGACCAA	CCAGGGAGTGGCCAATTTC	ATTTCTCGTTGCTGCTCA	900nM
MMP9	NM_004994	GGACGATGCCTGCAACGT	GTACTTCCCATCCTTGAACAAATACA	ATCTTCGACGCCATCG	900nM
MMP10	NM_002425	AGATGCATCAGGCACCAATTT	CAGGGAGTGGCCAAGTTCA	TTCCTCGTTGCTGCTC	900nM

MMP13	NM_002427	CCCCAGGCATCAC CATTCAAG	GACAAATCATCTT CATCACCACCAC	CTGCCTTCCTC TTC	900nM
IL-1α	NM_000575	ATGACGCCCTCAA TCAAAGTATAAT	TCAAATTTCACTG CTTCATCCAGAT	AGCCAATGAT CAGTACCT	900nM
IL-1β	NM_000576	CGGCCACATTTGG TTCTAAGA	AGGGAAGCGGTTG CTCATC	ACCCTCTGTCA TTCG	900nM
IL-R	NM_000877	AGGCTGATAAATG CAAGGAACGT	AGGACAGGGACGA ACATCAATT	TTTTAGTGTCA TCTGCAAATG	900nM
TNF-α	NM_000594	CGAACATCCAACC TTCCCAA	TGGTGGTCTTGTTG CTTAAAGTTC	CCAATCCCTTT ATTACCC	900nM
TNFR1A	NM_001065	CTCCTCTTCATTGG TTTAATGTATCG	CCCACAAACAATG GAGTAGAGCTT	TACCAACGGT GGAAGTC	900nM
TNFR1B	NM_001066	CGCTCTTCCAGTTG GACTGAT	ATGACACAGTTCA CCACTCCTATTATT AG	TGGGTGTGAC AGCCT	900nM
TIMP1	NM_003254	CTGACATCCGGTT CGTCTACAC	GTTGTGGGACCTG TGGAAGTATC	CCCGCCATGG AGAG	900nM
TIMP2	NM_003255	AGCATTTGACCCA GAGTGGAA	CCAAAGGAAAGAC CTGAAGGAA	CGTGGCCTATG CAGG	900nM
TIMP3	NM_000362	GCAGATAGACTCA AGGTGTGTGAAA	TCCCTCACTCTTAC ATGCAGACA	GTCCCAACCA GACTGTGT	900nM

2.2.7 Optimisation of Quantitative Real-Time PCR

2.2.7.1 Optimisation of Internal Reference Genes

A range of novel (RPLP0, β2-M, MRPL19 and EIF2B1) and classic (GAPDH and β-actin) qPCR internal reference genes were analysed in a small cohort of cervical (n=5) and lumbar (n=5) NP samples with varying levels of tissue degeneration to determine the most appropriate genes for this study (sample details in Table 2.4).

Table 2.4 Specimen Details for Optimisation of Internal Reference Genes

Sample ID	Age	Gender	Score	Classification
HH0063	58	M	5	Cervical Mildly Degenerate
HH0069	60	F	7	Cervical Degenerate
HH0070	59	M	7	Lumbar Mildly Degenerate
HH0081	47	M	6	Lumbar Mildly Degenerate
HH0082	48	M	10	Lumbar Degenerate
HH0095	48	F	9	Cervical Degenerate
HH0313	49	F	7	Cervical Mildly Degenerate
HH0327	27	F	5	Lumbar Mildly Degenerate
HH0329	52	F	12	Lumbar Degenerate
HH0384	47	F	6	Cervical Mildly Degenerate

An assay mastermix was prepared for each gene as follows: 5µl Lumino Ct qPCR Readymix, 2.5µl molecular biology-grade water and 0.5µl primer/probe set per well. As the primer/probe sets were pre-designed assay reagents (PDAR, Applied Biosystems), assays were performed according to manufacturer's instructions, and

thus no sequence information is available. Eight microlitres of assay mastermix was pipetted into each well of a 96-well plate using a positive displacement pipette, and 2µl target cDNA at a concentration of 5ng/µl also added. Each biological sample was repeated in triplicate and tested using the StepOnePlus Real-Time PCR machine as per the parameters outlined in 2.2.7. An average Ct value for each biological sample was determined and NormFinder software was used to establish the most appropriate reference genes for the cohort.

Stability values for each gene were determined by NormFinder. The lowest stability values are considered the most appropriate for use in qPCR. Table 2.5 details stability values for the genes tested.

Table 2.5 Stability Values for qPCR Reference Genes

Gene Name	Stability Value
β2-M	0.097
EIF2B1	0.103
GAPDH	0.114
MRPL19	0.129
RPLP0	0.172
β-actin	0.194

NormFinder software was then used to determine the best combination of 2 genes as the use of multiple internal reference genes increases the accuracy of reference gene expression levels and subsequently the normalised target gene expression values. A combined stability value of 0.076 defined β2-M and MRPL19 as the most appropriate combination. However, previous research has shown that β2-M expression in the human NP varies under differing loading conditions (Lee *et al.*, 2005). The next most stable combination (MRPL19, GAPDH, EIF2B1) was assessed. However, Ct values of cycle 16-18 were detectable for GAPDH, whilst MRPL19 and EIF2B1 were both detected at cycles 26-28. These differences in average Ct value meant fold-changes in target gene expression would be skewed by such large variations in average reference gene expression, and thus it was decided that the combination of MRPL19 and EIF2B1 was the most appropriate for this study.

2.2.7.2 Optimisation of qPCR Primer Concentrations

qPCR primer concentrations were optimised empirically to ensure reaction efficiency was between 95-105%. Reaction efficiencies were assessed at primer concentrations of 900nM, 600nM, 450nM and 300nM using an assay mastermix comprised of 5µl Lumino Ct qPCR Readymix, 1µl forward primer, 1µl reverse primer, 0.5µl 2.5µM probe and 0.5µl molecular biology-grade water. A five-fold serial dilution of either control total human cDNA or whole foetus cDNA (both reverse transcribed to cDNA in house from stock RNA) at 12.5ng/µl, 2.5ng/µl and 0.5ng/µl (diluted in molecular biology-grade water) was generated, with each primer concentration tested in triplicate repeats of each of the cDNA concentrations. A positive displacement pipette was used to add 8µl assay mastermix and 2µl cDNA to each well. Negative control wells contained 2µl molecular biology-grade water in place of cDNA. Plates were analysed using the StepOnePlus Real-Time PCR machine with the parameters detailed in 2.2.6. Standard curves were generated by plotting log cDNA concentration vs. average Ct value (at each cDNA concentration), and reaction efficiencies determined using StepOnePlus software. Specific details for each qPCR assay are detailed in Table 2.3.

2.2.8 Data Analysis

qPCR data was analysed according to the ΔCt method in accordance with the method outlined by (Livak and Schmittgen, 2001, Minogue *et al.*, 2010a, Minogue *et al.*, 2010b) where gene expression values are normalised to that of internal reference genes. A number of calculations were subsequently performed to obtain values to be used for graphs and statistical analysis, detailed in Table 2.6.

Table 2.6 Calculations for qPCR Analysis

Value Determined	Calculation
Average Ct of sample	Average of triplicate repeat
ΔCt of sample average	Average Ct (target gene)- Average Ct (ref. gene)
Standard error of the mean (SE)	STDEV((average ΔCt)/SQRT(n))
2-ΔCt	2^-(ΔCt average)
+ Standard error	2^-(ΔCt average +SE)
- Standard error	2^-(ΔCt average -SE)
+ Error bars	(-SE)- 2-ΔCt
- Error bars	2-ΔCt – (+SE)

2.2.9 Statistical Analysis

All statistical analysis was performed using GraphPad InStat and GraphPad prism software and Mann Whitney-U tests were employed where significance was defined as $p<0.05$.

2.3 General Histology

2.3.1 Equipment, Materials, Reagents and Solutions

2.3.1.1 Equipment

Vacuum oven	Binder
Histostation Embedding Centre	Thermo Electron Corporation
Rotary microtome	Thermo Scientific
Tissue processor	Thermo Electron Corporation

2.3.1.2 Materials

Positively charged microscope slides	Thermo Scientific
22x40mm glass coverslips	Scientific Laboratory Supplies
Histology cassettes	Surgipath

2.3.1.3 Reagents and Solutions

Avidin-biotin complex solution (ABC)	Vector
Bovine serum albumin	Sigma Aldrich
Citric acid anhydrous	Sigma Aldrich
Eosin	Surgipath
Ethylenediaminetetraacetic acid (EDTA)	Sigma Aldrich
Glacial acetic acid	Fisher Scientific
Hydrochloric acid	Fisher Scientific
Industrial methylated spirits (IMS)	Fisher Scientific
Mayer's haematoxylin	Solmedia
Normal goat serum	Sigma Aldrich
Normal donkey serum	Sigma Aldrich
Paraffin wax for embedding	Thermo Scientific
Paraformaldehyde	Sigma Aldrich
Pepsin from porcine gastric mucosa	Sigma Aldrich
Phloxin B	BDH
Phosphate buffered saline tablets (non-sterile)	Oxoid
Pronase protease	Calbiochem
Shandon consul mountant	Thermo Scientific
Sodium chloride	Fisher Scientific
Tris base	Fisher Scientific
Xylene	Fisher Scientific
3,3'-diaminobenzidine tetrahydrochloride (DAB)	Sigma Aldrich
30% (v/v) Hydrogen peroxide	Fisher Scientific

2.3.2 Tissue Fixation

Prior to processing of tissue specimens (as detailed in 2.1.3), a portion of each specimen containing both AF and NP tissue was washed twice in sterile PBS to remove traces of blood and culture media, and fixed for 24 hours in 25ml 4% (w/v) paraformaldehyde in PBS at 4°C. Fixed tissue was washed twice in PBS to remove excess fixative and stored at 4°C prior to processing.

2.3.3 Processing of Fixed Tissue Specimens

Tissue specimens were placed inside a histology cassette and processed on the Thermo Electron Tissue Processor overnight under the following parameters:

50% IMS	90 minutes
70% IMS	60 minutes
99% IMS	60 minutes
99% IMS	60 minutes
99% IMS	60 minutes
99% IMS	60 minutes
99% IMS	60 minutes
Xylene	90 minutes
Xylene	90 minutes
Xylene	90 minutes
Molten wax	90 minutes
Molten wax	120 minutes

Following completion of the processing programme, cassettes were transferred to molten wax under vacuum for 30 minutes to allow for thorough penetration of the wax in the tissue. Samples were then embedded using the Histostation Embedding Centre.

2.3.4 Haematoxylin and Eosin Staining

Five micrometre sections of wax-embedded tissue specimens were cut using a rotary microtome, and briefly floated in a waterbath at 42°C to allow the sections to flatten prior to mounting on positively charged microscope slides. Slides were placed on a hot plate at 37°C for two hours to allow for evaporation of excess water, and then

dried in a drying oven at 37°C for at least 48 hours. Before commencing the staining protocol, slides were baked on a hot plate set at 60°C to remove air bubbles trapped under the wax. Slides were subsequently dewaxed in xylene for 3x 5 minutes and rehydrated in 100% IMS for 4x 5 minutes. Sections were stained in freshly filtered Mayer's haematoxylin for 60 sections, and excess haematoxylin removed by washing slides in running tap water for 5 minutes. Slides were stained in eosin for 1 second, before dehydrating in IMS for 4x 5 minutes. Finally, sections were cleared in xylene for 3x 5 minutes, and covered using a 20x40mm glass coverslip and Shandon Consul mountant.

2.3.5 Histological Grading of Specimens for Level of Degeneration

Using the haematoxylin and eosin stained slides; specimens were graded histologically for their level of IVD degeneration in accordance with a previously established method (Sive *et al.*, 2002). A histopathologist (Professor A. Freemont) analysed four individual tissue features (loss of AF/NP demarcation, loss of NP proteoglycan, presence and extent of fissures and cell cluster formation) and awarded a score of 0-12 as detailed in Table 2.7.

Table 2.7 Histological Grading System for IVD Degeneration

Breakdown of the four groups of parameters used for the scoring system	
Loss of demarcation between the NP and AF	
0	Clear demarcation
1	Limited loss of demarcation
2	Substantial loss of demarcation
3	Complete loss of demarcation
Loss of proteoglycan from the NP	
0	No loss of haematoxophilia
1	Limited loss of haematoxophilia
2	Substantial loss of haematoxophilia
3	Complete loss of haematoxophilia
Presence and extent of fissures	
0	No fissures
1	Fissures present within NP
2	Fissures extending to NP/AF junction
3	Fissures extending to within AF
Cell cluster formation	
0	No cell clusters
1	<25% of cells formed into clusters
2	25-75% of cells formed into clusters
3	>75% of cells formed into clusters

Adapted from (Sive et al., 2002).

2.3.6 Immunohistochemistry

Five micrometer tissue sections were prepared as detailed in 2.3.4. Slides were dewaxed in xylene for 3x 5 minutes, and rehydrated in 100% IMS for 4x 5 minutes. Slides were then rinsed in deionised water to remove excess IMS. Where enzyme-only antigen retrieval was utilised, endogenous peroxidases were then blocked by immersing slides in 100% IMS containing 0.3% (v/v) H_2O_2 and 25mM HCl for 30 minutes at room temperature. Slides were then rinsed in TBS (50mM Tris-EDTA, 150mM NaCl) for 2x 5 minutes before performing antigen retrieval (as determined empirically). Where a heat-induced epitope retrieval technique was used, antigen retrieval was performed prior to blocking of endogenous peroxidases, with slides rinsed in TBS for 2x 5 minutes between the two steps. Following antigen retrieval and blocking of endogenous peroxidases, non-specific binding was blocked by the incubation of sections in the appropriate 25% animal serum in 1% BSA in TBS for 30 minutes at room temperature. Serum/BSA/TBS solution was removed from slides and the antibody diluted in 1% BSA in TBS (dilution determined empirically) applied to each section, and incubated overnight at 4°C in a humidified chamber.

Negative control sections containing appropriate IgG diluted in 1%BSA in TBS rather than primary antibody (but at an equivalent working concentration to the antibody) were used. Following overnight incubation, slides were rinsed in TBS for 3x 5 minutes and then incubated with an appropriate secondary antibody diluted 1:300 in 1% BSA in TBS for 30 minutes at room temperature. Slides were again rinsed in TBS for 3x 5 minutes and incubated with Avidin-Biotin Complex (ABC) reagent for 30 minutes at room temperature. Slides were again rinsed in TBS for 3x 5 minutes, and 3,3'-diaminobenzidine tetrahydrochloride (DAB) applied to each section, and incubated at room temperature for 20 minutes. Sections were rinsed in deionised water for 4 minutes and stained in freshly filtered Mayer's haematoxylin for 60 seconds. Excess haematoxylin was removed by washing slides in running tap water for 5 minutes. Finally, sections were dehydrated in 100% IMS for 4x 5minutes, cleared in xylene for 3x 5 minutes and glass coverslips applied and fixed using Shandon consul mountant. Assay specific parameters (serum, primary antibody/IgG details, antigen retrieval technique and secondary antibody details) are listed in Table 2.8. Additionally, 5μm sections of human foetal spine (aged 8 weeks post-conception) obtained under local ethical approval (08/H1010/28) were stained for all antibodies tested, in order to confirm that the notochordal cell markers investigated were in fact expressed in human notochordal cells.

Table 2.8 Assay Specific Parameters of Immunohistochemical Analysis

Primary Antibody	Primary Antibody Dilution	IgG Isotype Control	Positive Control Tissue	Blocking Serum	Epitope Retrieval Method	Secondary Antibody
Brachyury (Abcam ab57480)	1:10	Mouse IgG type 1 (Sigma M5284)	Chordoma	Goat	0.25% pepsin	Goat anti-mouse (Santa Cruz sc-3795)
Carbonic Anhydrase-12 (Sigma HPA008773)	1:50	Rabbit IgG (Dako X0936)	Kidney	Goat	Pressure cooker with citrate buffer	Goat anti-rabbit (Santa Cruz sc-3840)
CD24 (AbCam ab31622)	1:50	Mouse IgG type 1 (Sigma M5284)	Chordoma	Goat	Steamer with citrate buffer	Goat anti-mouse (Santa Cruz sc-3795)
Cytokeratin-8 (Zytomed 603-2156)	1:10	Mouse IgG type 1 (Sigma M5284)	Skin	Goat	0.25% pepsin followed by 0.1% pronase	Goat anti-mouse (Santa Cruz sc-3795)
Cytokeratin-18 (Dako M7010)	1:20	Mouse IgG type 1 (Sigma M5284)	Skin	Goat	0.25% pepsin followed by steamer with Tris/EDTA buffer	Goat anti-mouse (Santa Cruz sc-3795)
Cytokeratin-19 (Dako M0888)	1:10	Mouse IgG type 1 (Sigma M5284)	Skin	Goat	0.25% pepsin followed by steamer with Tris/EDTA buffer	Goat anti-mouse (Santa Cruz sc-3795)
FoxF1 (Santa Cruz sc-47591)	1:35	Goat IgG (R&D Systems AB-108-C)	Kidney	Donkey	0.25% pepsin	Donkey anti-goat (Santa Cruz sc-2042)
Galectin-3 (Santa Cruz sc-20157)	1:20	Rabbit IgG (Dako X0936)	Chordoma	Goat	0.25% pepsin followed by 0.1% pronase	Goat anti-rabbit (Santa Cruz sc-3840)
Pax-1 (Abcam ab114037)	1:600	Rabbit IgG (Dako X0936)	Placenta	Goat	Pressure cooker with citrate buffer	Goat anti-rabbit (Santa Cruz sc-3840)

2.3.7 Optimisation of Immunohistochemical Antibodies

All immunohistochemical antibodies required optimisation prior to use in this study, and the protocol followed is described in 2.3.6. For each antibody used, a positive control tissue was identified and 5µm sections mounted as detailed in 2.3.4. The tissue selected for analysis of each protein is listed in Table 2.8. For each assay, optimisations were conducted using 1x control tissue section and 1x adult IVD tissue

section for each antibody dilution assessed, and 1x control section/1x adult IVD section as a negative control. These quantities were repeated for each of the antigen retrieval methods tested. For the first set of optimisations for each antibody, 3 methods of epitope retrieval were assessed: enzymatic, heat-induced, and a combination of enzymatic and heat-induced. Experimental details of each enzymatic methodology and heat-induced antigen retrieval method are outlined in 2.3.7.1 and 2.3.7.2 respectively. Initially, antibodies were tested at dilutions of 1:10, 1:20, 1:50 and 1:100, with equivalent concentration of the appropriate IgG used as negative controls. Details of each antibody and the IgG utilised are listed in Table 2.8. The dilution of secondary antibody remained constant throughout at 1:300, but the antibody used varied according to the primary antibody host, and is clarified in Table 2.8. Where the initial optimisation did not identify an appropriate method of epitope retrieval, techniques were modified by altering either the buffer used in heat-induced retrieval methods, or the time allocated for retrieval. If intense staining of sections was detected even at a primary antibody dilution of 1:100, further tests were performed, diluting the antibody at 1:200, 1:300, 1:400 and 1:500.

2.3.7.1 Enzymatic Antigen Retrieval Methodologies

0.25% pepsin digestion:

0.25% pepsin (97066U/g) (w/v) was reconstituted in 10mM ice-cold HCl. Once dissolved, 150µl enzyme solution was applied to each tissue section and incubated at room temperature for 10 minutes.

0.1% pronase digestion:

0.1% pronase (3200U/mg) (w/v) was diluted in TBS pH 7.4 (50mM Tris-EDTA, 150mM NaCl). Once reconstituted, 150µl enzyme solution was applied to each tissue section and incubated at 37°C for 10 minutes.

2.3.7.2 Heat-Induced Antigen Retrieval Methodologies

Steamer retrieval:

Upon addition of 1L deionised water to the water compartment of the steamer, the apparatus was pre-heated for 10 minutes. Simultaneously, 800ml 10mM citrate buffer pH 6.0 (10mM citric acid) or 800ml Tris/EDTA buffer pH 9.0 (10mM Tris Base/1mM EDTA) was heated to 95°C in the microwave before transferring to the steamer and allowing the temperature to equilibrate for a further 5 minutes. Slides were then incubated in the buffer for 10 minutes, and following this, the basket containing the buffer/slides was removed from the steamer and placed on the bench for a further 10 minute incubation.

Pressure cooker retrieval:

Two litres citrate buffer pH 6.0 or Tris/EDTA buffer pH 9.0 was heated in the pressure cooker to for approximately 15 minutes until boiling. Slides were then placed into the chamber and the lid closed. Once pressure was reached, slides were subject to heating for 3 minutes. Following this, the chamber was removed from the heat and placed in running tap water until depressurised. The lid was then removed, and tap water run into the chamber for 10 minutes to cool the slides.

2.3.8 Image Analysis

All histological analysis was undertaken using a Leica Leitz DMRB Microscope, images obtained using an Infinity X digital camera DeltaPix camera software, and images prepared using ImageJ software.

Chapter 3:

The Adult Human Cervical Nucleus Pulposus Cell Phenotype

3.1 Background

Like LBP, chronic neck pain is a highly prevalent condition in developed societies (Makela *et al.*, 1991). However, unlike disorders of the lumbar spine, the cervical IVD and its associated pathologies are less well characterised. Features of IVD degeneration have also been identified in cervical discs (Christe *et al.*, 2005, Kolstad *et al.*, 2005), but the underlying aetiology of this degenerative process in the cervical region has not been comprehensively described, and it is often just assumed that the pathology mirrors that of the lumbar IVD.

Such an assumption may be flawed in that although the ontogeny of IVDs from both the cervical and lumbar region is identical, several distinctions exist between discs from the upper and lower human spine with regards to tissue matrix, load and anatomy. Compared with the lumbar spine, the cervical spine is weak with regards to flexion, with lumbar specimens resisting 35Nm in flexion, and cervical only 6.7Nm, suggesting that cervical discs have the capacity to withstand only 20% of the flexion strength of lumbar samples (Adams and Dolan, 1991, Przybyla *et al.*, 2007). This is also seen in extension, with cervical segment strength only 34% of that observed in the lumbar (Przybyla *et al.*, 2007). However, one of the limitations of this study is that only discs from patients aged 64+ were assessed, and although differences were noted between these findings and that reported for lumbar specimens, the authors failed to address whether this could be linked to the age of the samples. The extra strength observed in extension as compared to flexion is attributed to the large cervical apophyseal joints, which provide resistance to extension. The average compressive strength of cervical motion segments was 2.4kN, which is 45% of that observed in the lumbar region, and this is hypothesised to be due to decreased endplate area, with cervical endplates only 22% of the size of lumbar (Brinckmann *et al.*, 1989, Hutton and Adams, 1982, Przybyla *et al.*, 2007). Thus, the literature suggests that discs of the cervical and lumbar spine differ significantly in their mechanical properties; a feature which may affect cell phenotype within the region. As discussed in 1.3.2, disc structure also varies according to whether it is located within the cervical or lumbar spine. Briefly, disc diameter is markedly smaller in cervical IVDs as compared to lumbar, whilst the AF is crescentric in shape and only partially surrounds the NP (Mercer and Bogduk, 1999, Pooni *et al.*, 1986).

Currently, literature comparing the expression of matrix markers in cervical and lumbar IVD specimens is limited. It has been demonstrated that in primate discs, no distinctions exist between disc levels with regards to protein expression of types I and II collagen (Longo *et al.*, 2006), although no such comparison has been made utilising human specimens. However, gene expression analysis of human cervical and lumbar NP cells where degeneration has been induced following cytokine exposure demonstrated significantly higher expression levels of type I and II collagen in cervical as compared to lumbar discs (Park *et al.*, 2013). Interestingly, the same study identified that mRNA levels of aggrecan, alkaline phosphatase, osteocalcin and Sox9 did not differ significantly between lumbar and cervical specimens after growth factor and cytokine treatment, which indicates that cells from the two spinal regions may be similar with regards to phenotype. Thus, analysis of the existing literature has identified a clear requirement for elucidation of NP ECM marker expression in cervical discs and a comparison of this expression to that of lumbar specimens in human tissues. Additionally, expression of molecules associated with degeneration has been described briefly in the cervical IVD (detailed in section 1.6.2); however, no study has yet to comprehensively analyse expression of these markers (MMPs, ADAMTSs, TIMPs, pro-inflammatory cytokines) in the cervical NP, and compared it to that of lumbar samples. Given that distinctions exist between discs of the two spinal regions with regards to their anatomy, structure and load-bearing characteristics, it is possible that there may also be distinctions with regard to phenotype. Also, age and degeneration-associated alterations to the NP phenotype are well described in the lumbar IVD (see section 1.6), and it is therefore possible that such changes also occur in the cervical disc. However, understanding changes that occur to the cervical IVD with age and degeneration is limited by the scarcity of literature in which this is described as compared to the lumbar IVD. Thus, this investigation is being undertaken with a view to gaining an in-depth knowledge of cervical NP cell phenotype and IVD degeneration.

Additionally, a full comparison of cervical and lumbar NP cells with regards to matrix and degeneration-associated molecule expression may expand the number of human specimens available for research purposes, as currently, much of the literature focuses on lumbar tissues which are more comprehensively described. If cervical and lumbar tissues are in fact shown to be similar with regards to gene expression and

degeneration, it is possible then that tissues from the two spinal regions can be used interchangeably for research purposes.

3.2 Aims and Hypotheses

As discussed, the current understanding of the cervical NP cell phenotype is limited. Although various studies have noted expression of a handful of markers previously described as expressed in the lumbar IVD, no study has yet evaluated the cervical NP cell gene expression profile across a range of ages and levels of tissue degeneration, nor has it been established whether a comprehensive list of genes expressed during lumbar disc degeneration are also expressed by cervical NP cells. In order that cervical IVD specimens can be utilised for research of both LBP and chronic neck pain, a comparison of lumbar and cervical NP cell phenotypes must be made. Although evidence comparing cervical and lumbar IVDs is limited, some data has been presented which suggests that differences exist between the two regions, and it is therefore hypothesised that some significant differences will be noted between lumbar and cervical NP cell gene expression profiles.

Therefore, the aims of this study were twofold:

1) To assess whether cervical NP cells express markers previously described in lumbar NP specimens, and to assess expression across a range of ages and degenerative scores, with a view to characterising the cervical NP cell phenotype more fully.
2) To compare the phenotype of lumbar and cervical NP cells, with a view to determining whether cervical NP cells are comparable to those that are lumbar in origin in terms of gene expression.

3.3 Experimental Design

The adult human cervical NP cell phenotype was investigated by means of extensive gene expression analysis, assessing variations with ageing and degeneration, and a comparison of cervical and lumbar gene expression levels performed.

3.3.1 Tissue Histology and Morphological Characterisation

Tissue specimens detailed in Table 2.1 and 2.2 were fixed, processed and wax-embedded as detailed in sections 2.3.2 and 2.3.3. Sections were stained with H&E (protocol outlined in 2.3.4.) to characterise tissue structure and morphology, and samples assessed for histological features of IVD degeneration, used previously to grade lumbar specimens for their level of tissue abnormalities (Sive *et al.*, 2002). All image analysis was performed as detailed in 2.3.8.

3.3.2 Gene Expression Characterisation of Cervical NP Cells

The expression levels of a number of genes were assessed using RNA obtained from adult human cervical NP cells (sample details in Table 2.1) using quantitative real-time PCR, as outlined in sections 2.2.6, and 2.2.7, with cDNA generated from extracted total RNA using the protocols in 2.2.2, 2.2.3 and 2.2.4. These were categorised as classic chondrogenic genes: SOX9, COL2A1, ACAN and VCAN; catabolic enzymes: MMP1, MMP2, MMP3, MMP9, MMP10, MMP13, ADAMTS1, ADAMTS4, ADAMTS5, ADAMTS8, ADAMTS9 and ADAMTS13; inhibitors of catabolic enzymes: TIMP1, TIMP2 and TIMP3; pro-inflammatory cytokines and receptors: IL-1α, IL-1β, IL-1R, TNFα, TNFR1A and TNFR1B; and internal reference genes: MRPL19 and EIF2B1. Primer sequences are detailed in Table 2.3. Gene expression values were normalised to that of the internal reference genes, and analysed according to the 2-ΔCt method (Livak and Schmittgen, 2001). Mann Whitney-U tests were performed using GraphPad InStat and significance defined as $p<0.05$.

3.3.3 Comparison of Lumbar and Cervical Gene Expression Profiles

Gene expression data was further scrutinised through comparison of expression levels in lumbar and cervical NP specimens. Specimens were categorised according to their histological grade of degeneration: non-degenerate, moderately degenerate and severely degenerate. Non-degenerate tissues were defined as histological grades 0-4; moderately degenerate as 5-7; and severely degenerate as grades 8-12. Gene expression levels were compared between whole lumbar and cervical cohorts, lumbar and cervical moderately degenerate, and lumbar and cervical severely degenerate specimens (details in Tables 3.1 and 3.2), and statistical significance assessed as outlined in 3.3.2.

Table 3.1 Details of Lumbar and Cervical Moderately Degenerate NP Samples

Cervical NP (n=16)		**Lumbar NP (n=15)**	
Sample ID	Grade	Sample ID	Grade
HH0069	7	HH0117	6
HH0102	5	HH0267	5
HH0109	5	HH0285	7
HH0111	7	HH0292	6
HH0140	6	HH0301	6
HH0156	5	HH0360	6
HH0250	5	HH0363	7
HH0262	6	HH0389	7
HH0347	5	HH0395	7
HH0351	5	HH0404	7
HH0353	6	HH0418	7
HH0354	7	HH0422	6
HH0410	6	HH0445	7
HH0420	6	HH0446	7
HH0427	6	HH0447	7
HH0448	6		

Table 3.2 Details of Lumbar and Cervical Severely Degenerate Samples

Cervical NP (n=7)		**Lumbar NP (n=17)**	
Sample ID	Grade	Sample ID	Grade
HH0217	9	HH0215	10
HH0236	9	HH0272	8
HH0271	9	HH0273	10
HH0318	8	HH0281	8
HH0364	10	HH0283	10
HH0388	8	HH0291	9
HH0421	9	HH0332	9
		HH0349	8
		HH0355	8
		HH0359	8
		HH0386	11
		HH0416	8
		HH0428	8
		HH0430	10
		HH0439	9
		HH0440	9
		HH0442	10

3.4 Results

3.4.1 Histological Features of Degeneration in the Cervical IVD

Specimens stained with haematoxylin and eosin were assessed histologically for features of the degenerate IVD and graded for the severity of tissue degeneration accordingly. The criteria utilised in the method of grading discs (outlined by (Sive *et al.*, 2002)) relies on analysis of four individual characteristics: the presence and number of cell clusters; the presence and severity of fissures; the clarity of demarcation between the NP and AF tissues; and loss of proteoglycan content from the NP ECM, and has previously only been used on lumbar IVD tissues. Figure 3.1 demonstrates identification of the same features in IVD specimens taken from the cervical region. Cell clusters were localised within the NP (Figure 3.1D), and fissures extending into the NP tissue from the AF were also noted (Figure 3.1A). A reduction in the demarcation between the NP and AF could be seen (Figure 3.1B), as well as a loss of proteoglycan within the NP, evident as a loss of haemotoxyphilia in the matrix (Figure 3.1C). Such features confirm the validity of this method for histological grading of morphological features of IVD degeneration in the cervical spine.

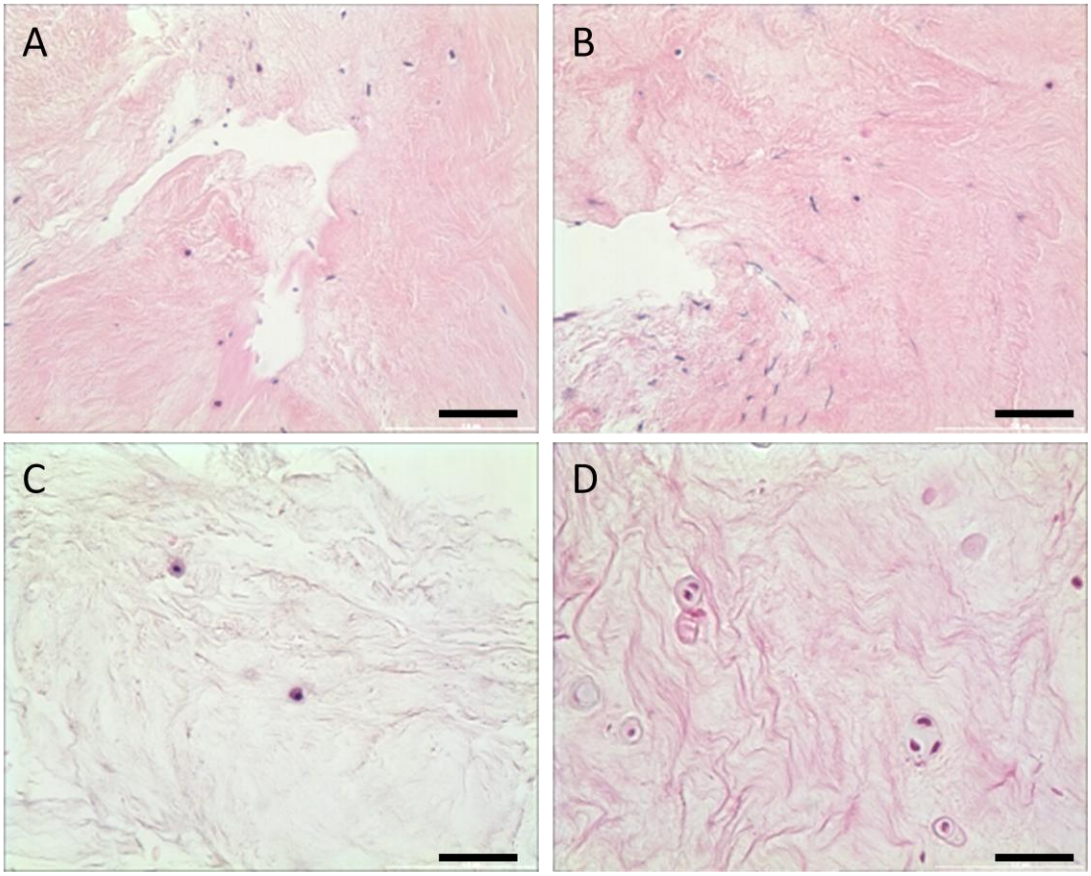

Figure 3.1 Histological features of IVD degeneration in the cervical IVD. Morphological features of degeneration were confirmed by the identification of fissures extending from the AF into the NP (A); poor demarcation between the NP and AF (B); a loss of haemotoxyphilia from the NP ECM (C); and NP cell clusters (D). Scale= 25μm

3.4.2 Variations in the Cervical NP Cell Phenotype with Ageing

3.4.2.1 Classic Markers of the NP Cell Phenotype

Expression levels of both SOX9 (Figure 3.2A) and COL2A1 (Figure 3.2B) did not vary significantly between young and mature adult ($p= 0.8712$ and $p= 0.7211$ respectively); young and elderly adult ($p= 0.2571$ and $p= 0.2672$ respectively); and mature and elderly adult specimens ($p= 0.8375$ and $p= 0.3002$ respectively). In terms of ACAN (Figure 3.2C) and VCAN (Figure 3.2D) expression, both genes were significantly more highly expressed in elderly as compared to mature adult samples ($p= 0.0145$ and $p= 0.0194$ respectively); expressed at similar levels between young adult and mature adult tissues ($p= 0.3104$ and $p= 0.1765$ respectively); and ACAN increased in young vs. elderly specimens ($p= 0.0095$), whilst VCAN expression did not differ significantly under the same comparison ($p= 0.4762$).

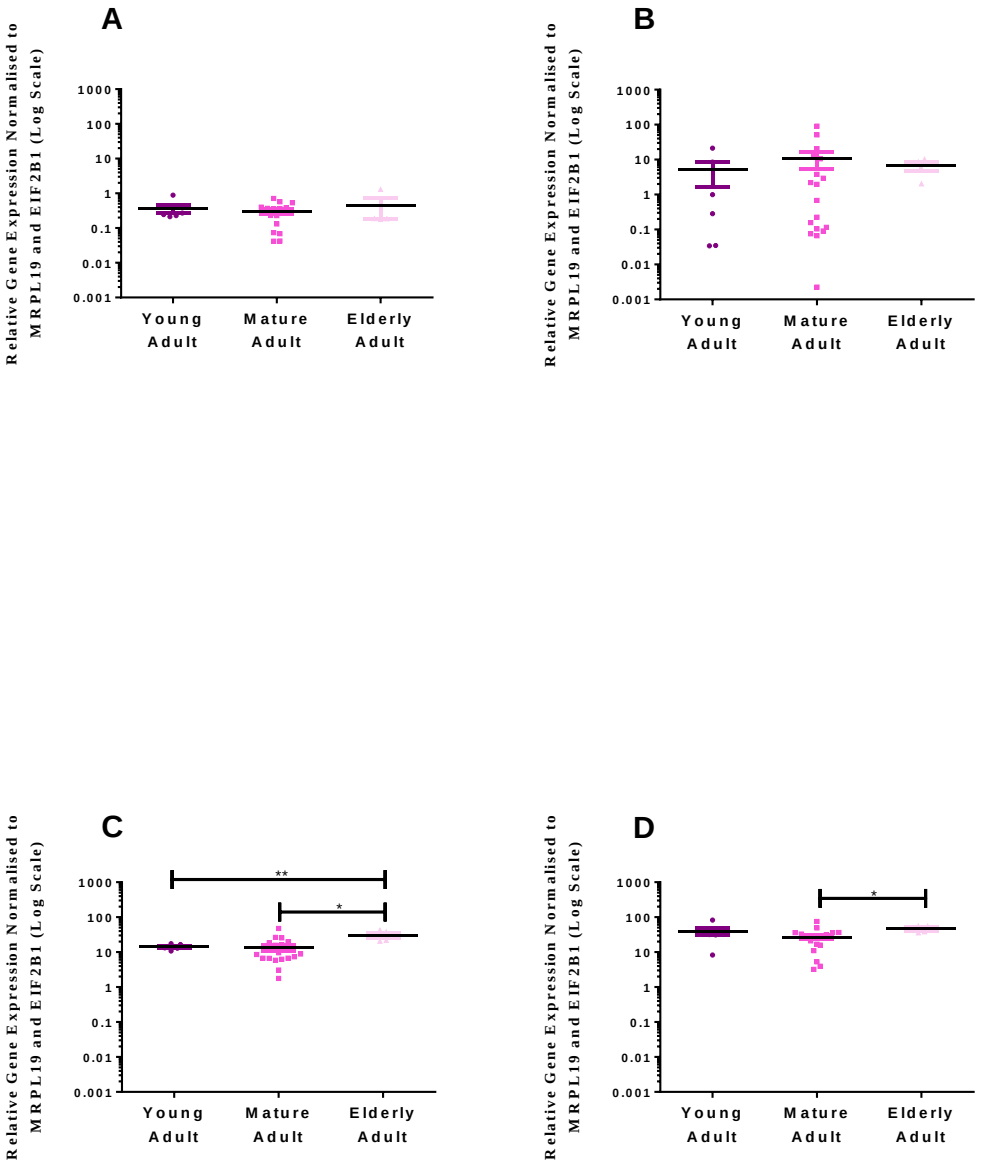

Figure 3.2 Classic NP cell marker gene expression in adult human cervical NP cells: Changes with ageing Gene expression levels of SOX9 (A), COL2A1 (B), ACAN (C) and VCAN (D) were compared between young adult (0-39 years); mature adult (40-59 years); and elderly adult (60+ years). *p=<0.05 **p=<0.01 ***p=<0.001.

3.4.2.2 ADAMTS, MMP and TIMP Expression

ADAMTS isoforms -1 (Figure 3.3A), -5 (Figure 3.3C), -8 (Figure 3.3D) and -9 (Figure 3.3E) demonstrated no significant variations in expression levels between young and mature adult (p= 0.3432; p= 0.0658; p= 0.1092; and p= 0.7211 respectively); young and elderly adult (p= 0.6095; p= >0.9999; p= >0.9999; and p= 0.9143 respectively); and mature and elderly adult specimens (p= 0.1178; p= 0.0659; p= 0.3034; and p= >0.9999 respectively). Both ADAMTS4 (Figure 3.3B) and ADAMTS15 (Figure 3.5F) isoforms were significantly decreased in mature adult as compared to young adult specimens (p= 0.0074; and p= 0.0077 respectively); demonstrated no significant variance between mature and elderly adult specimens (p= 0.3002; and p= >0.9999 respectively); and significantly lower expression of ADAMTS15 in elderly compared to young samples (p= 0.0095) but not ADAMTS4 (p= 0.7619).

Regarding the expression of MMPs, MMP2 (Figure 3.4B) and MMP10 (Figure 3.4E) demonstrated no age-associated variations in expression (young vs. mature p= 0.7198 and p= 0.5028 respectively; young vs. elderly= 0.7524 and p= >0.9999 respectively; mature vs. elderly p= 0.4845 and p= 0.6107 respectively). Both MMP9 (Figure 3.4D) and MMP13 (Figure 3.4F) were significantly decreased in mature adult samples as compared to young (p= 0.0118; and p= 0.0224 respectively), although no differential expression was noted between young and elderly (p= 0.4762; and p= 0.7619 respectively), and mature and elderly samples (p= 0.4342; p= 0.0807 respectively). MMP1 (Figure 3.4A) and MMP3 (Figure 3.4C) were significantly decreased in mature adult samples as compared to young (p= 0.0044; and p= 0.0118 respectively), and expressed at similar levels between young and elderly samples (p= 0.6095; and p= 0.9143 respectively). However, when mature and elderly adult specimens were compared, MMP1 expression was significantly decreased in elderly adult samples (p= 0.0424), whilst MMP3 was significantly increased in the same tissues (p= 0.0426).

TIMP3 (Figure 3.5C) expression did not differ significantly between young and mature (p= 0.0559); young and elderly (p= 0.4726); and mature and elderly specimens (p= 0.3002). TIMP1 (Figure 3.5A) and TIMP2 (Figure 3.5B) expression decreased significantly between young and mature adult samples (p= 0.0118; and p= 0.0330 respectively); did not differ significantly between young and elderly

specimens (p= 0.9143; and p= <0.9999); and TIMP1 expression increased again in elderly adult tissues as compared to mature (p= 0.0145), although TIMP2 demonstrated no such variation (p= 0.0982).

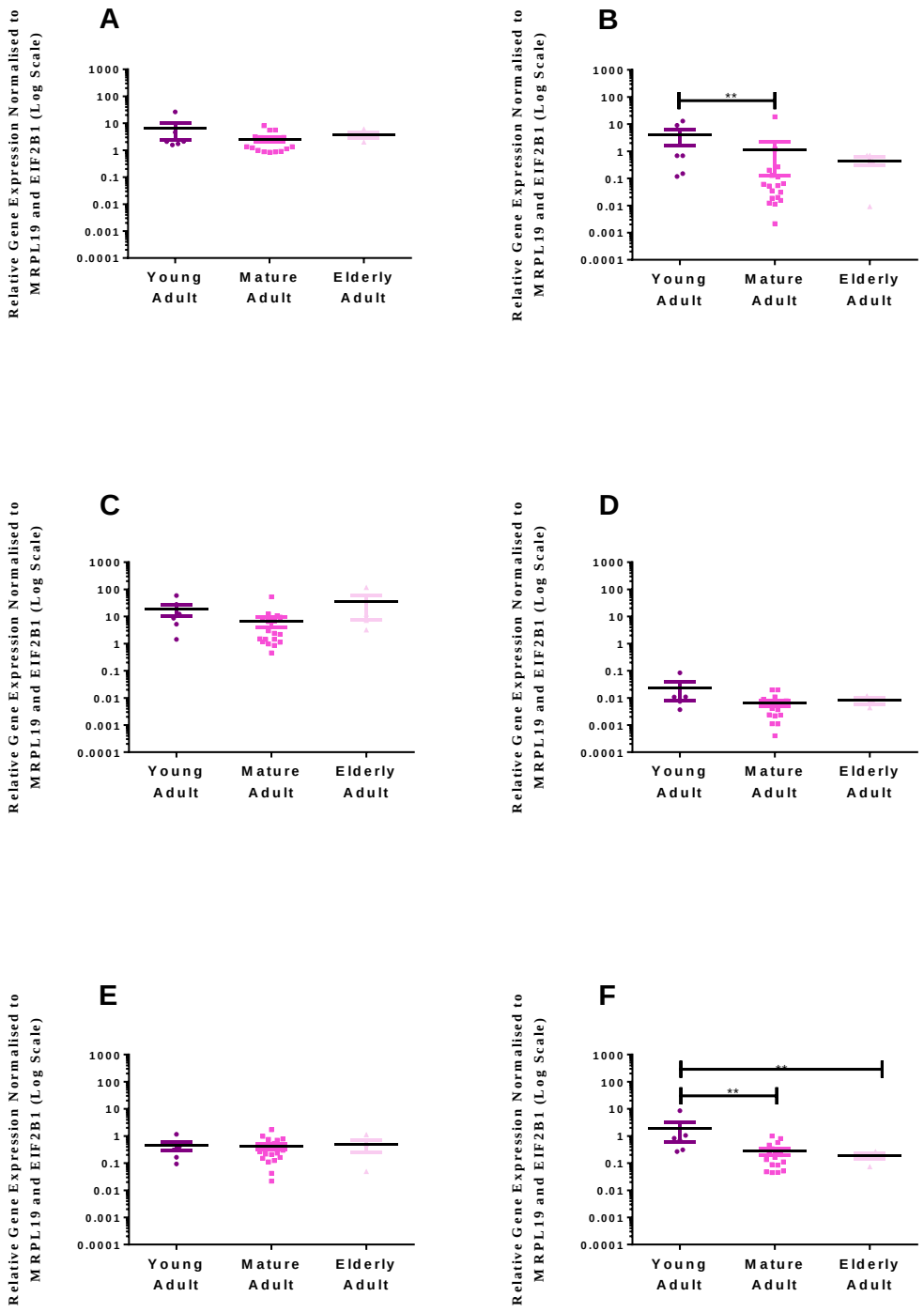

Figure 3.3 ADAMTS marker gene expression in adult human cervical NP cells: Changes with ageing. Gene expression levels of ADAMTS1 (A), ADAMTS4 (B), ADAMTS5 (C), ADAMTS8 (D), ADAMTS9 (E), and ADAMTS15 (F) were compared between young adult (0-39 years); mature adult (40-59 years); and elderly adult (60+ years) cervical NP specimens. *p=<0.05 **p=<0.01 ***p=<0.001.

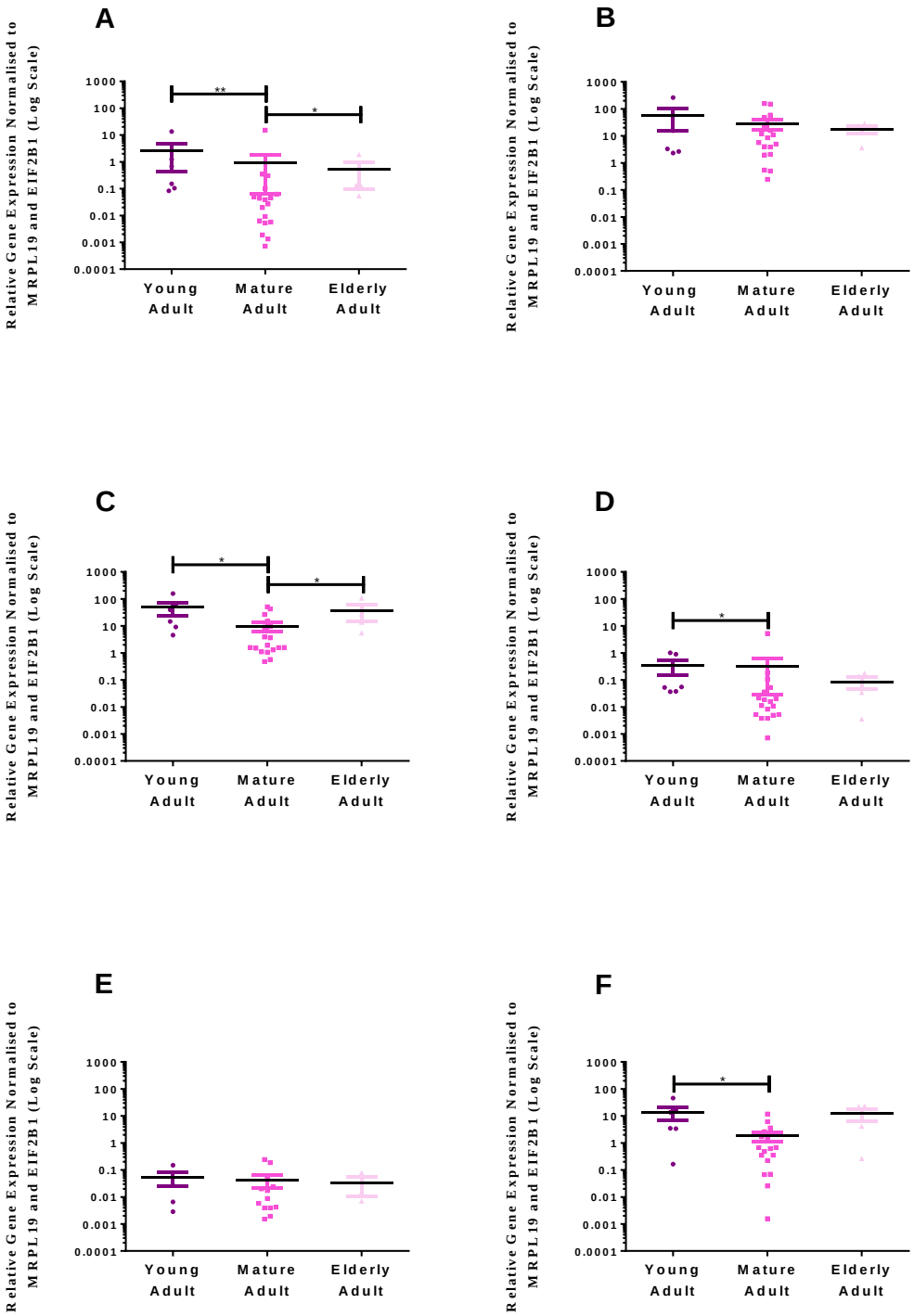

Figure 3.4 MMP marker gene expression in adult human cervical NP cells: Changes with Ageing. Gene expression levels of MMP1 (A), MMP2 (B), MMP3 (C), MMP9 (D), MMP10 (E), and MMP13 (F) were compared between young adult (0-39 years); mature adult (40-59 years); and elderly adult (60+ years) cervical NP specimens. *p=<0.05 **p=<0.01 ***p=<0.001.

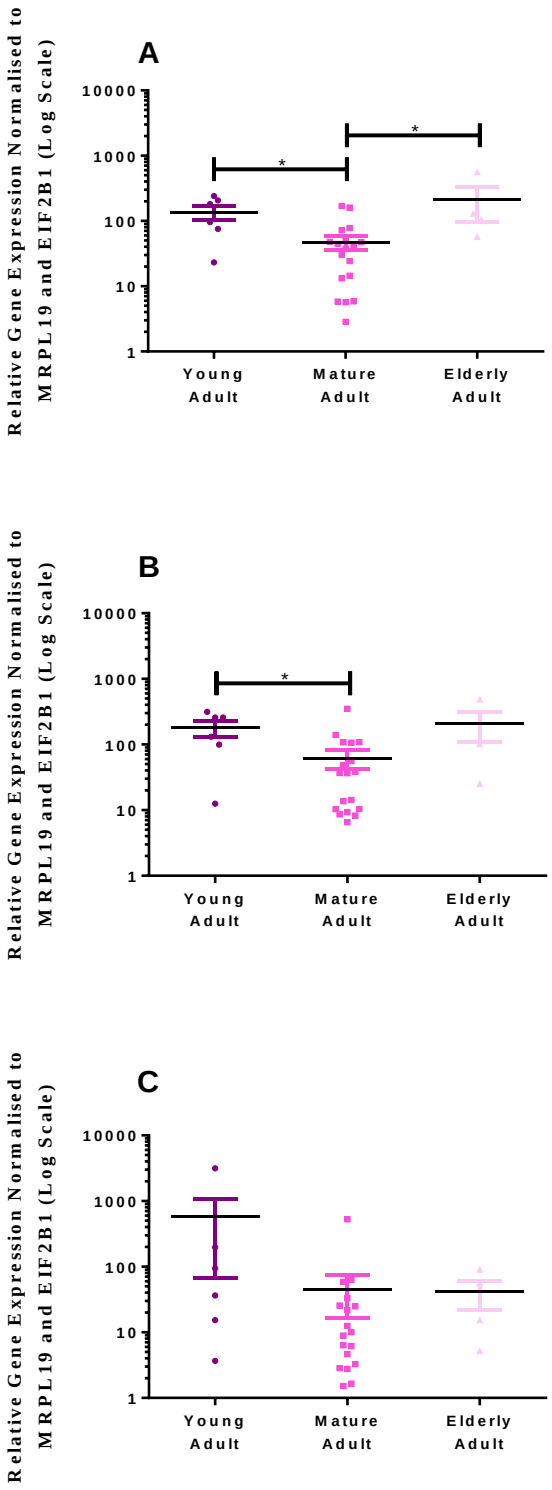

Figure 3.5 TIMP marker gene expression in adult human cervical NP cells: Changes with Ageing. Gene expression levels of TIMP1 (A), TIMP2 (B) and TIMP3 (C) were compared between young adult (0-39 years); mature adult (40-59 years); and elderly adult (60+ years) cervical NP specimens. *p=<0.05 **p=<0.01 ***p=<0.001.

3.4.2.3 Pro-Inflammatory Cytokine and Cytokine Receptor Expression

IL-1R (Figure 3.6C), TNF-α (Figure 3.6D), TNFR1A (Figure 3.6E) and TNFR1B (Figure 3.6F) expression levels did not differ significantly with ageing, when comparing young and mature adult ($p= 0.3781$; $p= 0.1014$; $p= 0.9144$; and $p= 0.2308$ respectively); young and elderly adult ($p= >0.9999$; $p= 0.3810$; $p= 0.7619$; and $p= >0.9999$ respectively); and mature and elderly adult specimens ($p= 0.4342$; $p= 0.0667$; $p= 0.6819$; and $p= 0.1775$ respectively). Expression levels of both IL-1α (Figure 3.6A) and IL-1β (Figure 3.6B) were significantly decreased in mature adult as compared to elderly adult specimens ($p= 0.0297$; $p= 0.0034$ respectively). There were no significant variations in expression levels when young and elderly adult expression levels were compared ($p= 0.1333$; $p= 0.6095$ respectively), although IL-1β expression was significantly greater in elderly adult as compared to mature adult specimens ($p= 0.0424$), but this was not noted for IL-1α ($p= 0.6593$).

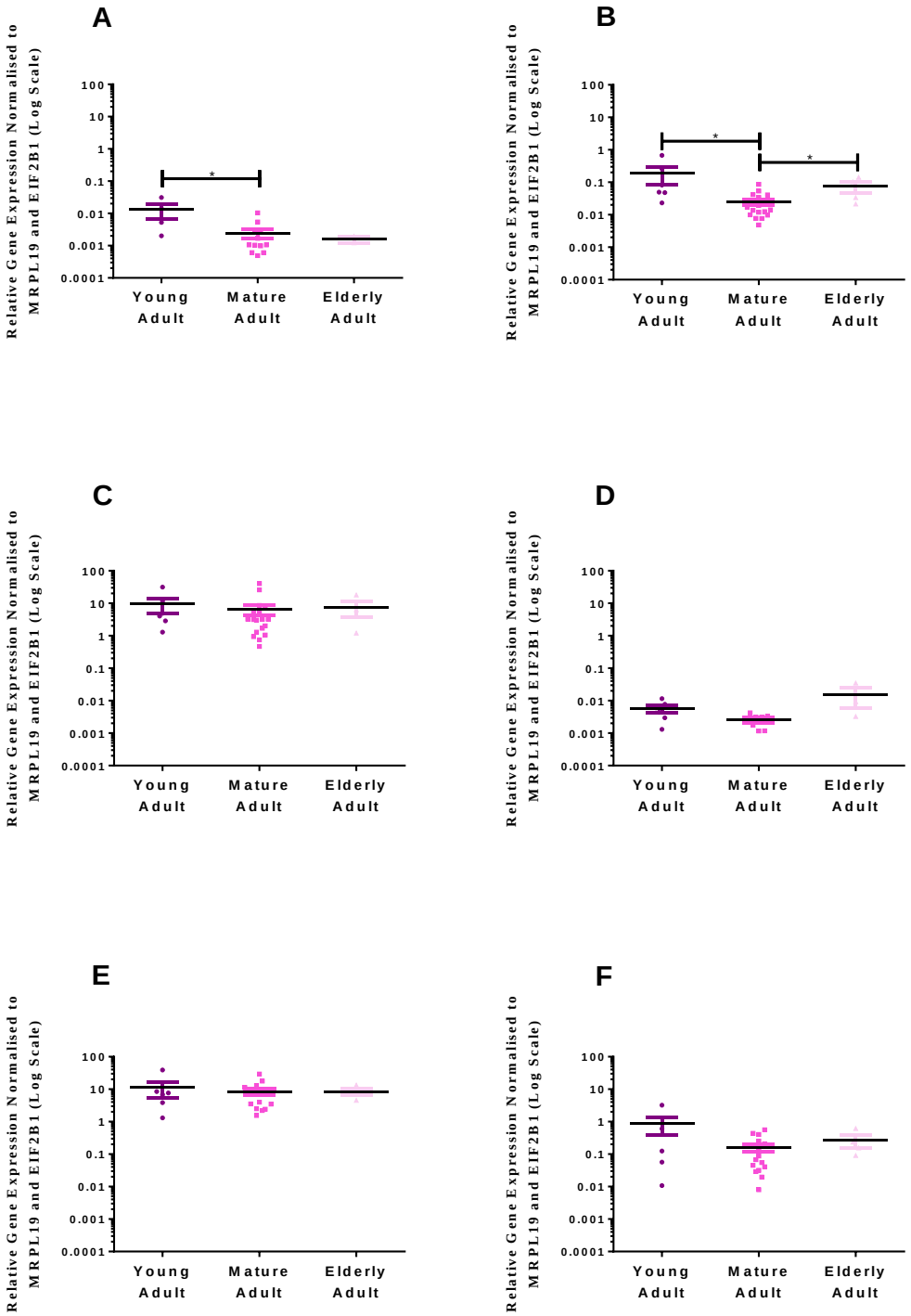

Figure 3.6 Pro-inflammatory cytokine and cytokine receptor gene expression in adult human cervical NP cells: Changes with Ageing Gene expression levels of IL-1α (A), IL-1β (B), IL-1R (C), TNF-α (D), TNFR1A (E) and TNFR1B (F) were compared between young adult (0-39 years); mature adult (40-59 years); and elderly adult (60+ years) cervical NP specimens. *p=<0.05 **p=<0.01 ***p=<0.001.

3.4.3 Variations in the Cervical NP Cell Phenotype with Degeneration

3.4.3.1 Classic Markers of the NP Cell Phenotype

Expression levels of SOX9 (Figure 3.7A), COL2A1 (Figure 3.7B) and VCAN (Figure 3.7D) did not differ significantly between non-degenerate and moderately degenerate ($p= 0.1213$; $p= 0.4157$; $p= 0.8402$ respectively); non-degenerate and severely degenerate ($p= 0.8586$; $p= 0.3308$; and $p= 0.2020$ respectively); and moderately and severely degenerate specimens ($p= 0.0988$; $p= 0.6223$; and $p= 0.1679$ respectively). ACAN (Figure 3.7C) expression significantly increased in moderately degenerate as compared to non-degenerate samples ($p= 0.0143$), and in moderately degenerate as compared to severely degenerate samples ($p= 0.0455$), although no significant variation was noted between non-degenerate and severely degenerate samples ($p= 0.9773$).

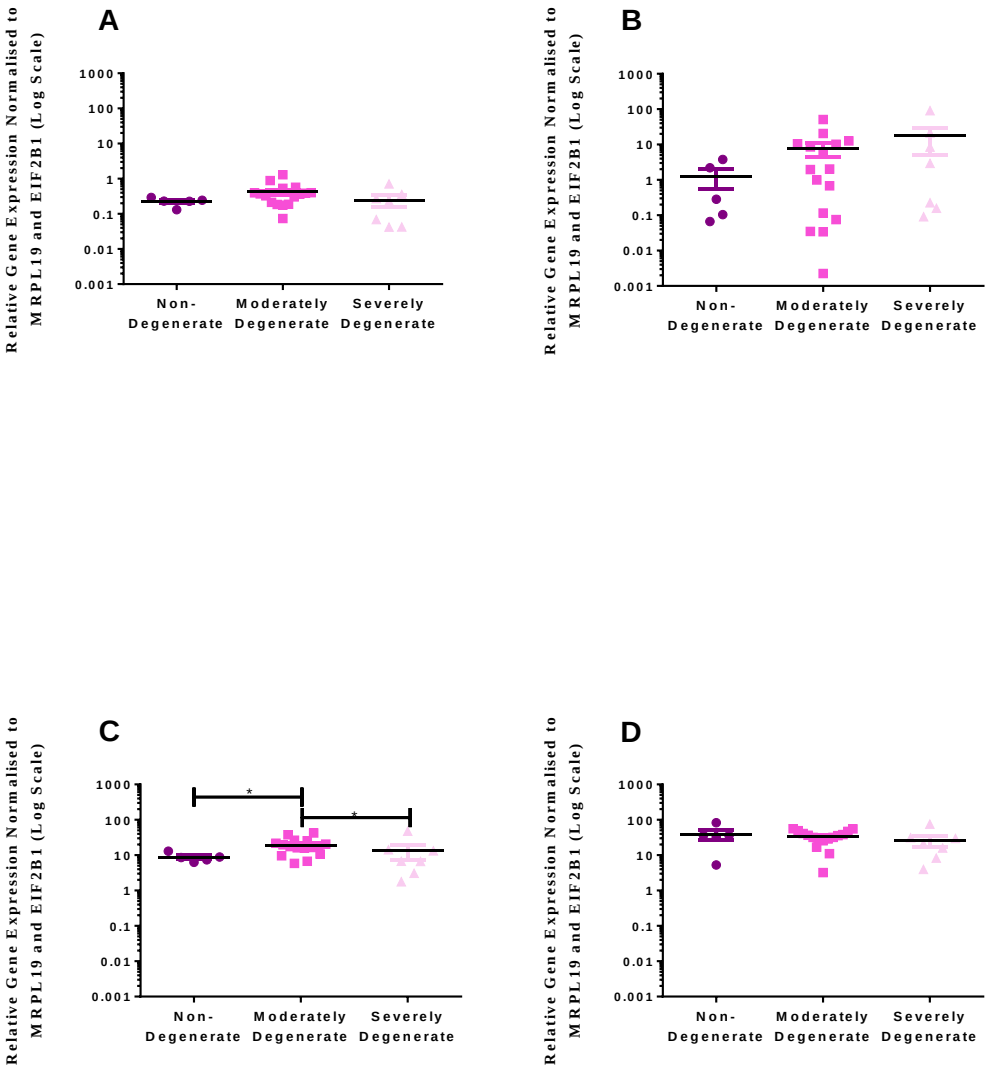

Figure 3.7 Classic NP cell marker gene expression in adult human cervical NP cells: Changes with Degeneration Gene expression levels of SOX9 (A), COL2A1 (B), ACAN (C) and VCAN (D) were compared between non-degenerate (grades 0-4); moderately degenerate (grades 5-7); and severely degenerate (grades 8-12) cervical NP specimens. *p=<0.05 **p=<0.01 ***p=<0.001.

3.4.3.2 ADAMTS, MMP and TIMP Expression

Expression levels of neither ADAMTS-1 (Figure 3.8A), -4 (Figure 3.8B), -5 (Figure 3.8C), -8 (Figure 3.8D), -9 (Figure 3.8E), or -15 (Figure 3.8F) demonstrated significant variation across the degenerative score categories analysed (non-degenerate vs. moderately degenerate p= 0.6021, p= 0.7355, p= 0.4157, p= 0.7729, p= 0.7355, and p= 0.6592 respectively; non-degenerate vs. severely degenerate p= 0.5253, p= 0.8586, p= 0.9773, 0.2468, p= 0.9779, and p= 0.4242 respectively; moderately degenerate vs. severely degenerate p= 0.4712, p= 0.4322, p= 0.2348, p= 0.1451, p= 0.5986, and p= 0.2472 respectively). Figure 3.9 illustrates MMP expression according to grade of degeneration. Expression levels of MMP1 (Figure 3.9A), MMP2 (Figure 3.9B), MMP3 (Figure 3.9C), MMP9 (Figure 3.9D), MMP10 (Figure 3.9E) and MMP13 (Figure 3.9F) did not vary significantly when non-degenerate and moderately degenerate (p= 0.4629; p= >0.9999; p= 0.6200; p= 0.3713; p= 0.3477; and p= 0.6768 respectively); non-degenerate and severely degenerate (p= 0.7069; p= 0.7424; p= 0.6010; p= 0.9773; p= 0.2424; and p= 0.5025 respectively); as well as moderately degenerate and severely degenerate specimens were compared (p= 0.2658; p= 0.7882; p= 0.8160; p= 0.3950; p= 0.5584; and p= 0.7170 respectively).

Variations in TIMP expression with degeneration are noted in Figure 3.10. TIMP1 (Figure 3.10A), -2 (Figure 3.10B) and -3 (Figure 3.10C) expression did not vary between non-degenerate and moderately degenerate specimens (p= 0.1937; p= 0.3713; p= 0.5652 respectively); and non-degenerate and severely degenerate specimens (p= 0.7424; p= 0.3434; p= 0.85856 respectively). TIMP1 and -3 expression did not vary between moderately degenerate and severely degenerate samples (p= 0.0537; and p= 0.1136 respectively), although TIMP2 expression levels were significantly decreased in severely degenerate specimens as compared to moderately degenerate (p= 0.0320).

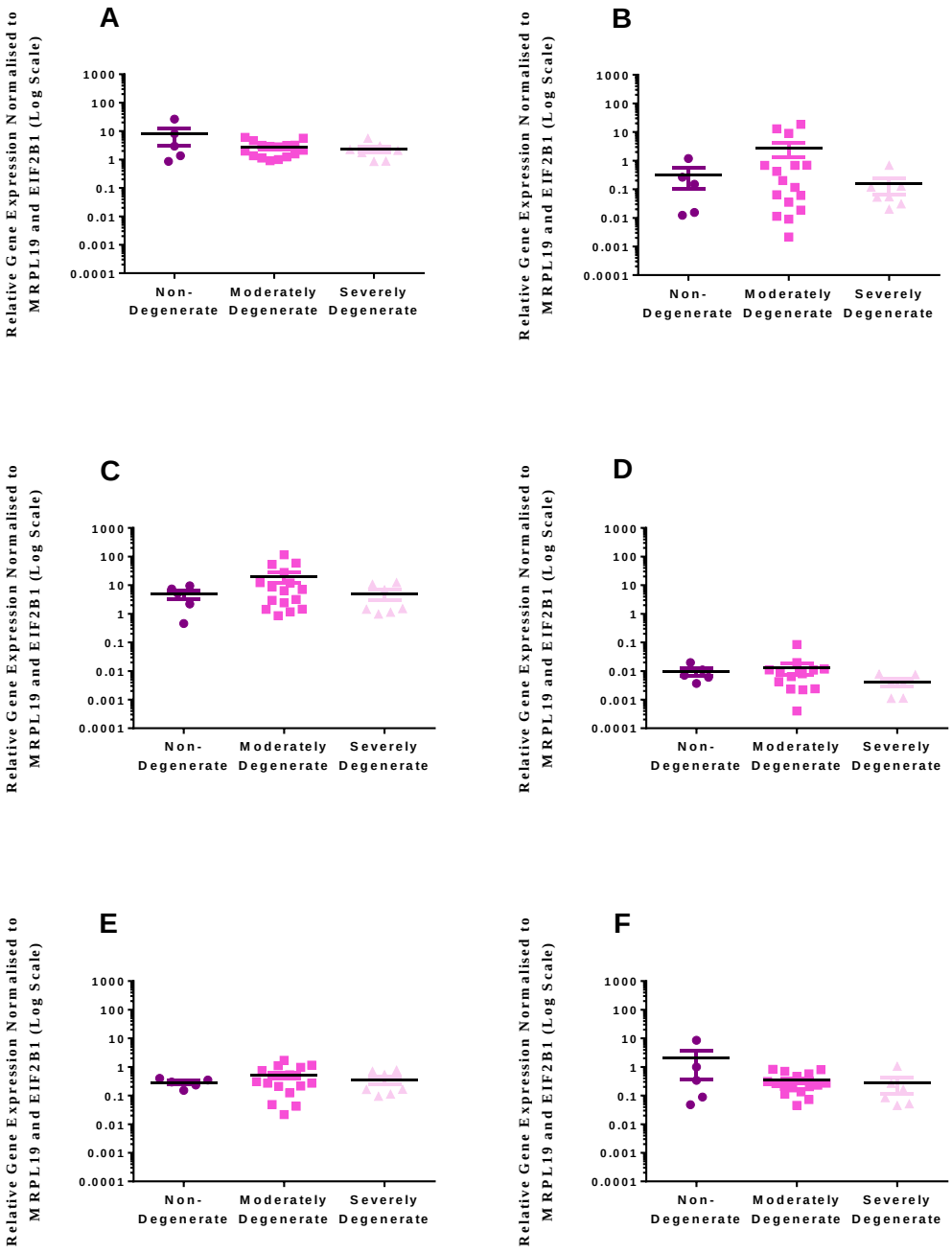

Figure 3.8 ADAMTS marker gene expression in adult human cervical NP cells: Changes with Degeneration. Gene expression levels of ADAMTS1 (A), ADAMTS4 (B), ADAMTS5 (C), ADAMTS8 (D), ADAMTS9 (E), and ADAMTS15 (F) isoforms were compared between non-degenerate (grades 0-4); moderately degenerate (grades 5-7); and severely degenerate (grades 8-12) cervical NP specimens. *p=<0.05 **p=<0.01 ***p=<0.001.

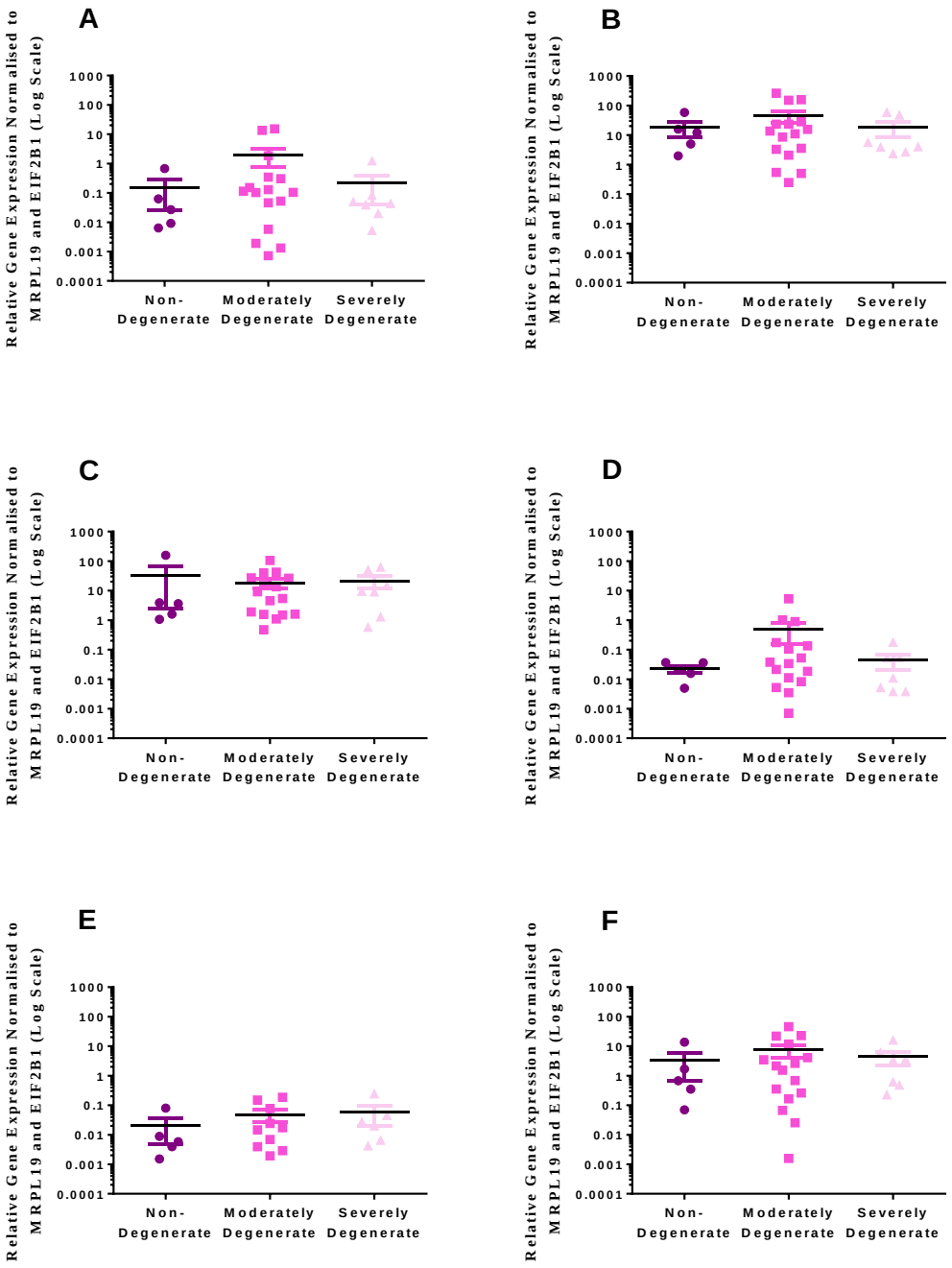

Figure 3.9 MMP marker gene expression in adult human cervical NP cells: Changes with Degeneration. Gene expression levels of MMP1 (A), MMP2 (B), MMP3 (C), MMP9 (D), MMP10 (E) and MMP13 (F) isoforms were compared between non-degenerate (grades 0-4); moderately degenerate (grades 5-7); and severely degenerate (grades 8-12) cervical NP specimens. *p=<0.05 **p=<0.01 ***p=<0.001.

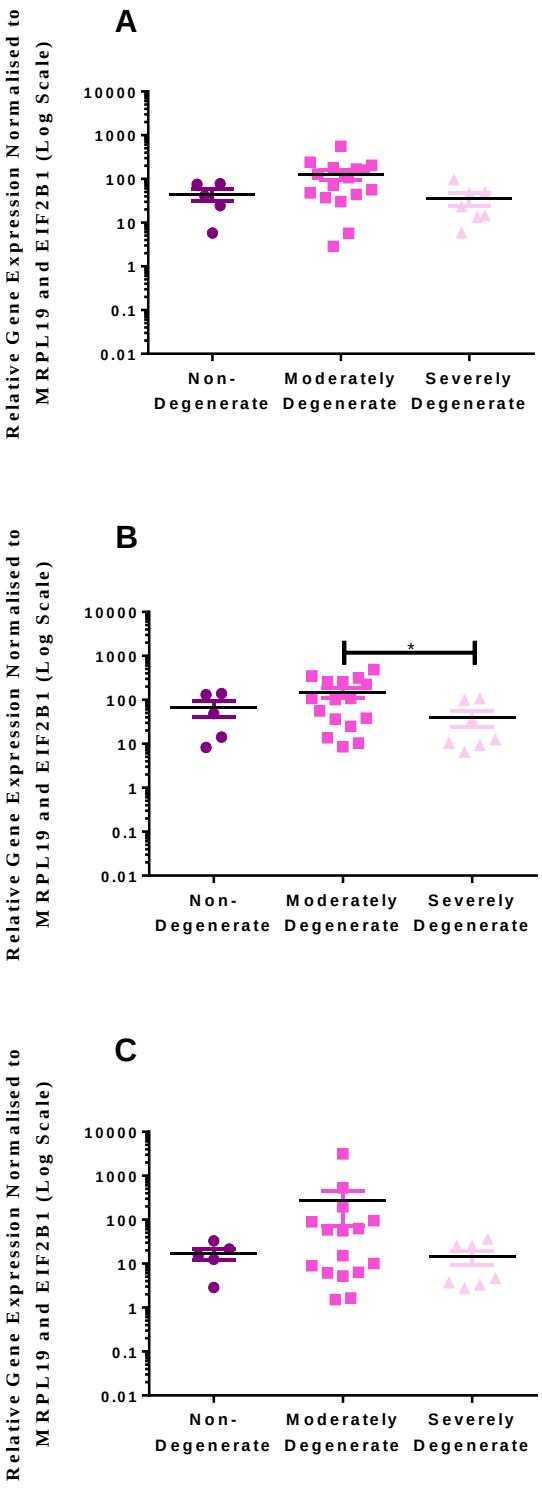

Figure 3.10 TIMP marker gene expression in adult human cervical NP cells: Changes with Degeneration. Gene expression levels of TIMP1 (A), TIMP2 (B), and TIMP3 (C) were compared between non-degenerate (grades 0-4); moderately degenerate (grades 5-7); and severely degenerate (grades 8-12) cervical NP specimens. *p=<0.05 **p=<0.01 ***p=<0.001.

3.4.3.3 Pro-Inflammatory Cytokine and Cytokine Receptor Expression

Figure 3.11 highlights the expression levels of pro-inflammatory cytokines and cytokine receptors when assessed according to severity of IVD degeneration. IL-1α (Figure 3.11A), IL-1β (Figure 3.11B), IL-1R (Figure 3.11C), TNF-α (Figure 3.11D), TNFR1A (Figure 3.11E) and TNFR1B (Figure 3.11F) expression analyses demonstrated no significant variations between non-degenerate and moderately degenerate specimens ($p= 0.5035$; $p= 0.7956$; $p= 0.6308$; $p= 0.9091$; $p= 0.3949$; and $p= 0.5730$ respectively); non-degenerate and severely degenerate specimens ($p= 0.8254$; $p= 0.9369$; $p= >0.9999$; $p= 0.5333$; $p= 0.4242$; and $p= 0.9004$ respectively); and moderately degenerate and severely degenerate specimens ($p= 0.4366$; $p= >0.9999$; $p= 0.5120$; $p= 0.2777$; $p= 0.9656$; and $p= 0.1691$ respectively).

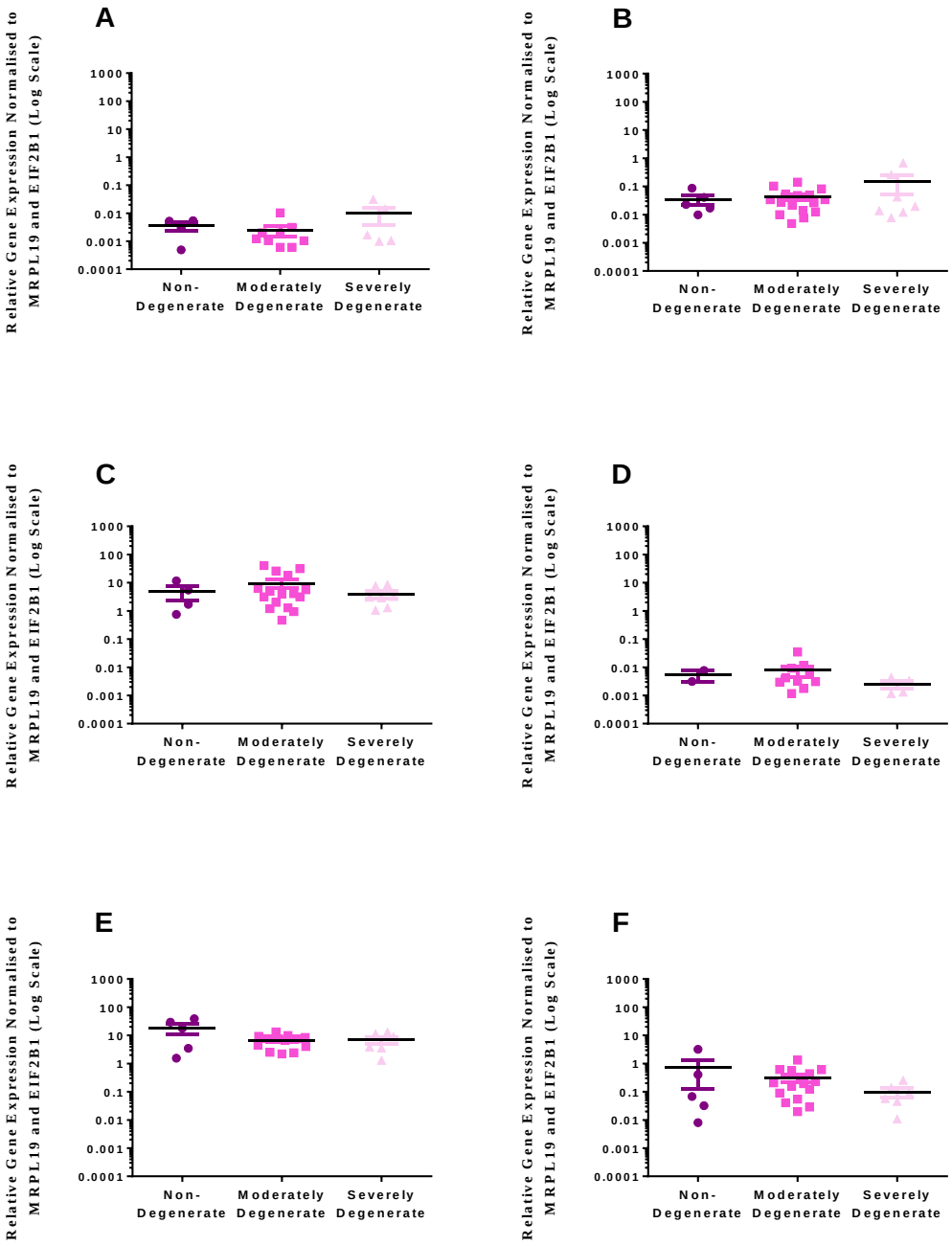

Figure 3.11 Pro-inflammatory cytokine and cytokine receptor gene expression in adult human cervical NP cells: Changes with Degeneration. Gene expression levels of IL-1α (A), IL-1β (B), IL-1R (C), TNF-α (D), TNFR1A (E), and TNFR1B (F) were compared between non-degenerate (grades 0-4); moderately degenerate (grades 5-7); and severely degenerate (grades 8-12) cervical NP specimens. *p=<0.05 **p=<0.01 ***p=<0.001.

3.4.4 Comparing the Lumbar and Cervical NP Cell Phenotype

3.4.4.1 Classic Markers of the NP Cell Phenotype

There were no significant differences in the gene expression levels of SOX9 (Figure 3.12A p=0.1611), COL2A1 (Figure 3.12B p=0.8103), ACAN (Figure 3.12C p=0.4642) or VCAN (Figure 3.12D p=0.1388) between NP cells of moderately degenerate lumbar and cervical discs. Additionally, gene expression levels of SOX9 (Figure 3.13A p=0.6312), COL2A1 (Figure 3.13B p=0.2441) and ACAN (Figure 3.13C p=0.1056) did not vary significantly between severely degenerate cervical and lumbar NP cells. Expression levels of VCAN (Figure 3.13D) however, were significantly greater in severely degenerate NP cells obtained from the lumbar region than that of the cervical (p=0.0166). When cohorts were compared irrespective of degenerative grade, SOX9 (Figure 3.14A), COL2A1 (Figure 3.14B) and ACAN (Figure 3.14C) did not vary between lumbar and cervical specimens (p= 0.3355, p= 0.3581 and p= 0.3418 respectively). VCAN expression (Figure 3.14D) was significantly greater in lumbar as compared to cervical samples (p= 0.0048).

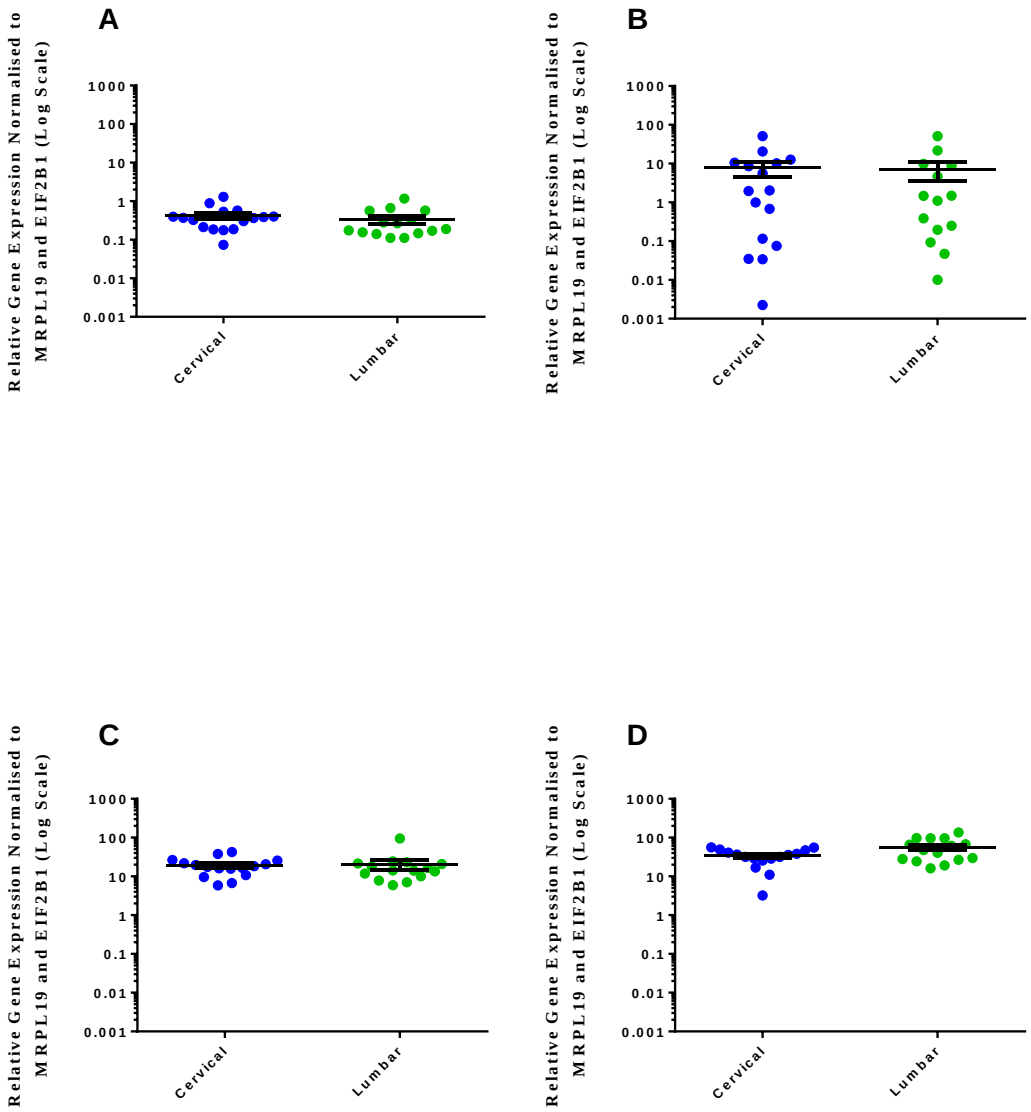

Figure 3.12 Classic NP cell marker gene expression in NP cells derived from adult human moderately degenerate cervical and lumbar NP tissue. Gene expression levels of SOX9 (A), COL2A1 (B), ACAN (C) and VCAN (D) were compared between cervical (blue) and lumbar (green) moderately degenerate specimens. *p=<0.05 **p=<0.01 ***p=<0.001.

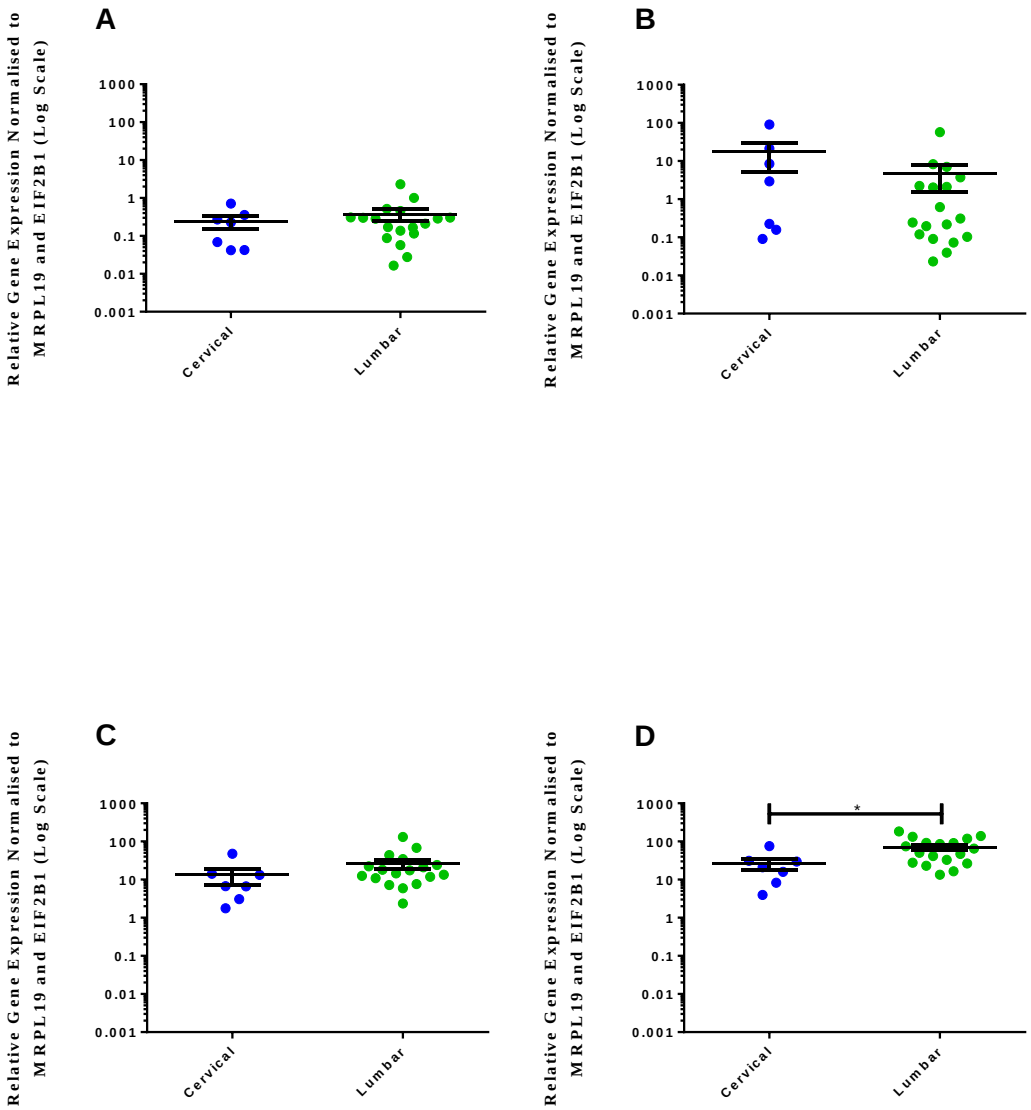

Figure 3.13 Classic NP cell marker gene expression in NP cells derived from adult human severely degenerate cervical and lumbar NP tissue. Gene expression levels of SOX9 (A), COL2A1 (B), ACAN (C) and VCAN (D) were compared between cervical (blue) and lumbar (green) severely degenerate specimens. *p=<0.05 **p=<0.01 ***p=<0.001.

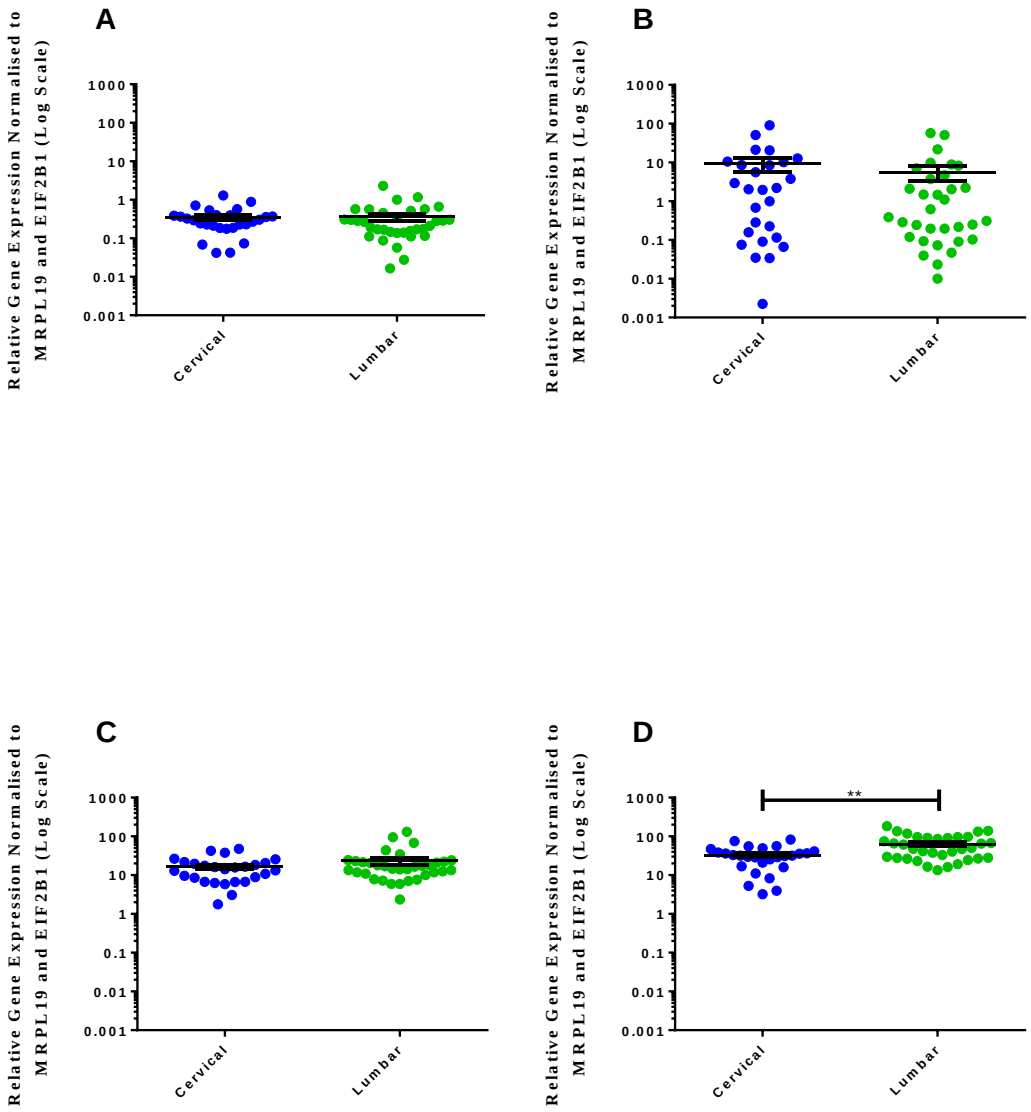

Figure 3.14 Classic NP cell marker gene expression in NP cells derived from adult human cervical and lumbar NP tissue. Gene expression levels of SOX9 (A), COL2A1 (B), ACAN (C) and VCAN (D) were compared between cervical (blue) and lumbar (green) specimens. *p=<0.05 **p=<0.01 ***p=<0.001.

3.4.4.2 ADAMTS, MMP and TIMP Expression

With regards to the expression of ADAMTSs, there were no significant variations in the gene expression levels of ADAMTS1 (Figure 3.15A p=0.2146), ADAMTS5 (Figure 3.15C p=0.1184), ADAMTS8 (Figure 3.15D p=0.5294), ADAMTS9 (Figure 3.15E p=0.3146) and ADAMTS15 (Figure 3,15F p=0.1863) in cervical and lumbar moderately degenerate NP samples. ADAMTS4 (Figure 3.15B) expression was significantly higher in moderately degenerate cervical NP cells as compared to lumbar (p=0.0490). In severely degenerate NP cells, there were no statistically significant differences in expression levels of any of the ADAMTS isoforms assessed (ADAMTS1 Figure 3.16A p=0.0616; ADAMTS4 Figure 3.16B p=0.6312; ADAMTS5 Figure 3.16C p=0.8796; ADAMTS8 Figure 3.16D p=0.2379; ADAMTS9 Figure 3.16E p=0.6556; and ADAMTS15 Figure 3.16F p=0.8344). When expression levels were compared irrespective of degenerative score, ADAMTS1 expression (Figure 3.17A) was significantly greater overall in lumbar as and compared to cervical specimens (p= 0.0213), but expression levels of ADAMTSs -4 (Figure 3.17B), -5 (Figure 3.17C), -8 (Figure 3.17D), -9 (Figure 3.17E) and -15 (Figure 3.17F) did not differ significantly (p= 0.2319, p= 0.1945, p= 0.9448, p= 0.1945 and p= 0.3681 respectively)

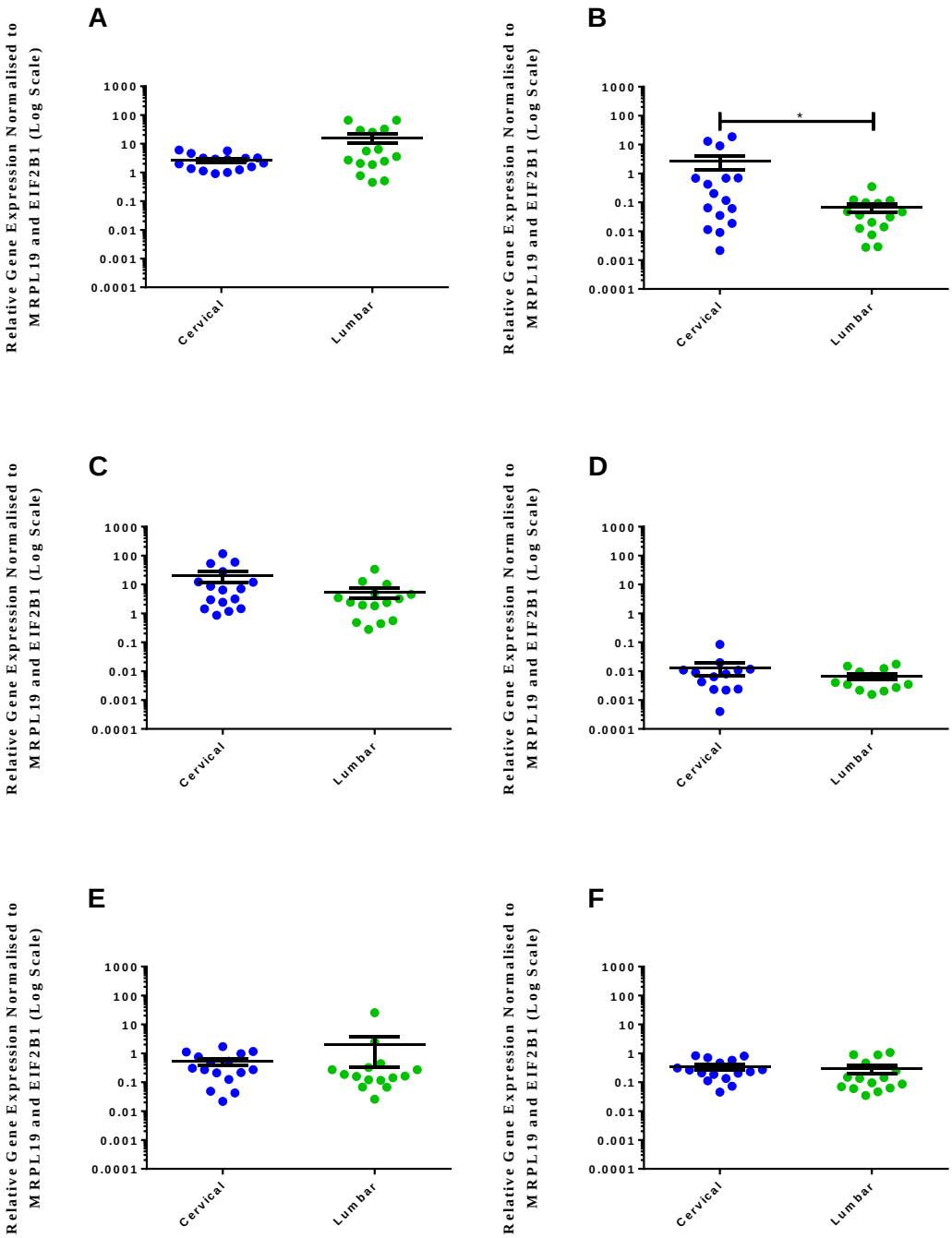

Figure 3.15 ADAMTS marker gene expression in NP cells derived from adult human moderately degenerate cervical and lumbar NP tissue. Gene expression levels of ADAMTS1 (A), ADAMTS4 (B), ADAMTS5 (C), ADAMTS8 (D), ADAMTS9 (E) and ADAMTS15 (F) were compared between cervical (blue) and lumbar (green) moderately degenerate specimens. *p=<0.05 **p=<0.01 ***p=<0.001

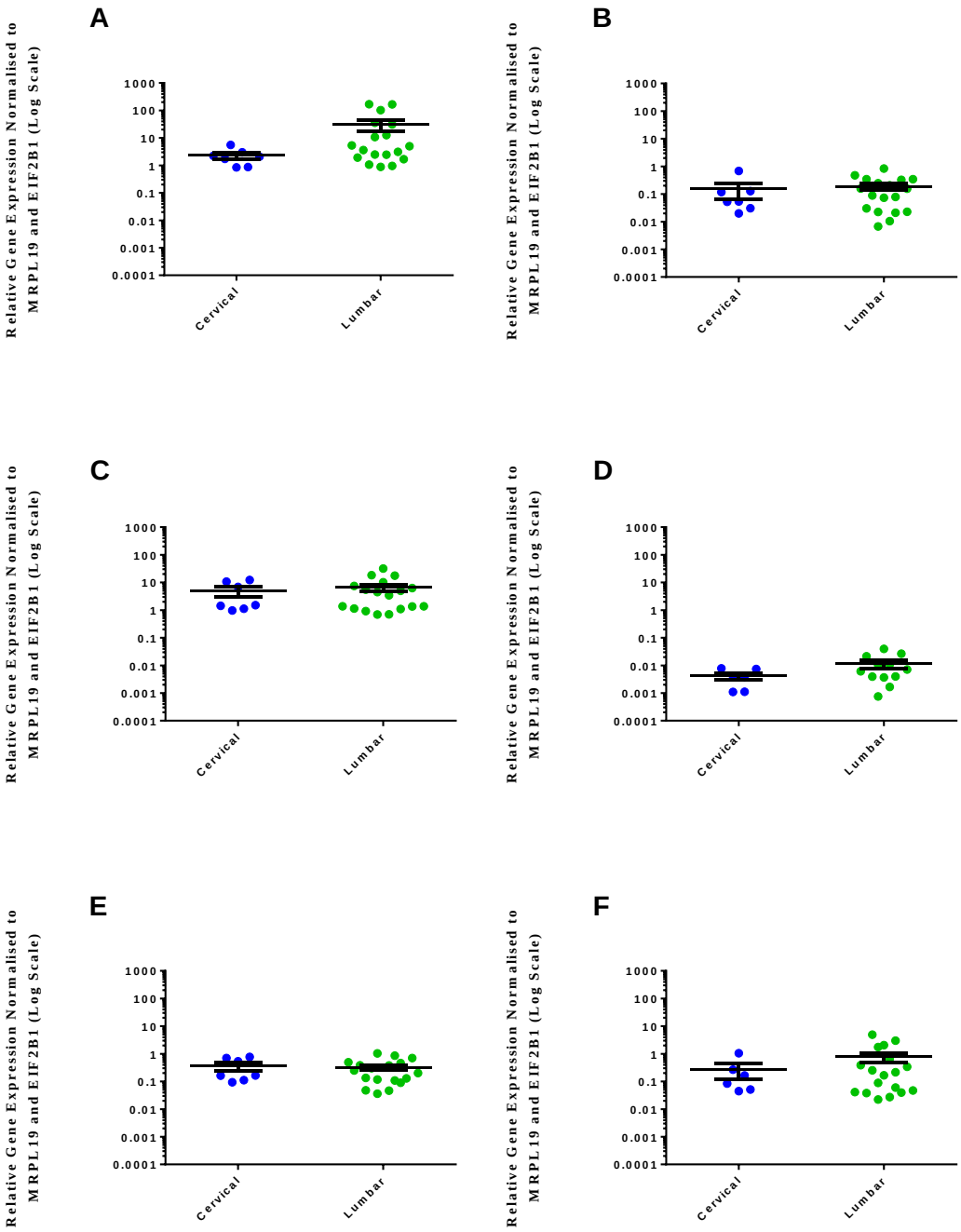

Figure 3.16 ADAMTS marker gene expression in NP cells derived from adult human severely degenerate cervical and lumbar NP tissue. Gene expression levels of ADAMTS1 (A), ADAMTS4 (B), ADAMTS5 (C), ADAMTS8 (D), ADAMTS9 (E) and ADAMTS15 (F) were compared between cervical (blue) and lumbar (green) severely degenerate specimens. *p=<0.05 **p=<0.01 ***p=<0.001.

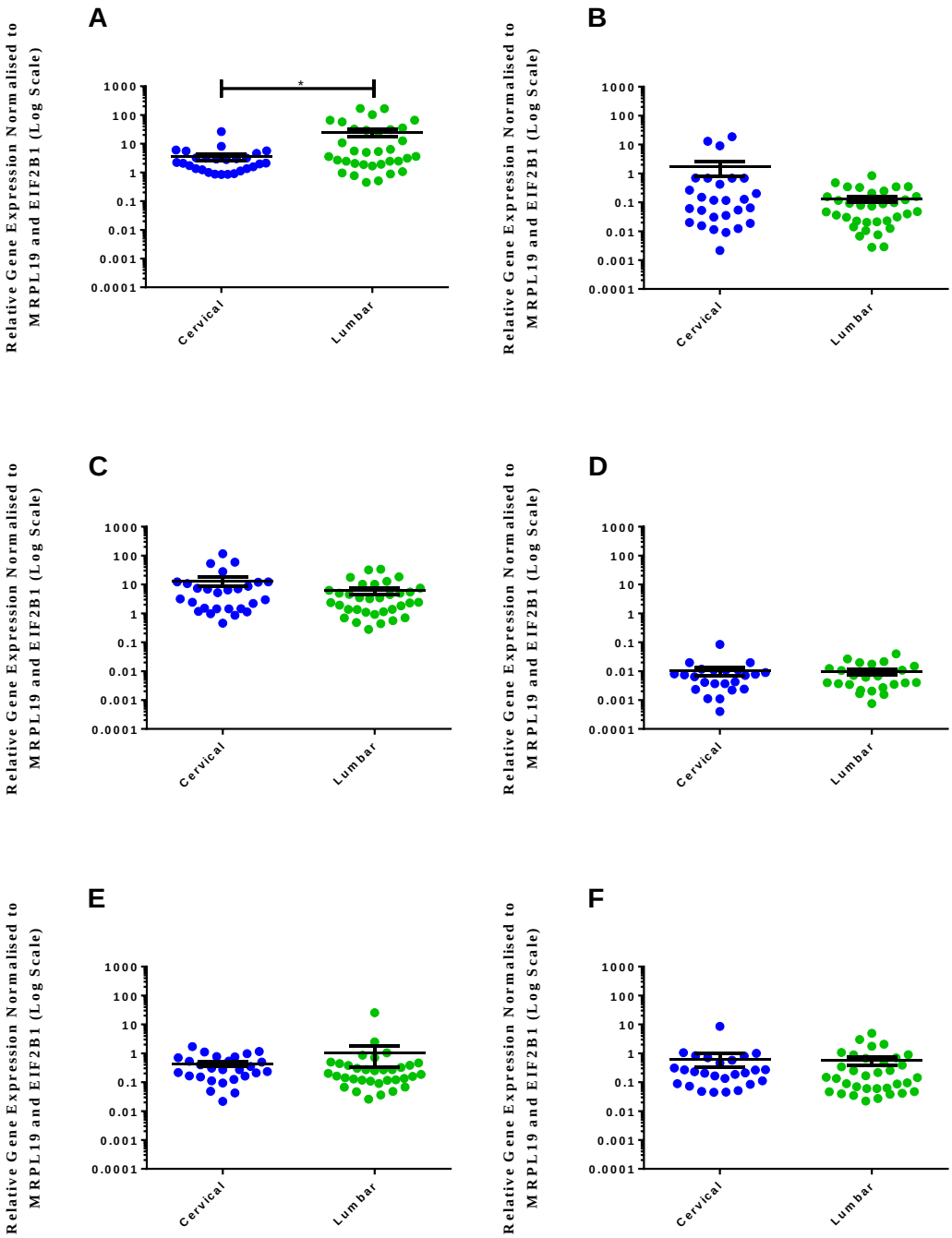

Figure 3.17 ADAMTS marker gene expression in NP cells derived from adult human cervical and lumbar NP tissue. Gene expression levels of ADAMTS1 (A), ADAMTS4 (B), ADAMTS5 (C), ADAMTS8 (D), ADAMTS9 (E) and ADAMTS15 (F) were compared between cervical (blue) and lumbar (green) specimens. *p=<0.05 **p=<0.01 ***p=<0.001.

Expression levels of MMPs were compared between moderately degenerate cervical and lumbar NP cells. No significant variations in gene expression levels were noted for any of the MMP isoforms analysed (MMP1 Figure 3.18A p=0.3293; MMP2 Figure 3.18B p=0.8200; MMP3 Figure 3.18C p=0.7311; MMP9 Figure 3.18D p=0.7604; MMP10 Figure 3.18E p=0.8210; and MMP13 Figure 3.18F p=0.0712). Similarly, gene expression levels of MMPs did not vary between severely degenerate specimens of cervical and lumbar NP cells, shown in Figure 3.19 (MMP1 Figure 3.19A p=0.3721; MMP2 Figure 3.19B p=0.1699; MMP3 Figure 3.19C p=0.9728; MMP9 Figure 3.19D p=0.0928; MMP10 Figure 3.19E p=0.7358; and MMP13 Figure 3.19F p=0.3257). When expression levels were compared between cohorts irrespective of degenerative score, again no variations were noted in expression for either MMP1 (Figure 3.20A, p= 0.9012), MMP2 (Figure 3.20B, p= 0.5176), MMP3 (Figure 3.20C, p= 0.9909), MMP9 (Figure 3.20D, p= 0.2369), MMP10 (Figure 3.20E, p=0.3349) or MMP13 (Figure 3.20F, p= 0.0725).

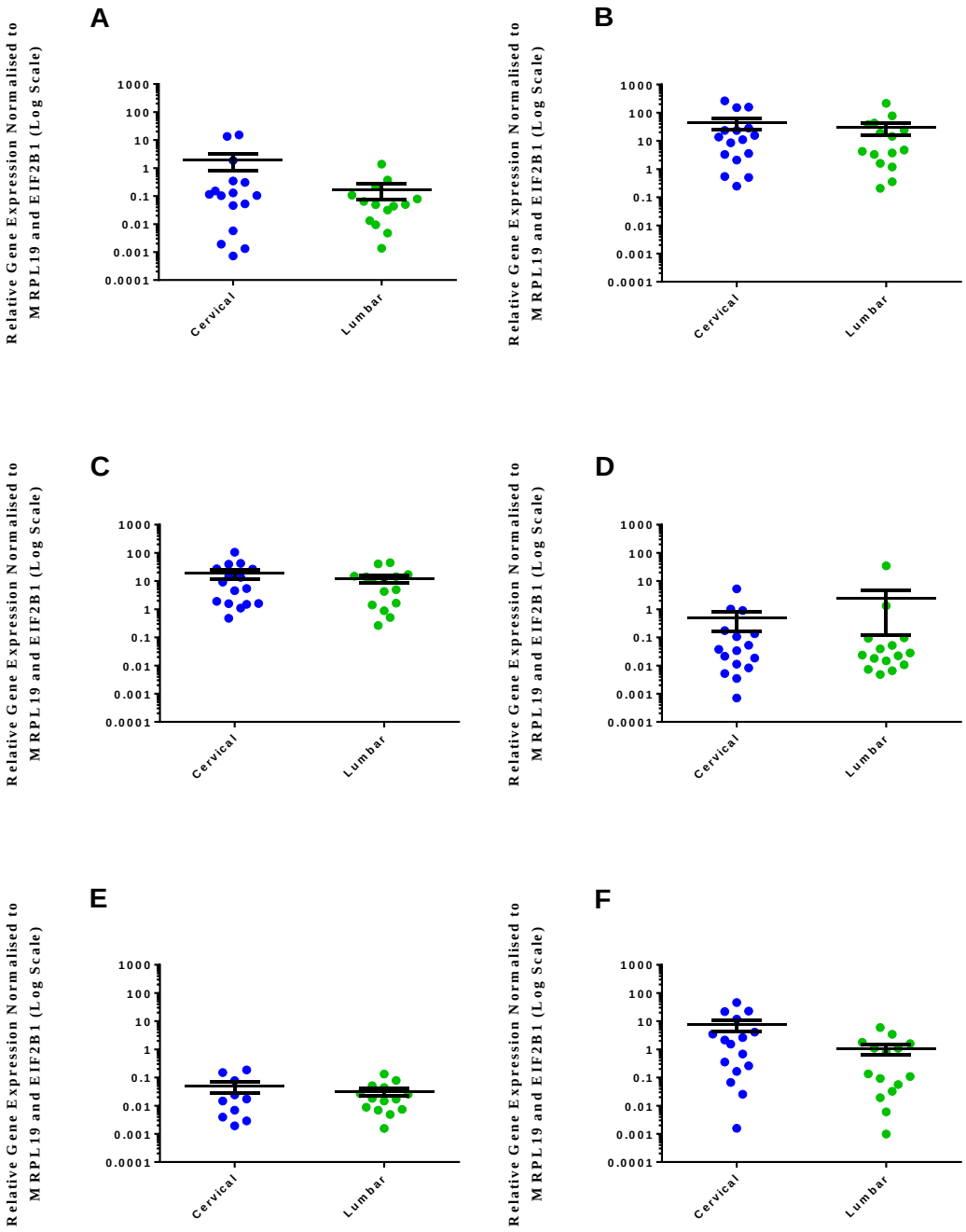

Figure 3.18 MMP marker gene expression in NP cells derived from adult human moderately degenerate cervical and lumbar NP tissue. Gene expression levels of MMP1 (A), MMP2 (B), MMP3 (C), MMP9 (D), MMP10 (E) and MMP13 (F) were compared between cervical (blue) and lumbar (green) moderately degenerate specimens. *p=<0.05 **p=<0.01 ***p=<0.001.

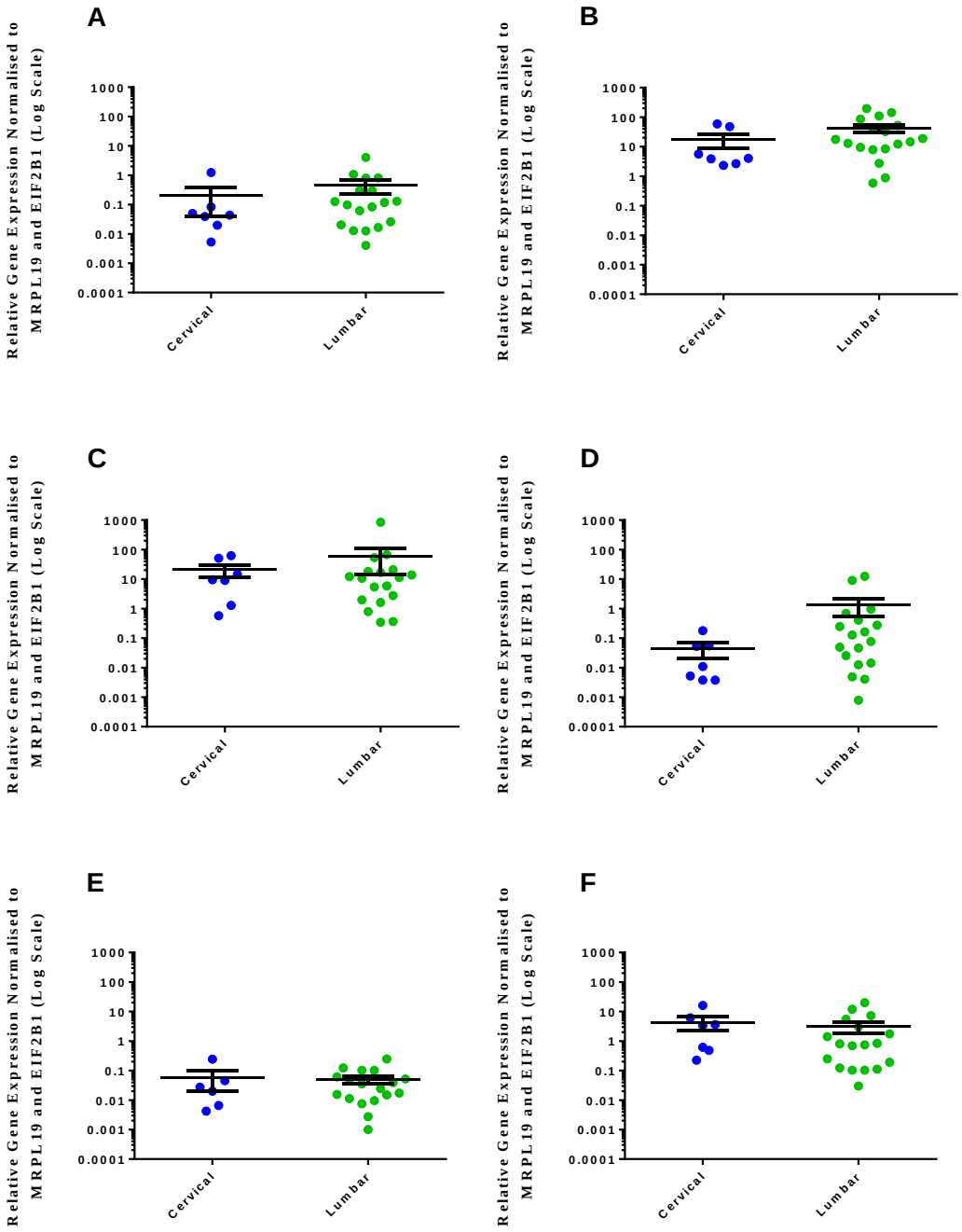

Figure 3.19 MMP marker gene expression in NP cells derived from adult human severely degenerate cervical and lumbar NP tissue. Gene expression levels of MMP1 (A), MMP2 (B), MMP3 (C), MMP9 (D), MMP10 (E) and MMP13 (F) were compared between cervical (blue) and lumbar (green) severely degenerate specimens. *p=<0.05 **p=<0.01 ***p=<0.001.

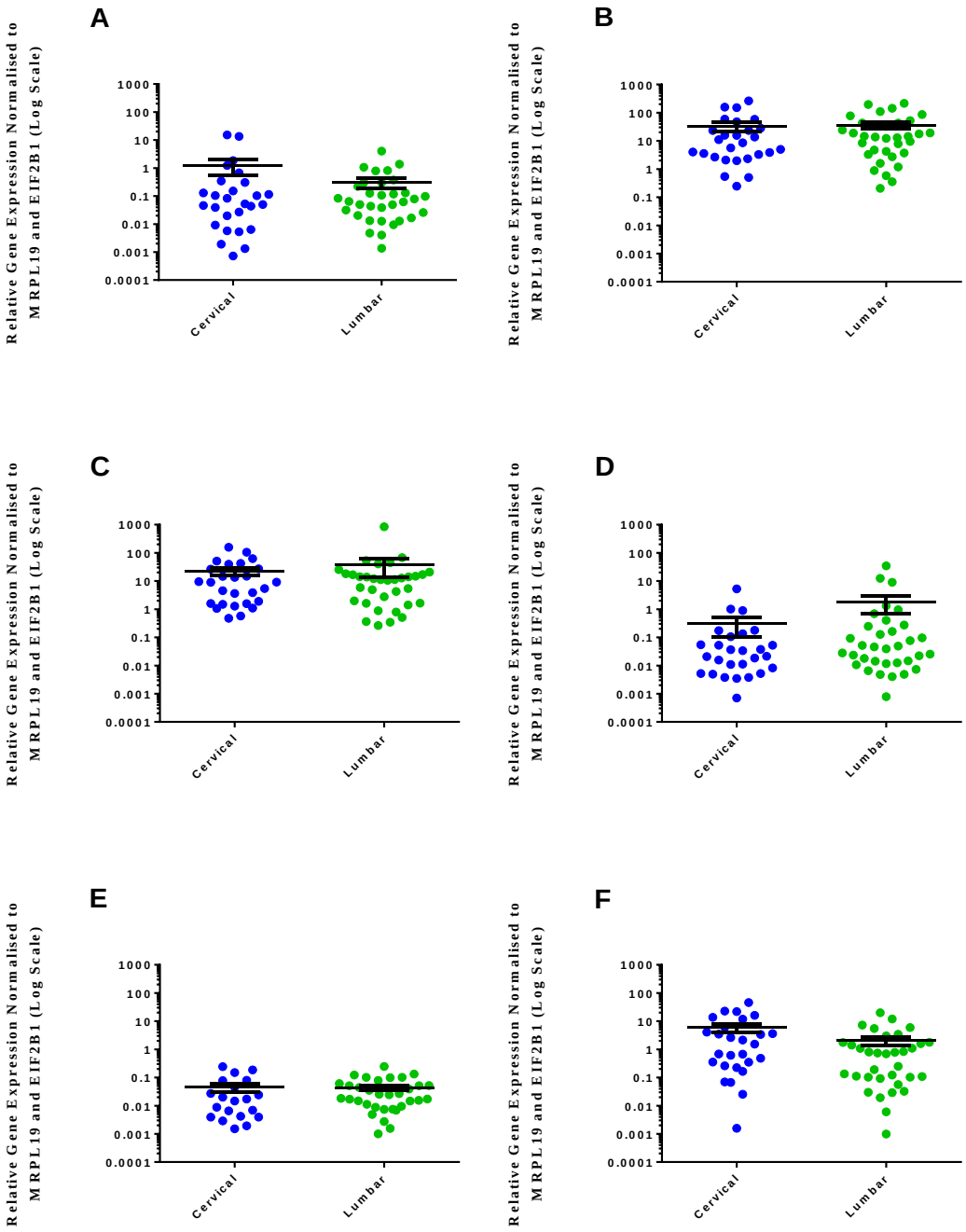

Figure 3.20 MMP marker gene expression in NP cells derived from adult human cervical and lumbar NP tissue. Gene expression levels of MMP1 (A), MMP2 (B), MMP3 (C), MMP9 (D), MMP10 (E) and MMP13 (F) were compared between cervical (blue) and lumbar (green) specimens. *p=<0.05 **p=<0.01 ***p=<0.001.

TIMPs are known to inhibit the actions of MMPs and ADAMTSs in IVD degeneration. Expression levels of three TIMP isoforms, previously demonstrated as expressed in the human IVD, were compared between lumbar and cervical NP specimens in order to ascertain whether cells of either region preferentially expressed these markers. In moderately degenerate NP cells, expression of TIMP1 (Figure 3.21A) was comparable between cells isolated from either spinal region ($p=0.1184$), whilst expression levels of TIMP2 (Figure 3.21B) and TIMP3 (Figure 3.21C) were significantly greater in cervical NP cells as compared to lumbar ($p=0.0002$ and $p=0.0119$ respectively). No significant differences in the expression of the TIMP isoforms were noted in severely degenerate NP samples from cervical and lumbar discs (TIMP1 Figure 3.22A $p=0.3721$; TIMP2 Figure 3.22B $p=0.7879$; and TIMP3 Figure 3.22C $p=0.3257$). When expression levels were compared between cohorts irrespective of degenerative grade, TIMP1 (Figure 3.23A) expression did not differ between lumbar and cervical specimens ($p= 0.5765$), whilst TIMP2 (Figure 3.23B) and TIMP3 (Figure 3.23C) expression was significantly greater in cervical as compared to lumbar samples ($p= 0.0009$ and $p= 0.0053$ respectively).

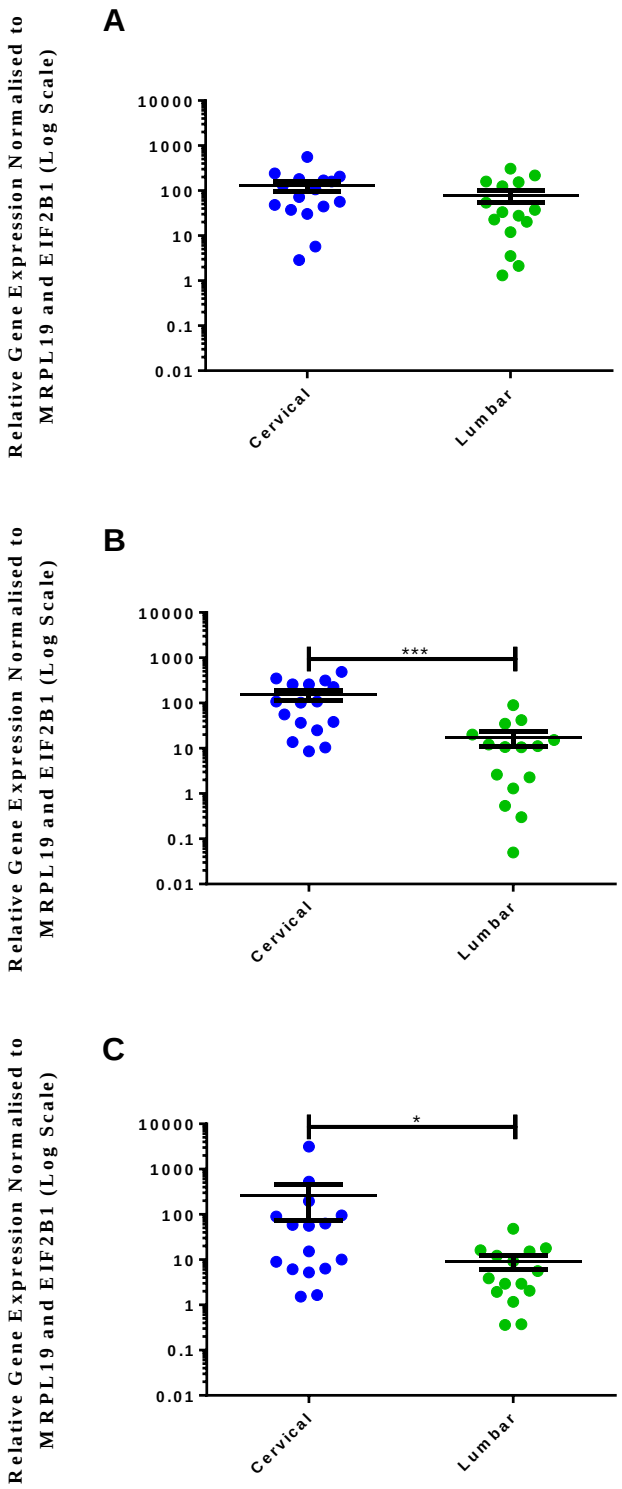

Figure 3.21 TIMP marker gene expression in NP cells derived from adult human moderately degenerate cervical and lumbar NP tissue. Gene expression levels of TIMP1 (A), TIMP2 (B) and TIMP3 (C) were compared between cervical (blue) and lumbar (green) moderately degenerate specimens. *p=<0.05 **p=<0.01 ***p=<0.001.

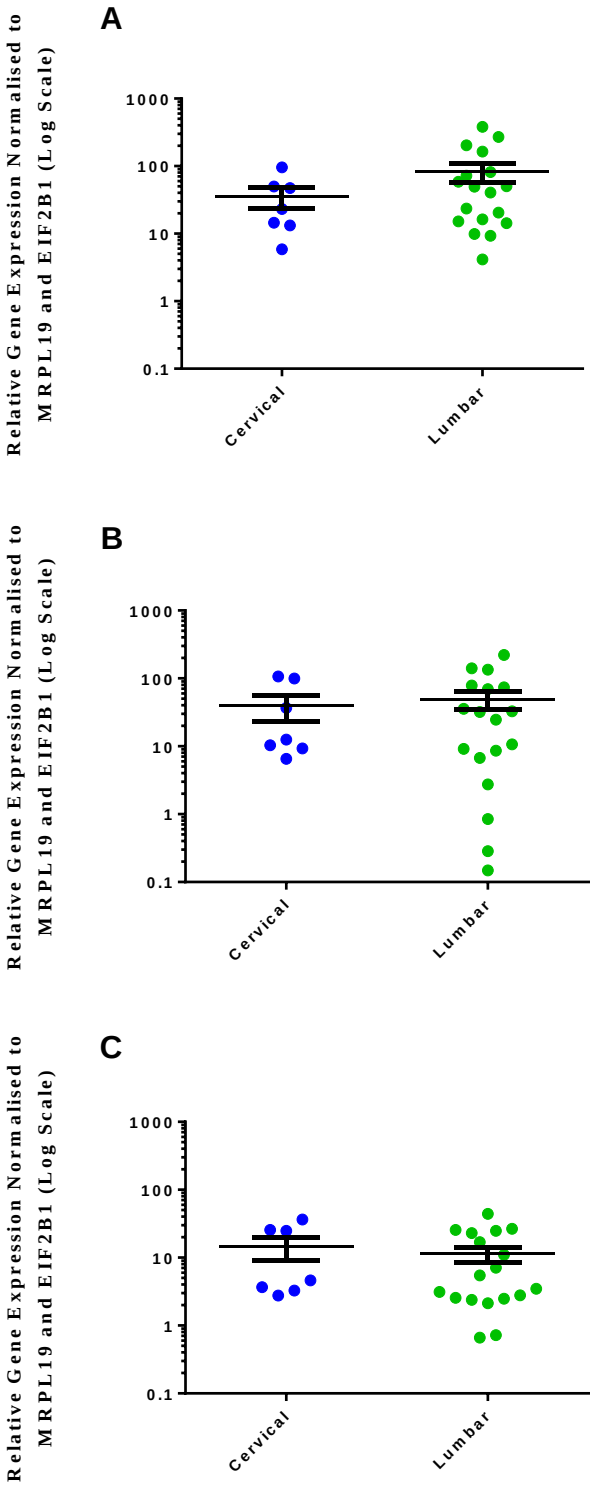

Figure 3.22 TIMP marker gene expression in NP cells derived from adult human severely degenerate cervical and lumbar NP tissue. Gene expression levels of TIMP1 (A), TIMP2 (B) and TIMP3 (C) were compared between cervical (blue) and lumbar (green) severely degenerate specimens. *p=<0.05 **p=<0.01 ***p=<0.001.

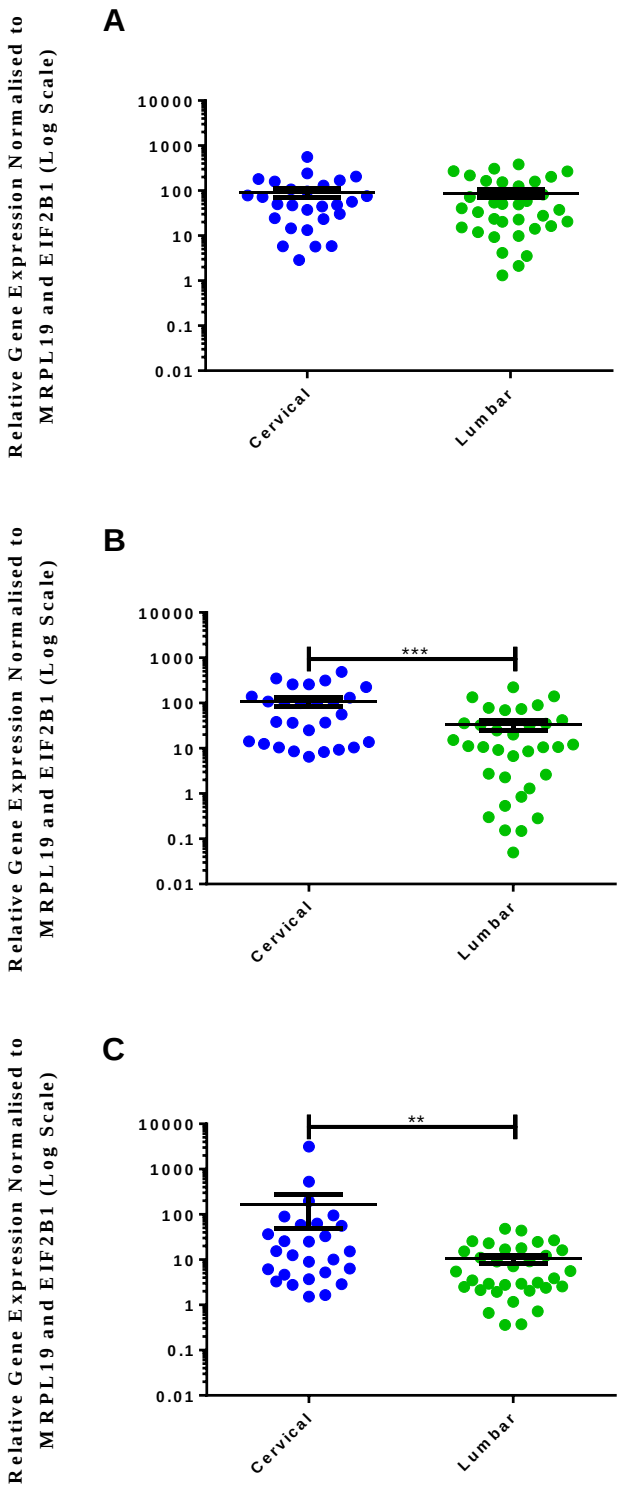

Figure 3.23 TIMP marker gene expression in NP cells derived from adult human cervical and lumbar NP tissue. Gene expression levels of TIMP1 (A), TIMP2 (B) and TIMP3 (C) were compared between cervical (blue) and lumbar (green) specimens. *p=<0.05 **p=<0.01 ***p=<0.001.

3.4.4.3 Pro-Inflammatory Cytokine and Cytokine Receptor Expression

The expression levels of IL-1α, IL-1β, IL-1R, TNF-α, TNFR1A and TNFR1B were assessed to again enable a comparison of the pathological process of disc degeneration in the cervical and lumbar NP. Expression levels of IL-1α (Figure 3.24A p=0.1751), IL-1β (Figure 3.24B p=0.7604), IL-R (Figure 3.24C p=0.2960), TNF-α (Figure 3.24D p=0.5082) and TNFR1A (Figure 3.24E p=0.3013) did not vary significantly between NP cells of the disparate spinal regions. Levels of the TNF-α receptor TNFR1B (Figure 3.24F) were significantly higher in cells of the moderately degenerate cervical NP, as compared to lumbar NP (p=0.0037). Similarly, when expression levels were compared in severely degenerate samples obtained from cervical and lumbar tissue, no significant differences in gene expression levels were noted for any of the pro-inflammatory markers and receptors assessed (IL-1α Figure 3.25A p=0.6445; IL-1β Figure 3.25B p=0.8334; IL-R Figure 3.25C p=>0.9999; TNFR1A Figure 3.25E p=0.9357; and TNFR1B Figure 3.25F p=0.8849), with the exception of TNF-α (Figure 3.25D), where significantly higher levels of expression were noted in lumbar NP specimens as compared to cervical (p=0.0449). When expression levels were compared irrespective of the severity of tissue degeneration, expression levels of IL-1α (Figure 3.26A), IL-1β (Figure 3.26B), IL-1R (Figure 3.26C), TNF-α (Figure 3.26D) and TNFR1A (Figure 3.26E) did not vary significantly between lumbar and cervical specimens (p= 0.3343, p= 0.6064, p= 0.4822, p= 0.0611 and p= 0.5057 respectively). Expression levels of TNFR1B (Figure 3.26F) were significantly greater in cervical as compared to lumbar samples (p= 0.0315).

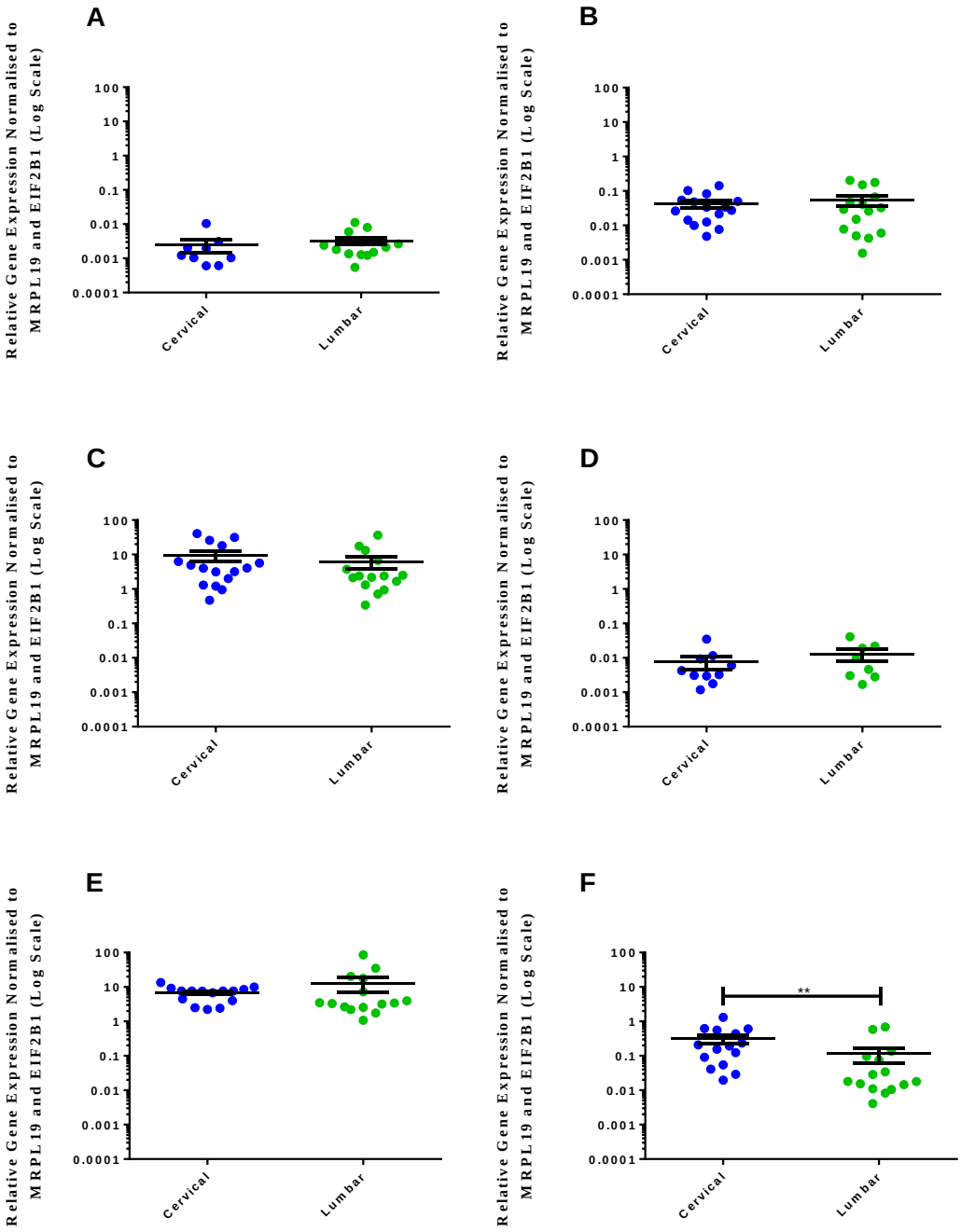

Figure 3.24 Pro-inflammatory cytokine and cytokine receptor gene expression in NP cells derived from adult human moderately degenerate cervical and lumbar NP tissue. Gene expression levels of IL-1α (A), IL-1β (B), IL-1R (C), TNF-α (D), TNFR1A (E), and TNFR1B (F) were compared between cervical (blue) and lumbar (green) moderately degenerate specimens. *p=<0.05 **p=<0.01 ***p=<0.001.

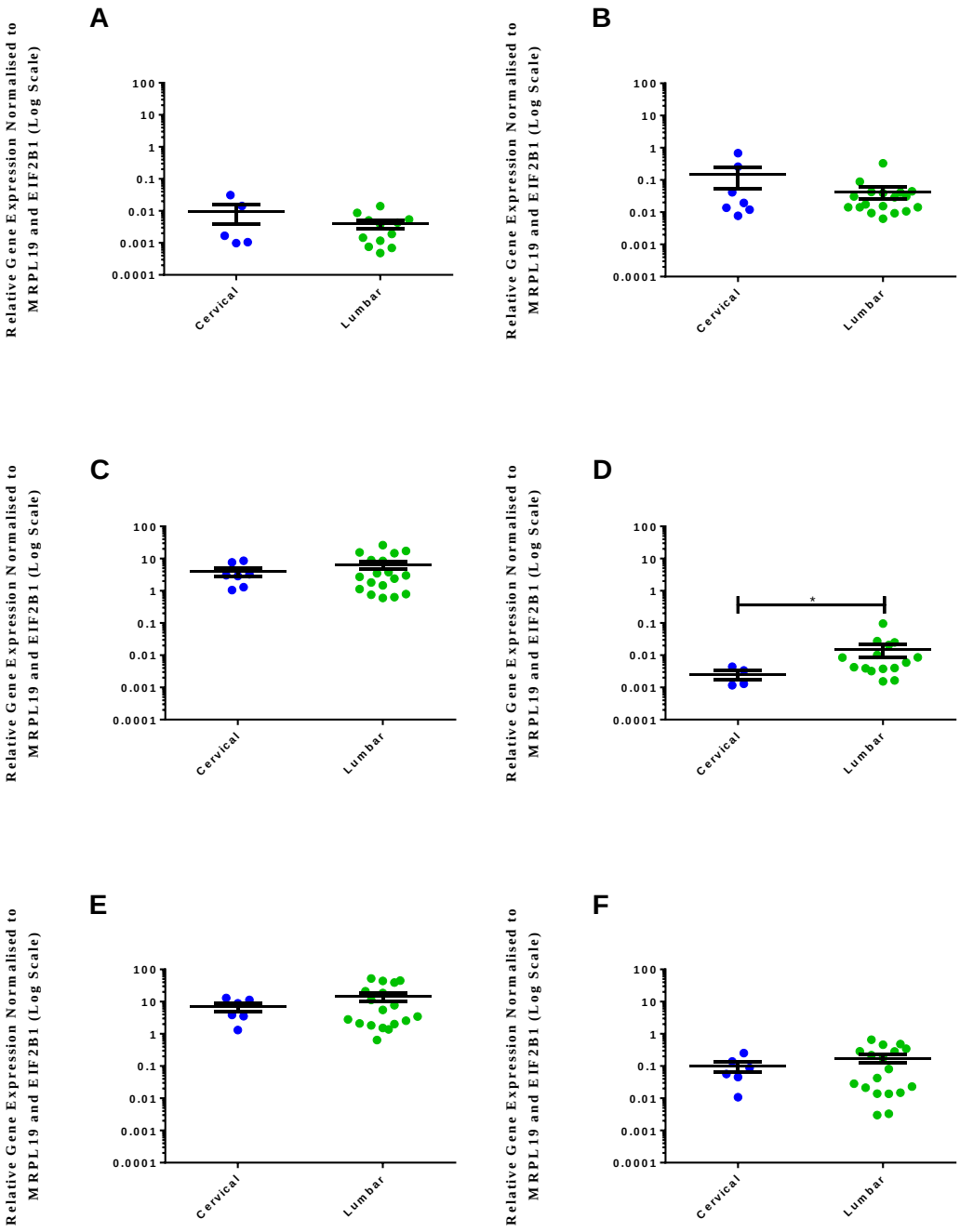

Figure 3.25 Pro-inflammatory cytokine and cytokine receptor gene expression in NP cells derived from adult human severely degenerate cervical and lumbar NP tissue. Gene expression levels of IL-1α (A), IL-1β (B), IL-1R (C), TNF-α (D), TNFR1A (E), and TNFR1B (F) were compared between cervical (blue) and lumbar (green) severely degenerate specimens. *p=<0.05 **p=<0.01 ***p=<0.001.

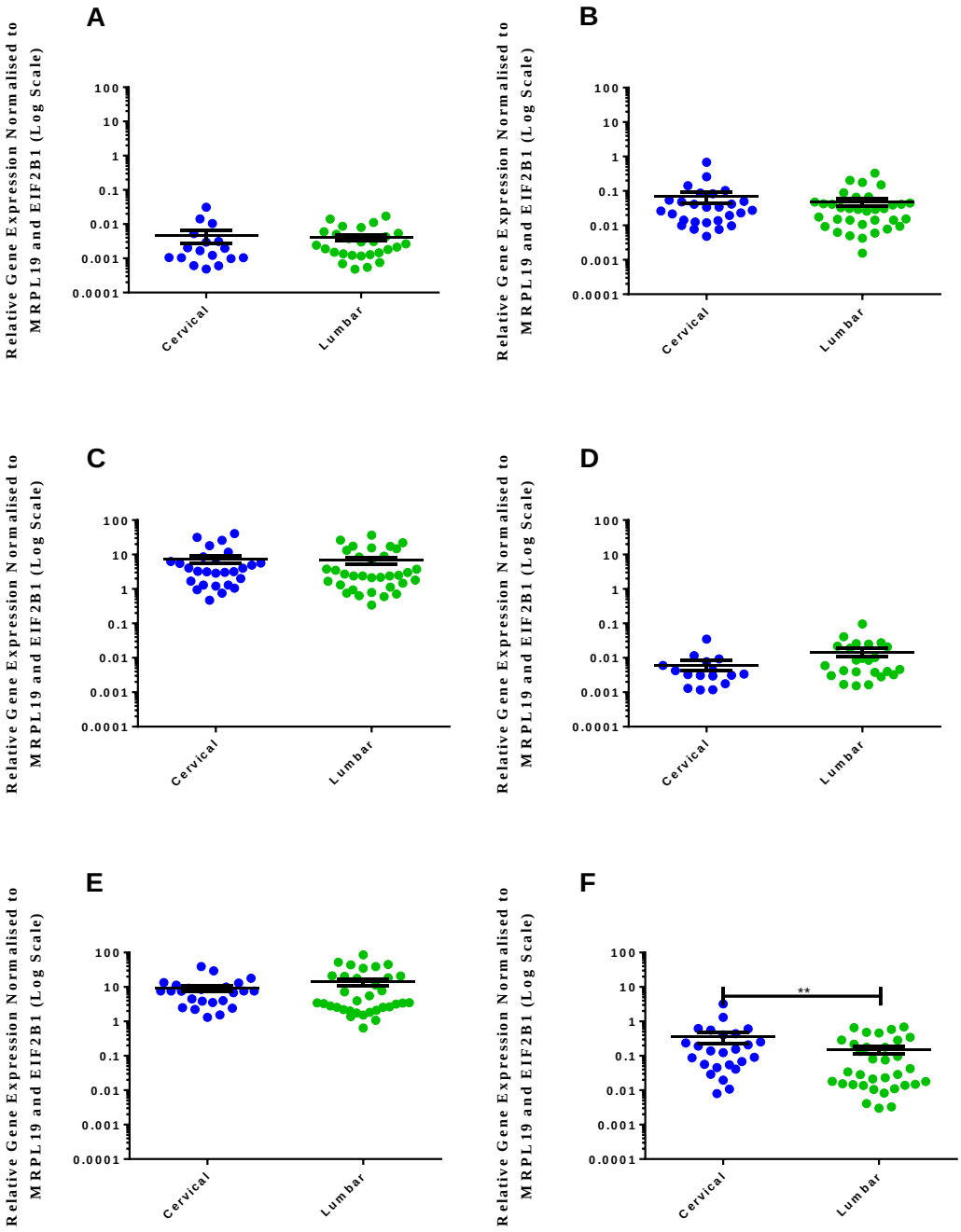

Figure 3.26 Pro-inflammatory cytokine and cytokine receptor gene expression in NP cells derived from adult human cervical and lumbar NP tissue. Gene expression levels of IL-1α (A), IL-1β (B), IL-1R (C), TNF-α (D), TNFR1A (E), and TNFR1B (F) were compared between cervical (blue) and lumbar (green) specimens. *p=<0.05 **p=<0.01 ***p=<0.001.

3.5 Discussion

This investigation has demonstrated that similarities exist between degenerate cervical and lumbar NP tissues in terms of both morphological features of tissue degeneration, as well as the phenotypic expression of genes known to be expressed by degenerate lumbar specimens. Additionally, few statistically significant differences were shown to exist between the gene expression profiles of cells isolated from NP tissue of the two distinct spinal regions.

3.5.1 Histology of Cervical Tissue

Here it has been shown that the criteria outlined by (Sive *et al.*, 2002) for histological grading of the lumbar IVD for severity of tissue degeneration is applicable to specimens isolated from the cervical region also. Tissue cleft formation is frequently observed in IVD degeneration (Gries *et al.*, 2000), and was apparent in numerous cervical disc specimens analysed here. It is hypothesised that clefts originate in the NP and extend into the AF; in extreme cases extending into the CEP also. Cleft formation has previously been identified in 49% of cervical disc specimens obtained during surgery (Kokubun *et al.*, 1996), although distinctions in the severity of the clefts were not made like that outlined previously (Sive *et al.*, 2002), nor was this feature utilised in the grading of samples. Additionally, cell clusters form within the NP with progression of IVD degeneration, and are well characterised in the lumbar NP, but are not well described in the cervical region. Studies have identified the presence of single and clustered cells within the adult human NP (Furusawa *et al.*, 2001), and it appears that clusters become larger with increasing severity of degeneration (Kokubo *et al.*, 2008), although these were graded using previously described magnetic resonance imaging methodologies, which are less sensitive to tissue alterations which might otherwise be identified histologically (Pfirrmann *et al.*, 2001). There is currently no evidence regarding the loss of haemotoxyphilia (due to loss of PG content) and demarcation between the AF/NP in the cervical IVD, and thus the current study is the first to identify these features and apply them to a grading system for use in discs obtained from various spinal regions. Christe *et al.*, adapted a grading system of histological changes (Berlemann *et al.*, 1998) for use in cervical IVDs, although with the exception of cleft formation, characterise none of the features described here. The findings here

are however limited by the exclusive use of surgical specimens and in order to fully confirm the validity of this grading system in the cervical spine, it is essential to test it using a cohort of samples obtained from healthy individuals with no history of neck pain.

3.5.2 Gene Expression in the Adult Human Cervical and Lumbar NP

The chondrocyte marker genes SOX9, COL2A1, ACAN and VCAN have been utilised as markers characteristic of the NP cell and its ECM (Sive *et al.*, 2002), and are expressed at all stages of tissue degeneration in the lumbar spine. However, similar profiling has not been performed in cells of the cervical NP, and as such, there is no existing literature with which to compare this data. In the present study, no variations in SOX9 and COL2A1 were noted with ageing or degeneration, which is in agreement with previously described literature for lumbar specimens (Sive *et al.*, 2002), and the limited data regarding type II collagen expression in the cervical region (Longo *et al.*, 2006, Park *et al.*, 2013). COL2A1 is known to be regulated by SOX9 (Zhao *et al.*, 1997), and thus the findings of parallel unchanged expression is unsurprising. Interestingly, significant increases in expression levels of ACAN and VCAN were noted with increasing age, but not with degeneration. A loss of PG expression with degeneration is well documented (Antoniou *et al.*, 1996), and thus the findings presented here contest the current status quo regarding NP matrix loss with degeneration. However, the specimens examined here were all obtained during surgery, and although some were classed as non-degenerate histologically, clinical symptoms must have been presented in order for the surgery to have been performed. The lack of specimens from asymptomatic individuals for analysis in the current study may therefore serve to explain why no variations were noted in terms of matrix marker expression with degeneration, and inclusion of such specimens in future investigations may yield some significantly different findings. It is possible that at the point of surgical acquisition of specimens, alterations to the phenotype of NP cells have already occurred, and may be indicative of such alterations being an early feature of tissue degeneration, existing prior to surgical intervention. Also, Antoniou *et al*. suggest that during degeneration of the NP ECM, there is evidence for increased denaturation of matrix components, but that parallel alterations to expression levels are not noted, and hence it is possible that the entirely degenerate

cohort of specimens utilised here demonstrate no variations in expression levels with progressing degeneration simply because they are already degenerate.

Additionally, no variations were identified in the gene expression levels of these markers when cervical and lumbar cohorts were compared, with the exception of significantly higher levels of VCAN expression in severely degenerate lumbar NP cells as compared to cervical. This implies that the cervical and lumbar NP cell gene expression profile is comparable, which may be indicative of highly similar ECM composition, and suggests that mechanisms controlling expression of these markers is identical in the upper and lower spine IVDs. Following the *in vitro* induction of degeneration in human cervical and lumbar NP cells, expression levels of type I and type II collagen levels were significantly different between lumbar and cervical samples, with higher expression noted in cervical NP cells (Park *et al.*, 2013), which does not match with the data generated here. However, the cells assessed in the aforementioned study were stimulated with TGF-β1 and BMP2 cytokines in order to assess the cellular response, and it is therefore possible that the similar expression levels of COL2A1 noted here are due to the varied cytokine milieu that NP cells are exposed to *in vivo*, which is not limited to a cocktail of two cytokines. The present study does however confirm the findings of similar SOX9 and ACAN gene expression in degenerate lumbar and cervical specimens elucidated previously (Park *et al.*, 2013). Versican is a hyaluronan-binding PG and is thought to play a role in cell adhesion, migration, proliferation and differentiation (Cattaruzza *et al.*, 2004, Landolt *et al.*, 1995, Zhang *et al.*, 1998). There is evidence from studies of other tissues that mechanical loading regulates expression of versican (Robbins *et al.*, 1997, Grande-Allen *et al.*, 2004). Tendon and mitral valve investigations have demonstrated that compressive load is associated with increased expression of versican (as much as 130% increased expression), but the underlying regulatory network has yet to be elucidated. Given that the compressive strength of cervical IVDs is only 45% that of the lumbar, it could be hypothesised that the differences in expression levels of this molecule can be attributed to their exposure to distinct mechanical loading stimuli (Przybyla *et al.*, 2007). As it was demonstrated that expression levels of SOX9, COL2A1 and ACAN did not vary, it would be reasonable to assume that the cervical and lumbar NP cell phenotype is comparable in terms of chondrogenic marker expression.

MMPs and ADAMTSs are molecules frequently identified in the degenerate intervertebral disc, where they break down extracellular matrix components. This is generally paralleled with decreased matrix anabolism, and this catabolic shift in NP cell phenotype results in a loss of ECM integrity (Richardson *et al.*, 2009, Pockert *et al.*, 2009, Millward-Sadler *et al.*, 2009, Le Maitre *et al.*, 2007c, Le Maitre *et al.*, 2006, Le Maitre *et al.*, 2004a). TIMPs are competitive inhibitors of numerous MMPs and ADAMTSs, and their expression is often thought to ameliorate the detrimental effects of matrix degrading enzymes (Le Maitre *et al.*, 2004a, Vo *et al.*, 2013). In this study, ADAMTS expression did not vary with degeneration across a cohort of cervical specimens, and most of the isoforms analysed showed no variation with ageing either. Similarly, MMP expression did not alter with degeneration, whilst some decreases in MMP expression with ageing were observed. TIMP expression demonstrated no clear trends with ageing or degeneration when assessed in the cervical cohort. This is in disagreement with previously described literature (Le Maitre *et al.*, 2004a, Pockert *et al.*, 2009), which indicates that expression of these markers is increased with progressing severity of degeneration, although these studies utilised non-degenerate specimens not obtained from surgery during analysis, which is not included in the present study, and may therefore explain why differences were noted. It could also be hypothesised that (like for the NP cell markers discussed previously) degenerative alterations to NP cell phenotypic expression precedes the onset of clinical symptoms, and comparisons of expression levels of specimens tested here, with those of asymptomatic individuals may confirm this.

ADAMTS expression was generally mirrored in lumbar and cervical NP cells, both in the moderate and severe stages of IVD degeneration and across the entire cohorts irrespective of degenerative score. ADAMTS4 was more highly expressed in moderately degenerate cervical NP cell specimens as compared to lumbar, but demonstrated no variation in the most severely degenerate specimens or across the cervical and lumbar cohorts as a whole. Evidence to explain these variations is limited. ADAMTS4 is known to regulate turnover of versican, which was also differentially expressed in this study, but at different stages of disc degeneration (Westling *et al.*, 2004, Gao *et al.*, 2002). Also, ADAMTS4 is known to be upregulated when exposed to greater compressive loads (Walter *et al.*, 2011), but

compressive loads are higher in lumbar than cervical IVDs (which may explain increased versican expression in the same specimens), and thus does not apply here. Additionally, the expression of ADAMTS4 has been demonstrated to be controlled by pro-inflammatory cytokine signalling (Tian *et al.*, 2013), but as IL-1β and TNF-α expression is unchanged here, is likely not the appropriate explanation for this variation either. Additionally, this variation was not noted at the most severe stages of IVD degeneration, as one might have expected. However, this may be due to the large differences in sample number between the cervical (n=7) and lumbar (n=17) severely degenerate cohorts, and perhaps more evenly matched specimen numbers would confer some significant differences in terms of ADAMTS4 gene expression.

Expression levels of all MMP isoforms analysed demonstrated no variations between lumbar and cervical NP cells. MMP expression has previously been demonstrated in the cervical IVD, but the novel data highlighted by this investigation has confirmed that degenerative processes involving these molecules may be comparable between cervical and lumbar discs. TIMP expression was not variable in severely degenerate specimens, but isoforms -2 and -3 were significantly more highly expressed in moderately degenerate cervical NP cells than lumbar, and in the total cervical cohort as compared to the total lumbar cohort. To date, the literature suggests that increases in TIMP expression in cartilage may be attributed to increased compressive load and/or IL-1-induced expression of degradative enzymes (Torzilli *et al.*, 2011). However, it has also been hypothesised that exposure to shorter periods of compressive load may result in increased TIMP expression as compared to those exposed to for a longer period of time (Wuertz *et al.*, 2009), however given that the cells of the lumbar NP are exposed to greater loads than that of the cervical NP and that TIMP expression is higher in cervical specimens, this cannot form a possible explanation. Thus, expression of matrix degrading enzymes and their inhibitors is largely comparable between cervical and lumbar specimens, indicating that cervical tissues are as applicable as lumbar for *in vitro* investigation and that phenotypic variation between samples from either spinal region will not influence such studies.

There was no variation in gene expression levels of either IL-1 isoform or their receptor between cervical and lumbar IVD specimens at either stage of tissue degeneration or across the cohorts as a whole; however TNF-α expression was significantly greater in severely degenerate lumbar specimens as compared to

cervical (but this was not noted when entire cohorts were compared), and increased TNFR1B in moderately degenerate cervical samples as compared to lumbar, as well as in the total cervical cohort as compared to lumbar. TNF-α has been demonstrated to play a role in degenerative processes in the lumbar IVD, although it was only expressed in 59% of specimens (Le Maitre *et al.*, 2007b); but to date there is no evidence of expression in the cervical IVD. This study has highlighted for the first time, that TNF-α is expressed in the cervical IVD, but confirms previous data of expression in approximately half of specimens tested, with 4/7 severely degenerate cervical NP specimens expressing the cytokine. The finding of increased TNF-α expression in severely degenerate lumbar specimens as compared to cervical may be as a consequence of differing mechanical loads between the two spinal regions. Increased load is known to induce expression of TNF-α (Wang *et al.*, 2007), and as it is also known that mechanical loads are greater in the lumbar as compared to cervical NP (Przybyla *et al.*, 2007), it is possible that although degenerative processes are similar in cervical and lumbar discs, differing environmental conditions (such as mechanical load) may influence the extent to which TNF-α is expressed. The literature has previously described the expression of TNFR1B in the lumbar IVD (Le Maitre *et al.*, 2007b), and this study is therefore the first to describe its expression in the cervical region. However, there is little evidence to explain why TNFR1B expression would be increased in cervical tissue specimens as compared to lumbar. Studies in the mammalian heart have demonstrated that load does not affect TNFR1 expression (Baumgarten *et al.*, 2002), although it appears that reactive oxygen species (ROS) may mediate increased expression of the receptor in murine neuronal cells (Ma *et al.*, 2009), but to date, there has been no comparison of ROS levels in cervical and lumbar IVDs. Thus, as the expression levels of NP cell phenotypic marker genes, and genes expressed in the degenerate lumbar NP are largely comparable, this would suggest that cervical NP tissue is applicable for use in *in vitro* techniques related to IVD biology and degeneration, thereby increasing the range of specimens available for study, rather than merely limiting to just lumbar samples. Given the differences in morphology of cervical and lumbar IVDs, it was hypothesised that some distinctions in the phenotype of the respective NP cells would be noted. Generally, this has not been found, however, given that load varies between the spinal regions, assessment of markers associated with load may elucidate phenotypic distinctions between lumbar and cervical NP cells. Regarding

the expression of markers associated with disc degeneration, the current study is limited by the lack of non-degenerate tissue specimens for comparison. However, as the vast majority of human specimens for research are obtained through surgery (as cadaveric tissue availability is extremely low), validation in degenerate cohorts such as these are of upmost importance, as it is samples such as these that will be utilised in *in vitro* research. Finally, a panel of novel markers of the NP cell phenotype have recently been identified by (Minogue *et al.*, 2010a, Minogue *et al.*, 2010b), and it would be useful to determine the expression levels of these markers in NP cells both cervical and lumbar in origin.

3.5.3 Implications of this Investigation

This investigation has confirmed that cervical NP tissues/cells are comparable to lumbar in terms of the expression of chondrocyte markers and molecules expressed in degeneration, thus providing a new model in which to study IVD biology, degeneration and regeneration, rather than being limited to lumbar specimens. For any study of human disease processes, it is preferential to investigate using human samples rather than those obtained from an animal model, which may not always be appropriate for study of the IVD. Also, given the limited numbers of investigations currently carried out in cervical IVDs, this work may enable a better understanding of cervical disc degeneration, perhaps aiding the development of novel treatments for chronic neck pain that overcome the limitations of commonly used conservative treatments.

Chapter 4:

Investigating the Cell Population of the Adult Human Nucleus Pulposus

4.1 Background

As described in 1.8, evidence has been presented over recent years that challenges the classic concept of the NP cell phenotype. Briefly, NP cells were previously considered chondrocyte-like, as demonstrated by their similar morphology and phenotype (Sive *et al.*, 2002). However, the elucidation of distinct differences in the ECM synthesised by NP and hyaline cartilage cells intimated that the two cell types were not phenotypically similar (Mwale *et al.*, 2004). Microarray investigations have profiled NP and AC cells in a range of animal models (Lee *et al.*, 2007, Sakai *et al.*, 2009), but were limited by the lack of agreement on the top differentially expressed marker genes; a feature attributed to interspecies variation. Analysis of the bovine and human NP and AC cell phenotypes described the expression of a number of novel NP cell marker genes (Minogue *et al.*, 2010a, Minogue *et al.*, 2010b, Power *et al.*, 2012), applicable to both species, which could subsequently be used to define adult human NP cells. However, a number of limitations still apply to these studies, and further investigation is required in order to fully characterise cells of the adult human NP tissue.

The major limitation of these microarray investigations is the small number of samples in the analysed cohorts. Specimens from no more than 6 patients were utilised in bovine and human array studies (Minogue *et al.*, 2010a, Minogue *et al.*, 2010b, Power *et al.*, 2012), which although sufficient for noting phenotypic differences between two distinct cell phenotypes, cannot allow for full characterisation of the NP cell phenotype across a range of ages and levels of tissue degeneration in the human population. It is therefore essential that the expression of these markers is assessed in a large cohort of adult human specimens, and expression levels correlated to both age and tissue degeneration. A small number of studies have, however, identified age as a factor influential to the NP cell phenotype. Gene expression levels of KRT19 have been demonstrated to decrease significantly with age (Rutges *et al.*, 2010), whilst CAXII expression is negatively correlated with both age and severity of IVD degeneration (Power *et al.*, 2012), and it is postulated therefore, that the age of specimens may denote the expression levels of NP cell markers, and this therefore requires investigation. Additionally, as highlighted by Table 1.3, much research has been conducted into gene expression levels, but little analysis has been performed investigating marker expression at the protein level. As

such, a full understanding of the NP phenotype can only be obtained when protein localisation of novel markers has been elucidated, and expression patterns analysed.

It is also imperative to identify whether any sub-populations of cells exist within the adult human NP, in order that the roles of such cells can be fully determined. Evidence has been presented which suggests that the adult human NP is comprised of a heterogeneous cell population (Gilson *et al.*, 2010, Weiler *et al.*, 2010) with regards to the expression of novel NP markers, and thus, these recently identified markers require localisation in order to determine whether they mark all, or a subset of, adult human NP cells. Additionally, the potential existence of NP cell sub-populations is also highlighted by the identification of progenitor cell populations within the adult human NP (Blanco *et al.*, 2010, Erwin *et al.*, 2013, Risbud *et al.*, 2007, Sakai *et al.*, 2012). Taken together, this evidence suggests that the NP may be comprised of cellular sub-populations. A comprehensive description of these cells with regards to phenotype is crucial as it may allow for the elucidation of the role of these discrete cell sub-populations *in vivo*. As a number of novel NP markers have recently been identified, the human NP cell phenotype can now be fully characterised, a unique aspect of NP cell biology not previously investigated. An understanding of whether the NP is comprised of a homogenous or heterogeneous cell population is essential in order that these novel NP markers can be used unquestionably in future research, and given the limited protein expression data previously described for these genes, it is essential that it is determined whether these markers are cell subset-specific. Finally, the discovery of NC cell marker gene expression in cells of the NP is suggestive of a common ontogeny between NP and NC cells (Minogue *et al.*, 2010a, Minogue *et al.*, 2010b, Weiler *et al.*, 2010), although it is a contentious issue as to whether adult human NP cells are notochordally-derived, or arise as a result of mesenchymally-derived AF cell infiltration into the NP during tissue maturation. It is postulated that tissue which will go on to form the adult NP is in fact synthesised by the surrounding mesenchyme during development; a process driven by NC cells which then undergo a form of cell death (Hunter *et al.*, 2003a, Vujovic *et al.*, 2006). Markers characteristic of bone marrow-derived MSCs have been noted as expressed within the human NP, supporting the theory than the NP may be mesenchymally-derived (Risbud *et al.*, 2007). However, AF cells are thought to infiltrate the NP during

degeneration, and this infiltration is hypothesised to be an endogenous attempt at repairing tissue damage (Walsh *et al.*, 2004), and would therefore explain the finding of mesenchymal marker expression in cells residing within NP tissue. Similarly, the detection of AF markers within NP tissue samples may be due to contamination of the tissue during dissection with AF specimens. The potential for NC cells to influence the differentiation of MSCs has been investigated through the use of NC cell-conditioned media, and demonstrated increased expression of GAG and collagen isoforms associated with disc development, suggesting that NC cells may directly influence the chondrogenic differentiation of MSCs; a process that may result in the formation of the NP *in vivo* (Korecki *et al.*, 2010). The expression of such markers is yet to be fully studied at either the gene or protein level, but such analyses may enable a better understanding of the developmental origins of adult human NP cells, whilst protein localisation analyses may also confirm whether adult human NP cells express a range of NC markers despite the fact that the cells populating the tissue no longer resemble NC cells in terms of morphology.

4.2 Aims and Hypotheses

As discussed, previous investigations have identified a range of novel NP markers using both human and animal models, but expression levels in a human cohort spanning a range of degenerative scores and ages has not been investigated. Additionally, evidence from microarray studies has suggested that NC cell marker genes are expressed by adult human NP cells, but it is unclear whether this expression is as a result of the postulated notochordal origin of adult NP cells, or whether a NC cell sub-population persists in the adult human NP that resembles NP cells in terms of morphology, whilst retaining expression of NC cell marker genes. Non-ubiquitous expression of some novel NP cell markers has been described, and is suggestive of the existence of phenotypically-distinct adult NP cell sub-populations, and this may be confirmed through localisation studies of novel NP and NC cell markers.

Given that a handful of studies have identified some age/degeneration related trends in the expression levels of some novel NP cell markers, it is hypothesised that expression levels of NP and NC cell marker genes will also vary here, with decreased NC cell marker expression associated with age and/or degeneration. As many of these novel NP cell markers were highly expressed in NP cell samples analysed by microarray, protein expression levels of these markers is likely to be ubiquitous throughout the NP, whilst it is hypothesised that NC cell marker proteins will be localised to only a subset of NP cells. Finally, if NC cell proteins are in fact shown to be expressed by a subset of NP cells, it is hypothesised that it will be the same sub-population of cells expressing all NC markers, identifying a distinct NC cell sub-population existing within the adult human NP.

The aims of this investigation were threefold:

1) To validate novel NP cell marker genes recently identified by microarray analysis in a large cohort of adult human specimens, and correlate levels of gene expression with patient age or severity of tissue degeneration.
2) To localise expression of novel NP and NC cell marker proteins to cells of the adult human NP in order to ascertain whether expression is noted in all

cells or a subset of NP cells. Expression levels will also be analysed according to age or histological level of degeneration.

3) To assess whether a subset of novel NP and NC cell marker genes are co-expressed by the same cells thereby identifying discrete NP cell sub-populations.

4.3 Experimental Design

A cohort of adult human NP specimens (including both lumbar and cervical disc levels, n=62) were utilised in this investigation of the adult NP phenotype. Gene expression analysis was first performed, followed by extensive protein localisation (immunohistochemistry) experiments, and multi-labelling flow cytometry protocols performed in order to investigate cell sub-populations within the NP.

4.3.1 Confirmation of Microarray Findings by Quantitative Real-Time PCR

Samples utilised are listed in Tables 2.1 and 2.2. Briefly, specimens were subject to cell isolation, RNA extraction and cDNA synthesis as described in sections 2.1.3, 2.2.2, 2.2.3 and 2.2.4. cDNA was then assessed by qPCR for a number of genes: novel NP genes (FOXF1, PAX-1, KRT8, KRT18, KRT19, CAXII), novel NP negative genes (IBSP, FBLN1) and notochordal genes (NOTO, T, FOXA2, CHRD, NOGGIN, LGALS3, CD24) in accordance with the protocol outlined in 2.2.6. Details of sequences for primers and probes, and optimal primer concentrations are listed in Table 2.3. Gene expression levels were analysed as explained in 2.2.8 and statistical significance determined as detailed in 2.2.9.

4.3.2 Immunohistochemical Analysis of Protein Expression

In order to assess whether phenotypic markers identified at the gene level were expressed as proteins and to determine whether they are expressed by all adult human NP cells, or a subset of cells, wax-embedded sections of all of the samples assessed by qPCR (listed in Tables 2.1 and 2.2) were then subject to protein expression analysis by means of immunohistochemistry for a number of proteins: FoxF1, Pax-1, Krt8, Krt18, Krt19, Carbonic anhydrase-12, Brachyury, Galectin-3 and CD24. The protocol is outlined in 2.3.6, with assay specific parameters detailed in Table 2.8. Image analysis was performed as described in 2.3.8. Staining levels were quantified by performing cell counts. Briefly, the tissue was first divided into NP and AF portions, and where the tissue was considered to be located in the IAF/NP boundary, this was excluded from analysis. The total number of cells within each region was counted, as well as the number of positively stained cells. The percentage of immunopositive cells was then calculated for both the NP and AF of

each sample. Additionally, the immunopositivity of single cells vs. clustered cells was calculated by counting the total number of cells localised in clusters (Figure 4.1) of 2 cells or more, as well as the number of these cells stained positively for the protein of interest.

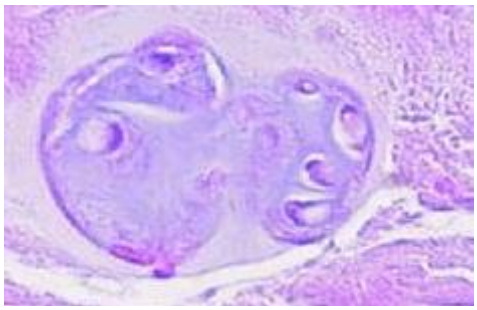

Figure 4.1 Morphology of NP cell clusters. NP cells localised in clusters have atypically-shaped cell nuclei, and are localised in clusters containing various numbers of cells. Adapted from (Sive *et al.*, 2002).

4.3.3 Multi-Labelling Flow Cytometry

Although immunohistochemical techniques are advantageous in that they allow for localisation of protein expression, flow cytometry was performed to elucidate expression levels of multiple proteins simultaneously.

4.3.3.1 Equipment and Reagents

4.3.3.1.1 Equipment

CyanADP Flow Cytometer	Beckman Coulter
405nm Laser	Beckman Coulter
488nm Laser	Beckman Coulter
635nm Laser	Beckman Coulter
450/50 bandpass filter	Beckman Coulter
530/40 bandpass filter	Beckman Coulter
575/25 bandpass filter	Beckman Coulter
665/20 bandpass filter	Beckman Coulter
Summit 4.1 Data Analysis Software	Beckman Coulter

4.3.3.1.2 Reagents

Bovine Serum Albumin (BSA)	Gibco
Dulbecco's Phosphate Buffered Solution (PBS)	Sigma Aldrich
EDTA	Sigma Aldrich
Methanol	Fisher Scientific

4.3.3.2 Flow Cytometry Methodology

Cells were isolated from fresh surgical tissue, as described in 2.1.3.1. Cells were washed in 1ml sterile PBS to remove excess media and tissue contaminants, and the cell suspension filtered using a 40µm cell sieve into a 15ml centrifuge tube. Cells were counted using a haemocytometer, and aliquoted into 1.5ml centrifuge tubes, so that each tube contained $1x10^6$ cells. For each sample stained using the conjugated antibodies, a duplicate sample was stained using the relevant conjugated IgG controls. Cells were pelleted by centrifugation at 700g for 7 minutes at 4°C. Cell membrane-bound antigens for CD24 were first stained prior to fixation and permeabilisation of cells for intracellular antigen staining in order to negate the issue of damaging the cell membrane antigens in the alcohol-based fixation method. Details of all flow cytometry antibodies can be found in Table 4.1. Briefly, CD24 antibody (2.5µg/µl) in buffer (PBS pH 7.2 supplemented with 0.5% (w/v) BSA and 2mM EDTA) and cells resuspended in 200µl antibody/buffer solution. A second sample was resuspended in 200µl isotype control/buffer solution. The specimens were incubated for 30 minutes at 4°C, and 800µl buffer added to each tube before centrifuging at 700g for 7 minutes at 4°C. The supernatant was aspirated from pelleted cells and the pellet resuspended in 1ml buffer. The samples were again centrifuged at 700g for 7 minutes at 4°C to pellet cells, and once complete, the supernatant aspirated. Cells were then fixed and permeabilised by resuspending cells in 1ml 100% methanol and incubating for 10 minutes at 4°C. Tubes were then centrifuged at 2000g for 7 minutes at 4°C to pellet cells, and methanol removed by aspiration. Excess methanol was removed by washing cells in 1ml buffer and centrifuging at 1000g for 7 minutes at 4°C. An antibody solution comprised of 200µl buffer and dilutions of the remaining 3 intracellular antibodies (Brachyury 150µg/µl, Galectin-3 200µg/µl, and Carbonic anhydrase-12 0.1µg/µl) was applied to pelleted cells, and samples incubated for 30 minutes at 4°C. The sample assigned as isotype control was incubated in a solution of buffer and a cocktail of the relevant conjugated isotype controls. After incubation, a further 800µl buffer was applied to each tube, and then centrifuged at 1000g for 7 minutes at 4°C. The antibody/buffer solution was removed by aspiration, and finally, cells were resuspended in 300µl buffer prior to analysis.

In order to allow for compensation of PE- and Alexa Fluor488-conjugated antibodies, staining was also assessed individually (i.e. antibodies used singularly rather than a cocktail of 4) using the same protocol outlined here. Appropriate isotype controls were also assessed individually. Samples were analysed using a CyanADP flow cytometer, using the following protocol:

- For detection of PE staining: 488nm laser; 575/25 bandpass filter
- For detection of APC staining: 635nm laser; 665/20 bandpass filter
- For detection of Alexa Fluor488 staining: 488nm laser; 530/40 bandpass filter
- For detection of Pacific Blue staining: 405nm laser; 450/50 bandpass filter

Table 4.1 Details of Antibodies used for Flow Cytometry

Protein of Interest	Supplier Information	Antibody Working Concentration	Isotype Control	Isotype Control Working Concentration
Brachyury (APC-conjugated)	R&D Systems (IC20851A)	150µg/µl	Mouse IgG 2B Isotype Control-APC (R&D Systems IC0041A)	150µg/µl
Carbonic Anhydrase-12 (PE-conjugated)	Bioss USA (bs-6025R-PE)	0.1µg/µl	Rabbit IgG Isotype Control PE-conjugated (Bioss USA bs-0295P-PE)	0.1µg/µl
CD24 (Pacific Blue-conjugated)	Exbio Antibodies (PB-503-T100)	2.5µg/µl	Mouse IgG1 Control Pacific Blue-conjugated (Exbio AntibodiesPB-457-C100)	2.5µg/µl
Galectin-3 (Alexa Fluor488-conjugated)	R&D Systems (IC1154G)	200µg/µl	Goat IgG Control Alexa Fluor488 (R&D Systems IC108G)	200µg/µl

4.3.3.3 Flow Cytometry Data Analysis

All data analysis was performed using Summit 4.1 software. Briefly, dual parameter dot plots of forward scatter versus pulse width and forward scatter versus side scatter were created to gate samples and remove cells in clusters and dead cells from analysis. Then, isotype controls were compared to staining observed in samples incubated with primary antibody to ensure that good separation of the two was noted. Dual parameter dot plots were then created for each possible fluorochrome combination. Firstly, isotype control data was loaded, and a quadrant drawn to indicate the boundary between isotype and non-isotype staining. The data from the antibody-stained samples was then loaded into these same plots, and the percentage positivity taken from these graphs. Expression levels were correlated to patient age and degenerative score, and statistical significance determined by Spearman's Rank correlation.

4.4 Results

4.4.1 Comparison of Gene Expression in Cervical and Lumbar IVD Specimens

The evidence presented in Chapter 3 indicated that gene expression levels between cervical and lumbar disc specimens is comparable, and that the samples can be used interchangeably for *in vitro* research purposes. In order to validate novel marker genes identified by microarray in a cohort comprised of tissues from both regions, the expression levels of NP and NC cell marker genes in cervical and lumbar NP specimens was assessed.

Analysis of novel NP markers FOXF1, PAX-1, KRT8, KRT18, KRT19 and CAXII (Figure 4.2) demonstrated that expression of FOXF1 (Figure 4.2A), PAX-1 (Figure 4.2B), KRT18 (Figure 4.2D), KRT19 (Figure 4.2E) and CAXII (Figure 4.2F) did not vary significantly between cervical and lumbar NP cells (p= 0.2626, p= 0.3853, p= p= 0.1327, p= 0.1917 and p= 0.1209 respectively). KRT8 gene expression levels (Figure 4.2C) were significantly higher in cervical specimens as compared to lumbar (p= 0.0014). When expression levels of notochordal cell marker genes NOTO, FOXJ1, T, FOXA2, CHRD, NOGGIN, LGALS3 and CD24 were compared between cervical and lumbar NP cells, FOXJ1 (Figure 4.3B), FOXA2 (Figure 4.3D), CHRD (Figure 4.3E), NOGGIN (Figure 4.3F), LGALS3 (Figure 4.3G) and CD24 (Figure 4.3H) did not vary significantly between samples (p= 0.3571, p= 0.2206, p= 0.9982, p= 0.4799, p= 0.2262, p= 0.1595 respectively). Expression levels of NOTO (Figure 4.3A) and T (Figure 4.3C) did however vary significantly, with NOTO more highly expressed in cervical as compared to lumbar NP cells (p= 0.<0001), whilst conversely, T was more highly expressed in lumbar NP samples (p= 0.0002). Thus, gene expression levels of novel NP and notochordal marker genes was largely comparable between lumbar and cervical specimens, confirming evidence presented in chapter 3, and intimating that samples from both spinal regions can be used interchangeably.

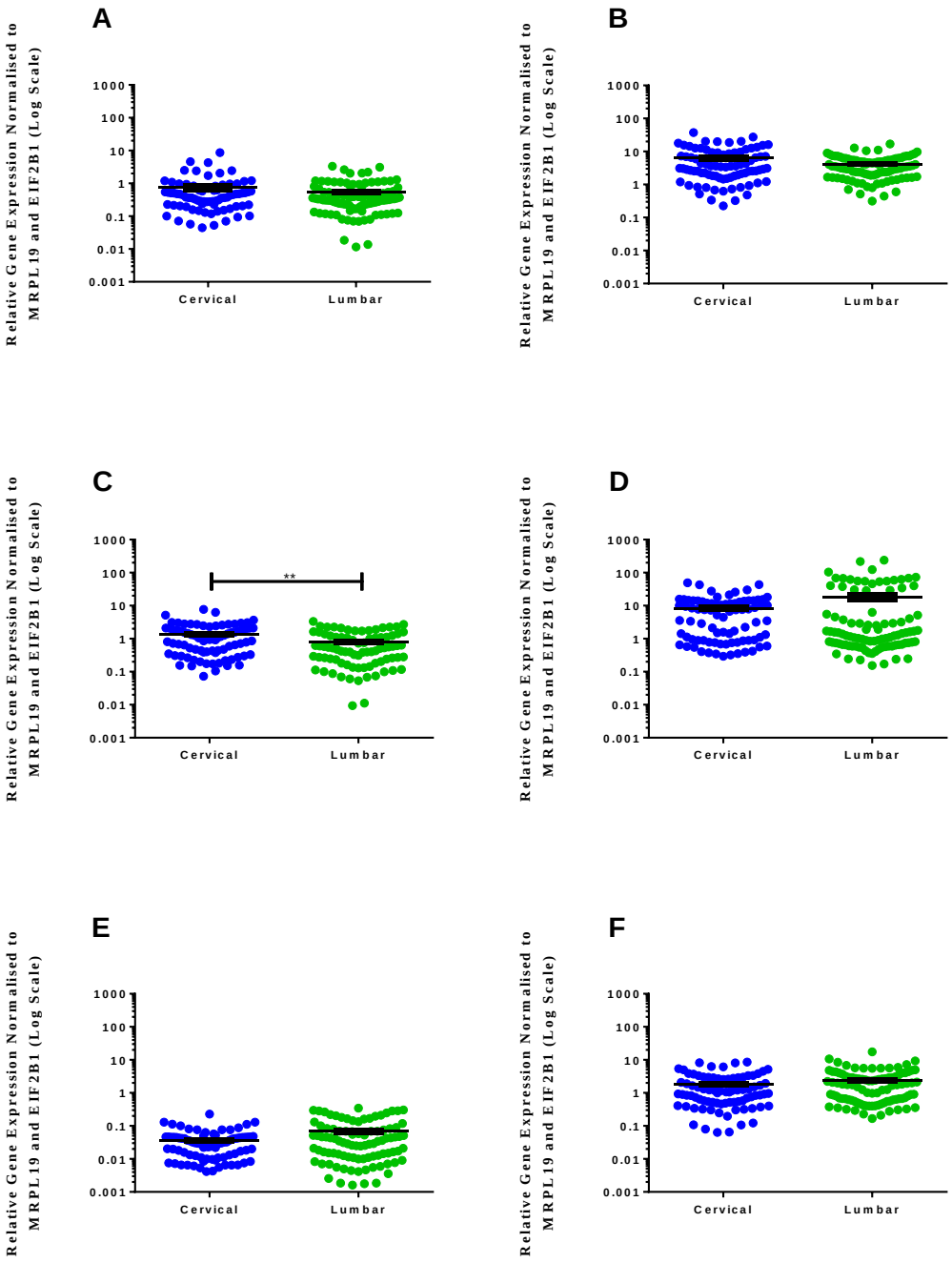

Figure 4.2 Novel NP cell marker gene expression in NP cells derived from adult human cervical and lumbar NP tissue. Gene expression levels of FOXF1 (A), PAX-1 (B), KRT8 (C), KRT18 (D), KRT19 (E), and CAXII (F) were compared between cervical (blue) and lumbar (green) cohorts. **p=<0.01.

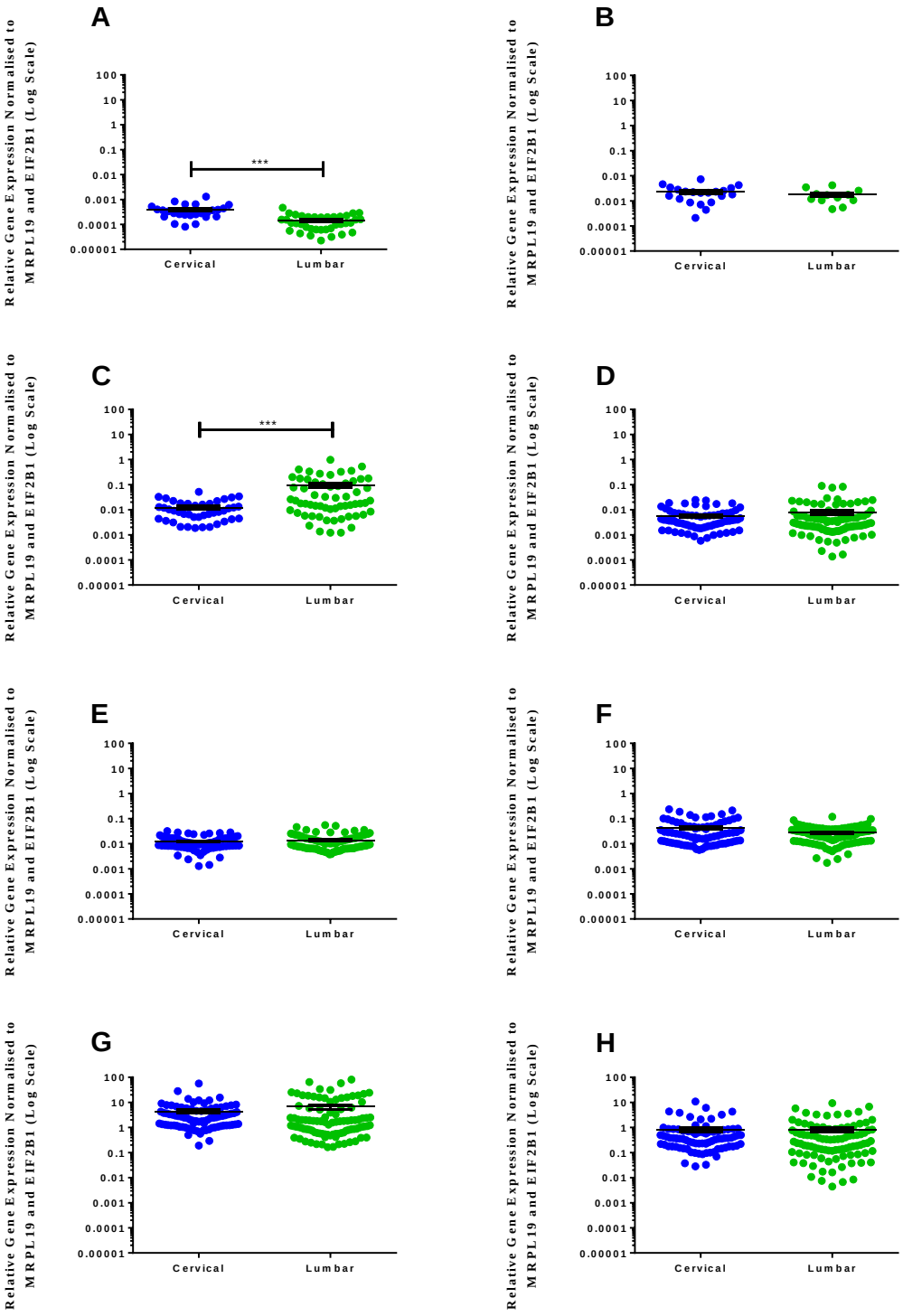

Figure 4.2 Notochordal cell marker gene expression in NP cells derived from adult human cervical and lumbar NP tissue. Gene expression levels of NOTO (A), FOXJ1 (B), T (C), FOXA2 (D), CHRD (E), NOGGIN (F), LGALS3 (G) and CD24 (H) were compared between cervical (blue) and lumbar (green) cohorts. ***p=<0.001.

4.4.2 Validation of Novel NP Cell Marker Genes

The expression of novel NP cell marker genes identified by microarray FOXF1, PAX-1, KRT8, KRT18, KRT19 and CAXII was assessed in a large cohort of human specimens and analysed according to age and level of degeneration. With regards to variations with patient age, FOXF1 (Figure 4.4A) gene expression was significantly greater in young adult as compared to mature adult specimens (p= 0.0077), but expression levels did not differ between young vs. elderly and mature vs. elderly samples (p= 0.5054 and p=0.3925 respectively). With regards to PAX-1 expression (Figure 4.4B), young adult specimens expressed significantly higher levels of the gene when compared to mature adult (p= 0.0495). There were no further variations in expression with regards to young adult vs. elderly adult and mature adult vs. elderly adult comparisons (p= 0.4292 and p= 0.5999 respectively). Expression levels of KRT8 (Figure 4.4C) and KRT18 (Figure 4.4D) did not vary significantly between young and mature adult specimens (p= 0.6918 and p=0.4352 respectively), young and elderly adult specimens (p= 0.8160 and p= 0.2859 respectively) and mature and elderly adult specimens (p= 0.9864 and p= 0.0808 respectively). KRT19 (Figure 4.4E) expression did not vary significantly between young and mature, and young and elderly specimens (p= 0.3434 and 0.1243 respectively), whilst expression was significantly higher in elderly adult specimens as compared to mature (p= 0.0283). Like for KRT8 and KRT18, expression levels of CAXII (Figure 4.4F) did not vary significantly between the age groups assessed (young vs. mature adult p= 0.4801; young vs. elderly adult p= 0.3054; mature vs. elderly adult p= 0.0704).

When expression levels were assessed according to histological level of degeneration, only FOXF1 (Figure 4.5A) and PAX-1 (Figure 4.5B) demonstrated any significant variations in expression levels. FOXF1 gene expression did not vary between non-degenerate and moderately degenerate specimens, or between non-degenerate and severely degenerate specimens (p= 0.9834 and p= 0.2082 respectively), although expression was significantly higher in moderately degenerate samples as compared to severely degenerate (p= 0.0490). Regarding PAX-1 expression, expression did not vary in non-degenerate vs. moderately degenerate and non-degenerate vs. severely degenerate specimens (p= 0.4806 and p= 0.1580 respectively), however, expression was significantly higher in moderately degenerate as compared to severely degenerate samples (p= 0.0201). KRT8 (Figure 4.5C),

KRT18 (Figure 4.5D), KRT19 (Figure 4.5E) and CAXII (Figure 4.5F) expression levels did not vary between either non-degenerate vs. moderately degenerate ($p= 0.5062$; $p= 0.6728$; $p= 0.8934$; and $p= 0.8618$ respectively), non-degenerate vs. severely degenerate ($p= 0.0595$; $p= 0.2683$; $p= 0.8639$; and $p= 0.9023$ respectively), or moderately degenerate vs. severely degenerate specimens ($p= 0.3230$; $p= 0.3825$; $p= 0.6662$; and $p= 0.9423$ respectively).

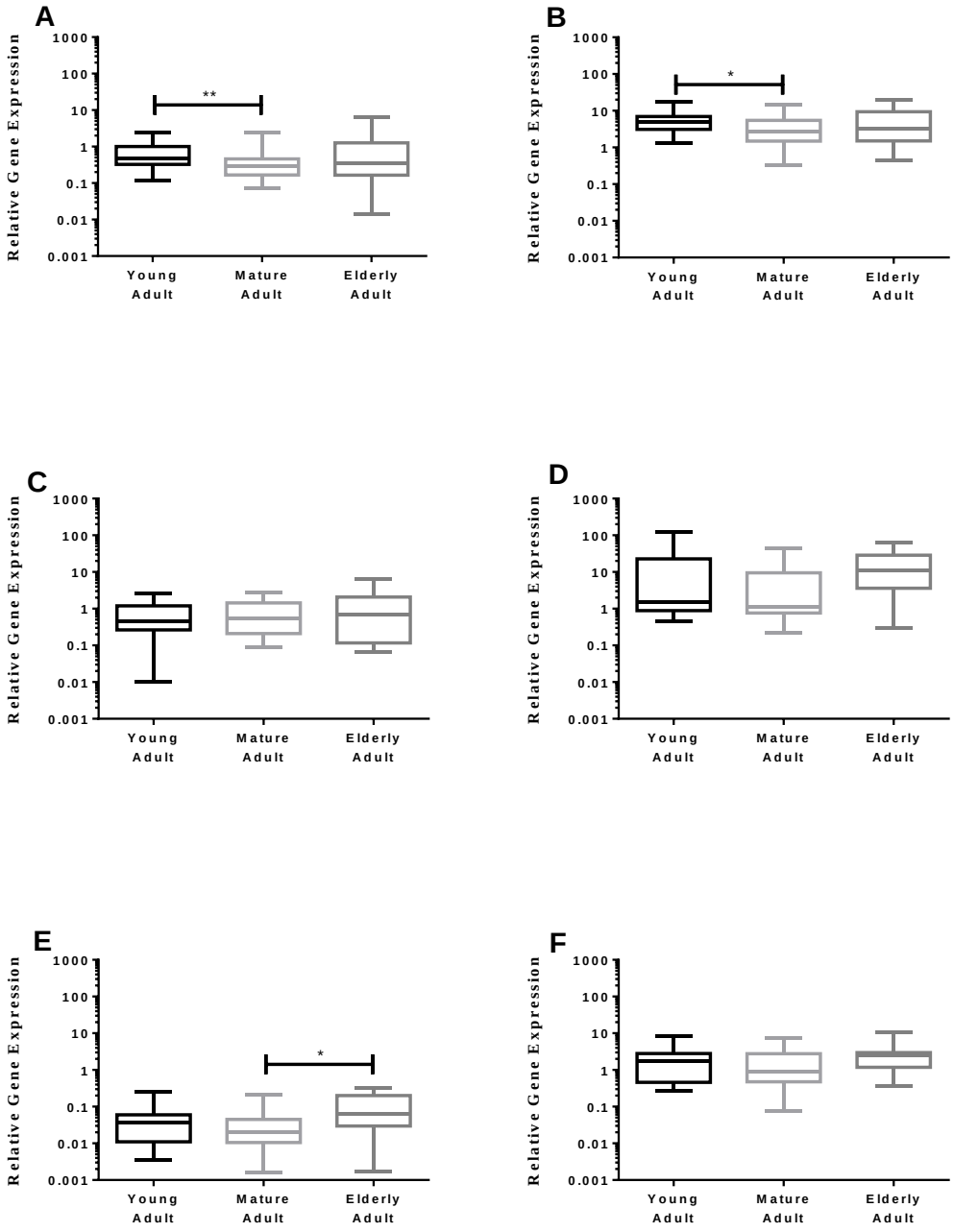

Figure 4.4 Correlation of novel NP cell marker gene expression with age. Expression levels of genes FOXF1 (A), PAX-1 (B), KRT8 (C), KRT18 (D), KRT19 (E) and CAXII (F) (normalised to the average gene expression of reference genes MRPL19 and EIF2B1) were assessed according to patient age at the time of surgery, categorised into three age groups: young adult (0-39 years, n=21); mature adult (40-59 years, n=31); elderly adult (60+ years, n=10). *p <0.05 **p<0.01.

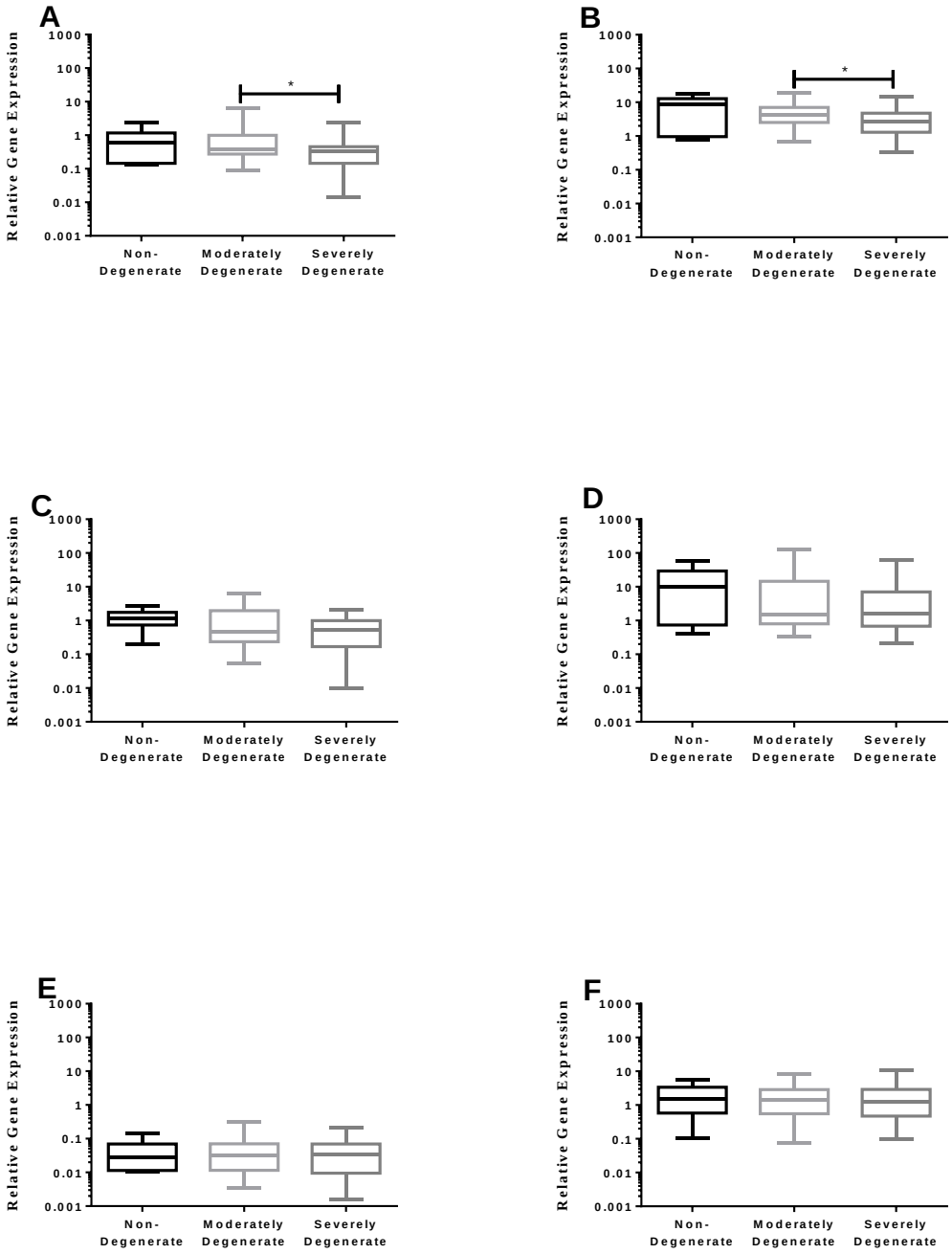

Figure 4.5 Correlation of novel NP cell marker gene expression with level of degeneration. Expression levels of genes FOXF1 (A), PAX-1 (B), KRT8 (C), KRT18 (D), KRT19 (E) and CAXII (F) (normalised to the average gene expression of reference genes MRPL19 and EIF2B1) were assessed according to level of tissue degeneration, as determined histologically, categorised into three degrees of degeneration: non-degenerate (grades 0-4, n=6); moderately degenerate (grade 5-7, n=31); severely degenerate (grades 8-12, n=25). *p <0.05.

4.4.3 Validation of Novel NP Cell Negative Marker Genes

IBSP and FBLN1 are genes identified by microarray as negative markers of the NP cell phenotype, in that they are more lowly expressed in adult human NP cells when compared to AC cells. With regards to variation with ageing, expression levels of FBLN1 (Figure 4.6B) did not differ significantly between young vs. mature adult specimens ($p= 0.4136$), young vs. elderly adult specimens ($p= 0.3039$) or mature vs. elderly adult specimens ($p= 0.1529$). IBSP (Figure 4.6A) gene expression was significantly lower in mature adult samples when compared to both young adult ($p= 0.0191$) and elderly adult ($p=0.0087$), whilst comparisons of young and elderly adult expression levels showed no significant variation ($p= 0.3723$).

When assessed according to the severity of tissue degeneration, expression levels of neither IBSP (Figure 4.7A) nor FBLN1 (Figure 4.7B) demonstrated any significant variations when comparisons were made between young and mature adult ($p= 0.7309$ and $p= 0.6412$ respectively); young and elderly adult ($p= 0.7596$ and $p= 0.7536$ respectively); and mature and elderly specimens ($p= 0.9492$ and $p= 0.4058$ respectively).

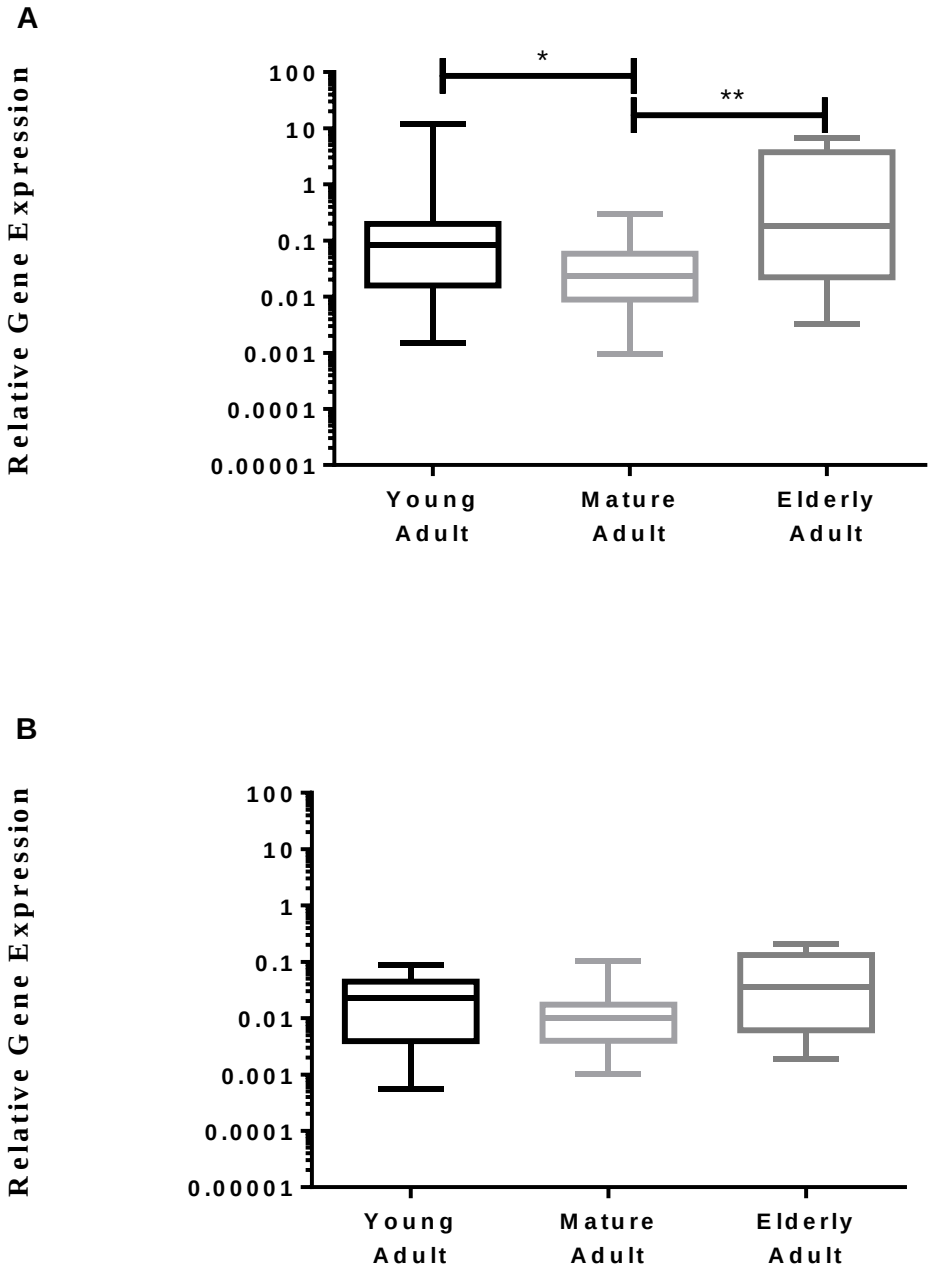

Figure 4.6 Correlation of novel NP cell negative marker gene expression with age. Expression levels of genes IBSP (A) and FBLN1 (B) (normalised to the average gene expression of reference genes MRPL19 and EIF2B1) were assessed according to patient age at the time of surgery, categorised into three age groups: young adult (0-39 years, n=21); mature adult (40-59 years, n=31); elderly adult (60+ years, n=10). *p <0.05 **p <0.01.

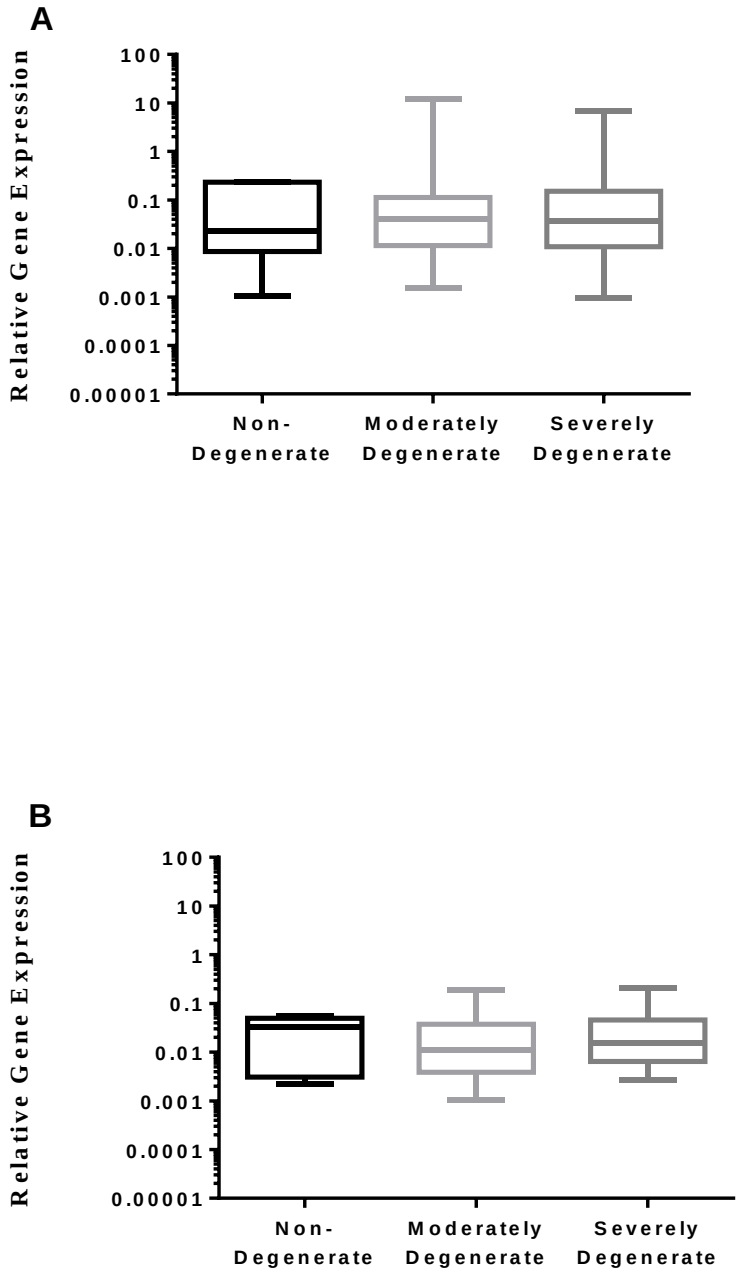

Figure 4.7 Correlation of novel NP cell negative marker gene expression with level of degeneration. Expression levels of genes IBSP (A) and FBLN1 (B) (normalised to the average gene expression of reference genes MRPL19 and EIF2B1) were assessed according to level of tissue degeneration, as determined histologically, categorised into three degrees of degeneration: non-degenerate (grades 0-4, n=6); moderately degenerate (grade 5-7, n=31); severely degenerate (grades 8-12, n=25).

4.4.4 Assessment of Notochordal Cell Marker Gene Expression in Adult NP Cells

The gene expression levels of a number of NC cell marker genes (NOTO, T, FOXA2, CHRD, NOGGIN, LGALS3 and CD24) were assessed in cells obtained from the adult human NP, and expression levels correlated to patient age or severity of IVD degeneration, as determined histologically. Overall, 100% of specimens analysed expressed NOGGIN, LGALS3 and CD24, whilst NOTO, T, FOXA2 and CHRD expression was only shown in 42%, 71%, 94% and 97% of samples respectively. Tables 4.2 and 4.3 indicate the percentage of specimens with detectable gene expression levels for the various age and degenerative score groups assessed. There appears to be no correlation between the percentage of specimens with detectable expression levels and patient age or severity of tissue degeneration.

Table 4.2 Percentage of Samples Expressing NC Cell Markers and Ageing

	Notochordal Marker Gene						
	NOTO	**T**	**FOXA2**	**CHRD**	**NOGGIN**	**LGALS3**	**CD24**
Young Adult	**48%**	**81%**	**100%**	**100%**	**100%**	**100%**	**100%**
Mature Adult	**39%**	**71%**	**88%**	**94%**	**100%**	**100%**	**100%**
Elderly Adult	**40%**	**50%**	**100%**	**100%**	**100%**	**100%**	**100%**

Young Adult (0-39 years); Mature Adult (4-59 years); Elderly Adult (60+ years).

Table 4.3 Percentage of Samples Expressing NC Cell Markers and Degeneration

	Notochordal Marker Gene						
	NOTO	**T**	**FOXA2**	**CHRD**	**NOGGIN**	**LGALS3**	**CD24**
Non-Degenerate	**17%**	**67%**	**100%**	**100%**	**100%**	**100%**	**100%**
Moderately Degenerate	**48%**	**61%**	**90%**	**97%**	**100%**	**100%**	**100%**
Severely Degenerate	**40%**	**64%**	**100%**	**100%**	**100%**	**100%**	**100%**

Non-Degenerate (grades 0-4); Moderately Degenerate (grades 5-7); Severely Degenerate (grades 8-12).

With regards to patterns of expression with ageing, significantly increased NOTO (Figure 4.8A) expression was noted in elderly adult specimens as compared to young adults (p= 0.0240), but there were no further variations in young vs. mature and mature vs. elderly samples (p= 0.3375 and p= 0.3044 respectively). Expression levels of T (Figure 4.8B), FOXA2 (Figure 4.8C), CHRD (Figure 4.8D), NOGGIN (Figure 4.8E) and CD24 (Figure 4.8G) did not vary between any of the age groups analysed: young adult vs. mature adult (p= 0.6200, p= 0.8142, p= 0.9153, p= 0.8692 and p= 0.5642 respectively); young adult vs. elderly adult (p= 0.7191, p= 0.7840, p= 0.6761, p= 0.1815 and p= 07212 respectively); and mature adult vs. elderly adult (p= 0.8412, p= 0.8777, p= 0.6091, p= 0.1244 and p= 0.3599 respectively). LGALS3 (Figure 4.8F) expression was significantly lower in mature adult as compared to young adult samples (p= 0.0281), although there were no significant variations in expression when comparisons of young adult/elderly adult and mature adult/elderly adult specimens were made (p= 0.9134 and p= 0.1119 respectively).

Regarding variations in gene expression levels with degeneration, with the exception of CD24, there were no significant differences in gene expression levels with increasing severity of degeneration. NOTO (Figure 4.9A) expression was only detected in 1 non-degenerate specimen and statistical comparisons could therefore not be made, and when moderately degenerate and severely degenerate specimens were compared, no significance was noted (p= 0.7715). For T (Figure 4.9B), FOXA2 (Figure 4.9C), CHRD (Figure 4.9D), NOGGIN (Figure 4.9E) and LGALS3 (Figure 4.9F), no significant variations in expression were noted between non-degenerate and moderately degenerate (p= 0.4095, p= 0.3248, p= 0.1508, p= 0.5819, and p= 0.9515 respectively); non-degenerate and severely degenerate (p= 0.3847, p= 0.2154, p= 0.2548, p= 0.6782 and p= 0.5743 respectively); and moderately degenerate and severely degenerate samples (p= 0.8729, p= 0.5989, p= 0.5476, p= 0.0857 and p= 0.3230 respectively). With regards to CD24 expression (Figure 4.9G), no significant differences in expression were noted between both non-degenerate and moderately degenerate (p= 0.8934) and non-degenerate and severely degenerate specimens (p= 0.1171). Expression was significantly lower in severely degenerate samples as compared to moderately degenerate (p= 0.0183).

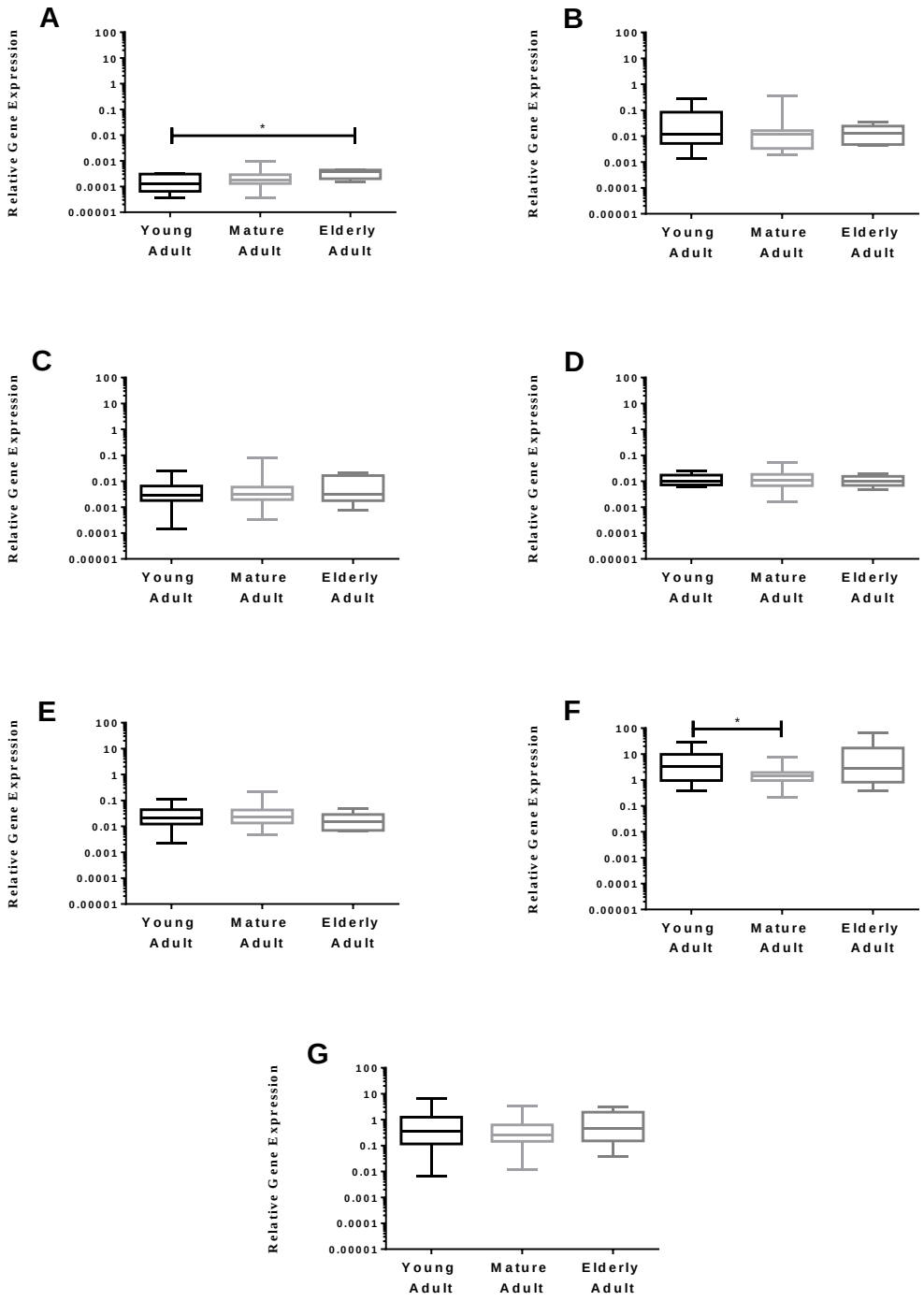

Figure 4.8 Correlation of NC cell marker gene expression with age. Expression levels of genes NOTO (A), T (B), FOXA2 (C), CHRD (D), NOGGIN (E), LGALS3 (F) and CD24 (G) (normalised to the average gene expression of reference genes MRPL19 and EIF2B1) were assessed according to patient age at the time of surgery, categorised into three age groups: young adult (0-39 years n=21); mature adult (40-59 years, n=31); elderly adult (60+ years, n=10). *p <0.05.

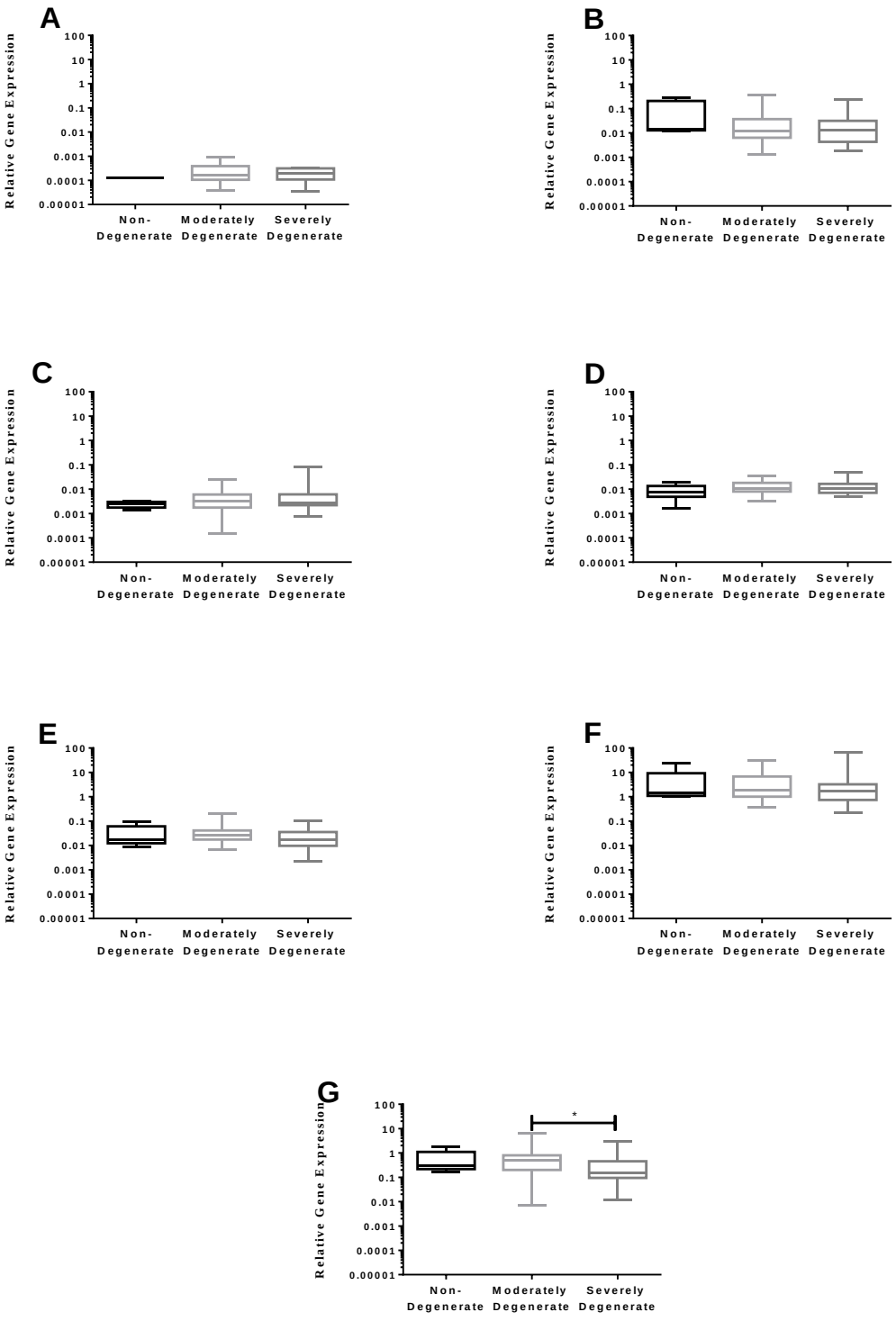

Figure 4.9 Correlation of NC cell marker gene expression with level of degeneration. Expression levels of genes NOTO (A), T (B), FOXA2 (C), CHRD (D), NOGGIN (E), LGALS3 (F) and CD24 (G) (normalised to the average gene expression of reference genes MRPL19 and EIF2B1) were assessed according to level of tissue degeneration, as determined histologically, categorised into three degrees of degeneration: non-degenerate (grades 0-4, n=6); moderately degenerate (grade 5-7, n=31); severely degenerate (grades 8-12, n=25). *p <0.05.

4.4.5 Localisation of Novel NP and NC Cell Marker Proteins in the Adult NP

A number of markers were selected from the panel of novel NP and NC cell marker genes assessed in 4.4.1 and 4.4.3. (FoxF1, Pax-1, Cytokeratin-8, Cytokeratin-18, Cytokeratin-19, Carbonic Anhydrase-12, Brachyury, Galectin-3 and CD24), and the protein expression of these analysed by immunohistochemistry with a view to confirming gene expression findings and to localise expression to cells of the adult human NP.

4.4.5.1 Identification of Protein Expression in Adult Human NP Cells

4.4.5.1.1 FoxF1

FoxF1 expression was detected in cells of the adult human NP (Figure 4.10A). AF cells of the same tissue demonstrated some expression (Figure 4.10B), whilst NC cell remnants present in the NP of an 18-year old were positive also (Figure 4.10C). When analysis was conducted in human foetal NC tissue, staining was noted in all NC cells, but also in the surrounding mesenchymal cells (Figure 4.10D). Human kidney tubule cells were utilised as a positive control tissue and demonstrated high levels of expression (Figure 4.10E) and adult human NP sections stained with an isotype control stained negatively throughout (Figure 4.10F).

4.4.5.1.2 Pax-1

Protein expression staining for Pax-1 was intense in cells of the adult human NP (Figure 4.11A), and like that observed for FoxF1, staining was also noted in some AF cells of the same specimens (Figure 4.11B). NC cell remnant clusters obtained from adolescent NP demonstrated low levels of expression for Pax-1, but expression was detected nonetheless (Figure 4.11C). Human foetal NC cells were ubiquitously positive for Pax-1 expression, as were cells of the surrounding mesenchyme (Figure 4.11D). Human placental cells (trophoblasts) were stained as positive control cells, and high levels of staining were shown (Figure 4.11E). Finally, sections of adult human NP tissue stained with an isotype control showed no staining throughout the tissue (Figure 4.11F).

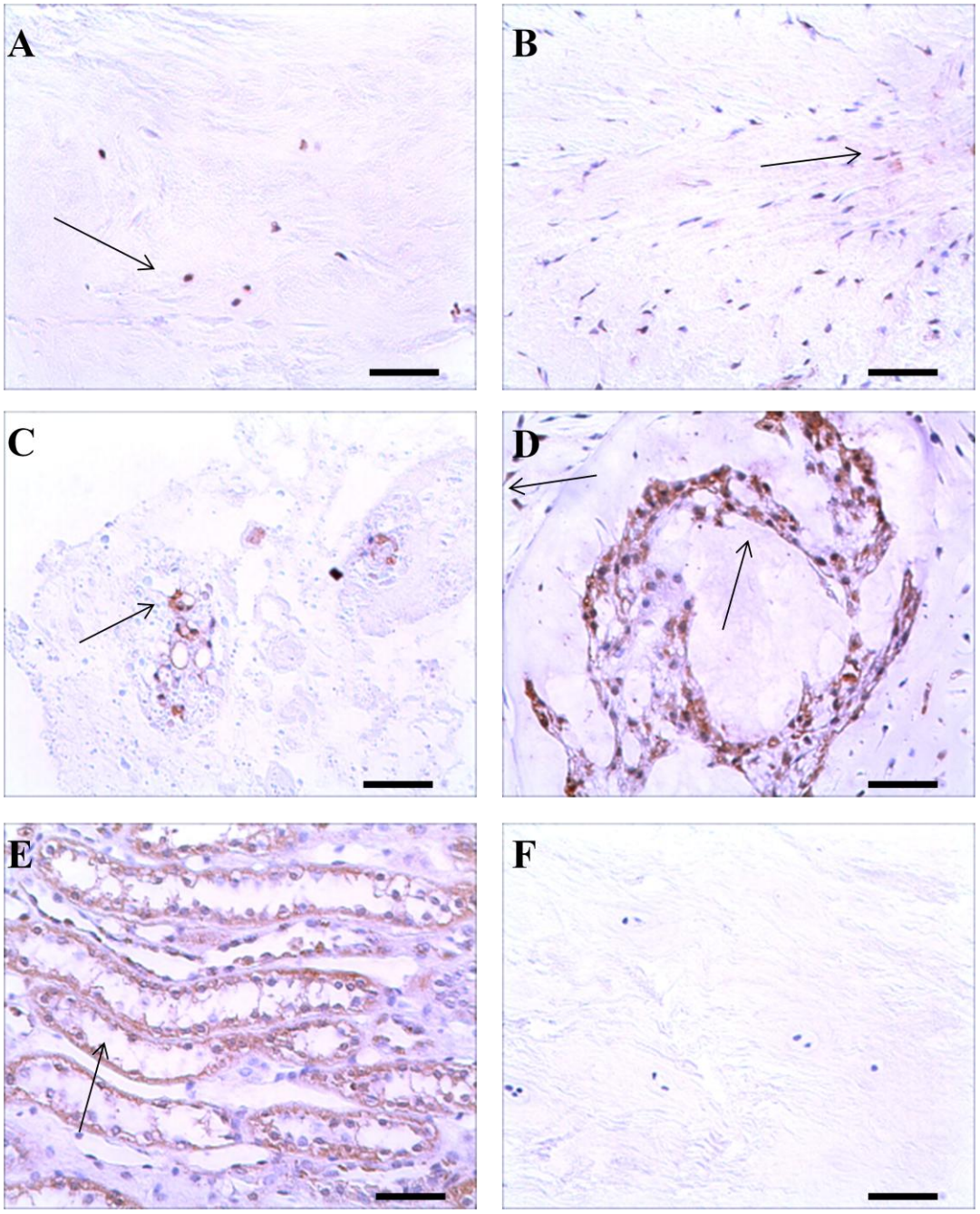

Figure 4.10 FoxF1 protein expression by immunohistochemistry. FoxF1 protein expression was assessed in mature adult human NP cells (A); mature adult human AF cells (B); 18 y/o adult human NC cell remnants (C); human foetal NC cells (D); human kidney tubule cells (E); and isotype negative control adult human NP cells (F). Black arrows indicate positive staining. Scale bar = 50μm.

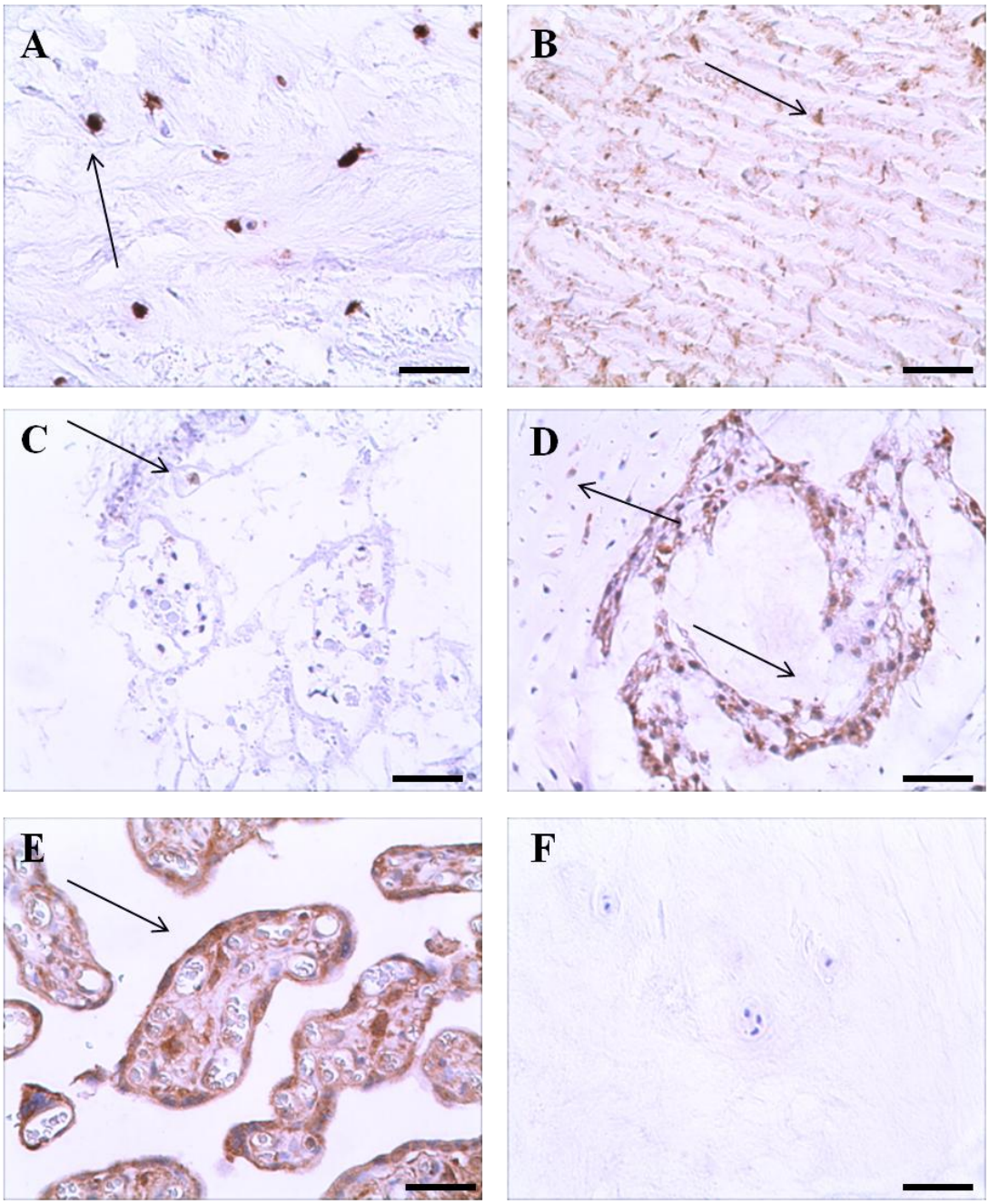

Figure 4.11 Pax-1 protein expression by immunohistochemistry. Pax-1 protein expression was assessed in mature adult human NP cells (A); mature adult human AF cells (B); 18 y/o adult human NC cell remnants (C); human foetal NC cells (D); human placental cells (E); and isotype negative control adult human NP cells (F). Black arrows indicate positive staining. Scale bar = 50μm.

4.4.5.1.3 Cytokeratin-8

Immunopositivity for cytokeratin-8 was detected in cells of the adult human NP (Figure 4.12A), whilst AF cells of the same tissue were negative (Figure 4.12B). NC cell remnant clusters in the NP of an 18-year old were highly positive for cytokeratin-8 (Figure 4.12C), as were human foetal NC cells (Figure 4.12D). Interestingly, mesenchymal cells surrounding the foetal NC cells were entirely negative for expression of cytokeratin-8 protein (Figure 4.12D). Glandular cells located in the sub-epidermal layers of human skin were stained as a positive control, and all cells showed high levels of expression (Figure 4.12E). Negative isotype control sections of adult human NP tissue demonstrated negative staining throughout (Figure 4.12F).

4.4.5.1.4 Cytokeratin-18

Cells of the adult human NP demonstrated positivity for cytokeratin-18 protein expression (Figure 4.13A), whilst little staining was noted in AF cells of the same samples (Figure 4.13B). High levels of positivity were noted in NC remnant cells present in the NP of an 18-year old's IVD (Figure 4.13C), and NC cells of a human foetal spine were also highly positive (Figure 4.13D). Human sub-epidermal glandular cells were stained as a positive control, and demonstrated high levels of expression (Figure 4.13E), whilst a negative control specimen (adult human NP stained with an isotype control) were negatively stained throughout the tissue (Figure 4.13F).

4.4.5.1.5 Cytokeratin-19

Protein expression of cytokeratin-19 could not be detected in cells of the adult human NP (Figure 4.14A), nor in AF cells of the same tissues (Figure 4.14B). However, NC cell remnants in 18-year old NP tissue displayed positive staining (Figure 4.14C), as did NC cells of human foetal spine (Figure 4.14D). Glandular cells located in the sub-epidermal layers of human skin also demonstrated positive expression as a positive control tissue (Figure 4.14E), whilst sections of human NP tissue stained with an isotype control showed no positivity (Figure 4.14F).

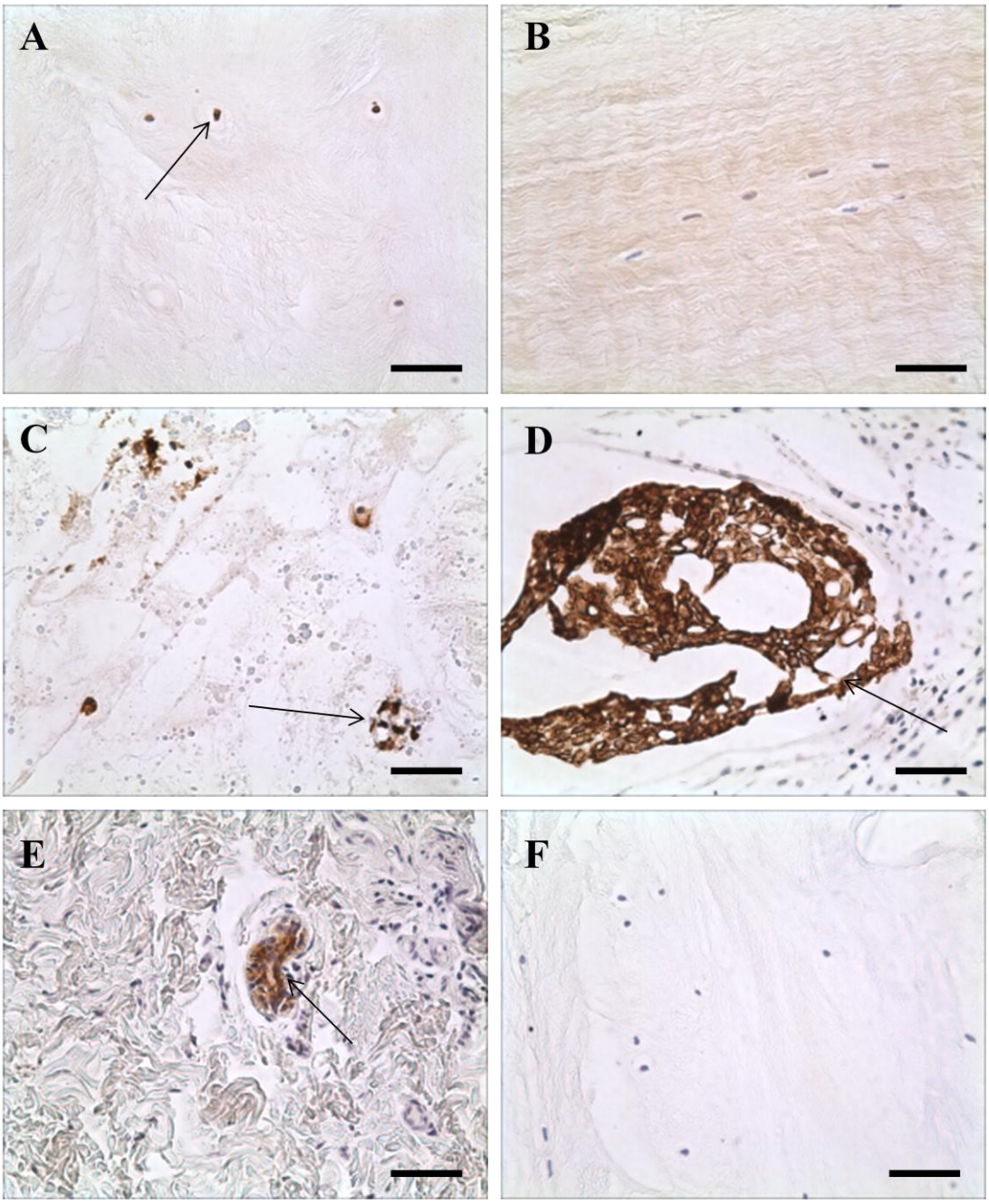

Figure 4.12 Cytokeratin-8 protein expression by immunohistochemistry. Cytokeratin-8 protein expression was assessed in mature adult human NP cells (A); mature adult human AF cells (B); 18 y/o adult human NC cell remnants (C); human foetal NC cells (D); human glandular epithelial cells (E); and isotype negative control adult human NP cells (F). Black arrows indicate positive staining. Scale bar = 50µm.

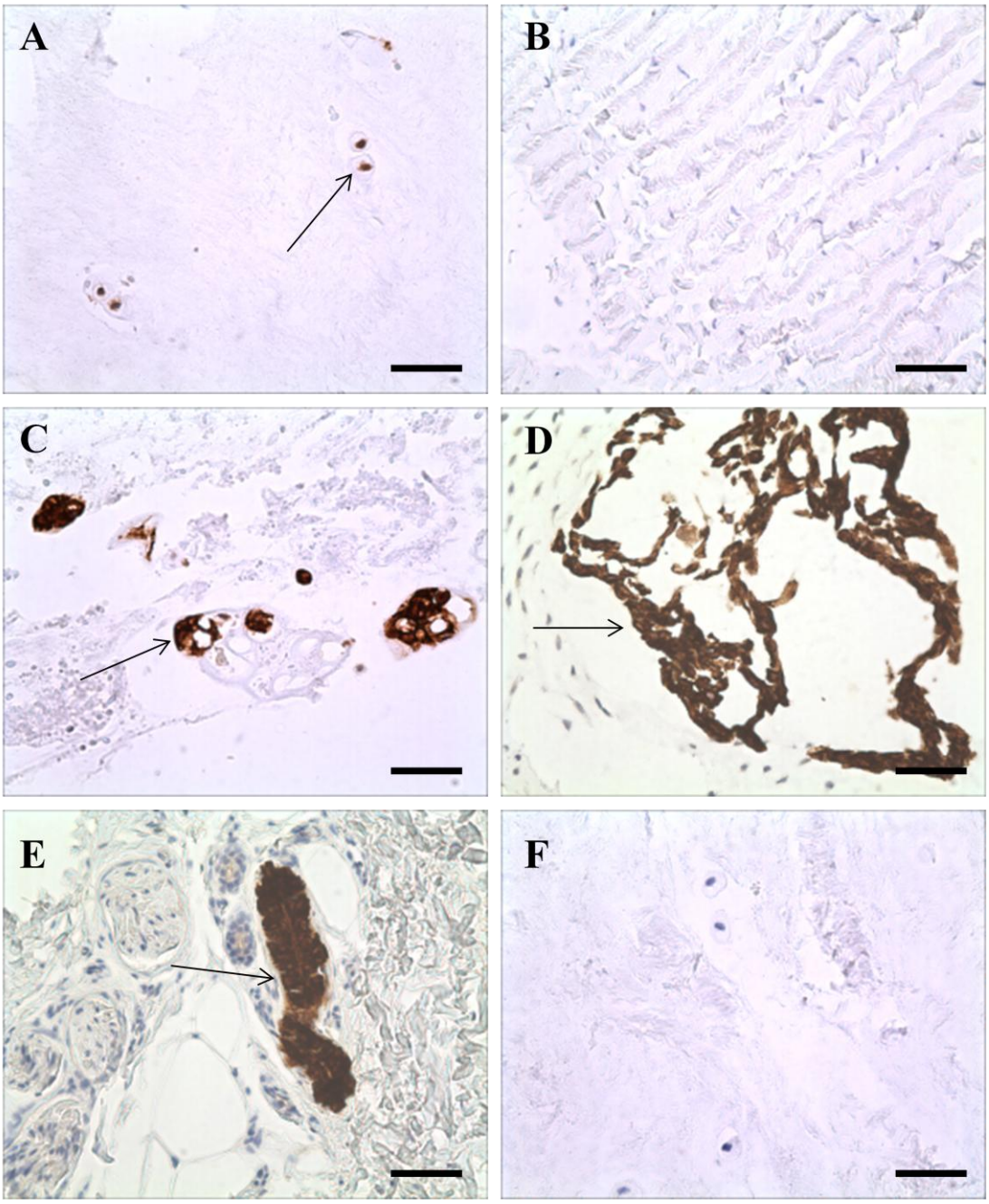

Figure 4.13 Cytokeratin-18 protein expression by immunohistochemistry. Cytokeratin-18 protein expression was assessed in mature adult human NP cells (A); mature adult human AF cells (B); 18 y/o adult human NC cell remnants (C); human foetal NC cells (D); human glandular epithelial cells (E); and isotype negative control adult human NP cells (F). Black arrows indicate positive staining. Scale bar = 50µm.

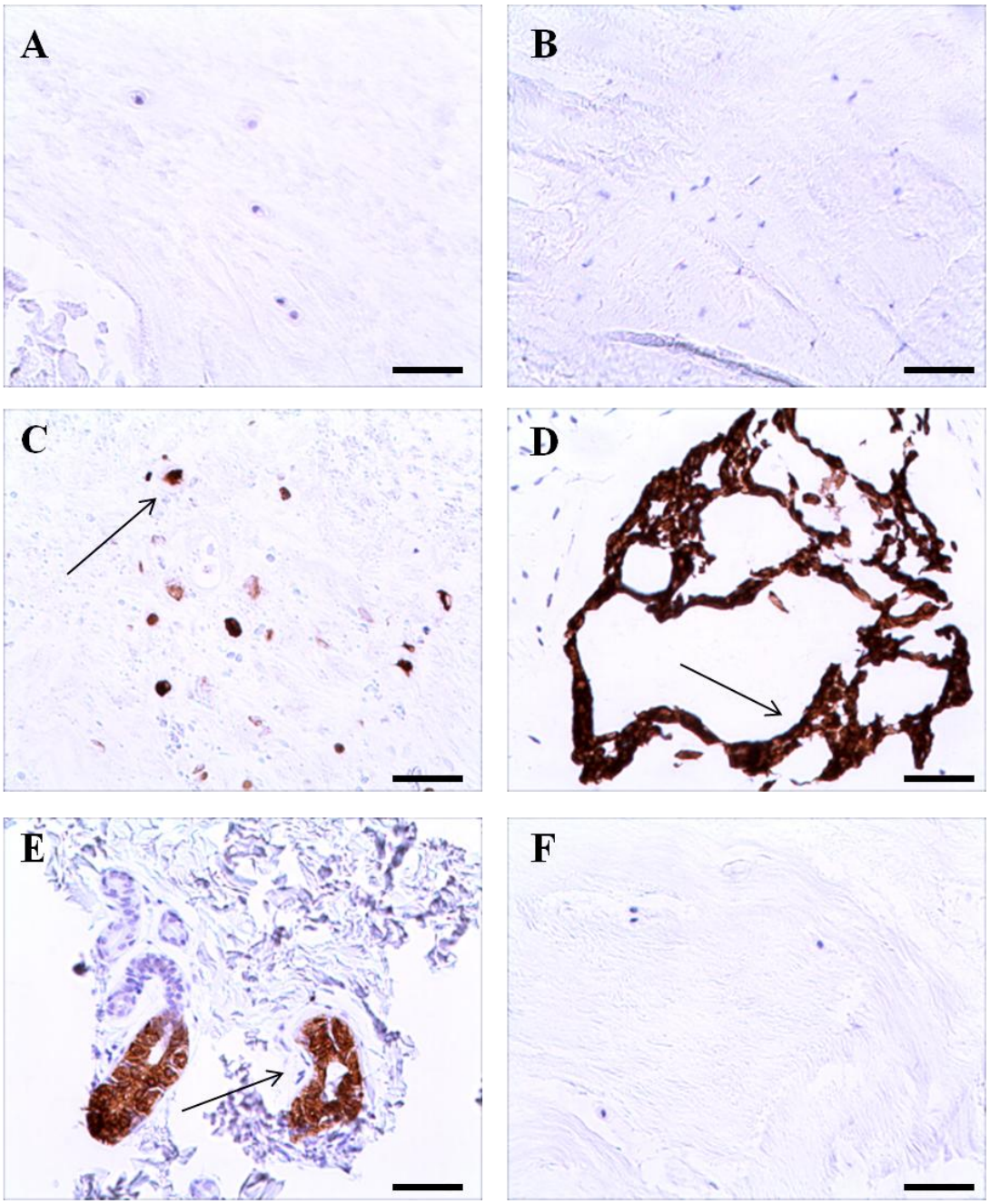

Figure 4.14 Cytokeratin-19 protein expression by immunohistochemistry. Cytokeratin-19 protein expression was assessed in mature adult human NP cells (A); mature adult human AF cells (B); 18 y/o adult human NC cell remnants (C); human foetal NC cells (D); human glandular epithelial cells (E); and isotype negative control adult human NP cells (F). Black arrows indicate positive staining. Scale bar = 50µm.

4.4.5.1.6 Carbonic Anhydrase-12

Carbonic Anhydrase-12 protein was detected in almost all cells of the adult human NP samples tested (Figure 4.15A), and positivity was also shown in adult human AF cells (Figure 4.15B). Low levels of immunopositivity were detected in NC cell remnants in 18-year old NP tissue (Figure 4.15C), and regarding positivity in human foetal NC cells, expression was shown in NC cells but also in cells of the surrounding mesenchyme (Figure 4.15D). Human kidney specimens were stained as a positive control, and staining noted in the tubule cells (Figure 4.15E), and negative control sections of adult human NP stained with an isotype control demonstrated no staining (Figure 4.15F).

4.4.5.1.7 Brachyury

Strong Brachyury expression was detected in adult human NP cells (Figure 4.16A), but also in a small number of AF cells from the same specimens (Figure 4.16B). NP tissue containing NC cell remnants from the IVD of an 18-year old stained mildly positive for the protein (Figure 4.16C), whilst NC cells of human foetal tissue were highly immunopositive, as were the surrounding mesenchymal cells (Figure 4.16D). Human chordoma tissue was utilised as a positive control tissue, and chordoma cells demonstrated high positivity (Figure 4.16E), whilst human NP tissue negative control slides stained with isotype control has no positively stained cells (Figure 4.16F).

4.4.5.1.8 Galectin-3

Protein expression of Galectin-3 was detected in NP cells of the adult human IVD (Figure 4.17A), as well as a minority of AF cells of the same tissue (Figure 4.17B). High levels of staining were noted in remnant NC cells of 18-year old's IVD (Figure 4.17C), as well as in NC cells and surrounding mesenchymal cells of human foetal spine (Figure 4.17D). Cells of human chordoma tissue were highly immunopositive as a positive control tissue (Figure 4.17E), whilst human NP cells stained with an isotype control were negatively stained throughout as a negative control section (Figure 4.17F).

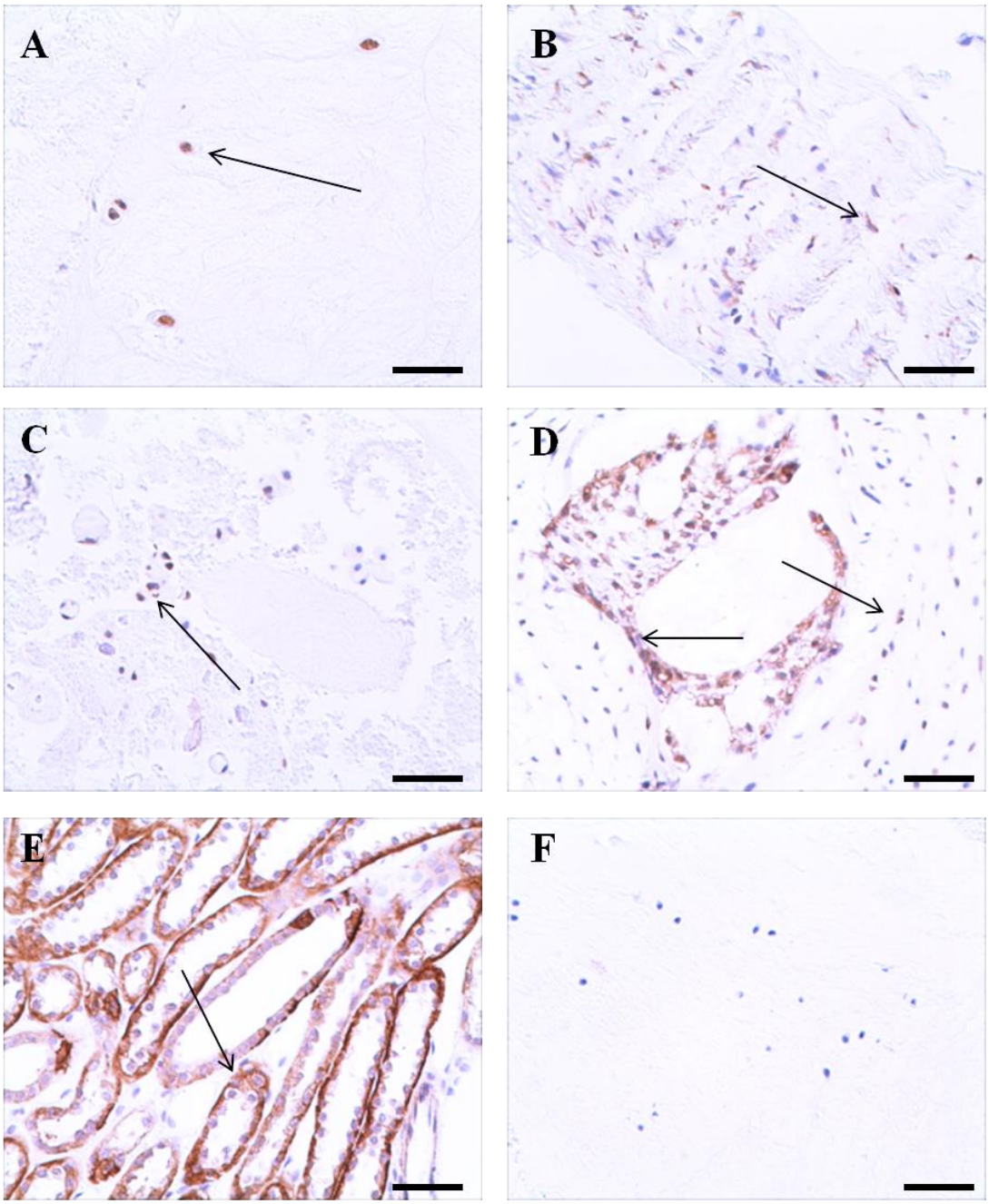

Figure 4.15 Carbonic Anhydrase-12 protein expression by immunohistochemistry. Carbonic Anhydrase-12 protein expression was assessed in mature adult human NP cells (A); mature adult human AF cells (B); 18 y/o adult human NC cell remnants (C); human foetal NC cells (D); human kidney tubule cells (E); and isotype negative control adult human NP cells (F). Black arrows indicate positive staining. Scale bar = 50μm.

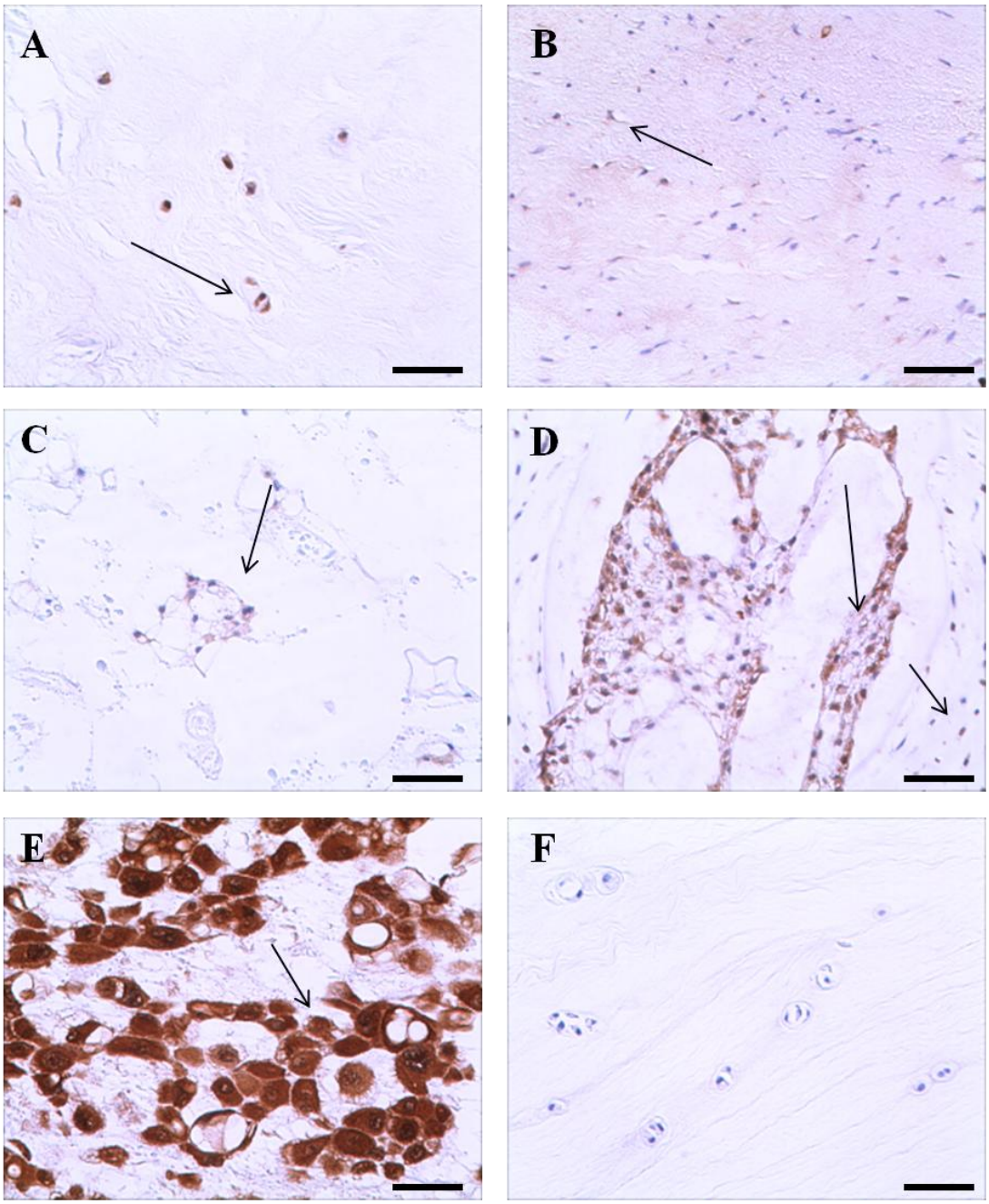

Figure 4.16 Brachyury protein expression by immunohistochemistry. Brachyury protein expression was assessed in mature adult human NP cells (A); mature adult human AF cells (B); 18 y/o adult human NC cell remnants (C); human foetal NC cells (D); human chordoma cells (E); and isotype negative control adult human NP cells (F). Black arrows indicate positive staining. Scale bar = 50µm.

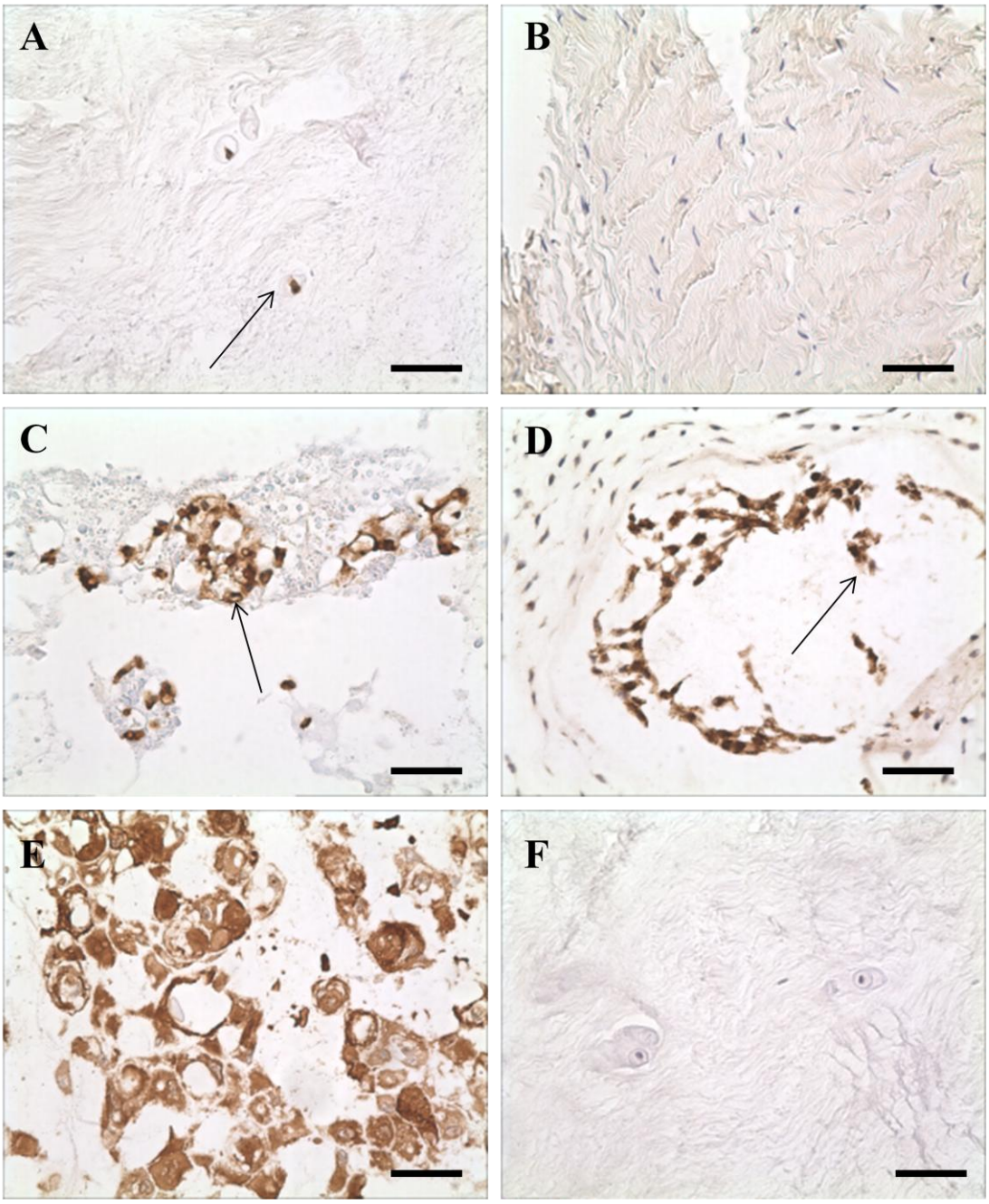

Figure 4.17 Galectin-3 protein expression by immunohistochemistry. Galectin-3 protein expression was assessed in mature adult human NP cells (A); mature adult human AF cells (B); 18 y/o adult human NC cell remnants (C); human foetal NC cells (D); human chordoma cells (E); and isotype negative control adult human NP cells (F). Black arrows indicate positive staining. Scale bar = 50µm.

4.4.5.1.9 CD24

Some staining was noted in NP cells of adult human IVD tissue (Figure 4.18A), as well as in a very small number of AF cells of the same specimens (Figure 4.18B). Human NC cells remaining in NP tissue of an 18-year old spine were mildly positively stained (Figure 4.18C), whilst NC and mesenchymal cells of human foetal spine were also positively stained (Figure 4.18D). Human chordoma tissue was stained as a positive control, and chordoma cells were highly immunopositive (Figure 4.18E), and negative control sections of human NP tissue stained with an isotype control were negatively stained throughout (Figure 4.18F).

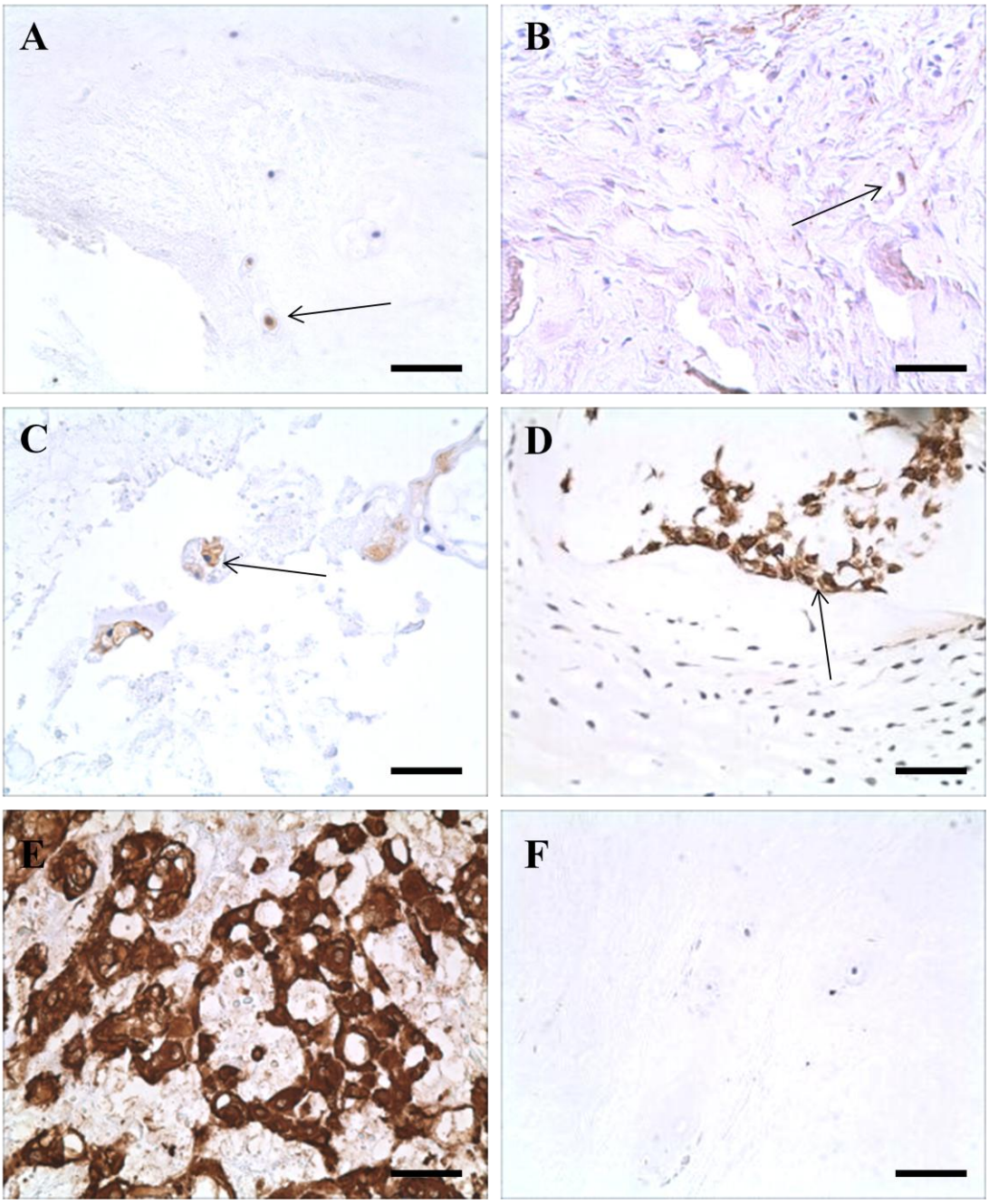

Figure 4.18 CD24 protein expression by immunohistochemistry. CD24 protein expression was assessed in mature adult human NP cells (A); mature adult human AF cells (B); 18 y/o adult human NC cell remnants (C); human foetal NC cells (D); human chordoma cells (E); and isotype negative control adult human NP cells (F). Black arrows indicate positive staining. Scale bar = 50μm.

4.4.5.2 Quantification of Immunohistochemical Protein Expression

For each of the markers assessed, percentage cell immunopositivity was quantified by counting all cells within the NP and AF tissues of each specimen, as well as the number of positively stained cells within these. Staining levels were then correlated against patient age and histological level of degeneration. Note, no assessment of cytokeratin-19 immunopositivity was made as no staining was detected in cells of the adult human NP or AF. Immunopositivity was noted in 100% of specimens stained for FoxF1, Pax-1, Carbonic Anhydrase-12 and Brachyury, whilst samples stained for Cytokeratin-8, Cytokeratin-18, Galectin-3 and CD24 displayed some degree of immunopositivity in 72%, 96%, 95% and 91% of specimens respectively.

4.4.5.2.1 Total Immunopositivity within NP Cells

Figure 4.19 illustrates the mean percentage immunopositivity within NP tissues noted for each of the markers tested. The average NP cell immunopositivity values were as follows: FoxF1 74.73%±2.728; Pax-1 68.21%±3.278; Cytokeratin-8 10.59%±1.858; Cytokeratin-18 29.01%±3.459; Carbonic Anhydrase-12 72.08%±3.918; Brachyury 43.32%±2.739; Galectin-3 50.02%±3.631; and CD24 16.76%±2.065. Crucially, this data highlights that for all of the markers assessed, expression is not ubiquitous throughout the NP. Novel NP cell markers demonstrated greater mean NP cell immunopositivity than notochordal cell markers, but there was also huge variation in expression levels between samples.

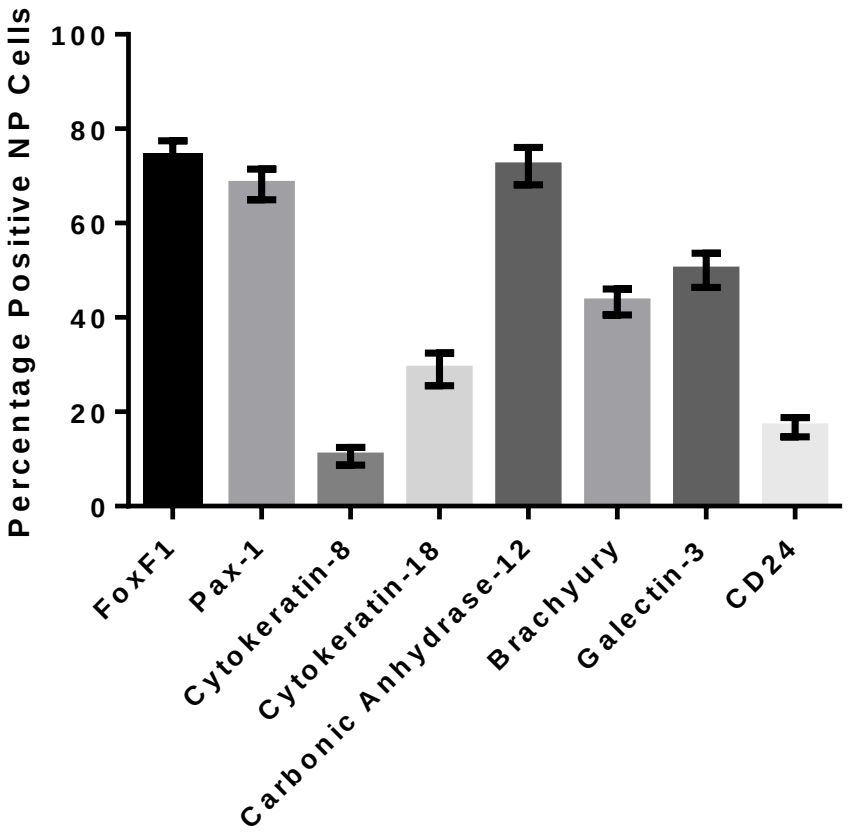

Figure 4.19 Mean NP cell immunopositivity as a percentage of total NP cell count. Error bars calculated from standard error of the mean.

4.4.5.2.2 Novel NP Cell Marker Protein Expression in the Adult Human NP: Changes with Age

The percentage immunopositivity of novel NP cell marker proteins (FoxF1, Pax-1, Cytokeratins-8, -18, -19 and Carbonic Anhydrase-12) in cells of the adult human NP were initially assessed according to patient age at the time of surgery. No significant variation was demonstrated in the cell positivity of FoxF1 (Figure 4.20A), Pax-1 (Figure 4.20B), Cytokeratin-8 (Figure 4.20C), Cytokeratin-18 (Figure 4.20D), or Carbonic Anhydrase-12 (Figure 4.20E) with increasing age in young vs. mature adult ($p= 0.1731$; $p= 0.2555$; $p= 0.9698$; $p= 0.8269$; and $p= 0.6122$ respectively), young vs. elderly adult ($p= 0.4000$; $p= 0.6023$; $p= 0.9736$; $p= 0.2479$; and $p= 0.4188$ respectively), and mature vs. elderly adult specimens ($p= 0.8342$, $p= 0.1888$; $p= 0.7450$; $p= 0.4993$; and $p= 0.6899$ respectively).

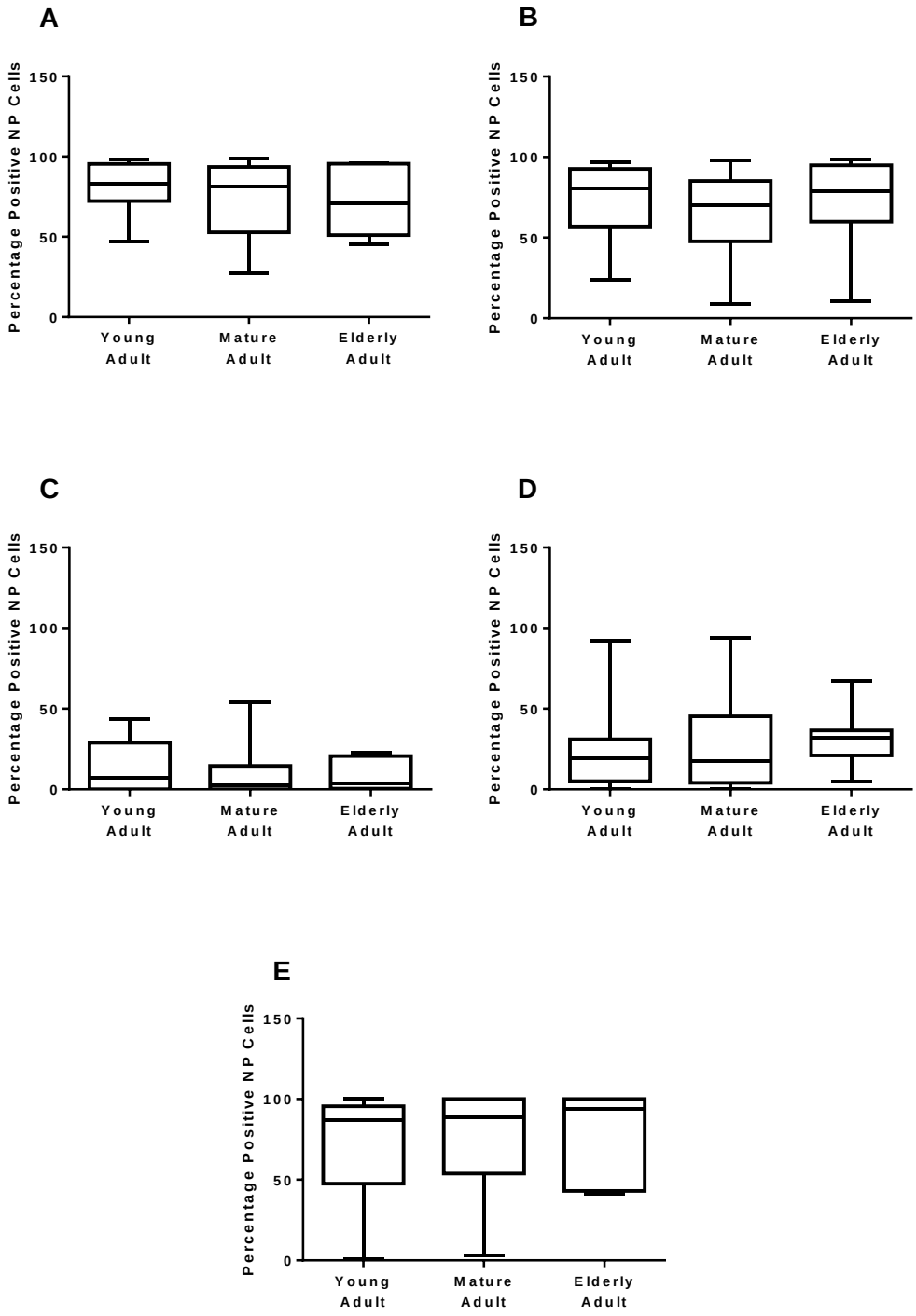

Figure 4.20 Immunopositivity for Novel NP Cell Marker Proteins: Changes with Age. The percentage of adult human NP cells that stained positively for novel NP cell marker proteins FoxF1 (A), Pax-1 (B), Cytokeratin-8 (C), Cytokeratin-18 (D) and Carbonic Anhydrase-12 (E) was assessed according to patient age at the time of surgery (young adult 0-39 years n=20; mature adult 40-59 years, n=28; elderly adult 60+ years, n=7).

4.4.5.2.3 Novel NP Cell Marker Protein Expression in the Adult Human NP: Changes with Degeneration

When the same markers were assessed according to degenerative score, FoxF1 (Figure 4.21A), Pax-1 (Figure 4.21B), and Cytokeratin-8 (Figure 4.21C) demonstrated no significant variations in percentage cell positivity between non-degenerate and moderately degenerate samples ($p= 0.3121$; $p= 0.6935$; and $p= 0.2793$ respectively), non-degenerate and severely degenerate samples ($p= 0.0925$; $p= 0.8162$; and $p= 0.1033$ respectively) and moderately and severely degenerate samples ($p= 0.6855$; $p= 0.3073$; and $p= 0.2355$ respectively). Expression of Cyokeratin-18 (Figure 4.21D) and Carbonic Anhydrase-12 (Figure 4.21E) was not significantly variable between non-degenerate and moderately degenerate tissues ($p= 0.2771$ and $p= 0.1196$ respectively) and non-degenerate and severely degenerate specimens ($p= 0.9427$ and $p= 0.7764$ respectively), although the number of positive cells was significantly greater in severely degenerate NP cells as compared to moderately degenerate ($p= 0.0474$ and $p= 0.0184$ respectively).

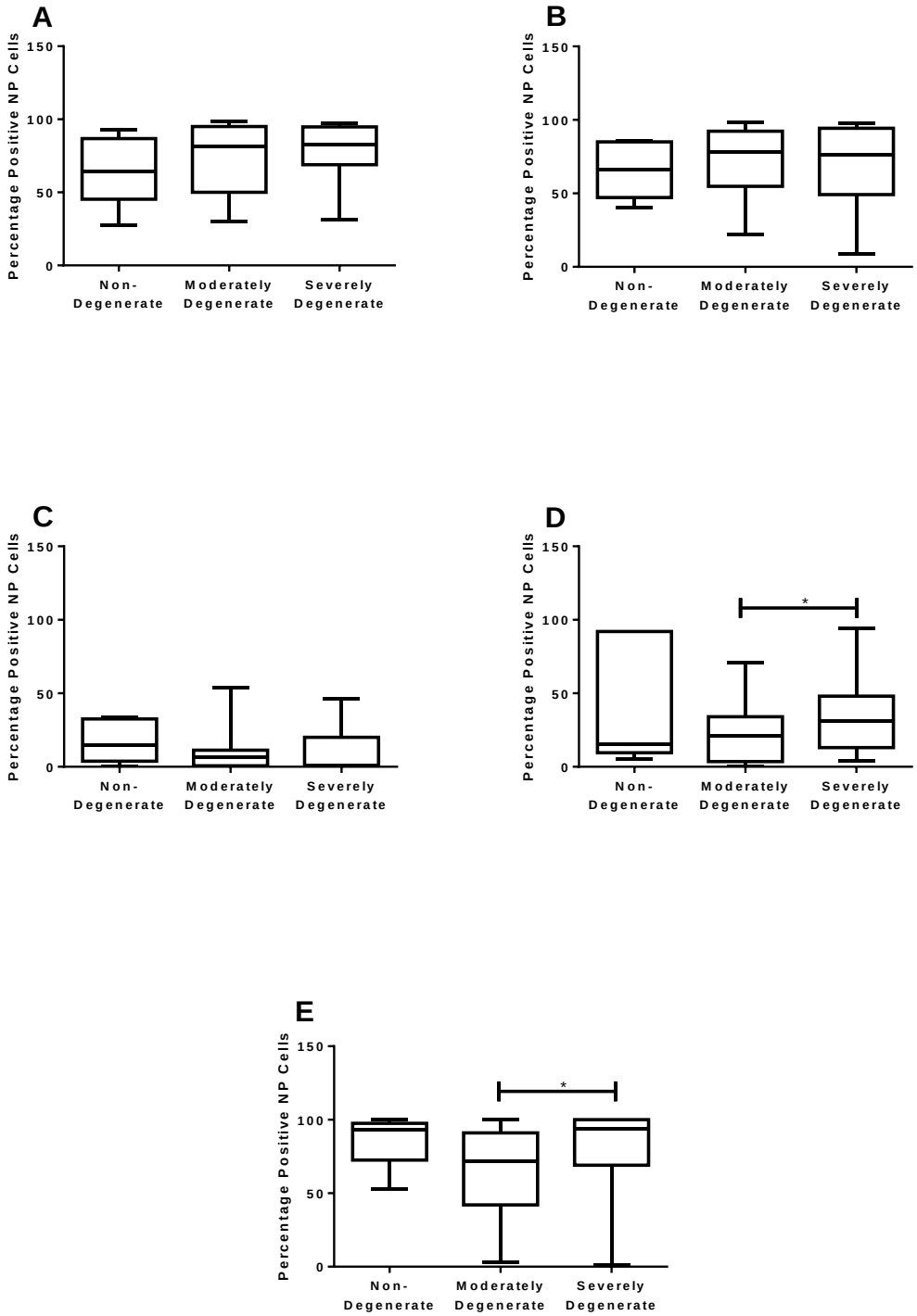

Figure 4.21 Immunopositivity for Novel NP Cell Marker Proteins: Changes with Degeneration. The percentage of adult human NP cells that stained positively for novel NP cell marker proteins FoxF1 (A), Pax-1 (B), Cytokeratin-8 (C), Cytokeratin-18 (D) and Carbonic Anhydrase-12 (E) was assessed according to histological grade of tissue degeneration (non-degenerate grades 0-4, n=5; moderately degenerate grades 5-7, n=27; severely degenerate grades 8-12, n=23). *p <0.05.

4.4.5.2.4 Notochordal Marker Cell Protein Expression in the Adult Human NP: Changes with Age

Notochordal cell marker proteins Brachyury, Galectin-3 and CD24 were also localised to adult human NP cells, and staining levels correlated with patient age. CD24 positivity (Figure 4.22C) did not vary with increasing age (young vs. mature adult $p= 0.4173$; young vs. elderly adult $p= 0.0684$; and mature vs. elderly adult $p= 0.2280$). Brachyury (Figure 4.22A) cell positivity was significantly lower in mature adult as compared to young specimens ($p= 0.0218$), but no variation between young and elderly specimens ($p= 0.0609$) and mature and elderly specimens ($p= 0.6847$). Galectin-3 (Figure 4.22B) immunopositivity was significantly higher in mature adult samples when compared to young adult ($p= 0.0139$), but no further variations were noted between young and elderly tissues ($p= 0.1390$) and mature and elderly tissues ($p= 0.7852$).

4.4.5.2.5 Notochordal Cell Marker Protein Expression in the Adult Human NP: Changes with Degeneration

Notochordal cell marker protein expression was analysed according to grade of degeneration, and cellular staining for Galectin-3 (Figure 4.23B) and CD24 (Figure 4.23C) demonstrated no variation in the percentage of immunopositive cells in non-degenerate vs. moderately degenerate ($p= 0.3576$ and $p= 0.7773$ respectively), non-degenerate vs. severely degenerate ($p= 0.7051$ and $p= 0.8095$ respectively) and moderately degenerate vs. severely degenerate specimens ($p= 0.0939$ and $p= 0.9854$ respectively). Positivity for Brachyury protein (Figure 4.23A) did not differ between either non-degenerate and moderately degenerate samples ($p= 0.0602$) or moderately degenerate and severely degenerate tissues ($p= 0.7391$), although a comparison of non-degenerate and severely degenerate tissue staining levels did show variability, with greater staining noted in non-degenerate specimens ($p= 0.0385$).

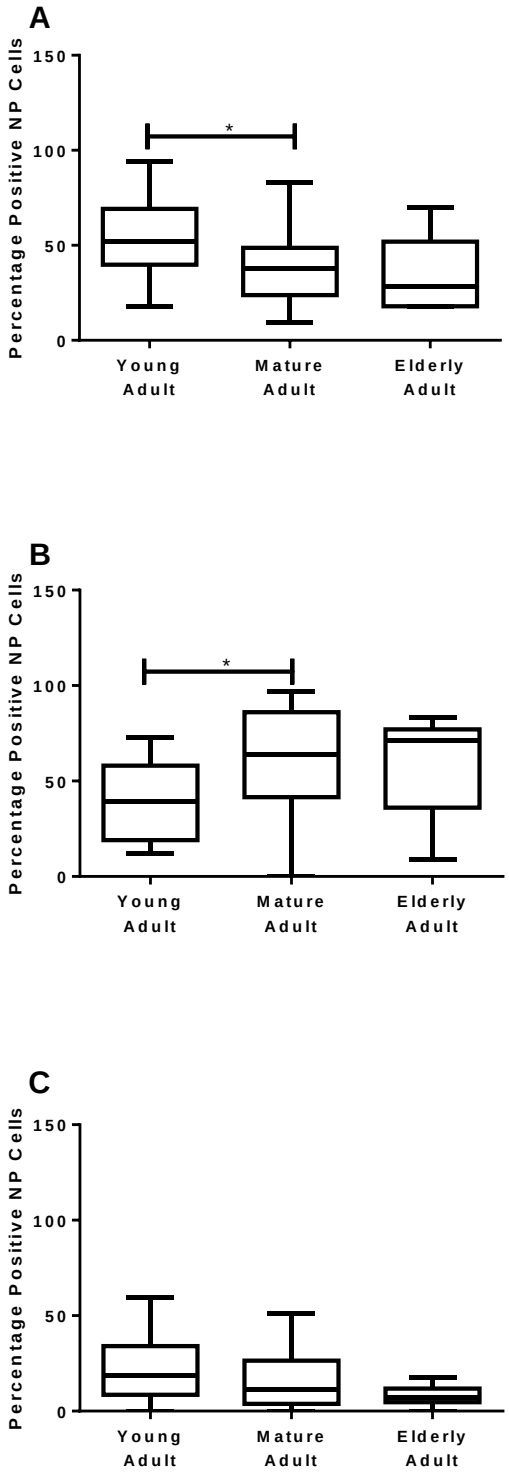

Figure 4.22 Immunopositivity for Notochordal Cell Marker Proteins: Changes with Age. The percentage of adult human NP cells that stained positively for notochordal cell marker proteins Brachyury (A), Galectin-3 (B) and CD24 (C) was assessed according to patient age at the time of surgery (young adult 0-39 years n=20; mature adult 40-59 years, n=28; elderly adult 60+ years, n=7). *p <0.05.

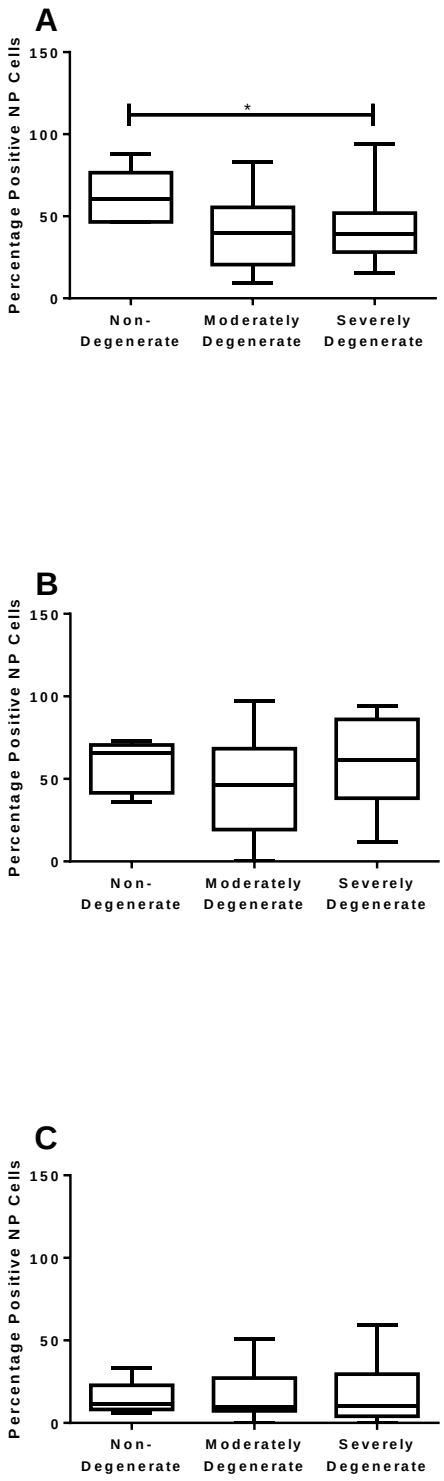

Figure 4.23 Immunopositivity for Notochordal Cell Marker Proteins: Changes with Degeneration. The percentage of adult human NP cells that stained positively for notochordal cell marker proteins Brachyury (A), Galectin-3 (B) and CD24 (C) was assessed according to histological grade of tissue degeneration (non-degenerate grades 0-4, n=5; moderately degenerate grades 5-7, n=27; severely degenerate grades 8-12, n=23). *p <0.05.

4.4.5.2.6 The Effects of Ageing and Degeneration on the Proportion of Clustered and Single NP Cells

The proportion of single NP cells and NP cell clusters within the tissue was first determined for each of the specimens assessed. On average across the cohort, 87.69%±1.154 of NP cells were single cells, whilst an average of 12.31%±1.154 of NP cells were localised within NP cell clusters. Figure 4.24 illustrates the average percentage of NP cells localised within clusters or as single cells for each of the antibodies assessed. Of note, variation in these proportions was comparable between each antibody specimen cohort, with no significant variation the percentage of singular and clustered NP cells noted between antibody cohorts, irrespective of age or degeneration (p=>0.9999 and p=>0.9999 respectively), and therefore any trends identified correlated to the presence of single or clustered NP cells was not associated with variations in the proportions of these populations between tissue sections.

When the proportion of NP cells in clusters was correlated against the histological grade of degeneration, a significant positive correlation was noted (Figure 4.25A) (r= 0.3055, p= 0.0209, 95% CI), indicating that increasing severity of disc degeneration results in increased NP cell cluster formation. A significant negative correlation was noted when the proportion of single NP cells was correlated to the histological grade of degeneration (Figure 4.25B) (r= -0.3640, p= 0.0054, 95% CI), indicating that the proportion of single NP cells declines with progressing severity of tissue degeneration. In terms of variation in the proportion of cell clusters with ageing and degeneration, there was no significant correlation between patient age and the proportion of NP cell clusters (Figure 4.25C) (r= -0.03305, p= 0.8072, 95% CI). Similarly, the proportion of single NP cells was not found to be correlated with patient age (Figure 4.25D) (r= -0.05983, p= 0.6584, 95% CI),

Figure 4.24 Protein Expression in Single and Cell Clusters. The average percentage of single (dark purple) and clustered NP cells (light purple) was determined for FoxF1 (A), Pax-1 (B), Cytokeratin-8 (C), Cytokeratin-18 (D), Carbonic Anhydrase-12 (E), Brachyury (F), Galectin-3 (G) and CD24 (H). Data taken from the average of all specimens tested with each antibody.

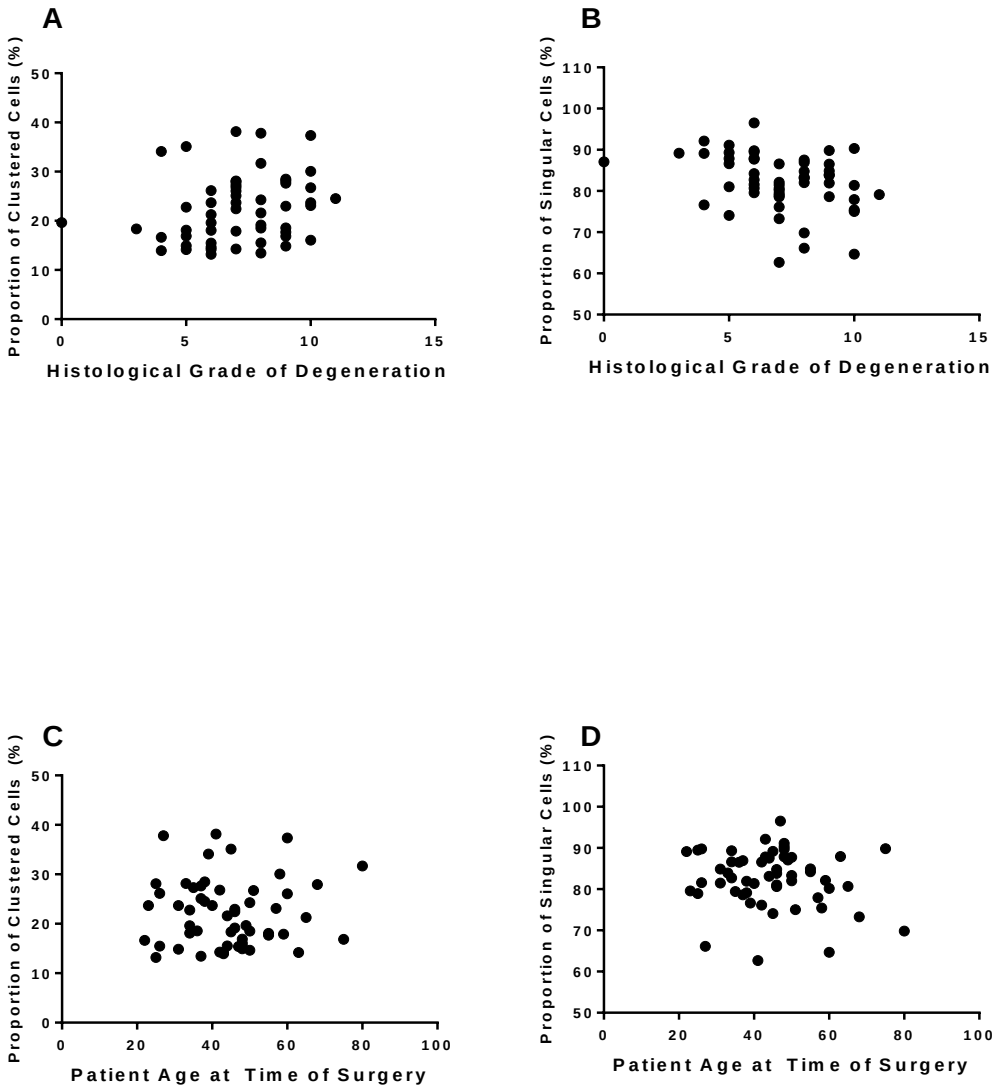

Figure 4.25 Variation in the proportion of singular and clustered NP cells with degeneration and ageing. The proportions of total NP cells within NP tissue localised within cell clusters (A and C) and as singular cells (B and D) was correlated against histological grade of degeneration (A and B) and patient age at the time of surgery (C and D).

4.4.5.2.7 Immunopositivity within Single NP Cells and NP Cell Clusters

Comparisons of the proportion of single NP cells and NP cell clusters within the immunopositive cell populations were then made. Figure 4.26 illustrates the mean proportions of immunonegative and immunopositive NP cells for each marker assessed (grey pie charts), and of this positive population, the respective mean proportions localised as single and positive cells (green pie charts). With regards to FoxF1 expression, 74.73% of the total NP cell population was immunopositive, and of these cells, 75.23% were located as single cells, and 24.77% as NP cell clusters (Figure 4.26a). Similarly, Pax-1 was detected in 68.21% of all NP cells, with 80.18% immunopositive cells being single NP cells, and 19.82% cell clusters (Figure 4.26b). On average, Cytokeratin-8 was only detected in 10.59% of all NP cells, and 97.36% of these were single cells, versus 2.64% in cell clusters (Figure 4.26c). Cytokeratin-18 staining was detected in an average of 29.01% of total NP cells, and of these positively stained cells, 82.59% of cells were single NP cells, and 17.41% NP cell clusters (Figure 4.26d). Carbonic Anhydrase-12 protein was present in an average of 72.08% of the total NP cell population, with 64.08% in single NP cells, and 35.92% in NP cell clusters (Figure 4.26e). Regarding the notochordal cell marker proteins, Brachyury expression was demonstrated in an average of 43.32% of NP cells, and of these cells, 83.76% were single cells, and 16.24% in clusters (Figure 4.26f). An average of 50.02% of all NP cells was shown to express Galectin-3, and of this immunopositive cell population, 83.72% of cells were located as single NP cells, and 16.28% within NP cell clusters (Figure 4.26g). Finally, CD24 immunopositivity was only demonstrated in 16.76% of all NP cells, and the majority (94.93%) of positively stained cells were single NP cells, and only 5.07% were clustered NP cells (Figure 4.26h).

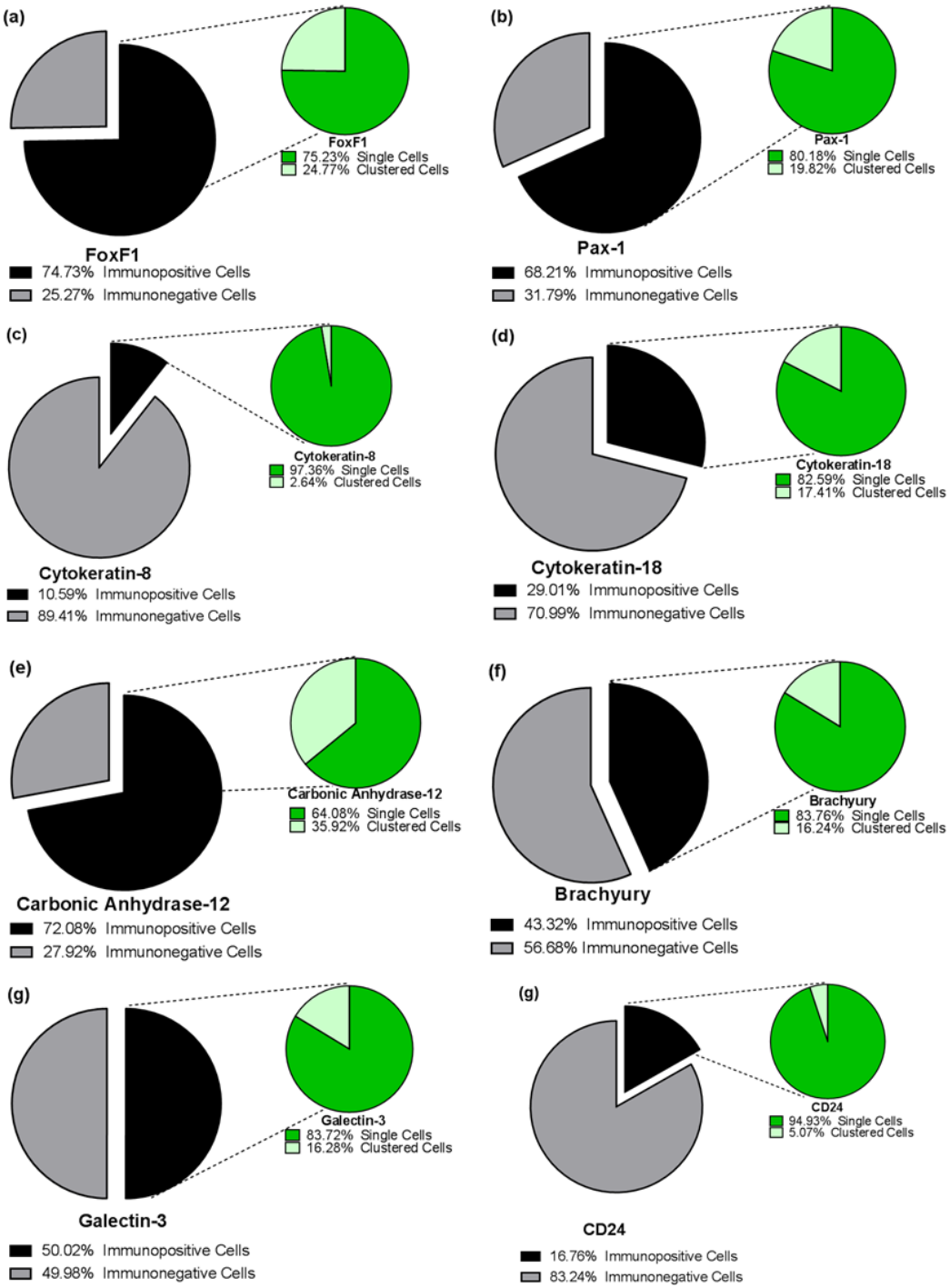

Figure 4.26 Mean immunopositivity in the total NP cell population, and average proportions of positive NP cells in clusters and single cells. The total NP cell population is represented by the grey pie chart. Of the immunopositive cells (black segment), the mean proportion of NP cells located as single cells (dark green) and clustered cells (light green) was determined for the markers FoxF1 (a); Pax-1 (b); Cytokeratin-8 (c); Cytokeratin-18 (d); Carbonic Anhydrase-12 (e); Brachyury (f); Galectin-3 (g); and CD24 (h).

4.4.5.2.8 Immunopositivity within All Single NP Cells and All NP Cell Clusters

As the proportion of staining was noted to vary between cell clusters and single NP cells, the immunopositivity of these sub-populations of cells were further investigated. Figure 4.27 illustrates the immunopositivity of total single NP cells and total clustered NP cell cluster groups for each of the proteins investigated. Of the total single cell population assessed for FoxF1 expression, 40.60% of cells were immunopositive, compared to 60.08% of the total population of NP cells localised within cell clusters. Regarding Pax-1 expression, 43.08% of all single NP cells demonstrated positivity, whilst 70.26% of clustered NP cells were immunopositive. The total single NP cell population was comprised of only 8.03% cytokeratin-8 immunopositive cells, whilst 46.05% of clustered NP cells were positively stained. Regarding Cytokeratin-18 staining, 41.42% of single NP cells demonstrated positivity, compared to 37.48% of clustered NP cells. Of the single NP cell sub-population, 36.34% of cells were positive for Carbonic Anhydrase-12, whilst 80.74% of NP cell clusters were positive for the same marker. In terms of NC cell marker protein expression, 41.10% of single NP cells demonstrated immunopositivity for Brachyury, in addition to 56.49% of clustered NP cells. Galectin-3 positivity was shown in 41.67% of all single NP cells and 60.87% of all clustered NP cells, whilst CD24 was detected in 47.91% of single NP cells, versus 28.44% of clustered NP cells. Thus, although a greater proportion of the total immunopositive NP cells are single NP cells as compared to clustered, analysis of the single NP cell and NP cell cluster populations individually highlight that with the exception of Cytokeratin-18 and CD24, a greater proportion of the NP cells localised within cell clusters are immunopositive for these markers, as compared to single cell populations.

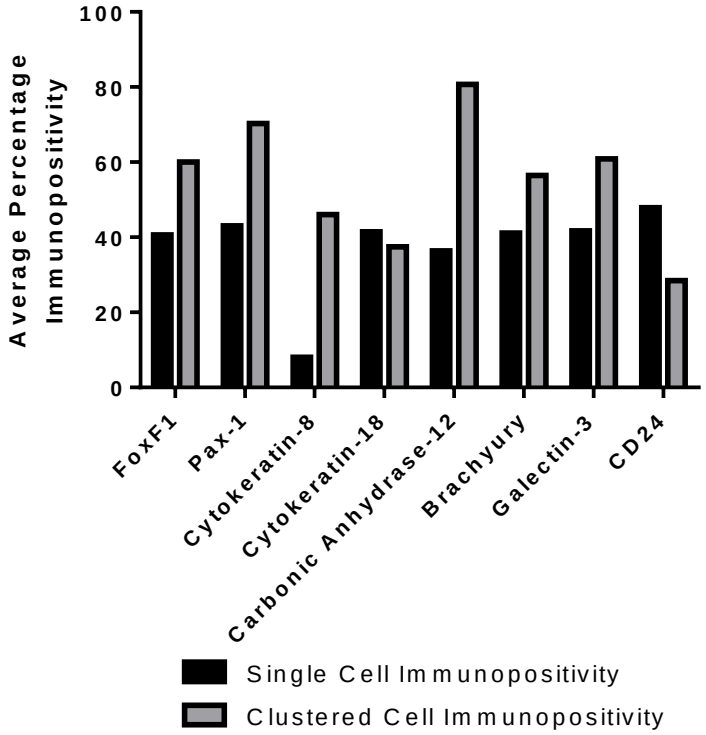

Figure 4.27 Mean immunopositivity of total single NP cell and total clustered NP cell populations. The percentage of single NP and clustered NP cells were counted for each specimen tested, as well as the positive staining demonstrated in each of these groups. For each marker, the mean percentage of immunopositive cells was determined for single (black bars) and clustered NP cell (grey bars) categories.

4.4.5.2.9 Variation in Single NP Cell Immunopositivity with Ageing

Variations in the immunopositivity of the single NP cells and NP cell clusters with ageing and degeneration were determined. Figure 4.28 illustrates variation in single NP cell immunopositivity with ageing. The number of positively stained single NP cells for Cytokeratin-8 (Figure 4.28C), Cytokeratin-18 (Figure 4.28D), Carbonic Anhydrase-12 (Figure 4.28E), Brachyury (Figure 4.28F) and Galectin-3 (Figure 4.28G) did not vary significantly between young and mature adult cohorts ($p= 0.4449$; $p= 0.1679$; $p= 0.2477$; $p= 0.1028$; and $p= 0.0559$ respectively); young and elderly adult cohorts ($p= 0.5116$; $p= 0.0764$; $p= 0.1809$; $p= 0.1204$; and $p= 0.1989$ respectively); and mature and elderly adult cohorts ($p= 0.5906$; $p= 0.2265$; $p= 0.3519$; $p= 0.7612$; and $p= 0.6179$ respectively). FoxF1 (Figure 4.28A) and Pax-1 (Figure 4.28B) immunopositivity did not vary significantly between young and mature adult specimens ($p= 0.1464$; and $p= 0.0534$ respectively), or mature and elderly adult specimens ($p= 0.2759$; and $p= 0.1705$ respectively), although the number of positively stained cells was significantly higher in young adult vs. elderly adult samples ($p= 0.0402$; and $p= 0.0164$ respectively). Regarding CD24 staining (Figure 4.28H), a comparison of young vs. mature adult staining levels demonstrated greater positivity in young specimens, as compared to mature ($p= 0.0333$), although no further variations were noted for young/elderly ($p= 0.1080$) and mature/elderly cohort ($p= 0.7910$) comparisons.

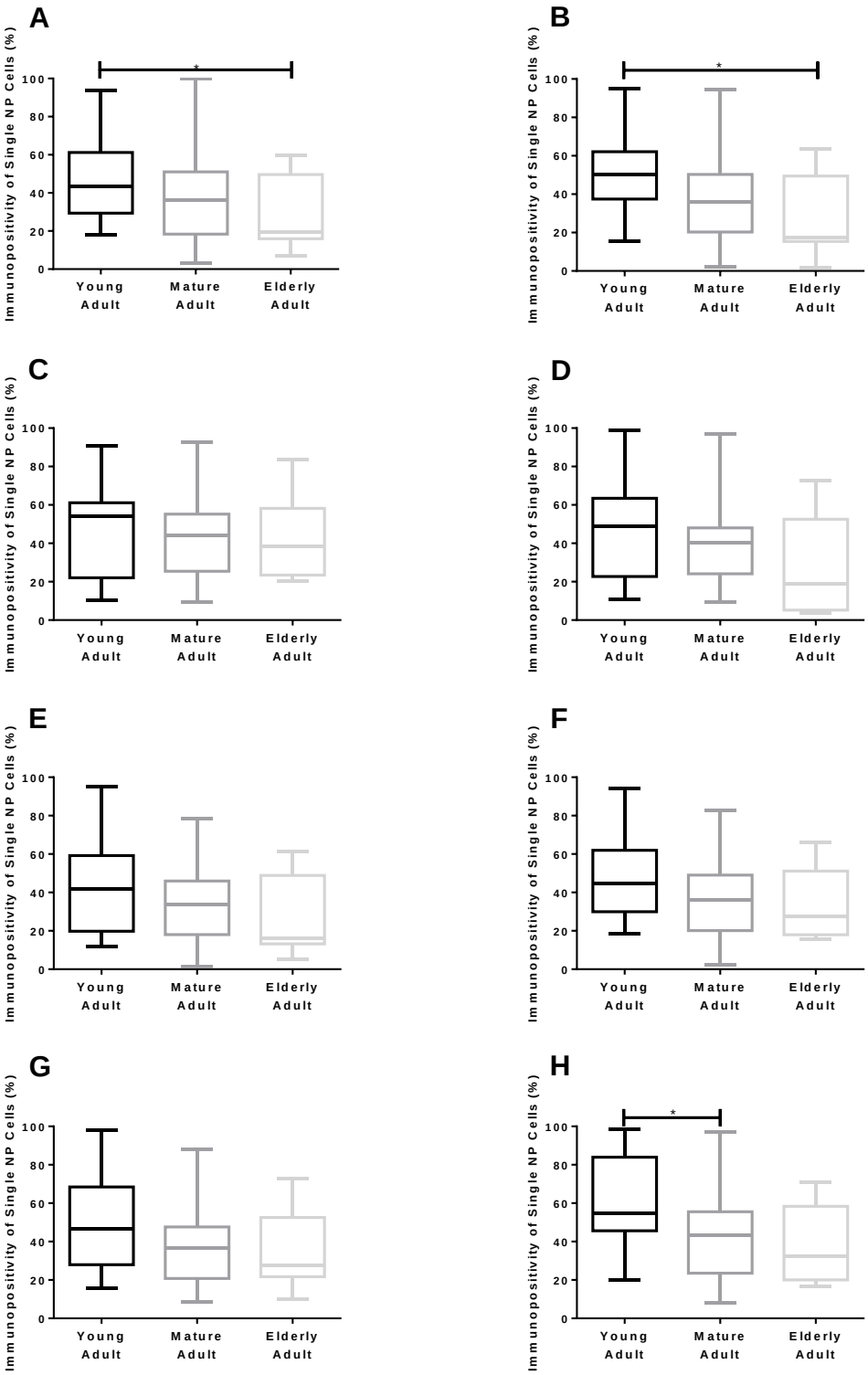

Figure 4.28 Variation in the immunopositivity of total single NP cell population and ageing. The immunopositivity of the total single NP cell population was assessed according to patient age for FoxF1 (A), Pax-1 (B), Cytokeratin-8 (C), Cytokeratin-18 (D), Carbonic Anhydrase-12 (E), Brachyury (F), Galectin-3 (G) and CD24 (H). Young adult (0-39 years, n=20); Mature adult (40-59 years, n=28); and Elderly adult (60+ years, n=7). *p= <0.05.

4.4.5.2.10 Variation in Single NP Cell Immunopositivity with Degeneration

Regarding variation in single cell immunopositivity with degeneration, expression levels of Pax-1 (Figure 4.29B), Cytokeratin-8 (Figure 4.29C), Galectin-3 (Figure 4.29G) and CD24 (Figure 4.29H) did not demonstrate any significant variations when either non-degenerate and moderately degenerate ($p= 0.0561$; $p= 0.5705$; $p= 0.0994$; and $p= 0.0642$ respectively); non-degenerate and severely degenerate ($p= 0.0819$; $p= 0.2636$; $p= 0.0938$; and $p= 0.1732$ respectively); or moderately degenerate and severely degenerate ($p= 0.6448$; $p= 0.8491$; $p= 0.6712$; and $p= 0.2113$ respectively) specimens were compared. Immunopositivity of FoxF1 (Figure 4.29A), Carbonic Anhydrase-12 (Figure 4.29E) and Brachyury (Figure 4.29F) significantly decreased with degeneration. When comparisons of non-degenerate and moderately degenerate staining levels were compared, significant decreases in the number of positively stained cells were noted ($p= 0.0436$; $p= 0.0383$; and $p= 0.0334$ respectively); which was also noted when non-degenerate and severely degenerate samples were compared ($p= 0.0229$; $p= 0.0128$; and $p= 0.0229$ respectively), but not when moderately degenerate and severely degenerate specimens were analysed ($p= 0.9522$; $p= 0.6693$; and $p= 0.6061$ respectively). With regards to Cytokeratin-18 (Figure 4.29D) immunopositivity, no significant variations were noted between non-degenerate and moderately degenerate ($p= 0.0712$); and moderately degenerate and severely degenerate samples ($p= 0.5064$), although the number of positively stained cells was significantly greater in non-degenerate vs. severely degenerate tissues ($p= 0.0128$).

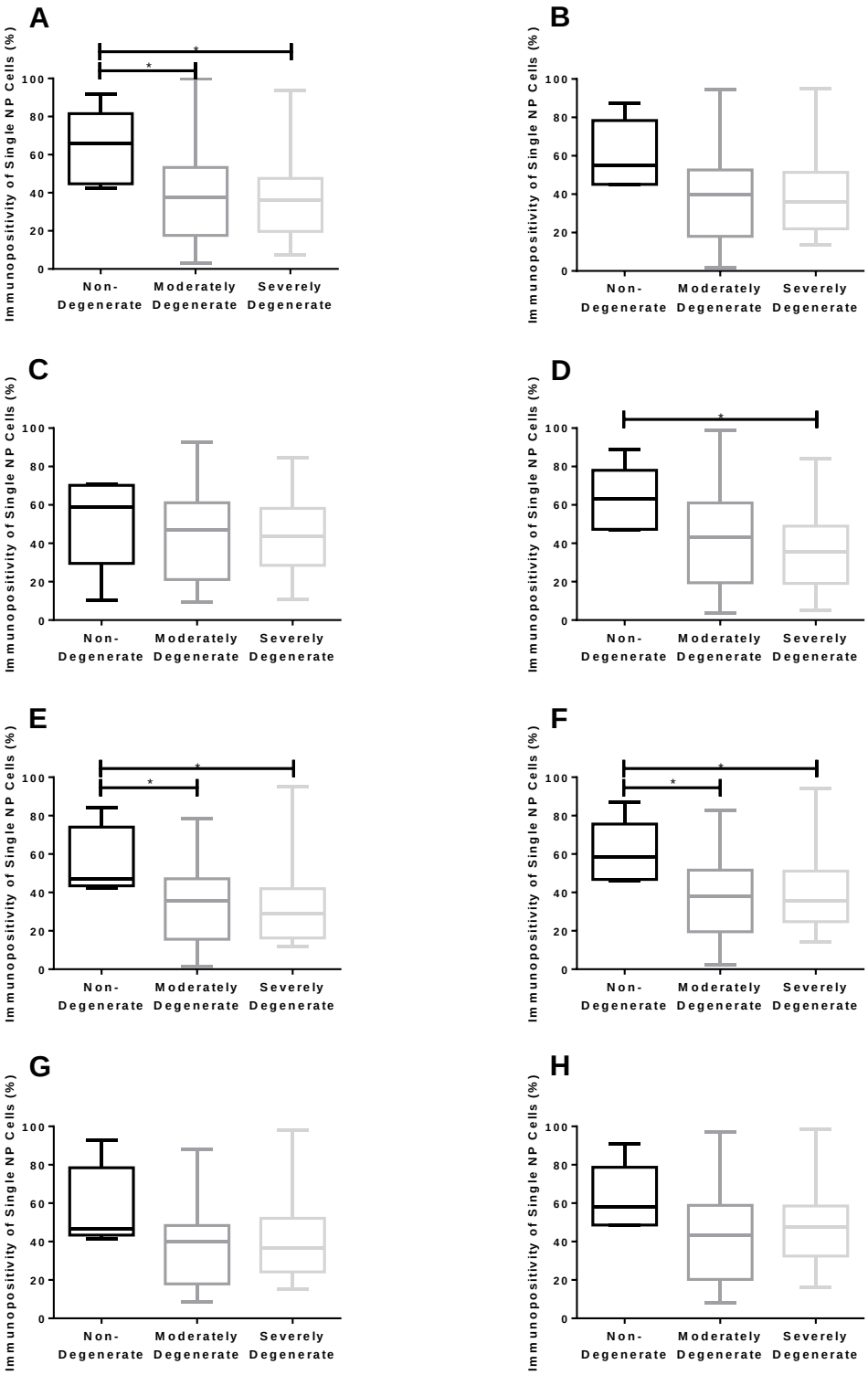

Figure 4.29 Variations in the immunopositivity of total single NP cell population and degeneration. The immunopositivity of the total single NP cell population was assessed according degenerative score for FoxF1 (A), Pax-1 (B), Cytokeratin-8 (C), Cytokeratin-18 (D), Carbonic Anhydrase-12 (E), Brachyury (F), Galectin-3 (G) and CD24 (H). Non-degenerate (grades 0-4, n=5); Moderately degenerate (grades 5-7, n=27); and Severely degenerate (grades 8-12, n=23). *p= <0.05.

4.4.5.2.11 Variation in NP Cell Cluster Immunopositivity with Ageing

Variations in the immunopositivity of the NP cell clusters with ageing and degeneration was also investigated. Variations with age are shown in Figure 4.30. There was no significant variations in the NP cell cluster immunopositivity of any of the markers analysed (FoxF1 (Figure 4.30A), Pax-1 (Figure 4.30B), Cytokeratin-8 (Figure 4.30C), Cytokeratin-18 (Figure 4.30D), Carbonic Anhydrase-12 (Figure 4.30E), Brachyury (Figure 4.30F), Galectin-3 (Figure 4.30G) and CD24 (Figure 4.30H)) when young and mature adult specimens ($p= 0.0797$; $p= 0.4140$; $p= 0.1952$; $p= 0.3764$; $p= 0.6433$; $p= 0.1760$; $p= 0.7515$; and $p= 0.4968$ respectively); young and elderly adult specimens ($p= 0.4668$; $p= 0.8094$; $p= 0.3910$; $p= 0.4906$; $p= 0.5395$; $p= 0.0721$; $p= 0.4600$; and $p= 0.6656$ respectively); and mature and elderly adult specimens were compared ($p= 0.4120$; $p= 0.7621$; $p= 0.8199$; $p= 0.2389$; $p= 0.2911$; $p= 0.3609$; $p= 0.2241$; and $p= 0.6250$ respectively).

4.4.5.2.12 Variation in NP Cell Cluster Immunopositivity with Degeneration

Regarding variations in the NP cell cluster immunopositivity and degeneration, with the exception of Cytokeratin-18, no significant variations in the number of positively stained clustered NP cells for the novel NP and NC cell markers were noted. FoxF1 (Figure 4.31A), Pax-1 (Figure 4.31B), Cytokeratin-8 (Figure 4.31C), Carbonic Anhydrase-12 (Figure 4.31E), Brachyury (Figure 4.31F), Galectin-3 (Figure 4.31G) and CD24 (Figure 4.31H) immunopositivity did not vary between non-degenerate and moderately degenerate ($p= 0.0756$; $p= 0.7137$; $p= 0.9552$; $p= 0.7365$; $p= 0.9201$; $p= 0.6750$; and $p= 0.6912$ respectively); non-degenerate and severely degenerate ($p= 0.1080$; $p= 0.7390$; $p= 0.8320$; $p= 0.7713$; $p= 0.2187$; $p= 0.6347$; and $p= 0.5975$ respectively); and moderately degenerate and severely degenerate tissue specimens ($p= 0.4544$; $p= 0.9523$; $p= 0.6145$; $p= 0.4502$; $p= 0.4417$; $p= 0.8586$; $p= 0.9298$ respectively). Cytokeratin-18 (Figure 4.31D) immunopositivity was significantly higher in severely degenerate as compared to moderately degenerate specimens ($p= 0.0238$), although no variation was noted between non-degenerate and moderately degenerate ($p= 0.3126$) and non-degenerate and severely degenerate specimens ($p= 0.8685$).

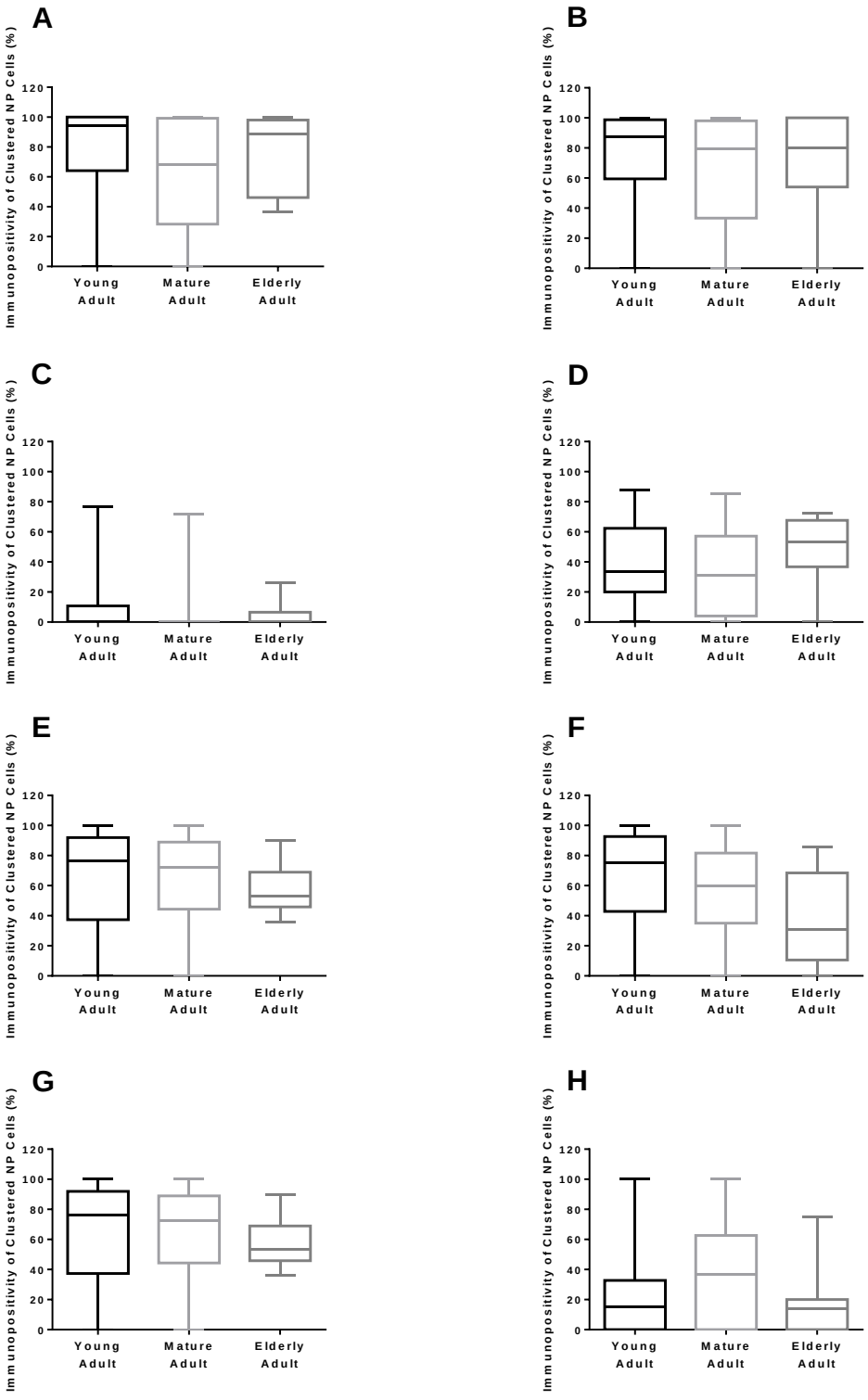

Figure 4.30 Variations in the immunopositivity of total NP cell clusters and ageing. The immunopositivity of the total NP cell cluster was assessed according to patient age for FoxF1 (A), Pax-1 (B), Cytokeratin-8 (C), Cytokeratin-18, (D) Carbonic Anhydrase-12 (E), Brachyury (F), Galectin-3 (G) and CD24 (H). Young adult (0-39 years, n=20); Mature adult (40-59 years, n=28); and Elderly Adult (60+ years, n=7).

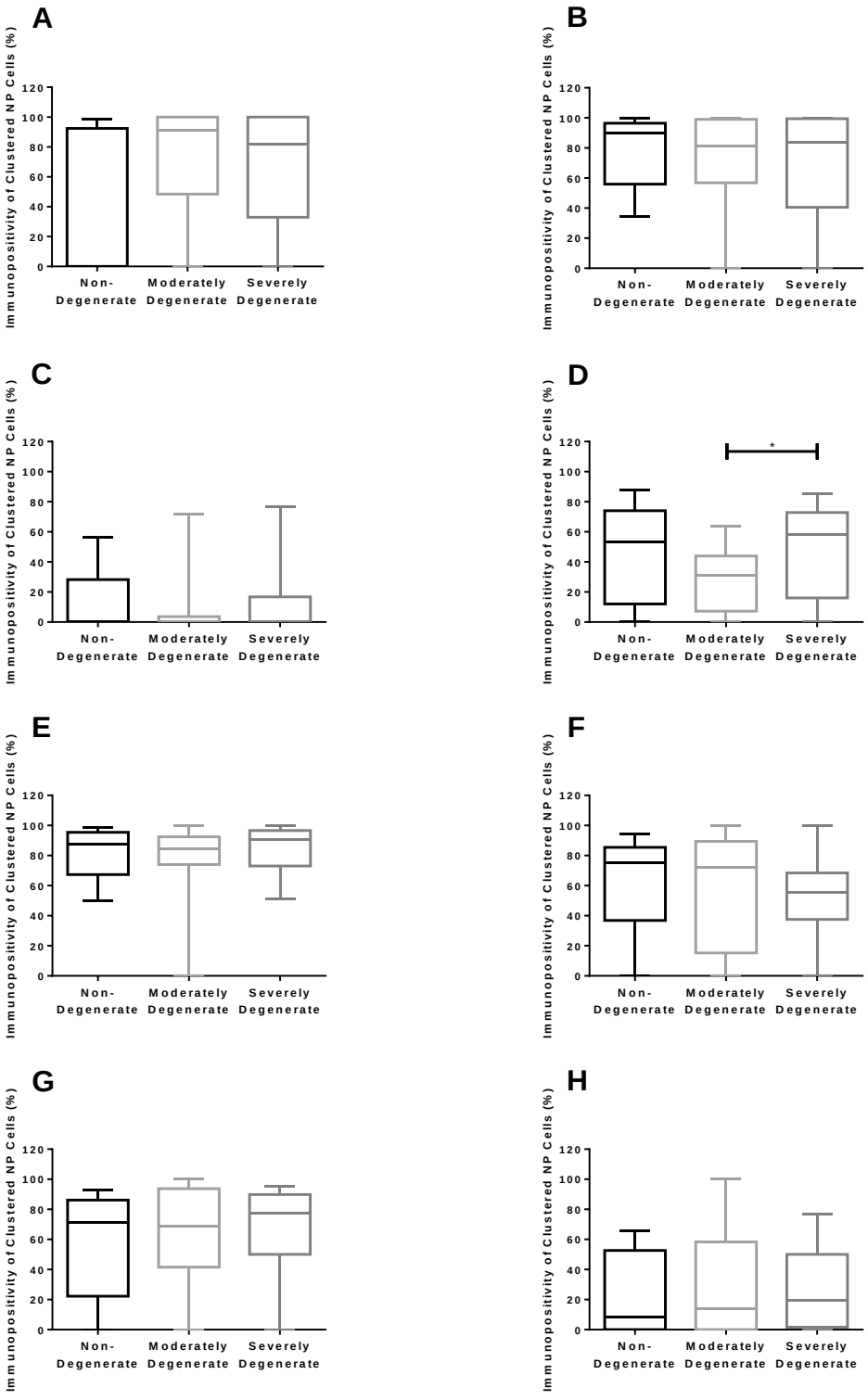

Figure 4.31 Variations in the immunopositivity of total NP cell clustersand degeneration. The immunopositivity of the total NP cell clusters was assessed according to degenerative score for FoxF1 (A), Pax-1 (B), Cytokeratin-8 (C), Cytokeratin-18 (D), Carbonic Anhydrase-12 (E), Brachyury (F), Galectin-3 (G) and CD24 (H). Non-degenerate (grades 0-4, n=5); Moderately degenerate (grades 5-7, n=27); and Severely degenerate (grades 8-12, n=23). *p= <0.05.

4.4.5.2.13 Influence of Increasing Proportion of NP Cell Clusters on Immunopositivity

Variations in the total NP cell immunopositivity with increasing proportion of NP cells in clusters were investigated (Figure 4.32), in order to ascertain whether a progenitor cell population was potentially residing within the NP tissue. Given that increased proportions of clustered NP cells with progressing degeneration were noted here (and described previously by (Pritzker, 1977, Sive *et al.*, 2002)), and it has been suggested that these may be a progenitor cell population, increased expression of novel NP and NC cell markers here may be indicative of such a population of cells. There was no significant correlation between the total NP cell immunopositivity and proportion of clustered NP cells when assessing immunopositivity of Pax-1 (Figure 4.32B) (r= 0.2295; p= 0.0859; 95% CI); Cytokeratin-8 (Figure 4.32C) (r= -0.04044, p= 0.7652, 95% CI); Carbonic Anhydrase-12 (Figure 4.32E) (r= 0.2043, p= 0.1277, 95% CI); and CD24 (Figure 4.32H) (r= 0.08622; p= 0.5237, 95% CI). However, immunopositivity for FoxF1 (Figure 4.32A) (r= 0.3711, p= 0.0045, 95% CI); Cytokeratin-18 (Figure 4.32D) (r= 0.4297, p= 0.0009, 95% CI); Brachyury (Figure 4.32F) (r= 0.2634, p= 0.0477, 95% CI); and Galectin-3 (Figure 4.32G) (r= 0.5635, p= <0.0001, 95% CI) was significantly positively correlated with the proportion of NP cells located within clusters.

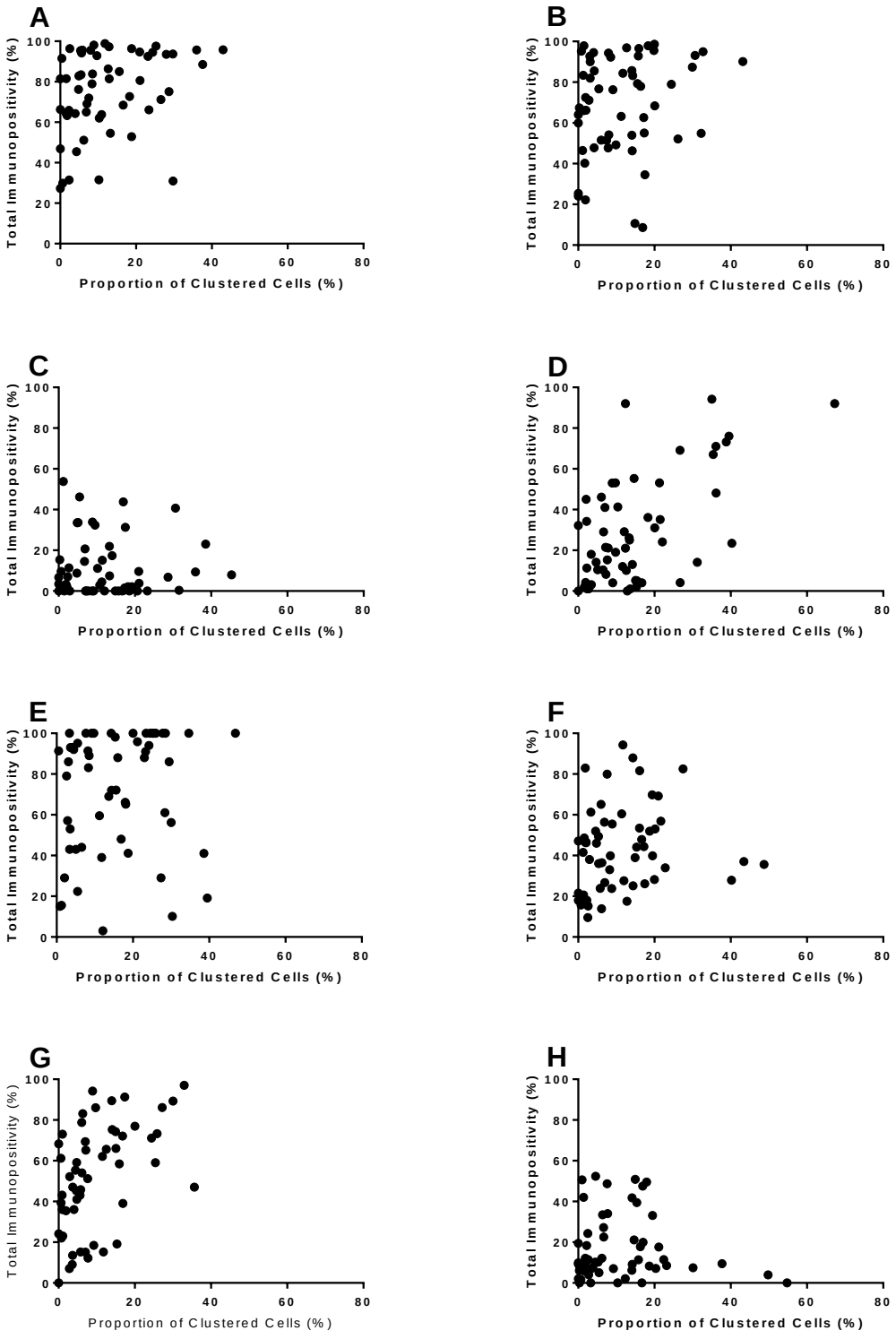

Figure 4.32 Variations in total NP cell immunopositivity with increasing proportion of clustered NP cells. Total NP cell immunopositivity for FoxF1 (A), Pax-1 (B), Cytokeratin-8 (C), Cytokeratin-18 (D), Carbonic Anhydrase-12 (E), Brachyury (F), Galectin-3 (G) and CD24 (H) was correlated with the percentage of NP cells localised in cell clusters.

4.4.5.2.14 NP and NC Cell Marker Protein Expression in the Adult Human AF

Percentage cell immunopositivity of novel NP cell markers (FoxF1, Pax-1, Cytokeratin-8, Cytokeratin-18 and Carbonic Anhydrase-12) and notochordal cell marker (Brachyury, Galectin-3 and CD24) proteins in adult human AF tissues were calculated. Figure 4.33 illustrates the mean percentage immunopositivity within AF tissues noted for each of the markers tested. The average AF cell immunopositivity values were as follows: FoxF1 72.25%±5.659; Pax-1 50.36%±7.507; Cytokeratin-18 1.871%±0.5610; Carbonic Anhydrase-12 36.31%±5.640; Brachyury 9.978%±3.036; Galectin-3 4.061%±1.295; and CD24 6.357%±1.818. Of note, there was no detectable staining of Cytokeratin-8 in cells of the adult human AF. Interestingly, the novel NP cell markers FoxF1, Pax-1 and Carbonic Anhydrase-12 demonstrated the greatest percentage of AF immunopositivity, whereas NC cell markers (Brachyury, Galectin-3 and CD24) were lowly expressed by AF cells.

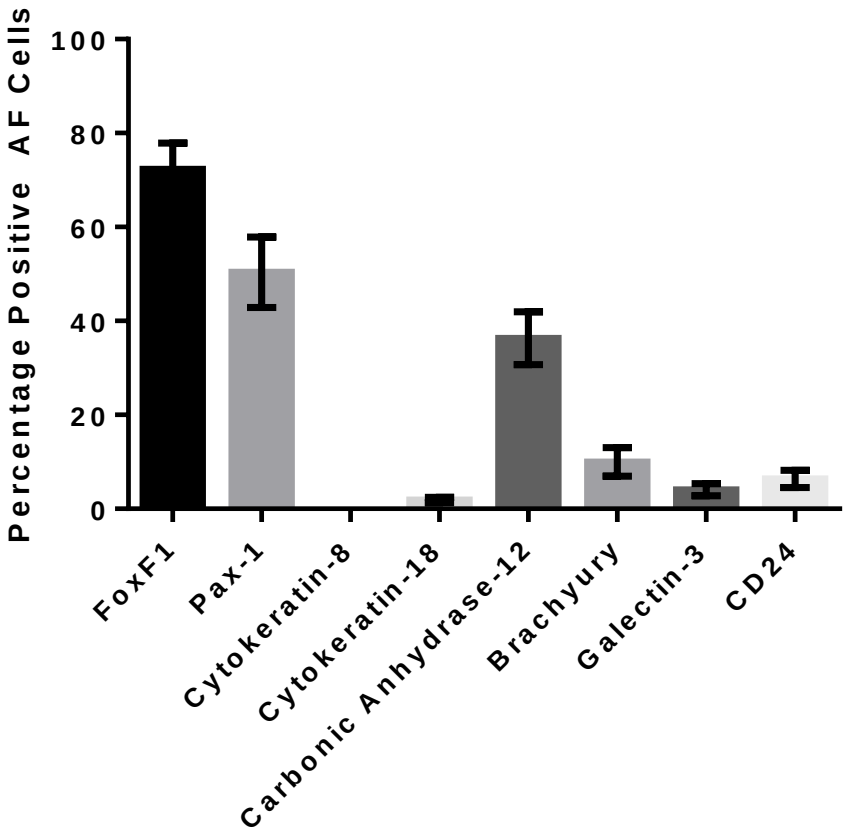

Figure 4.33 Mean AF cell immunopositivity as a percentage of total AF cell count. Error bars calculated from standard error of the mean.

4.4.5.2.15 NP Cell Marker Protein Expression in the AF: Changes with Ageing and Degeneration

Figure 4.34 illustrates the relationship between novel NP cell marker protein expression in adult human AF cells and patient age. Of note, as only 21 specimens contained distinct AF tissue, analysis according to age and degeneration was performed as a scatter plot and Spearman's Rank correlation rather than box plots and Mann Whitney-U tests. No statistically significant correlation between FoxF1 (Figure 4.34A) AF immunopositivity and ageing was shown ($r = 0.03905$, $p = 0.8655$, 95% CI). Similarly, no significant correlations were demonstrated for Pax-1 (Figure 4.34B), Cytokeratin-18 (Figure 4.34D), and Carbonic Anhydrase-12 (Figure 4.34E) immunopositivity and ageing ($r = -0.09974$, $p = 0.6671$, 95% CI; $r = -0.3657$, $p = 0.1031$, 95% CI; $r = -0.3729$, $p = 0.0959$, 95% CI respectively). As demonstrated by Figure 4.35, there was also no significant correlation between degenerative score and the immunopositivity of novel NP cell markers FoxF1 (Figure 4.35A) ($r = 0.03027$, $p = 0.8964$, 95% CI), Pax-1 (Figure 4.35B) ($r = -0.05338$, $p = 0.8182$, 95% CI), Cytokeratin-18 (Figure 4.35D) ($r = 0.1396$, $p = 0.5461$, 95% CI), and Carbonic Anhydrase-12 (Figure 4.35E) ($r = 0.2270$, $p = 0.3224$, 95% CI). In summary, there was no significant correlation between AF cell immunopositivity for novel NP cell marker proteins and age or level of degeneration.

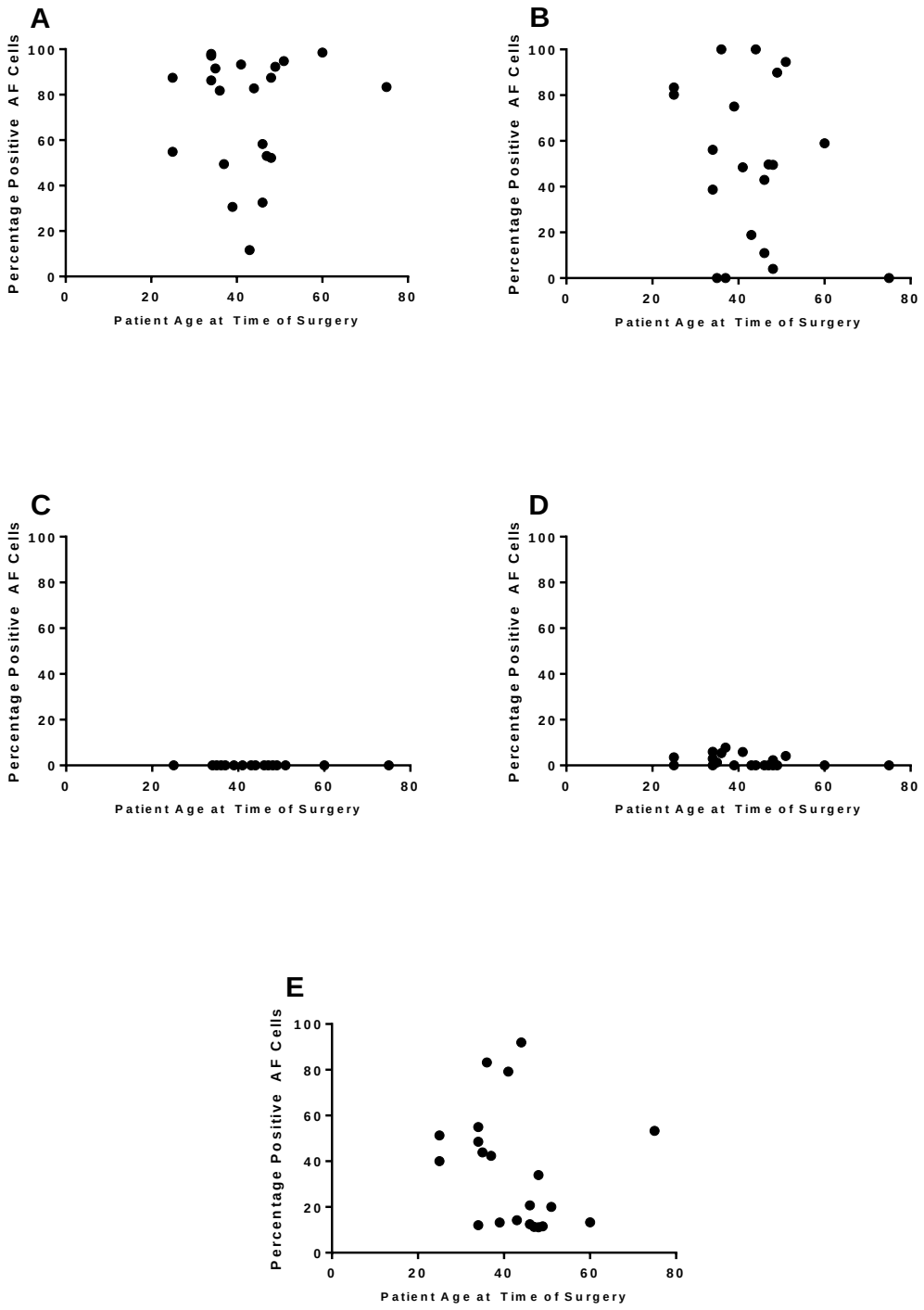

Figure 4.34 Immunopositivity for novel NP cell marker proteins: Changes with Age. A correlation of AF cell immunopositivity against patient age at the time of surgery was performed for FoxF1 (A), Pax-1 (B), Cytokeratin-8 (C), Cytokeratin-18 (D) and Carbonic Anhydrase-12 (E).

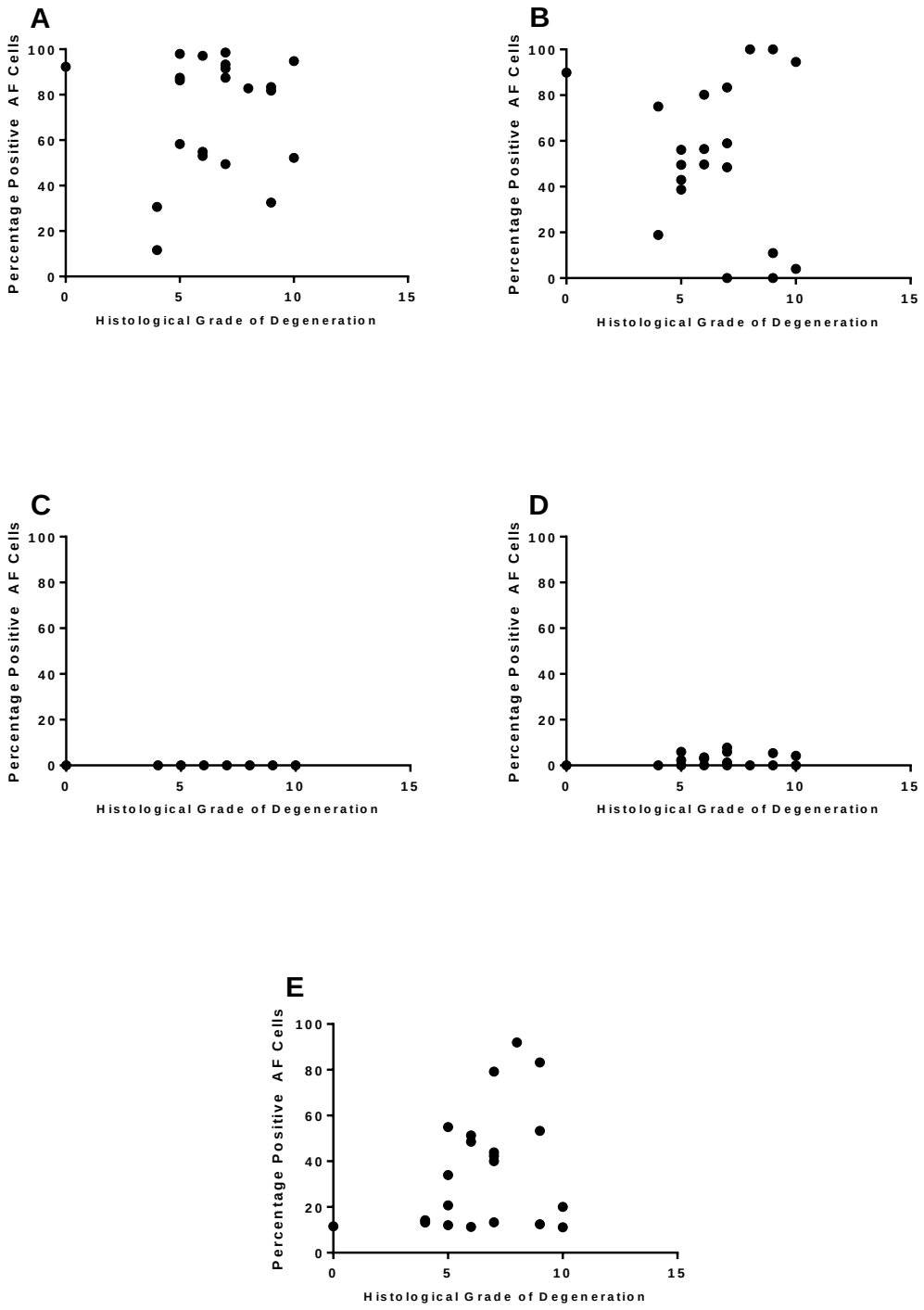

Figure 4.35 Immunopositivity for novel NP cell marker proteins: Changes with Degeneration. A correlation of AF cell immunopositivity against histological score of degeneration was performed for FoxF1 (A), Pax-1 (B), Cytokeratin-8 (C), Cytokeratin-18 and Carbonic Anhydrase-12 (E).

4.4.5.2.16 NC Cell Marker Protein Expression in the AF: Changes with Ageing and Degeneration

Notochordal cell marker protein expression in cells of the adult human AF was correlated with age and degenerative score. The correlation between Brachyury (Figure 4.36A), Galectin-3 (Figure 4.36B) and CD24 (Figure 4.36C) immunopositivity and patient age was not statistically significant ($r = -0.06168$, $p = 0.7906$, 95% CI; $r = -0.07049$, $p = 0.7614$, 95% CI; and $r = -0.06913$, $p = 0.7659$, 95% CI). Similarly, when correlated against histological grading of IVD degeneration, immunopositivity of Brachyury (Figure 4.37A) ($r = -0.1939$, $p = 0.3997$, 95% CI), Galectin-3 (Figure 4.37B) ($r = 0.02467$, $p = 0.9155$, 95% CI) and CD24 (Figure 4.37C) ($r = -0.03632$, $p = 0.8758$, 95% CI) was also not statistically significant.

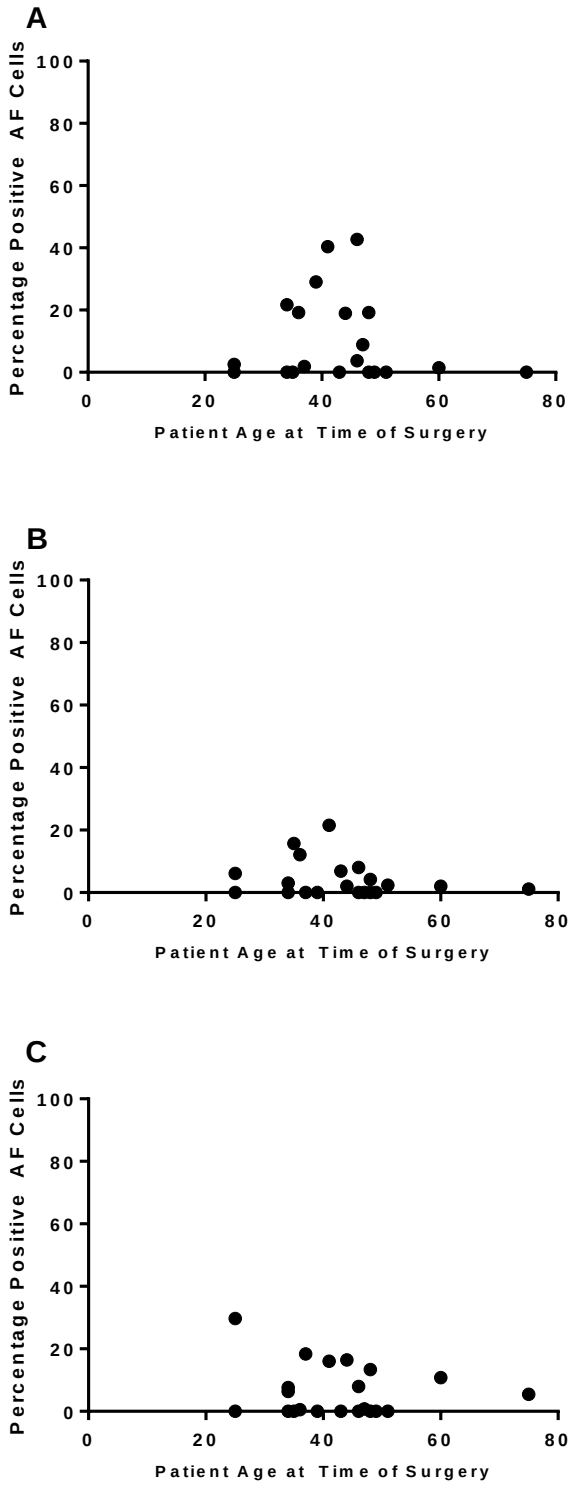

Figure 4.36 Immunopositivity for notochordal cell marker proteins: Changes with Ageing. A correlation of AF cell immunopositivity against patient age at the time of surgery was performed for Brachyury (A), Galectin-3 (B) and CD24 (C).

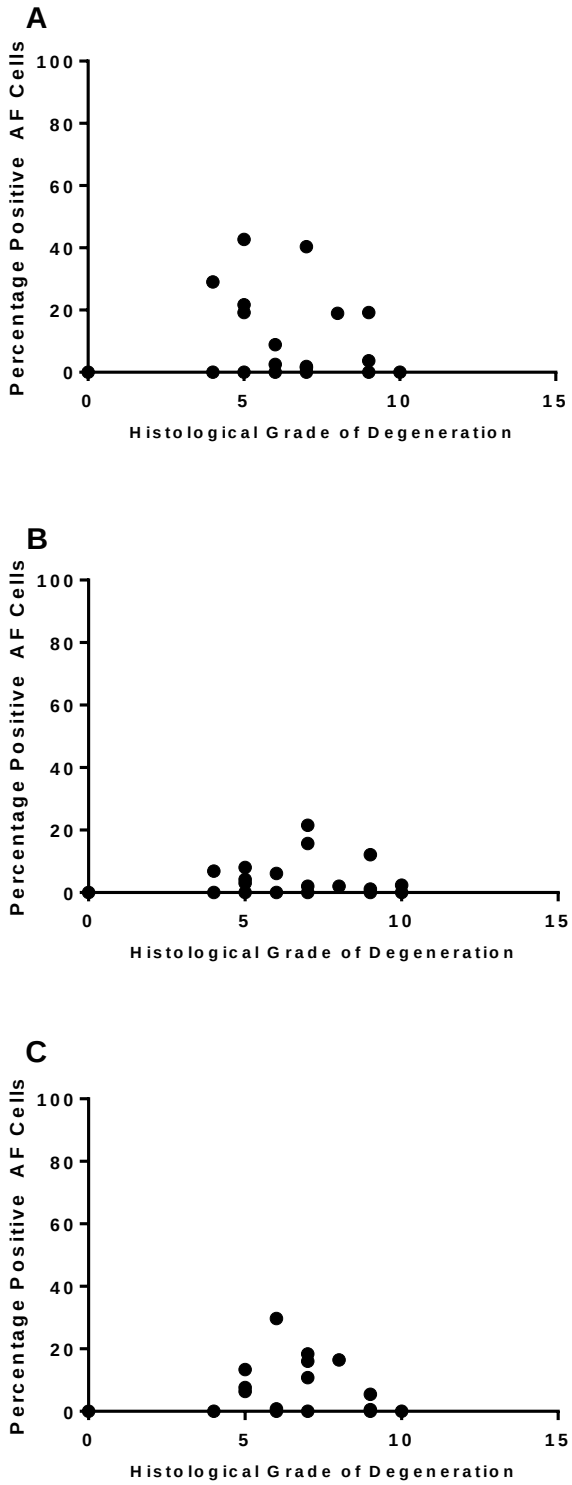

Figure 4.37 Immunopositivity for notochordal cell marker proteins: Changes with Degeneration. A correlation of AF cell immunopositivity against histological score of degeneration was performed for Brachyury (A), Galectin-3 (B) and CD24 (C).

4.4.6 Analysis of Co-Expression in Adult Human NP Cell Populations

Of the markers demonstrating differential expression levels by immunohistochemistry in 4.4.4, four were selected for analysis of co-expression in adult human NP cells: Carbonic Anhydrase-12, Brachyury, Galectin-3 and CD24. Figures 4.38-4.42 demonstrate expression levels of these proteins when investigated separately, and the relevant measurements of immunopositivity are summarised in Table 4.4.

Table 4.4. Protein Expression Levels of Markers Assessed by Flow Cytometry

Specimen	Carbonic Anhydrase-12 Positivity (%)	Brachyury Positivity (%)	Galectin-3 Positivity (%)	CD24 Positivity (%)
HH0295	99.92	70.45	97.96	6.75
HH0298	99.99	84.39	99.92	12.64
HH0581	99.93	94.92	98.01	41.64
HH0593	100.00	31.28	99.97	33.35
HH0613	99.93	96.96	97.92	5.38

Analysis by flow cytometry demonstrated that an average of 99.95%±0.01691 of adult NP cells expressed Carbonic Anhydrase-12. Similarly, an average 98.75%±0.4857 of adult NP cells were shown to be Galectin-3 immunopositive. However, immunopositivity of Brachyury and CD24 was found to be far more variable, with Brachyury positivity ranging from 31% to 97% (mean 75.60%±12.04), and CD24 from 5% to 42% (mean 19.93%±7.382). All isotype controls (shown in Figures 4.36-4.40) were almost entirely negatively stained.

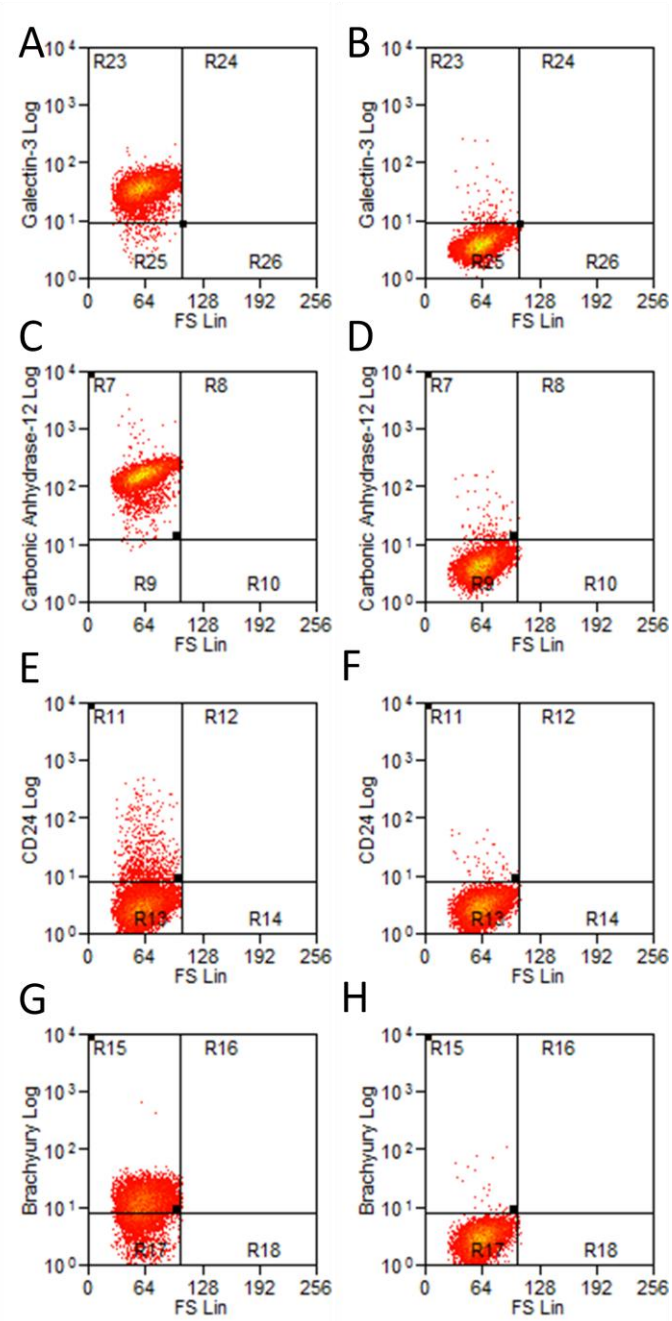

Figure 4.38 Flow cytometric analysis of novel NP and NC cell protein expression in adult human NP cells. Expression of Galectin-3 (A, B); Carbonic Anhydrase-12 (C, D); CD24 (E, F); and Brachyury (G, H) was investigated (sample HH0295). Isotype controls were utilised as negative controls (B, D, F, H). Cellular fluorescence detected in the upper left and right quadrants indicate positive staining.

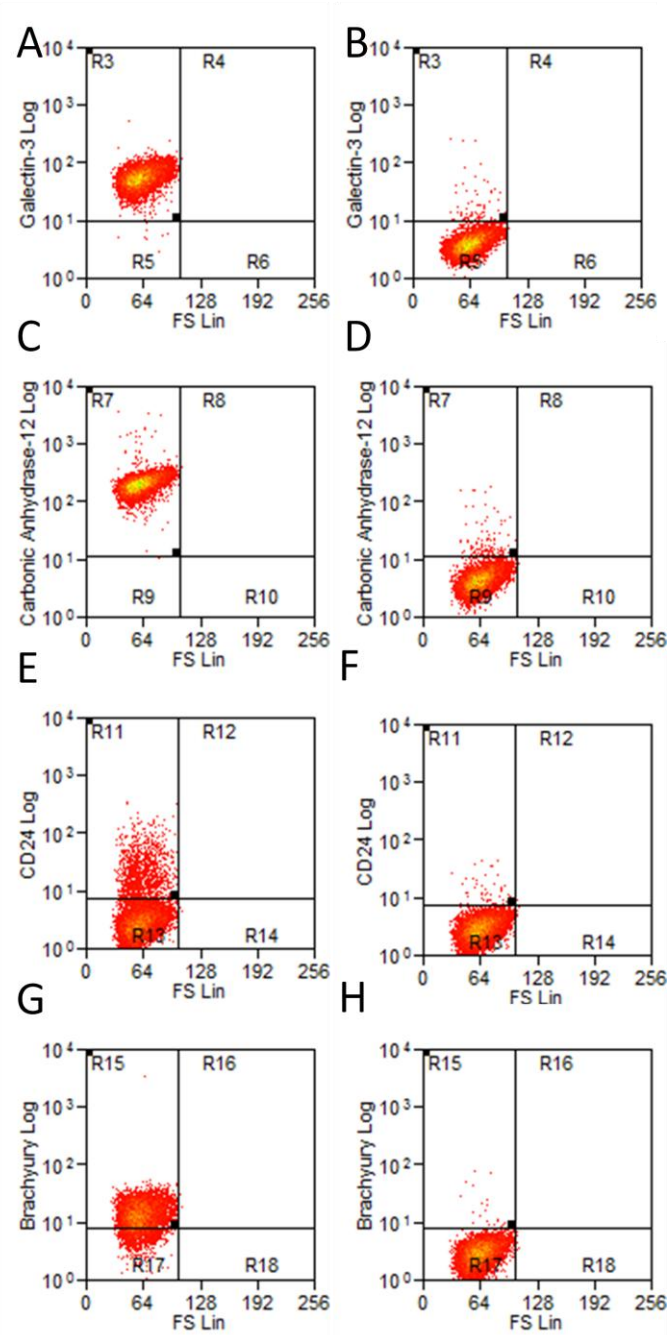

Figure 4.39 Flow cytometric analysis of novel NP and NC cell protein expression in adult human NP cells. Expression of Galectin-3 (A, B); Carbonic Anhydrase-12 (C, D); CD24 (E, F); and Brachyury (G, H) was investigated (sample HH0298). Isotype controls were utilised as negative controls (B, D, F, H). Cellular fluorescence detected in the upper left and right quadrants indicate positive staining.

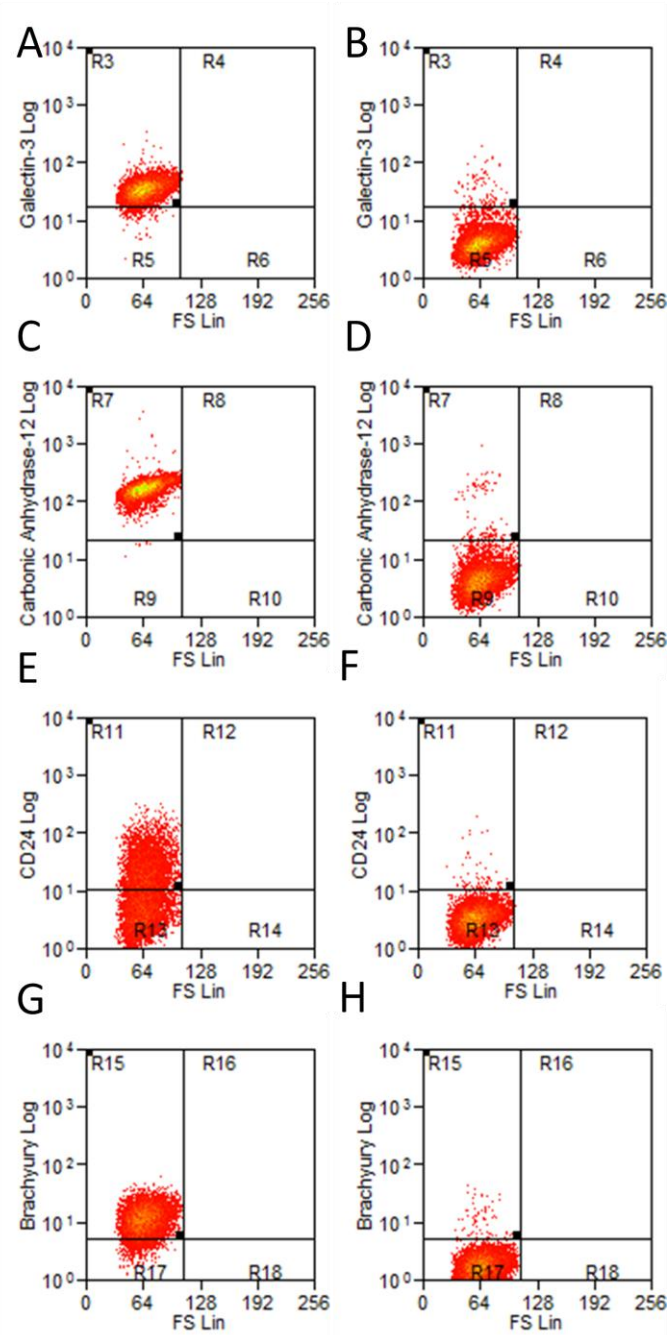

Figure 4.40 Flow cytometric analysis of novel NP and NC cell protein expression in adult human NP cells. Expression of Galectin-3 (A, B); Carbonic Anhydrase-12 (C, D); CD24 (E, F); and Brachyury (G, H) was investigated (sample HH0581). Isotype controls were utilised as negative controls (B, D, F, H). Cellular fluorescence detected in the upper left and right quadrants indicate positive staining.

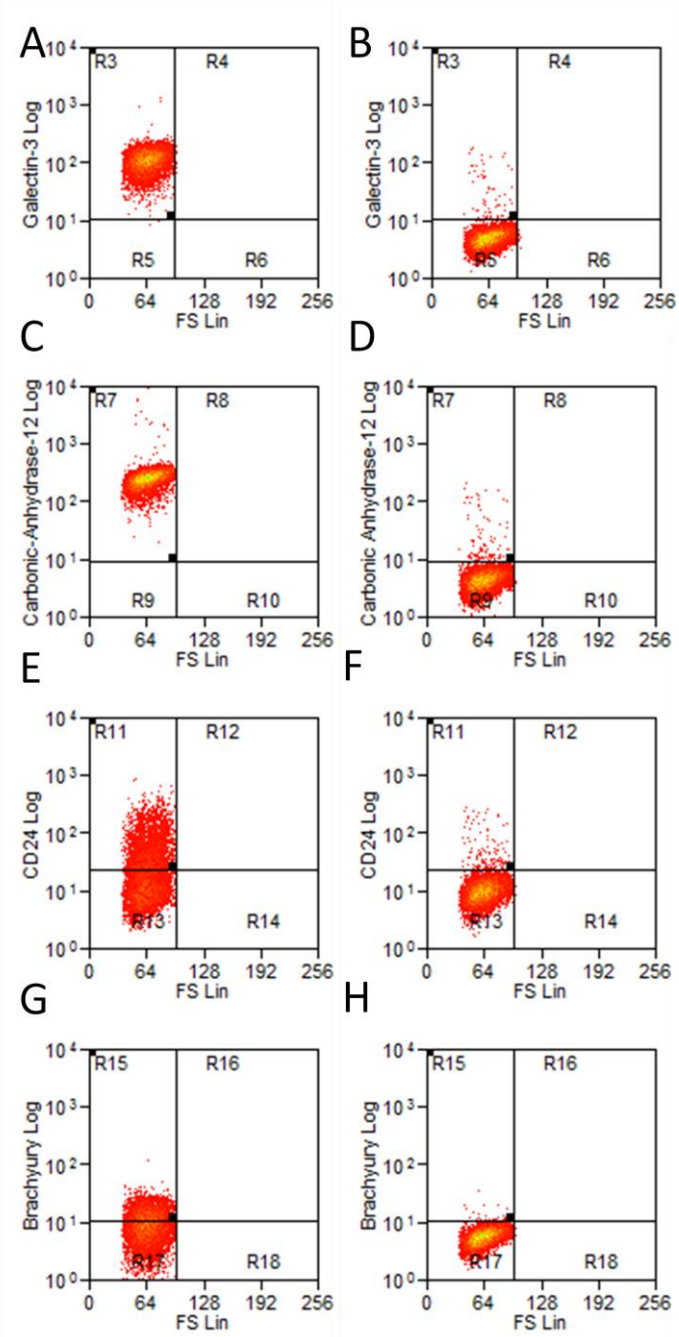

Figure 4.41 Flow cytometric analysis of novel NP and NC cell protein expression in adult human NP cells. Expression of Galectin-3 (A, B); Carbonic Anhydrase-12 (C, D); CD24 (E, F); and Brachyury (G, H) was investigated (sample HH0593). Isotype controls were utilised as negative controls (B, D, F, H). Cellular fluorescence detected in the upper left and right quadrants indicate positive staining.

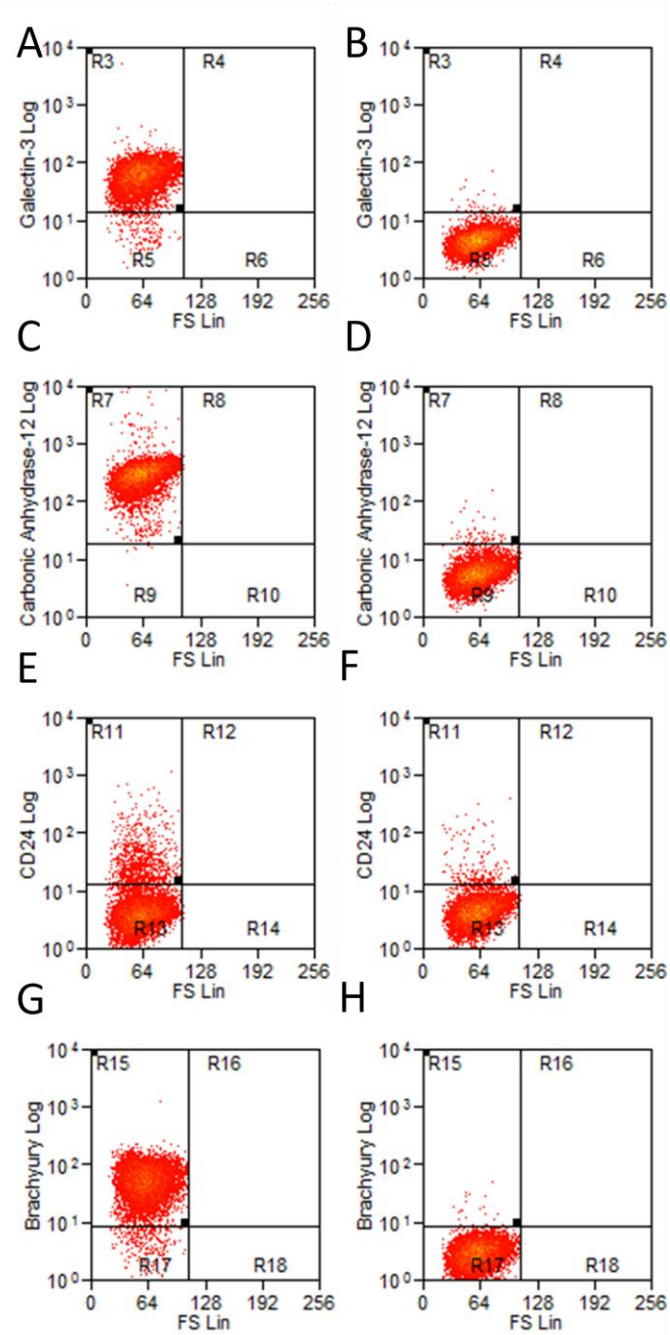

Figure 4.42 Flow cytometric analysis of novel NP and NC cell protein expression in adult human NP cells. Expression of Galectin-3 (A, B); Carbonic Anhydrase-12 (C, D); CD24 (E, F); and Brachyury (G, H) was investigated (sample HH0613). Isotype controls were utilised as negative controls (B, D, F, H). Cellular fluorescence detected in the upper left and right quadrants indicate positive staining.

Variations in expression levels were subsequently investigated with relation to patient age and severity of tissue degeneration, as shown in Figures 4.43 and 4.44. There appeared to be no trend with regards to age and percentage immunopositivity for Carbonic Anhydrase-12 (Figure 4.43A), Brachyury (Figure 4.43B), Galectin-3 (Figure 4.43C) or CD24 (Figure 4.43D). Similarly, no correlation between degenerative score and percentage positivity was demonstrated for Carbonic Anhydrase-12 (Figure 4.44A), Brachyury (Figure 4.44B), Galectin-3 (Figure 4.44C) and CD24 (Figure 4.44D). Of noted, sample HH0581 could not be graded histologically as insufficient NP tissue was present in the fixed specimen with which to gain an accurate grade.

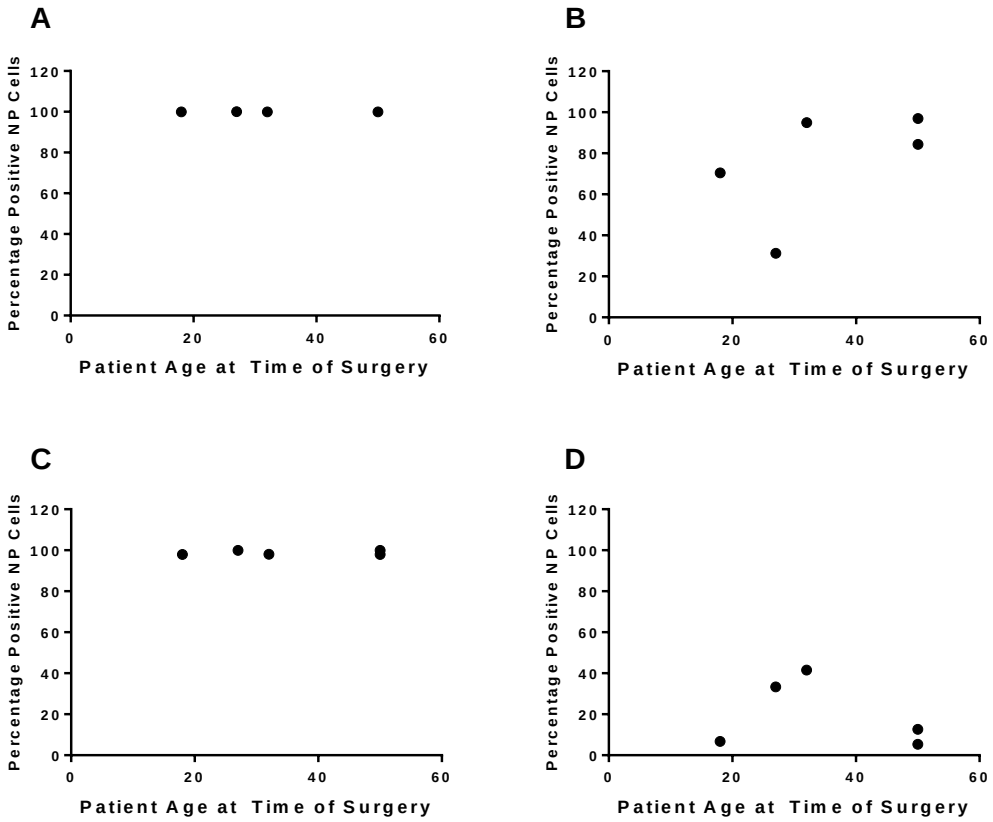

Figure 4.43 Correlation between patient age and flow cytometric immunopositivity. Immunopositivity for Carbonic Anhydrase-12 (A), Brachyury (B), Galectin-3 (C) and CD24 (D) were plotted against the age of the specimen.

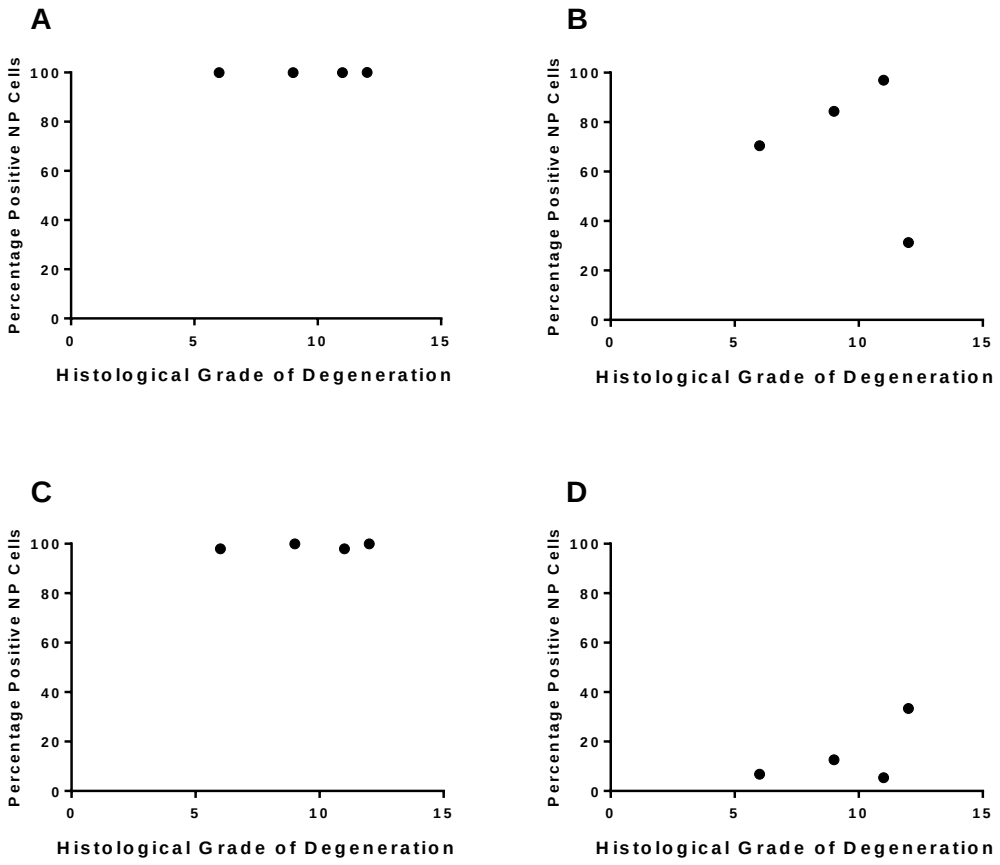

Figure 4.44 Correlation between degenerative score and flow cytometric immunopositivity. Immunopositivity for Carbonic Anhydrase-12 (A), Brachyury (B), Galectin-3 (C) and CD24 (D) were plotted against the histological score of degeneration.

Finally, as it could be assumed that almost all cells would express both Carbonic Anhydrase-12 and Galectin-3, and as Brachyury and CD24 staining levels demonstrated variability, further analysis of the Brachyury+ and CD24+ cell populations were undertaken, with a view to elucidating whether the same cells were largely expressing both of these proteins. Figure 4.45 illustrates simultaneous analysis of both Brachyury and CD24 positivity, and these results are summarised in Table 4.5. The results demonstrate that although Brachyury and CD24 are expressed by a subset of NP cells they are not necessarily co-expressed by the same population of NP cells, as demonstrated by the presence of both Brachyury+/CD24- and Brachyury-/CD24+ populations (indicated by regions R19 and R22 in Figure 4.45 respectively). However, further analysis shows that an average of 78.9%±6.586 of

total CD24+ cells also express Brachyury (region R20 in Figure 4.45), although only 21.1%±7.769 of all Brachyury+ cells also express CD24.

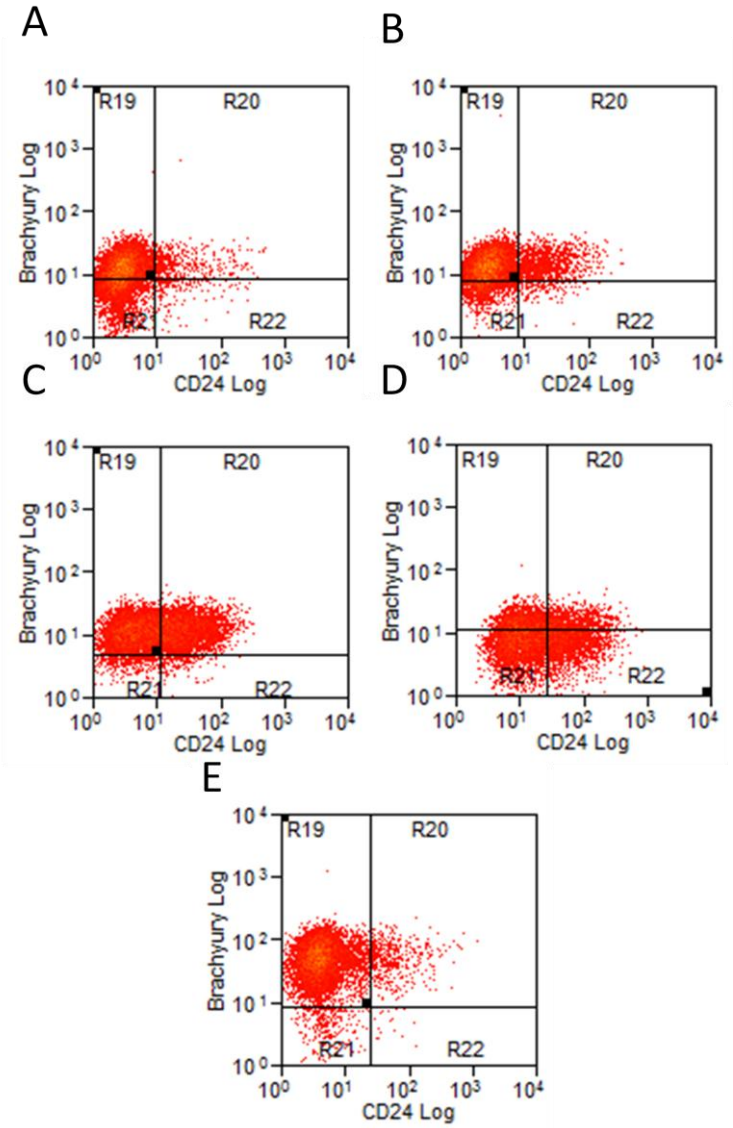

Figure 4.45 Simultaneous analysis of Brachyury and CD24 expression. Specimens HH0295 (A); HH0298 (B); HH0581 (C); HH0593 (D); and HH0613 (E) were assessed multi-parametrically for positivity of Brachyury and CD24 staining. Region R19 highlights Brachyury+/CD24- cells; region R20 highlights Brachyury+/CD24+ cells; region R21 is indicative of Brachyury-/CD24- cells; and region R22 shows Brachyury-/CD24+ cells.

Table 4.5 Summary of Multiple Staining Analysis

Phenotype	**Sample HH0295**	**Sample HH0298**	**Sample HH0581**	**Sample HH0593**	**Sample HH0613**
Brachyury-/CD24-	27.87%	14.34%	3.57%	46.87%	2.86%
Brachyury+/CD24-	65.36%	73.02%	54.46%	19.78%	91.76%
Brachyury-/CD24+	1.66%	1.27%	1.18%	21.85%	0.18%
Brachyury+/CD24+	5.09%	11.37%	40.46%	11.50%	5.20%

4.5 Discussion

Recent gene profiling studies are yet to validate novel NP marker genes in a large cohort of human specimens, nor have variations in expression of such markers been investigated with regards to ageing or degeneration. Additionally, localisation of these markers to specific cells of the adult human NP has not been fully elucidated and thus requires definition. This study has confirmed microarray findings of a panel of genes as novel markers of the adult human NP cell phenotype, and has also identified expression of NC cell marker genes in the same adult NP cells. Protein expression analysis confirmed that novel NP cell markers are expressed by the majority of NP cells, but also by a proportion of cells of the AF, while NC cell marker proteins were localised to a subset of adult NP cells and only a few AF cells. Furthermore, multi-parametric protein analysis identified sub-populations of NP cells with differential expression profiles.

4.5.1 Gene Expression Findings

Importantly, novel NP cell markers identified by microarray analysis have been confirmed as such in a large cohort of adult human specimens and generally, expression of these markers did not vary with age or tissue degeneration. FOXF1 and KRT8 were first identified as novel NP markers in a bovine IVD model (Minogue *et al.*, 2010b), and also assessed for their expression in adult human cells in the same study. However, only 5 non-degenerate and 5 degenerate IVD specimens were utilised, and thus, a more representative investigation of these markers in a larger cohort of specimens (n=62 spanning a greater range of ages and levels of tissue degeneration) was required. FOXF1 is a member of the forkhead transcription factor family, and has been shown to be involved in numerous cell processes, including cell growth, proliferation and differentiation (Kalinichenko *et al.*, 2002, Mahlapuu *et al.*, 2001, Ormestad *et al.*, 2006). FOXF1 is activated by SHH which is required for post-natal growth and differentiation of the IVD (Dahia *et al.*, 2012) and FOXF1 expression was demonstrated to be decreased in degenerate human NP cells as compared to non-degenerate (Minogue *et al.*, 2010b), a finding which was not replicated here. Again, this may be due to the increased cohort size used for investigation in this study, and the composition of the cohort being solely surgical specimens, all of which must display clinical, if not histological features of

degeneration in order to be considered for surgical intervention. FOXF1 expression was further described in a second gene profiling investigation, but variations with ageing and degeneration were not described, and only 5 specimens (all of which were non-degenerate) were used in the study (Minogue *et al.*, 2010a).

CAXII has been identified in two human microarray investigations as a novel marker of the NP cell phenotype (Minogue *et al.*, 2010a, Power *et al.*, 2012). CAXII is a membrane-associated member of the carbonic anhydrase family of enzymes, which function to catalyse the reversible hydration of carbon dioxide to bicarbonate and protons, thereby buffering intracellular pH (Lindskog, 1997). CAXII is regulated by HIF-1α – a molecule previously described as highly expressed in the NP (Risbud *et al.*, 2006) – and thus determination of this gene as a novel NP cell marker is largely unsurprising. A negative correlation in CAXII expression with both age and degeneration was noted by Power *et al*. which was not found here, although Power and colleagues only assessed 7 specimens (Thompson grades 1-4), and perhaps the larger cohort of 62 specimens investigated here is more indicative of expression in the wider human population. Additionally, Power *et al*. merely correlated expression with grade of degeneration rather than breaking down the grade of degeneration into non-degenerate, mildly degenerate and severely degenerate as performed here, which may have affected the outcome and explain this discrepancy. Given that CAXII functions to buffer intracellular pH, and that IVD pH decreases with degeneration, a decrease in CAXII expression may be indicative of the degenerative state of the tissue. PAX-1 is a novel NP cell marker also identified by human microarray analysis (Minogue *et al.*, 2010a). PAX-1 is a transcription factor involved in pattern formation during development, and interestingly is expressed in the embryonic sclerotome (the developmental origin of AF tissue) (Koseki *et al.*, 1993, Mcgaughran *et al.*, 2003). Its role in adult human NP cells is unclear, although like FOXF1, it is activated by SHH; a gene required for postnatal growth and differentiation of the NP (Dahia *et al.*, 2012). Interestingly, PAX-1 has recently been described as a negative regulator of chondrogenic maturation, and PAX-1 mis-expressing chondrocytes have been demonstrated to have decreased expression of the genes SOX9, COL2A1 and ACAN (Takimoto *et al.*, 2013). Thus, expression of PAX-1 so highly in adult human NP cells is surprising. To date, no investigations have been undertaken to investigate the expression of this marker with ageing and

degeneration in the adult human NP, and thus, the data presented here is entirely novel. PAX-1 expression may decrease with ageing (young vs. mature) and degeneration (moderately vs. severely) because of changes to SHH expression, as loss of such signalling has been shown to result in a loss of differentiation markers of NP cells (Dahia *et al.*, 2012), although FOXF1 and PAX-1 were not investigated.

KRT8 expression did not vary with age or degeneration in this study, suggesting that it is constitutively expressed by adult human NP cells, although this does not marry with the findings of Minogue *et al*., where it was demonstrated to be significantly decreased in degenerate NP specimens as compared to non-degenerate. This significant decrease in expression was also demonstrated by (Sun *et al.*, 2013b). However, it is possible that expansion of this comparison to a cohort of human specimens containing 62 samples is more representative of KRT8 expression in the human population, although such differences may also be due to the use of cadaveric non-degenerate specimens in previous studies (compared to the solely surgical specimens utilised in this investigation). Additionally, the inclusion of only 5 non-degenerate specimens in the present study may also affect the significance of KRT8 expression levels. KRT18 and -19 were first identified as novel NP markers in microarray investigations undertaken in canine and rat models respectively (Lee *et al.*, 2007, Sakai *et al.*, 2009), and were subsequently validated in bovine and human specimens (Minogue *et al.*, 2010a, Minogue *et al.*, 2010b, Rutges *et al.*, 2010). Classically, cytokeratins are integral to protein structure formation within the cytoplasm, and as such, are protective from mechanical (and non-mechanical) stressors (Karantza, 2011). KRT8 is known to dimerise with KRT18, and in the absence of KRT18, KRT19 dimersation acts as compensation (Kulesh *et al.*, 1989, Oshima, 2002), and it is therefore unsurprising that each of these genes were identified as novel NP markers. No variation in KRT18 expression was found with ageing or degeneration here, although KRT18 gene expression has previously been demonstrated to decrease significantly with degeneration (Minogue *et al.*, 2010b). Similarly, previously literature has demonstrated a significant decrease in KRT19 with ageing, which was not shown here (Rutges *et al.*, 2010). Again, these studies only utilised small cohorts of human samples, and thus, the data presented here may be giving a more representative indication of gene expression levels by comparison. However, the presence of an entirely surgical cohort in the present investigation

compared to some non-surgical specimens in previous investigations may also serve to explain such findings.

Novel NP negative markers FBLN1 and IBSP were first identified by bovine and human microarray investigations (Minogue *et al.*, 2010a, Minogue *et al.*, 2010b), where it was demonstrated that although these genes were expressed in adult human NP cells, they are expressed at significantly lower levels than AC cells. In this study, neither gene demonstrated significant variation with degeneration in terms of expression levels, although FBLN1 has previously been demonstrated to be increased in degenerate adult human NP cells as compared to non-degenerate (Minogue *et al.*, 2010b), which as stated previously, may be due to differences in the samples used between the two studies. Interestingly, this is the first study to investigate variations in IBSP expression with ageing, and has shown a decrease in IBSP expression in mature adult as compared to young adult samples, but then an increase again in elderly adult as compared to mature adult samples. The rationale for such variations are unclear; however, similar patterns of expression were noted for CAXII and KRT19 proteins in previous literature (Power *et al.*, 2012, Rutges *et al.*, 2010).

Overlapping gene expression profiles of bovine NP and NC cells (Minogue *et al.*, 2010b), and the recent demonstration of a common ontogeny between developmental NP and adult NP cells in the mouse (Choi *et al.*, 2008), prompted the investigation into the expression of NC cell markers in adult human NP cells shown here. NOTO has previously been used to characterise node and notochordal cells (Winzi *et al.*, 2011), and is involved in regulation of notochord ciliogenesis, left/right patterning, and node morphogenesis (Beckers *et al.*, 2007). To date, this is the first study to investigate NOTO expression in the adult human NP; a major novel finding, and although no variations were noted with degeneration, a significant increase in expression was noted with ageing. This in itself is surprising, as NOTO has recently been used in lineage tracing studies of NC cells in a mouse model (Mccann *et al.*, 2012), and given the loss of morphologically distinct NC cells with maturity in humans, it would be expected that NOTO expression would in fact decrease. NOTO acts downstream of other NC cell marker genes T and FOXA2 (Abdelkhalek *et al.*, 2004), although no such variation in expression of these genes was noted here. There is currently no existing literature to support a correlation between NOTO expression

and ageing/hypoxia/degeneration/inflammation, which may have explained the finding presented here. In the present study, NOTO expression was determined only at the gene level, and thus it is not possible to infer whether the gene expression is translated to protein. No previous study has characterised NOTO expression at the protein level, and further investigation is therefore required before the function of NOTO in cells of the adult human NP can be elucidated.

T and FOXA2 have both been described as expressed in the embryonic NC (Harrelson *et al.,* 2012, Wilkinson *et al.*, 1990), and are reportedly co-expressed (Weinstein *et al.*, 1994). Until now, FOXA2 expression has not been demonstrated in adult human NP cells, although it has been shown as pivotal to IVD formation in a mouse model in combination with FOXA1 expression (Maier *et al.*, 2013). T was demonstrated as expressed by both bovine NP and NC cells, and when validated in human NP specimens, expression did not vary with degeneration, although expression was not correlated to age (Minogue *et al.*, 2010a). Here, no variations in expression of either of these markers with ageing or degeneration were observed, suggestive of constitutive expression of these genes by cells across ages and throughout the degenerative process. The genomic targets of T during differentiation have been demonstrated in a mouse model, including components of the WNT, MAPK, TGF-β and FGF signal transduction pathways, which are known to be expressed in the IVD (Dahia *et al.*, 2009). As such signalling pathways are integral to normal function of the IVD, continuous expression of T with ageing and degeneration may be required for maintenance of normal cell signalling processes. Similarly, FOXA2 expression has been demonstrated as required for expression of SHH (Maier *et al.*, 2013), but given that SHH expression is also linked to regulation of FOXF1 and PAX-1 expression and that changes to SHH expression might be linked to alterations in gene expression with ageing and degeneration, it is unclear as to whether SHH expression is linked to the static FOXA2 expression noted here.

This study identified no variations in the expression of CHRD and NOGGIN with either ageing or increasing severity of degeneration. Both act as bone morphogenic protein (BMP) antagonists, by binding directly with the proteins, and preventing them from binding to their appropriate receptors (Groppe *et al.*, 2002). CHRD expression in the adult human IVD has not been identified before. NOGGIN has been identified as expressed throughout the developing mouse embryo, but was

localised solely in the AF (Dipaola *et al.*, 2005). In articular chondrocyte cells, CHRD has been demonstrated to increase with degeneration of the cartilage tissue (Tardif *et al.*, 2006), which was not observed here, suggesting that like the expression of other NC cell markers, the lack of variation with ageing and degeneration may be due to the need for expression in order to maintain tissue function (and prevent the formation of bone in the cartilaginous NP).

Finally, the NC cell marker gene LGALS3 has previously been localised to the embryonic notochord (Gotz *et al.*, 1997b), whilst CD24 has been described as expressed specifically in rat NP cells (Fujita *et al.*, 2005), although the suitability of CD24 as an NP cell marker has since been discredited (Minogue *et al.*, 2010b, Rutges *et al.*, 2010). This study has demonstrated that CD24 expression does not vary with ageing, but was decreased in severely degenerate as compared to moderately degenerate specimens, whilst LGALS3 expression was decreased in mature adult as compared to young adult samples, but levels were unaffected by degeneration. Although Rutges *et al*. investigated the expression of CD24 in adult human specimens, expression was not correlated to age or degeneration, and thus, the findings presented here are not comparable.

Another interesting finding of the notochordal gene expression analysis was that the notochordal cell genes investigated were not expressed in all adult human NP samples analysed. Furthermore, the data appears to suggest that genes expressed earlier in embryonic NP tissue development are expressed in fewer samples than those expressed at later stages. As this is the first study to extensively investigate expression of such markers in adult human NP cells, there is little evidence to explain why this might be. However, it can be postulated that the presence or absence of expression of these genes is related to different stages of NP cell maturation. Thus the loss of morphologically-distinct NC cells from the tissue with age, may be due to differentiation to adult NP cells, expressing fewer notochordal-associated genes, but resembling small NP cells in terms of morphology. However, this requires further investigation.

One of the limitations of gene expression analysis is that it is not possible to infer from such information whether expression is ubiquitous throughout cells of the entire NP tissue, or specific to a subset of NP cells. Additionally, the detection of

expression of such markers at the gene level is not necessarily indicative of protein expression, and thus, such investigations must be undertaken. Therefore, protein localisation by immunohistochemistry using the same larger cohort was performed.

4.5.2 Localisation of NP and NC Cell Protein Expression

The data presented here indicates that novel NP cell marker proteins are more highly expressed throughout the adult human NP than NC cell marker proteins. Additionally, novel NP cell marker proteins are also expressed by AF cells of the same tissue. Novel NP cell marker protein expression appears to be largely unaffected by ageing and degeneration, although this may be due to the use of solely surgical specimens obtained only from adult patients. It is possible that protein expression changes would be noted if paediatric or adolescent samples, as well as adult specimens from asymptomatic individuals, were analysed. These tissues would generally be entirely non-degenerate and allow for the inclusion of specimens younger than those assessed here.

This is the first study to assess the expression of FoxF1 and Pax-1 proteins in the adult human IVD, and has demonstrated high levels of expression in NP and AF cells. This matches gene expression findings for FOXF1, where it has been shown that human NP and AF cells express similar levels of the marker (Minogue *et al.*, 2010b); however, such comparisons have not been performed for PAX-1, but the data presented here suggests that it too is a marker of both NP and AF cells. Carbonic Anhydrase-12 protein expression has been shown here to be unaffected by ageing, and increased in the most severe stages of degeneration. This fits with observations by Power *et al.*, where the most intense staining was noted in the most severely degenerate NP cells; however it should be noted that the staining quantification methods utilised in the present study involved counting all cells within a tissue section, whilst Power *et al.*, merely count positivity of cells within a chosen field of view, and therefore may not be representative of staining throughout the NP tissue. Additionally, Power *et al.*, report immunonegativity in AF cells, although it is not clear whether like the NP data, this was concluded from analysis of only one field of view. With regards to both FOXF1 and PAX-1, gene expression analysis revealed significantly lower expression in mature adult as compared to young adult,

and in severely degenerate as compared to non-degenerate specimens, which was not noted at the protein level. Conversely, CAXII gene expression did not vary with age or degenerative score, but at the protein level was significantly more highly expressed in severely degenerate as compared to moderately degenerate specimens. Although factors influencing the transcription of FOXF1 and PAX-1 are well documented, mechanisms involved in their post-transcriptional regulation (which would explain the disparities between gene and protein expression noted here) are less well defined. Similarly, elucidation of human CAXII gene sequences has identified two isoforms generated by alternative splicing (Haapasalo *et al.*, 2008), and it may therefore be possible that the antibody used for protein analysis does not detect both transcript variants. For FOXF1, PAX-1 and CAXII, no evidence exists as to the modification of genes post-transcriptionally by either RNA editing, capping of the 5' mRNA sequence or poly(A) tail addition, which may serve to explain the differences noted in terms of trends in expression for gene and protein levels in the present study, but further study may enable definition of this. Evidence exists which suggests that protein and gene expression levels are not necessarily correlated and factors including protein stability (which is highly variable), rate of transcription vs. translation, post-transcriptional regulation, alternative splicing and RNA processing may affect the relationship between gene and protein expression (Vogel and Marcotte, 2012), and it is therefore possible that such parameters may have resulted in the differences noted here.

Regarding the expression of Cytokeratins -8, -18 and -19, the fact that these have been identified as novel NP cell markers and yet are expressed at the protein level so lowly throughout the adult human NP is surprising. Interestingly, the cytokeratins investigated here have previously been identified as expressed in the developing IVD (Gotz *et al.*, 1995), which provides further evidence of a notochordal origin of some adult human NP cells. Cytokeratin-8 protein expression has been demonstrated to be localised to only 10% of bovine NP cells, although details of the quantification method utilised were not given (Gilson *et al.*, 2010). Similarly, Cytokeratin-8 expression has been demonstrated to be decreased in degenerative human disc samples as compared to non-degenerate and scoliotic specimens, although an explanation of how staining was quantified was again not given (Sun *et al.*, 2013b). However, given that the samples assessed here are all degenerate, this may serve to

explain why low levels of staining were noted. Additionally, Cytokeratin-8 expression has been demonstrated to decrease with compressive load application, and this may explain why expression appears to decrease in adult specimens as compared to foetal NP samples (Sun *et al.*, 2013a). Cytokeratin-18 expression has previously been investigated by (Weiler *et al.*, 2010) and has shown immunonegativity in surgical AF specimens, largely confirming the findings presented here. Expression of Cytokeratin-18 protein was noted in younger NP specimens, but was absent in older specimens, which was not noted here (Weiler *et al.*, 2010). Like Power *et al*., the method for staining quantification only categorised staining as <10%; 10-50%; and >50%, which may not be accurate enough to note some trends, and thus may serve to explain why the data presented here showed no age-associated variations in expression levels, with expression detected in elderly adult specimens. Interestingly, in the same investigation, Cytokeratin-8 and -19 protein expression was investigated by utilising a Pan-Cytokeratin antibody that stains both proteins. From this data it is impossible to infer which of the cytokeratin isoforms the observed staining relates to, but given the data shown here, it is likely to be Cytokeratin-8 rather than -19 staining. Previous investigations of Cytokeratin-19 protein expression in human specimens have shown that samples over the age of 25 are generally immunonegative for expression, confirming the data presented here (Rutges *et al.*, 2010). However, this previous study also used a staining quantification method where the number of positive cells per field of view was considered representative of staining throughout the tissue, and this therefore differs from the method employed here, thus explaining the discrepancies in findings between studies. The absence of Cytokeratin-19 staining in the present study may be due to preferential dimerisation of Cytokeratin-8 with Cytokeratin-18. It has been shown that when Cytokeratins-8 and -18 are co-expressed, levels of Cytokeratin-19 protein are undetectable, thought to be because Cytokeratin-8 assembly with Cytokeratin-18 is more efficient that Cytokeratin-8/-19 interaction (Pankov *et al.*, 1997). It has been demonstrated previously that Cytokeratin-18 is rapidly degraded in the absence of a Cytokeratin-8 binding partner (although the methods of degradation are not elucidated) (Kulesh *et al.*, 1989). Given that Cytokeratin-19 also binds to Cytokeratin-8, it is possible that in the adult human NP, that Cytokeratin-8 is only bound to Cytokeratin-18 (as is this is a more efficient form of keratin filament assembly), and Cytokeratin-19 protein may therefore be degraded in the

same manner as previously described for Cytokeratin-18, thereby explaining the lack of Cytokeratin-19 protein expression in the current study.

With regards to the protein expression of NC cell markers, this is the first study to undertake detailed investigation of Brachyury protein expression in the adult human IVD. Previously, Brachyury expression has been demonstrated in rat NP cells (Tang *et al.*, 2012), and in human specimens by means of Western blot (Risbud *et al.*, 2010). Brachyury immunonegativity has previously been described in adult human NP cells (Vujovic *et al.*, 2006), although this was investigated using a cohort of only 7 specimens, and no information as to the age and grade of these tissues was given. Here, decreases in Brachyury expression with ageing and degeneration were found, which does not mirror the gene expression findings of no variation. As described previously, this may be due to post-transcriptional modification of Brachyury, and although the evidence regarding modifications to Brachyury are limited, other T-Box transcription family members have been demonstrated to undergo alternative splicing to form transcript variants (Campbell *et al.*, 1998). To date, no literature exists that suggests that Brachyury expression alters with nutrient supply, oxygen state, inflammation or pH, and thus, such differences are difficult to explain. The detection of Brachyury protein in cells of the AF is not a surprising finding, given that it is a marker of the embryonic mesoderm, and mesodermal tissues go on to form both the AF and NP. Galectin-3 protein has previously been localised to cells of the adult human IVD (Gotz *et al.*, 1997b, Weiler *et al.*, 2010). In one study, only 2 specimens were analysed (Gotz *et al.*, 1997b), whilst the other only demonstrates staining in samples < 31 years old, although again, the method for quantification of staining differs from that used in the current study (Weiler *et al.*, 2010). In this study, there were few variations in NC cell protein immunopositivity with age or degeneration; mirroring the gene expression findings. In the present investigation, expression of NC cell marker proteins was demonstrated in cells of the AF, in agreement with previous literature that has demonstrated immunopositivity for Galectin-3 in both rat AF and NP at various ages (Oguz *et al.*, 2007), and paired with the data presented here suggests that it may not be the most appropriate marker of the NC cell phenotype. Finally, CD24 has previously been localised to NP cells of the human and rat IVD (Fujita *et al.*, 2005, Tang *et al.*, 2012); however, quantification of staining levels in the human IVD has not been demonstrated in the

literature, and specificity to NP tissues remains unaddressed also. Here, CD24 expression is not demonstrated to alter with degeneration, which matches data from Fujita *et al*., where expression is maintained in herniation (albeit in a rodent model). Similarly, the data shown here demonstrates no variation in expression level with ageing, although investigation in a rat model shows decreased expression with age (Tang *et al.*, 2012). However, this disparity may be attributed to the fact that rodent age and human age are not comparable, and as such, this may not be an appropriate model for studying age-related alterations as it cannot be extrapolated to human ageing.

The present study is the first to characterise such an extensive range of proteins in tissues of both adult human IVD and foetal NC specimens. The data has demonstrated the expression of all markers in cells of the foetal NC, as well as expression of some proteins in surrounding mesenchymal cells (FoxF1, Pax-1, Carbonic Anhydrase-12, Brachyury, Galectin-3 and CD24). Overlapping protein expression profiles between human NP and NC cells (including NC cell remnants of adolescent IVD) may support evidence of a common ontogeny of the two cell types. Minogue *et al*. demonstrated using a bovine model that such cells do display overlapping gene expression profiles, and suggest it is indicative of a shared ontogeny. Recent lineage tracing studies have concluded also that the adult NP is notochordally-derived (Choi *et al.*, 2008, Mccann *et al.*, 2012).

To date, many studies have investigated the expression of the markers studied here, but have not related this expression to single NP cells and NP cells localised within clusters, with the exception of a recent study (Sun *et al.*, 2013b). Healthy NP cells contain few cellular clusters, but these are noted to increase with degeneration (Pritzker, 1977, Sive *et al.*, 2002), and have been linked to increased cellular proliferation within the NP tissue (Johnson *et al.*, 2001). Evidence presented here supports such findings, with a significant correlation noted between the proportion of NP cells localised as clusters and histological grade of degeneration. For each of the markers analysed, the majority of immunopositive cells were single NP cells. Analysis of the single and cell cluster populations individually demonstrates that generally, a greater proportion of the cell clusters are immunopositive for the markers investigated here as compared to single cells, which may intimate that NP

cell clusters represent a more NC cell-like remnant population as compared to single cells.

One of the limitations of the data presented here is that only one section per specimen was stained for each marker, and thus may not give a representative view of expression throughout the entire NP tissue. However, the methods used for quantification here are far more detailed than those in the current literature, and in addition to the large cohort of samples utilised in this study ensures that such methodologies are sufficient.

4.5.3 Multi-Protein Analysis of the NP Cell Phenotype

Immunohistochemical methods are limited in that from such staining you cannot determine whether it is the same cells expressing the same markers, and whether distinct sub-populations of cells exist within the tissue. Use of flow cytometric methods is advantageous because it allows for elucidation of such findings using a combination of markers. The immunohistochemistry data here indicated the presence of NP cell sub-populations, as the proteins analysed were not ubiquitously expressed throughout the NP, and the findings of the flow cytometry confirmed this matter. The finding that almost all adult human NP cells express Carbonic anhydrase-12 is unsurprising given that immunohistochemical analysis showed high levels of expression; however, the detection of Galectin-3 positivity in virtually all NP cells did differ from the earlier protein expression analysis, and does not match with previous data of non-ubiquitous expression in adult human specimens (Gotz *et al.*, 1997b, Weiler *et al.*, 2010). The expression of Galectin-3 in all adult human NP cells may be due to a culture-associated artefact, where certain sub-populations of cells (perhaps those positive for Galectin-3) are preferentially selected and expanded, or that cultured cells alter their phenotype. The preferential selection of cell sub-populations may be analysed through monitoring of cell growth and proliferation, labelling certain cell populations with fluorescent proteins to measure this by means of either flow cytometry or cell sorting if required for further culture or analysis. Unlike Galectin-3, expression levels of Brachyury and CD24 were far more variable, and perhaps indicative of NP cell sub-populations, but these populations are not

distinct (with varying degrees of positivity for both Brachyury and CD24); the proportion of which are not related to age or degeneration.

An abundance of evidence has come to light over recent years regarding the presence of NP cell sub-populations. A possible stem cell niche has been identified within the rabbit outer AF that may become active during disc degeneration and expression of such markers was confirmed also in human specimens (Henriksson *et al.*, 2009, Henriksson *et al.*, 2012). Additionally, an MSC-like cell population has been identified as present in adult human IVDs in two studies (Blanco *et al.*, 2010, Risbud *et al.*, 2007). However, Risbud *et al*., did not compare their findings to control MSC cells, and Blanco *et al*., do not achieve adipogenic differentiation of the MSC-like cells, which suggests that it is not a true MSC cell population. Similarly, a stem cell population has been isolated from canine NP cells and unlike native canine NP cells, did not express Brachyury, and comprised 1% of the total cell population (Erwin *et al.*, 2013). However, differences between these isolated canine cells and traditional stem cells were identified, and as such, these cells were described as a regenerative niche. Another recent study has identified a sub-population of NP cells that are $Tie2^{+}GD2^{+}$, that possess the ability to differentiate down each of the mesenchymal lineages, and whose number decreases with ageing and IVD degeneration (Sakai *et al.*, 2012). However, none of the aforementioned studies have investigated the possibility of a NC cell sub-population by utilisation of NC cell markers for characterisation. Here it has been demonstrated that the adult human NP is heterogeneous in its composition, and that such cells express differing levels of a range of NP and NC markers. Previous investigations have suggested that NC cells may confer some protective effects over NP cells through maintenance of disc integrity and ECM (Aguiar *et al.*, 1999, Cappello *et al.*, 2006), and through protection from degradation and apoptosis (Erwin *et al.*, 2011). Thus, the presence of cell populations expressing NC cell markers may indicate a progenitor cell type existing within the adult human NP. This matter however is only speculative at present, and requires extensive further investigation as to the function of these cells before such conclusions can be confirmed. Moreover, the distinctions in adult human NP cells with regards to phenotype may represent distinctions with regards to cellular ontogeny. As it is currently hypothesised that the adult human NP is populated by cells that either derive from the embryonic NC or from the infiltrating

AF/CEP during maturity of the tissue, differential cell phenotypes may arise as a result of this. Thus, the heterogeneous cell population identified here may in fact intimate that the adult human NP contains cells originating from both the NC and mesenchymally-derived AF, thereby explaining these distinctions. However, this hypothesis is not confirmed in the present study and thus requires further assessment.

4.5.4 Implications of this Investigation

Morphologically distinct NC cells have been demonstrated to disappear from NP tissue with ageing, replaced by the smaller chondrocyte-like cells of the adult NP (Louman-Gardiner *et al.*, 2011). However, data presented here suggests that sub-populations of NP cells persist in mature specimens that differentially express a range of NC cell markers, with the markers associated with the developmental NC lower in abundance than those characteristic of adult NP cells. These cells may be distinct from other NP cells in terms of function, and it is hypothesised here that given the high levels of notochordal cell marker expression in these cells, they represent a notochordal cell-like population that may act as a progenitor cell population in the degenerate IVD. However, this is purely speculative, and isolation of cell subpopulations and functional analysis of these will elucidate if such distinct functions exist. Additionally, what remains unclear are the processes underlying the apparent loss of these specialised cells from NP tissue during childhood, and this requires investigation. If this can be elucidated, the function of NC-like cell sub-populations in adult specimens such as those investigated here may then be fully understood. A more full understanding of the discrete role that these cell sub-populations play *in vivo* may then allow for a more informed decision as to the optimal cell phenotype for recapitulation in novel cell-based regenerative therapies targeting IVD degeneration.

Chapter 5:

Development of an *Ex Vivo* Model System to Study the Effect of the Adult IVD Microenvironment on Notochordal Cell Phenotype

5.1 Background

Work from the previous chapter has demonstrated that the adult human NP is comprised of a heterogeneous cell population, with cells expressing differential levels of both NP and NC cell markers. Whilst the expression of NC cell markers in cells of the adult human NP intimates a common ontogeny, it remains unclear as to why only a subset of NP cells expresses these markers, but it could be postulated that they are functionally distinct as well as phenotypically distinct, and given the high levels of notochordal cell marker expression in some cell sub-populations, that certain cells are progenitor-like. Findings presented in this investigation previously suggest the presence of an NC cell-like population persisting in the adult IVD, but also indicate that the adult human NP is populated by cells both morphologically and phenotypically distinct from those of the developing IVD. However, mechanisms underlying the change in NP cell population in adult as compared to developing or neonate IVD remain undefined.

5.1.1 Alterations to the NP Cellular Composition with Growth and Ageing

As described previously, during human development the NP is comprised of morphologically-distinct NC cells (Taylor, 1975), but it has been demonstrated that alterations to the cellular population of the NP occur with ageing and subsequent maturity of the tissue. The infant NP contains NC cell clumps and strands (Trout *et al.*, 1982a) which gradually disappear by age 8, replaced with smaller, rounded chondrocyte-like cells, that populate the NP throughout adulthood (Louman-Gardiner *et al.*, 2011). Additionally, the NP tissue itself becomes softer and relatively hypocellular (Taylor, 1975). Of note, the loss of notochordal cells from the human NP is thought to precede the onset of IVD degeneration, as it is at the point of NC cell loss that the first signs of disc degeneration are observed (Nerlich *et al.*, 1997). However, the precise mechanisms underlying the loss of these distinct cells from NP tissue is unknown.

The unknown fate of NC cells in the human IVD also casts controversy regarding the developmental origin of smaller NP cells within adult tissues. It is thought that NC cells form the NP and remain as developmental remnants within the IVD. Fate-mapping studies of adult mouse intervertebral disc cells found that all cells of the NP

are in fact derived from the embryonic notochord (Choi *et al.*, 2008) and this has subsequently been confirmed through the use of a Noto-Cre mouse model (Mccann *et al.*, 2012). It can be postulated that NC cells exist as remnants within the disc in order to support the chondrocyte-like cells of the disc in maintaining a normal phenotype. Bovine NP and NC cell co-cultures have demonstrated increased PG expression by NP cells in the presence of NC cells, suggesting that NC cells promote maintenance of healthy disc ECM (Aguiar *et al.*, 1999). Similarly, NC cells have been shown to secrete connective tissue growth factor (CTGF), which may play a role in ECM anabolism (Erwin *et al.*, 2006). In support of this theory, expression of Cytokeratin-8 (also expressed by NC cells) has been isolated in small clusters of cells of the mature bovine IVD, suggestive therefore of a sub-population of bovine NC cells persisting during maturity (Gilson *et al.*, 2010). Expression of known notochordal cell markers in a proportion of adult human NP cells has been demonstrated in another study (Weiler *et al.*, 2010), again suggesting that at least some of the adult NP cells may be notochordally-derived.

However, what remains unaddressed in such studies is whether NC cells are actually lost from the tissue and replaced by the familiar chondrocyte-like cells of the adult human NP, or whether they in fact differentiate to chondrocyte-like cells that mature and subsequently lose expression of NC cell markers to some degree. The finding that notochordal cell markers were identified in a sub-population of NP cells in much older adult specimens, and that these cells themselves do not resemble the morphologically distinct NC cells as noted during foetal development is supportive of the latter theory (Weiler *et al.*, 2010). Thus, this may suggest that the NP is derived from the embryonic notochord, but that the NC cells that populate the tissue during development go on to differentiate into chondrocyte-like cells, whilst still retaining the expression of some NC cell markers (Cappello *et al.*, 2006). A chondrocyte-like phenotype (expressing SOX9, COL2 and ACAN) in NC cells has been demonstrated, suggesting that NC cells could potentially differentiate to chondrocyte-like cells (Kim *et al.*, 2009). However, the authors fail to address whether this differentiation is indicative of *in vivo* processes, or whether it is merely a consequence of *in vitro* culture methods. Similarly, NC cells cultured *in vitro* under hypoxia have been demonstrated to produce a highly organised cellular construct mimicking that observed *in vivo*, which suggests that in a microenvironment akin to

that of the adult human disc, NC cells produce an NP-like ECM (Erwin *et al.*, 2009). A mouse degeneration model (employing needle-puncture techniques) demonstrated a chondrogenic-like differentiation of notochordal cells as defined by increased type II collagen expression, supporting the hypothesis that such cells undergo differentiation to smaller NP cells in the mature human disc (Yang *et al.*, 2009). Interestingly, the injury was caused to the AF, and the authors suggest that NC cells may be susceptible to physical alterations within the annulus, but this was merely speculation and investigated no further. Annular alterations are commonly observed in human disc degeneration (Peng *et al.*, 2005), raising the question of whether resultant atypical load influences the loss of morphologically distinct NC cells.

The evidence presented so far in this investigation is indicative of sub-populations of cells existing within the adult human NP that express differential levels of NC cell markers, thereby suggesting that the hypothesis of NC cell differentiation to NP cells with a subsequent loss of NC cell marker expression is most likely. The aforementioned studies however, fail to elucidate the exact mechanisms of NC cell differentiation and loss of distinct morphology within the human IVD, and thus, this requires investigation. The IVD, particularly NP, microenvironment is known to alter as the IVD ages, with increasing hypoxia, increased load-bearing, decreased pH, reduced nutrient supply and induction of a catabolic cytokine milieu noted (Diamant *et al.*, 1968, Grunhagen *et al.*, 2006, Le Maitre *et al.*, 2007b, Ohshima and Urban, 1992). Given the simultaneous loss of morphologically distinct NC cells from the NP, it is possible that the IVD microenvironment is influential to this process.

5.1.2 The Influence of Microenvironment on NC Cells

The effect of a number of microenvironmental factors on NC cell phenotype and function has been investigated. Firstly, regarding tissue pH, levels of lactic acid are high in the centre of the IVD. Lactic acid is a bi-product of anaerobic respiration by glycolysis, and the high acidity is due to increased distance for removal of metabolic waste products through the endplate via diffusion (Diamant et al., 1968). Survival of IVD cells is dependent on expression of ASIC3 when cells are exposed to this low-pH microenvironment (Uchiyama et al., 2007). Carbonic anhydrases are metalloenzymes that function to maintain intracellular pH through the catalysis of

the reaction $CO_2 + H_2O \leftrightarrow H+ HCO_3^-$ and carbonic anhydrase-12 has recently been demonstrated as expressed by adult human NP cells, where it is postulated that it functions to maintain pH levels in this highly acidic environment (Minogue et al., 2010a). It has been demonstrated that cultures of porcine and bovine NC cells in a variety of acidic levels differed in terms of glycolysis and cell survival rates (Guehring *et al.*, 2009). A standard pH of 7.4 was demonstrated to promote both glycolysis rates and cellular survival as compared to culture in a pH of 6.8; however, no investigation as to the effect of pH on notochordal cell phenotype was undertaken.

Low glucose levels are also characteristic of the adult human intervertebral disc microenvironment (Grunhagen *et al.*, 2006). The increased distance across which small molecules such as glucose must diffuse in the adult IVD results in low glucose concentrations in the most central portions of the NP. Disc cells cannot survive in an environment where glucose levels are less than 0.5mM (Horner and Urban, 2001) and it has been demonstrated that reductions in glucose concentrations result in decreased expression of ECM molecules aggrecan and type II collagen (Neidlinger-Wilke et al., 2012). High glucose concentration has been shown to be detrimental to NC cell proliferation and survival, with increased expression of apoptotic markers and MMPs in cells cultured on 0.4M glucose as compared to those cultured with no glucose (Park and Park, 2013a). Subsequent investigation showed that high glucose-induced oxidative stress resulted in cell death via the autophagic pathway (Park and Park, 2013b). However, both of these studies undertook culture of rat NC cells in monolayer, whilst most of the existing literature demonstrates that a 3D culture environment is most appropriate for NC cell culture. Decreased cellular proliferation and lactate production rates by NC cells cultured in high glucose were also noted (Guehring *et al.*, 2009). However, the effect of glucose on NC cell phenotype and differentiation has yet to be investigated, and thus it is still unclear whether this culture condition is influential to the loss of NC cells noted in human IVD development.

Mechanical load has previously been demonstrated to influence NC cell phenotype. In a rabbit model, compression was applied to discs for up to 56 days and histological observations showed that the NP became far more fibrous, with disappearance of vacuolated tissue also noted (Guehring *et al.*, 2010). Additionally,

cytokeratin-8 immunopositivity was significantly decreased in discs exposed to mechanical loading as compared to controls. However, a more extensive investigation as to the effects of mechanical load on NC cell phenotype in this study would have provided more conclusive evidence as to the detrimental effects of this environmental factor on phenotypic maintenance. Interestingly, evidence has shown that daily pressurisation increases matrix marker and NOGGIN expression in porcine NC cells, whilst T was shown to be maintained, and KRT18 expression decreased (Purmessur *et al.*, 2012), but a comprehensive description of loss of NC cell phenotypic marker expression, and induction of NP cell marker expression was not described.

Finally, with regards to oxygen state, the healthy adult IVD is generally avascular, (Freemont, 2009, Raj, 2008), although some vascularity is noted in the outer AF region (Boos et al., 2002). Thus, cells in the central NP of larger lumbar IVDs reside up to 20mm from the nearest blood supply (Moore, 2006), and oxygen levels in this portion of the tissue are subsequently low (Bartels et al., 1998, Grunhagen et al., 2006). The number of blood vessels supplying oxygen to the tissue decreases with ageing, and IVD cells therefore generate energy through metabolism of glucose to form lactic acid, and not via respiration, reducing their need for oxygen (Holm et al., 1981). Hypoxic culture of canine NC cells has been demonstrated to promote formation of an organised cellular construct similar to that observed *in vivo*; a level of organisation absent from concurrent normoxic cultures (Erwin *et al.*, 2009). Additionally, histological analysis of these 3D cultures demonstrated superior levels of PG deposition in the hypoxic specimens, as compared to normoxic. However, this study failed to assess the effect of oxygen state on the phenotype of cells within the constructs, relying solely on histological analysis, and thus this requires investigation. The effect of low oxygen culture on the metabolism and survival of porcine and bovine NP and NC cells has also been investigated, and demonstrated that cellular survival is comparable in both normoxic and hypoxic cultures, but that lactic acid production is significantly elevated in hypoxic specimens as compared to normoxic (Guehring *et al.*, 2009). Like the investigation by (Erwin *et al.*, 2009) the authors here also fail to elucidate the impact of low oxygen culture on the phenotype of NC cells. Although an understanding of histological differences and alterations to intrinsic cellular processes are important, it is vital given the evidence presented that

suggests NC cell differentiation precedes the population of NP tissue with chondrocyte-like cells, that differences in phenotype in response to oxygen state are also described. Such differences were briefly described in a rat model of NC cells, and normoxia was shown to promote maintenance of CD24 expression, although the authors also suggest that the findings may show that hypoxia induces chondrogenic differentiation of NC cells, given increased expression of SOX9 and type IIA procollagen (Rastogi *et al.*, 2009). However, as expression levels of only 3 genes were investigated, a more extensive description of phenotypic alterations is needed.

Finally, high levels of inflammatory cytokine expression are noted as a feature of the degenerate IVD microenvironment (Le Maitre *et al.*, 2007b). Bovine NP cells cultured in the presence of IL-1β with the addition of NC cell-conditioned media demonstrated decreased cell death via apoptosis and increased expression of ECM markers compared to those cultured in conditioned media obtained from NP cells, thereby leading the authors to conclude that NC cells secrete factors protective against the deleterious effects of IL-1β (Erwin *et al.*, 2011). However, no evidence currently exists as to the direct effects of IL-1β and other pro-inflammatory cytokines on the phenotype of NC cells, or their transition to NP cells, and thus, further investigation is required.

5.1.3 The Use of *Ex Vivo* Models and Cell Systems for the Study of the IVD

The scarcity of developmental human IVD tissue available for research of factors influencing the change in cell types populating the NP tissue with ageing in humans requires the development of a cell system or *ex vivo* model to enable such studies. A number of small animal models have been employed in numerous IVD investigations, including rat, mouse and rabbit (Mccann *et al.*, 2013, Miyagi *et al.*, 2012, Mwale *et al.*, 2011), but distinct differences in terms of animal age and the load exerted on these discs suggests that these models may not be appropriate for such studies, thus necessitating the use of larger animal models. Additionally, rodent aggrecan molecules are distinct from that of all other mammalian species (Barry *et al.*, 1994), and other animal models may therefore be more appropriate. Ovine disc biomechanics have been shown to vary significantly with that of the human IVD, implying that this may not be the most appropriate model for investigation

(Showalter *et al.*, 2012), whilst some canine breeds retain NC cells within the IVD and demonstrate a resistance to development of IVD degeneration (Erwin and Inman, 2006), which again may not be optimal for study of the human pathology. The relative abundance of NC cells in non-chondrodystrophic breeds, and the similarities in terms of biochemistry with human discs (Bergknut *et al.*, 2012) makes it an attractive source of cells or tissue for investigation of NC cell loss; however, the current investigation would rely on the use of cadaveric specimens for analysis, where a number of variables could not be controlled for (age, disease state etc.) and thus, an alternative species is likely more suitable.

Species bred for agricultural purposes are advantageous as they are numerous, can be age-matched, and are raised in similar environments, reducing the number of variables which may introduce bias. The cell population of the porcine NP is comprised predominantly of NC cells (Guehring *et al.*, 2009, Purmessur *et al.*, 2012), although some anatomical differences between human and porcine discs have been identified (Bozkus *et al.*, 2005, Dath *et al.*, 2007, Sheng *et al.*, 2010, Showalter *et al.*, 2012), and these must be accounted for if *in vivo* models were to be developed. Although anatomical variations have also been noted between bovine and human IVDs (Sheng *et al.*, 2010), the biomechanics of discs obtained from bovine tails have been shown as similar to that of humans (Ishihara *et al.*, 1996, Oshima *et al.*, 1993). Similarities have also been observed between bovine coccygeal discs and humans in terms of ECM production (Miyazaki *et al.*, 2009, Oshima *et al.*, 1993). Additionally, bovine tails have been demonstrated as populated by both smaller NP cells characteristic of the adult human disc, as well as NC cells (Minogue *et al.*, 2010b). This is advantageous because when studying alterations to NC cell morphology or phenotype, a resident cell population can be utilised for comparison which is phenotypically similar to adult human NP cells (Minogue *et al.*, 2010b).

Whilst selection of the optimal species for investigation is crucial, it is also important to design an appropriate model for study, whether that is a cell system, or an *in vitro* or *ex vivo* model. The obvious choice would be to culture NC cells in monolayer *in vitro*, expose them to a range of microenvironmental factors and study the effects. However, NC cells are not plastic adherent, thus necessitating the use of a 3D construct in which these cells can be cultured and remain viable (Erwin *et al.*, 2006, Erwin *et al.*, 2009, Guehring *et al.*, 2009, Kim *et al.*, 2009). Additionally,

porcine NC cell explants have been cultured in sterile bags under hydrostatic pressure, and maintenance of cell viability was noted (Purmessur *et al.*, 2012). The effects of load on NC cell-rich discs have been investigated through the use of *ex vivo* organ culture models, whereby whole motion segments were cultured intact and exposed to load (Guehring *et al.*, 2010, Le Maitre *et al.*, 2009), with viability noted after long-term culture. Both sterile bag culture methods and *ex vivo* whole disc culture systems are advantageous as cells are not removed from their highly specialised ECM, and explants can be exposed to a range of factors, including load, simultaneously. A method for separation of NC cells in a mixed population of cells obtained from NP tissue has been developed (Cappello *et al.*, 2006, Minogue *et al.*, 2010b). The sized-based separation of cell populations would allow for the characterisation of both small NP cells (akin to that of the adult human IVD) and NC cells simultaneously, and the use of a bovine model is advantageous over a porcine model as expression of novel NP marker genes applicable to the human NP cell phenotype has already been described (Minogue *et al.*, 2010b). However, previous studies have failed to assess the purity of isolated cell populations, which must first be determined if this methodology is to be utilised for investigation of alterations to NC cell populations specifically.

5.2 Aims and Hypotheses

The findings of the current investigation indicate that a proportion of adult human NP cells express NC cell markers, and it is hypothesised that these are differentiated NC cells, that undergo a change in morphology and phenotype with ageing of the adult human IVD. The mechanisms underlying this cellular change is unknown, but prior to investigation, a suitable model for study must be developed. Human NC cell-rich NP tissue is scarce, thus necessitating the use of animal specimens, and given that NC cells have previously been isolated from adult bovine coccygeal discs, this will be the first animal model investigated. It is hypothesised that cells isolated by size-filtration will be distinct in terms of morphology, and the larger cells (>15μm) will resemble NC cells and the smaller cells (<8μm) will resemble mature chondrocyte-like NP cells, and may share similarities with regards to phenotype. Previous literature describing the effects of hypoxia on NC cells is conflicting, but it is hypothesised that hypoxic culture will result in decreased expression of NC cell phenotypic markers in NP cells and increased expression of NP markers, as hypoxic *in vitro* culture is representative of the *in vivo* oxygen state thought to precede the loss of NC cells. Similarly, as the loss of morphologically distinct NC cells is thought to coincide with the onset of disc degeneration, and that expression of pro-inflammatory cytokines is characteristic of disc degenerative processes, culture of NC cells in the presence of inflammatory cytokines is hypothesised to be detrimental to the maintenance of NC cell phenotype and morphology.

Thus, the aims of this investigation were two-fold

1) To establish a cell/tissue model system suitable for studying the hypothesised transition of developmental NC cells to a more NP cell-like phenotype and morphology, through investigation of histology and gene expression profiles.

2) To assess the influence of microenvironmental factors on the maintenance and/or loss of the NC cell phenotype *in vitro* with a view to elucidating the mechanisms underlying the loss of morphologically distinct NC cells with maturity *in vivo*.

5.3 Experimental Design

Initially, isolation of bovine NP and NC cells was performed using previously described methods (Cappello *et al.*, 2006, Minogue *et al.*, 2010b), but due to non-homogenous separation of cells, a porcine model where discs are comprised predominantly of NC cells was then employed, negating the need for size-based separation of cells. In order to maintain culture of NC cells, explants of porcine NP tissue were used, as 3D culture has been demonstrated as crucial to maintenance of NC cell viability *in vitro*. Cells were exposed to microenvironmental factors akin to that of the adult human IVD, and effects on both the gene and protein expression profiles of these cells analysed. Sub-optimal results necessitated the further development of this porcine model to include the culture of porcine whole motion segments, thereby maintaining both the 3D culture environment required for NC cell culture, as well as applying constraint to NP tissues in both normoxia and hypoxia.

5.3.1 Isolation of Bovine IVD Tissue

5.3.1.1 Equipment, Materials and Reagents

5.3.1.1.1 Equipment

Orbital shaking incubator	Hybaid
Cytospin	Thermo Scientific

5.3.1.1.2 Materials

1ml syringe	BD Biosciences
5ml syringe	BD Biosciences
8µm cell filter	BioDesign Inc.
15µm cell filter	BioDesign Inc
24-blade scalpel	Swann Morton
50ml tubes	BD Biosciences
250ml sterile bottle	BD Biosciences
Autoclaved bone saw	Morton Swann
Positively charge microscope slides	Thermo Scientific
Sterile forceps	Morton Swann
Sterile petri dish	Sterilin Limited

5.3.1.1.3 Reagents

Antibiotic/antimycotic	Sigma Aldrich
Dulbecco's Modified Eagle Medium (DMEM)	Sigma Aldrich
Heparin (25kU)	Sigma Aldrich
Methanol	Thermo Scientific
Dulbecco's Phosphate Buffered Saline (PBS)	Sigma Aldrich

5.3.1.2 Protocol for Isolation of Bovine Coccygeal IVDs

Bovine tails were obtained from the local abattoir and processed within 18 hours of slaughter (stored at 4°C upon arrival). The board used for dissection was autoclaved prior to use and opened within the sterile class II microbiology cabinet. Starting at the apex of the tail (where IVDs are largest), excess muscle, fat and connective tissue were removed using a sterile 24-blade scalpel in order that the disc to be removed could be exposed. A sterile bone saw was used to cut into the vertebrae as close to the bony endplate as possible. As the disc was isolated from the tail, 2ml heparin solution (20U/ml) was administered to the endplate using a 5ml syringe in order to prevent blood from clotting on the endplate. A bone saw was used to cut at the other bony endplate boundary, thereby isolating the disc whole, and discs were then submerged in a dish of dilute heparin solution (20U/ml) for 15 minutes. A total of 6 discs were isolated. One disc was fixed in 4% (w/v) paraformaldehyde for 3 days, then processed and wax embedded as detailed in 2.3.3.

5.3.1.3 Enzymatic Digestion of Bovine NP Tissue and Sized-Based Cell Separation

For the remaining 5 discs, NP tissue was enzymatically digested as detailed in 2.1.3.1. The cell suspension was passed through a 40µm cell strainer into a 50ml tube. Cells were centrifuged at 500g for 5 minutes, the supernatant removed by aspiration, and cells resuspended in 10ml of serum-free DMEM containing 4500mg/L glucose, L-alanyl-L-glutamine, $NaHCO_3$ and pyridoxine HCl, supplemented with antibiotic/antimycotic (10,000U/ml penicillin, 10mg/ml streptomycin, 25µg/ml amphotericin). Sized-based filtration of cells was then undertaken. Figure 5.1 illustrates the materials used for the cell separation. The cell suspension was poured into the tube in Figure 5.1 using a 10ml stripette, allowing for control of flow rate through the filter, so that the sufficient time was allowed for the solution to pass through the membrane and so that an appropriate volume of cell suspension poured into the apparatus initially. The aspirator tube was intermittently applied to the 1ml syringe tip inserted into the side of the 50ml tube, thereby creating a light vacuum forcing the solution to pass through the filter. Cells were first filtered through the 15µm cell filter, and the filter was subsequently washed in 20ml media to detach cells (>15µm in size). The filtrate that passed through the 15µm filter was filtered a second time through an 8µm cell filter using the same technique. The filter

was washed in 20ml media to detach cells (8-15µm in size) and the filtrate retained as it contained the small NP cells (<8µm). Following this, cells were resuspended in an appropriate amount of media to allow for a proportion of cells to be subject to RNA extraction (as detailed in 2.2.2 and 2.2.3) and a proportion to be cytospun for histological analysis.

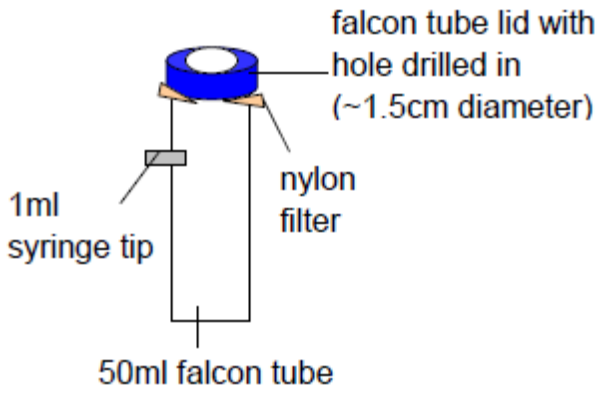

Figure 5.1 Materials utilised in bovine cell separation.

5.3.1.4 Cytospinning of Cells

Positively-charged microscope slides were inserted into the cytospin apparatus, and 100µl of the appropriate cell suspension pipetted into the funnel. Slides were spun at 800rpm for 10 minutes. The filter paper was removed carefully so as to not disturb the spun cells, and slides were fixed in 100% methanol for 5 minutes at room temperature. Slides were then transferred to PBS for short-term storage at 4°C, prior to histological staining by Giemsa stain (described in 5.3.9.2).

5.3.2 Isolation of Porcine IVD Tissue

5.3.2.1 Materials and Reagents

5.3.2.1.1 Materials

24-blade scalpel	Morton Swann
Sterile petri dish	Sterilin Limited

5.3.2.1.2 Reagents

Antibacterial mouthwash	Tesco
Antibiotic/antimycotic	Sigma Aldrich
Dulbecco's Modified Eagle Medium (DMEM)	Sigma Aldrich
Foetal bovine serum	Gibco
Gentamicin	Invitrogen
Hank's balanced salt solution (HBSS)	Sigma Aldrich

Heparin (25kU)	Sigma Aldrich
HEPES	Sigma Aldrich
L-Ascorbic acid	Sigma Aldrich
Paraformaldehyde	Sigma Aldrich
Phosphate buffered solution (PBS)	Sigma Aldrich

5.3.2.2 Protocol for Isolation of Porcine IVD Tissue

Pigs (11 weeks old) sacrificed at a local abattoir and transferred to the laboratory within 4 hours were utilised in this study. Dissection of the spine was performed under sterile conditions, and care was taken when removing the spine as to leave the spinal cord intact *in situ* to avoid issues of contamination. Excess muscle and connective tissue was removed from the spine prior to NP tissue dissection. The lower lumbar disc levels could not be removed due to the presence of the pelvic bone, whilst the upper most cervical disc levels had such large bony processes that a smooth excision was not possible. Once the remaining portion of the spine was dissected, specimens were transferred to a class II microbiology cabinet for further dissection. Where the NP tissue was to be cultured as an explant, a sterile 24-blade scalpel was used, and an incision made in the posterior AF, close to the boundary with one of the CEPs. Keeping the incision close to the edge of the IVD allowed removal of the whole NP rather than tissue fragments, which was essential for this experiment. Using a fresh scalpel blade and sterile spatula, NP tissue was detached from the surrounding AF and placed into a sterile petri dish containing PBS to remove any blood contaminants prior to culture. This process was repeated for each of the disc levels. Approximately 15 NP explants were excised from each spine.

Where discs were to be cultured as whole motion segments, the IVD was dissected using a 24-blade scalpel. The discs were excised so that 1-2mm of anterior and posterior endplate was located at either end of the IVD segment, with the AF and NP constrained between the two. Upon complete excision, discs were soaked in 250ml 0.02kU/ml heparin in Hank's Balanced Salt Solution (HBSS) for 15 minutes to remove blood clots. Sterile forceps were then used to transfer discs to a sterile culture pot containing 250ml 10% (v/v) mouthwash in PBS and soaked for 15 minutes. Following this, discs were soaked in PBS for 10 minutes and then briefly washed in medium (DMEM containing 4500mg/L glucose, L-alanyl-L-glutamine, $NaHCO_3$ and pyridoxine HCl, supplemented with 10% FBS and antibiotic/antimycotic (10,000U/ml penicillin, 10mg/ml streptomycin, 25µg/ml

amphotericin) 25µg/ml ascorbate, 20mM HEPES and 50µg/ml gentamicin). Discs were subsequently cultured as outlined in 5.3.4.

5.3.3 Culture of NP Explants

5.3.3.1 Equipment, Materials and Reagents

5.3.3.1.1 Equipment

Hypoxic culture chamber	Laboratory Products Inc
Hypoxic culture incubator	Binder
Normoxic culture incubator	Binder

5.3.3.1.2 Materials

24-well culture plate	BD Falcon
Bottle top filter	BD Falcon
Cell culture inserts (0.4µm)	BD Falcon

5.3.3.1.3 Reagents

Antibiotic/antimycotic	Sigma Aldrich
Dulbecco's Modified Eagle Medium (DMEM)	Sigma Aldrich
Foetal bovine serum	Gibco
L-ascorbic acid	Sigma Aldrich
Recombinant IL-1β	Peprotech

5.3.3.2 Explant Culture Protocol

Sterile cell culture inserts were placed inside the wells of a 24-well culture plate using sterile forceps, and 600µl culture media (DMEM containing 4500mg/L glucose, L-alanyl-L-glutamine, $NaHCO_3$ and pyridoxine HCl, supplemented with 10% FBS, 25µg/ml ascorbate and antibiotic/antimycotic (10,000U/ml penicillin, 10mg/ml streptomycin, 25µg/ml amphotericin)) pipetted into the bottom of each well. The NP tissue explant was placed into each insert using sterile forceps and 200µl culture media applied to the top of each explant. Where explants were exposed to IL-1β in the culture media, this was added to the media just prior to pipetting into the wells. The same plate set-up was duplicated in hypoxia, and set up in a sterile hypoxic chamber (2% O_2). For each of the following experimental parameters, an n=7 tissue explants was employed:

- Normoxic culture, standard media
- Normoxic culture, media supplemented with 10ng/ml recombinant IL-1β
- Hypoxic culture, standard media
- Hypoxic culture, media supplemented with 10ng/ml recombinant IL-1β

Explants were cultured for 14 days in either hypoxic (2% O_2, 37°C, 5% CO_2) or normoxic (21% O_2, 37°C, 5% CO_2) incubators, with media changed every 48 hours. Oxygen was removed from media for hypoxic culture by filtration through a bottle-top filter in a hypoxic chamber. Non-cultured tissue explants served as controls, and following excision, one explant was fixed for histological analysis (see 2.3.2 and 2.3.3) and six explants were subject to RNA extraction placing in sealed tin foil, snap-freezing in liquid nitrogen and stored at -80°C prior to RNA extraction as detailed in 5.3.5. Following the 14 days in culture, one explant from each condition was processed for histological analysis. Six further explants were sealed in tin foil, snap frozen in liquid nitrogen and stored at -80°C as above.

5.3.4 Culture of IVD Whole Motion Segments

5.3.4.1 Equipment and Materials

5.3.4.1.1 Equipment

Hypoxic culture chamber	Laboratory Products Inc
Hypoxic culture incubator	Binder
Normoxic culture incubator	Binder
Waterbath	Stuart Scientific

5.3.4.1.2 Materials

24-blade scalpel	Swann Morton
Whirl-pak bags	SLS

5.3.4.2 Whole Motion Segment Culture Protocol

For initial testing, 4 excised whole motion segments were placed in Whirl-pak bags using sterile forceps, and 50ml medium added to each bag using sterile 25ml stripettes (DMEM containing 4500mg/L glucose, L-alanyl-L-glutamine, $NaHCO_3$ and pyridoxine HCl, supplemented with 10% FBS and antibiotic/antimycotic (10,000U/ml penicillin, 10mg/ml streptomycin, 25µg/ml amphotericin) 25µg/ml ascorbate, 20mM HEPES and 50µg/ml gentamicin). Air bubbles were removed from

the bags, and bags tightened and incubated in a 37°C waterbath (prepared using sterile deionised water) for 7 days, with media changed every 48 hours. One disc was processed for histological analysis as a day 0 control (as outlined in 2.3.2 and 2.3.3), and one disc dissected into NP and AF tissue using a 24-blade scalpel, placed sealed in tin foil, snap-frozen in liquid nitrogen and stored at -80°C prior to RNA extraction (see 5.3.5). During media changes, discs were placed into fresh Whirl-pak bags using sterile forceps, exposing the tissue to air for as short time as possible. After 7 days, one disc was processed whole for histological analysis (detailed in 2.3.2 and 2.3.3) and the remaining 3 discs processed for RNA extraction, as outlined for day 0 specimens.

Following initial testing, the effect of hypoxic culture on the phenotype of porcine NP cells was assessed by culturing whole motion segments in normoxia and hypoxia. As it was not possible to expose discs to a hypoxic environment using the Whirl-pak bag and waterbath method, 8x discs were placed in sterile sample pots containing 50ml complete medium (detailed above) and 4x pots incubated in a normoxic culture incubator (37°C, 5% CO_2, 21% O_2) and 4x pots incubated in a hypoxic culture incubator (37°C, 5% CO_2, 2% O_2) for 7 days, with media changed every 48 hours. The lids of the pots were left slightly loose when in the incubators to allow for gaseous exchange to occur. Oxygen was removed from media for hypoxic cultures as outlined in 5.3.3.2 and all media changes for the hypoxic cultures performed in a hypoxic chamber, with normoxic cultures changed in a class II microbiology cabinet. One whole disc was processed for histological analysis at day 0 to serve as a control (detailed in 2.3.2 and 2.3.3) and NP dissected from 3x discs and processed for RNA extractions. After 7 days, 1x disc cultured in normoxia, and 1x disc cultured in hypoxia were processed whole for histological analysis (detailed in 2.3.2 and 2.3.3) and the remaining 3 discs at each oxygen tension processed for RNA extraction.

5.3.5 Extraction of Total RNA from Porcine Tissue Explants

5.3.5.1 Equipment, Materials and Reagents

5.3.5.1.1 Equipment

Homogenising apparatus	Amazon
Rubber mallet	B&Q
Vice	B&Q
Vortex	Grant Instruments

5.3.5.1.2 Materials

RNase-free microcentrifuge tubes	Axygen
RNase-free pipette tips	Corning

5.3.5.1.3 Reagents

TriReagent	Invitrogen

5.3.5.2 RNA Extraction Protocol

Specimens frozen at -80°C were transferred again to liquid nitrogen to ensure that they were as cold as possible. Following baking of the apparatus for tissue homogenisation (Figure 5.2) at 225°C for 18 hours, it was cooled to -80°C overnight. The apparatus was removed from the freezer just prior to use to ensure that it remained cool for as long as possible. Specimens were removed from the tin foil packets using sterile forceps and placed into the base of the apparatus (indicated by the red arrow) and the piston placed on top. The apparatus was placed into a vice and a force applied to the piston using a mallet, resulting in the tissue being powdered. Using a sterile spatula, powdered tissue was transferred to 1.5ml RNase-free MCTs, and 1ml TriReagent applied. Each MCT was vortexed briefly to ensure maximum recovery of RNA from the tissue and incubated at room temperature for 15 minutes, vortexing briefly every 5 minutes. Tubes were then stored at -80°C prior to RNA extraction, following the procedure outlined in 2.2.2. Specimens were then subject to DNase treatment and cDNA synthesis as detailed in 2.2.3 and 2.2.4.

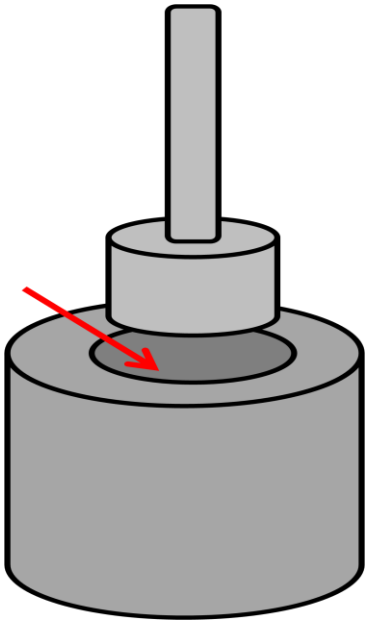

Figure 5.2 Apparatus for homogenising disc tissues. Specimens were placed in the base of the unit (red arrow) and the piston placed on top, prior to application of a force resulting in the tissue being powdered.

5.3.6 Optimisation of Bovine and Porcine qPCR Primers

5.3.6.1 Equipment, Materials and Reagents

5.3.6.1.1 Equipment

Centrifuge	Thermo Scientific
Positive displacement pipette	Gilson
StepOnePlus Real Time PCR Machine	Invitrogen

5.3.6.1.2 Materials

96-well PCR plate	Starlab
Optical Adhesive film	Starlab
Positive displacement pipette tips (10µl)	Gilson

5.3.6.1.3 Reagents

Fast SYBR Green Universal Mastermix	Applied Biosystems
Molecular biology-grade water	VWR
Bovine oligonucleotides	Applied Biosystems
Porcine oligonucleotides	Sigma Aldrich

5.3.6.2 qPCR Primer Optimisation

Primers required optimisation prior to use in gene expression analyses. The porcine primers differed from that used previously in that they were designed for use with SYBR Green mastermix, and therefore do not require the use of a fluorescent probe.

Primers were assessed at concentrations of 750nM and 500nM, diluted in molecular biology-grade water. Each primer concentration was tested in triplicate across 3 dilutions of control cDNA: 12.5ng/µl, 2.5ng/µl and 0.5ng/µl. Mastermix for the experiment was generated as follows: 5µl Fast SYBR Green Universal Mastermix, 1µl forward primer, 1µl reverse primer and 1µl molecular biology-grade water per well. Eight microlitres of mastermix was pipetted using a positive displacement pipette into each well of a 96-well PCR plate, and 2µl of control cDNA (from bovine genomic DNA or whole porcine organ cDNA generated in-house) added to the relevant wells. The plate was sealed using optical adhesive film, centrifuged at 2000g for 60 seconds and PCR performed using a StepOnePlus Real Time PCR Machine using the following experimental parameters: 95°C for 20 seconds followed by 40 cycles of 95°C for 1 seconds and 60°C for 20 seconds. As these assays did not use a probe, melt curves were also generated in order to ensure that only the desired products were being formed, rather than non-specific secondary products. Standard curves were constructed using the serial dilution of control cDNA for each primer concentration and primers were considered optimal when the reaction efficiency was 95-105%.

5.3.7 Gene Expression Analysis by qPCR

5.3.7.1 Quantitative Real-Time PCR Methodology

The expression levels of various genes were assessed using qPCR: COL1A1, COL2A1, ACAN, KRT8, KRT18, KRT19, CAXII, IBSP, NOTO, FOXJ1, T, FOXA2, LGALS3 and NOGGIN. Expression levels were normalised to that of the internal reference gene GAPDH. Bovine-specific primer sequence information and optimal concentration information is detailed in Table 5.1, whilst those pertaining to analysis of porcine specimens are listed in Table 5.2. An assay mastermix was generated as outlined in 5.3.6.2. Each sample was analysed in triplicate, with two negative and two positive control wells also tested. The negative control wells contained 2µl molecular biology-grade water in place of cDNA, whilst the positive control wells contained 2µl of the porcine whole organ cDNA or bovine genomic DNA used for primer optimisation in 5.3.6.2. Experimental parameters were the same as that described in 5.3.6.2.

Table 5.1 Bovine qPCR Primer Details

Gene Name	Forward Primer Sequence 5'-3'	Reverse Primer Sequence 5'-3'	Optimal Primer Concentration
GAPDH	TGCCGCCTGGAGAAACC	CGCCTGCTTCACCACCTT	500nM
SOX9	GGGAAGCCTCACATCGACTTC	GGACATTACCTCATGGCTGATCT	500nM
COL2A1	CGGGCTGAGGGCAACA	CGTGCAGCCATCCTTCAGA	500nM
ACAN	GGGAGGAGACGACTGCAATC	CCCATTCCGTCTTGTTTTCTG	500nM
CAXII	CCAACAACGGCCACTCAGT	CCCCGGACCTGCATGTC	500nM
IBSP	GTTTTAATTTTGCTCAGCATTTTGG	GGCTCTTCGATTCAAATTTTTCA	500nM
FBLN1	GCAGCGCAGCCAAGTCAT	AGATATGTCTGGGTGCTACAAACG	500nM
T	ACTTCGTGGCGGCTGACA	GCACCCACTCCCCATTCA	500nM
LGALS3	AGGCCTCGCATGCTGATAAC	AAGCAAGTCTGTTCGCATTGG	500nM
CD24	TTCTGGCGCTGCTCTTACCT	GGGAGGAGTTACTTGGTGTTACAAC	500nM

Table 5.2 Porcine qPCR Primer Details

Gene Name	Forward Primer Sequence 5'-3'	Reverse Primer Sequence 5'-3'	Optimal Primer Concentration
GAPDH	GTATGATTCCACCCACGG	GATCTCGCTCCTGGAAGA	500nM
COL1A1	AGTTGTCTTATGGCTATGATGAG	GACCACGAGGACCAGAAG	500nM
COL2A1	TATAATGATAAGGATGTGTGGAA	GATTATGTCGTCGCAGAG	500nM
ACAN	GACTTTAGTGAACTTCCATCT	GCCCAAATGTTTCTCCAG	500nM
KRT8	CCTCTGATGTCCTGTC	TGAATTGGCTTGGAGT	500nM
KRT18	CAGGGACTGGAGTCATTA	GCATTGTCCACAGAACTT	500nM
KRT19	AAGAAGAACCACGAGGAG	GGAGCCGAATCAACCT	500nM
CAXII	ACACACATGGATGACCC	CAGCCTCTCGTCAAACT	750nM
NOTO	CGATACCAGCGTCCAG	CCTCTGTCCCCATCCT	250nM
FOXJ1	GCTCGTGGATGTTGAC	TTGGCGTTGAGAATGG	250nM
FOXA2	AGCATTCTCATTCTTGACA	GCAGTAGGAACACACATT	500nM
T	CCTTCAGCAAAGTCAAGC	CGTACTTATGTAAGGAGTTCAG	250nM
NOGGIN	AGTGCTCATGCTAGAACT	GAAAGCTAGGTCTCTGTAG	500nM

5.3.7.2 qPCR Data Analysis

Data was analysed according to both the ΔCt and ΔΔCt method (Livak and Schmittgen, 2001). In experiments where specimens did not undergo culture for a 7 or 14 day timepoint, RNA from day 0 control specimens was not generated to normalised data back to in the ΔΔCt method. In these conditions, ΔCt analysis was performed. In order to assess for statistical significance, Mann Whitney-U tests were employed, and GraphPad InStat software utilised for analysis.

5.3.8 Confirmation of Cell Viability by Total Message *In Situ* Hybridisation

Cellular viability at the end of the culture period was assessed in order to ensure that the culture protocol was not detrimental to explant viability.

5.3.8.1 Equipment, Materials and Reagents

5.3.8.1.1 Equipment

Humidity chamber	Patolab
UV Transilluminator	RS Component

5.3.8.1.2 Materials

22x40mm coverslips	Scientific Laboratory Supplies
Loctite glue	Loctite
Positively charged microscope slides	Thermo Scientific

5.3.7.1.3 Reagents

30% (v/v) hydrogen peroxide	Thermo Scientific
Anti-Dig-AP, Fab fragments	Roche
Boehringer Blocking Reagent	Boehringer
Cobalt chloride ($CoCl_2$)	Sigma Aldrich
Diethylpyrocarbonate (DEPC)	Sigma Aldrich
Dig-11-UTP	Roche
Diemthyl formamide	Sigma Aldrich
Ethylenediaminetetraacetic acid (EDTA)	BDH
Fast red ITR	Sigma Aldrich
Glycine	Fisher Scientific
Hydrochloric acid (HCl)	Fisher Scientific
Industrial methylated spirits (IMS)	Fisher Scientific
Levamisole	Sigma Aldrich
Magnesium chloride	BDH
Mayer's haematoxylin	Solmedia
Naphthol AS-BI phosphate	Sigma Aldrich

Paraformaldehyde	Sigma Aldrich
PIPES	Sigma Aldrich
Poly-dTTP (2.5mM)	Roche
Poly-d(T) probe	Roche
Polyethylene glycol 6000	Sigma Aldrich
Proteinase K	Promega
Salmon sperm DNA	Life Technologies
Sodium acetate	Sigma Aldrich
Sodium barbitone	Sigma Aldrich
Sodium chloride (NaCl)	Fisher Scientific
Sodium citrate	Sigma Aldrich
Terminal transferase (400U)	Roche
Terminal transferase tailing buffer (5x)	Roche
Tris-Base	Fisher Scientific
Triton-X 100	Sigma Aldrich
Xylene	Fisher Scientific

5.3.8.2 *In Situ* Hybridisation Methodology

At completion of the 14-day culture protocol, explants were removed from the culture inserts using sterile forceps, and washed briefly in sterile PBS to remove any traces of culture media. Explants were then placed in a 15ml centrifuge tube containing 5ml 4% (w/v) paraformaldehyde, and incubated at 4°C for 24 hours. Specimens were then washed in PBS twice before being processed and wax-embedded as outlined in 2.3.3.

All glassware used in this experiment was treated for ubiquitous RNase contamination by treating with 3% (v/v) hydrogen peroxide and baking at 250°C for 3 hours. Additionally, all solutions were treated with 0.1% (v/v) diethylpyrocarbonate (DEPC) or prepared in DEPC-treated water followed by autoclaving. Wax-embedded sections were cut and mounted as detailed in 2.3.4. Prior to commencing the protocol, slides were incubated at 60°C for 48 hours to ensure that specimens were firmly attached to the slide surface. Slides were then heated on a hotplate to thoroughly melt the wax, before dewaxing in xylene for 3 x 5 minutes and rehydrating in IMS for 4 x 3 minutes. Sections were rinsed in DEPC-treated water for 10 minutes, and then immersed in 0.2N HCl for 20 minutes. Sections were rinsed in 2X SSC (300mM NaCl, 30mM sodium citrate) for 2 x 3 minutes and then rinsed in 50mM Tris HCl pH 7.4 for 3 minutes. Slides were placed in humidity chambers and 5µg/ml proteinase K applied to each, before incubating at 37°C for 1 hour. Slides were then rinsed in 0.2% glycine (v/v) in PBS for 2 x 3

minutes and then in PBS alone for 2 x 3 minutes. Specimens were then subject to post-fixation, by incubating in cold 0.4% (w/v) paraformaldehyde for 20 minutes, followed by rinsing in DEPC-treated water.

A pre-hybridisation step was then conducted in order to block non-specific binding sites and decrease background signal. Hybridisation buffer (2ml) was made up as follows: 240µl 5M NaCl, 200µl 10X PE (100mM PIPES pH 6.8, 10mM EDTA), 20µl 10mg/ml salmon sperm DNA, 400µl 50% (v/v) polyethylene glycol 6000 and 1140µl DEPC-treated water. Slides were placed in a humidity chamber and 100µl of pre-hybridisation buffer applied to each slide. A coverslip was placed over negative control sections. All slides were incubated at 37°C for 1 hour. The probe was then prepared as follows: 10µl 5x terminal transferase tailing buffer, 10µl 25mM $CoCl_2$ solution, 3.5µl 2.5mM poly dTTP, 2µl 1mM Dig-11-UTP, 1µl 1µg/ml poly d(T) probe, 22.5µl DEPC-treated water and 1µl terminal transferase (400U). The prepared probe was incubated at 37°C for 15 minutes, and the labelling reaction stopped by adding 5µl 0.2M EDTA pH 8.0. This probe was then utilised in making the hybridisation buffer as follows: 120µl 5M NaCl, 100µl 10X PE, 10µl 10mg/ml salmon sperm DNA, 200µl 50% (v/v) polyethylene glycol 6000, 520µl DEPC-treated water and 50µl of the prepared Dig-labelled poly d(T) probe. The pre-hybridisation buffer was poured off the sections (excluding the negative control) and 50µl of hybridisation buffer applied to each test slide. Negative control sections were not tested with probe. Each was covered with a coverslip and incubated at 37°C overnight.

Post-hybridisation washes were then performed. Coverslips were removed from sections by rinsing in 4X SSC (600mM NaCl, 60mM sodium citrate). Slides were then washed in 2X SSC (300mM NaCl, 30mM sodium citrate) for 3 x 10 minutes at 37°C. Slides were then washed in 0.1% Triton-X 100 (v/v) in TBS at room temperature for 15 minutes. Detection of the Dig-labelled probe was then performed using alkaline phosphatase, visualised with fast red and naphthol salt. Briefly, sections were rinsed in ISH buffer (0.15M NaCl, 0.1M Tris, pH 7.5) for 5 minutes. Non-specific binding sites were then blocked by incubating sections in 100µl 0.5% (w/v) Boehringer blocking reagent in ISH buffer for 30 minutes at room temperature. The blocking solution was poured off slides and tissue used to wipe around the section. The antibody conjugate (Anti-Dig-AP, Fab fragments) was diluted 1:250 in

blocking solution and applied to each section, followed by incubation at room temperature for 2 hours. The antibody conjugate was poured off the slides, which were then rinsed in ISH buffer for 2 x 15 minutes. Sections were then rinsed briefly in veronal acetate buffer (30mM sodium acetate, 30mM sodium barbitone, 100mM sodium chloride, 50mM magnesium chloride pH 9.2). A detection solution was prepared as follows: 0.5mg/ml fast red ITR and 0.2mg/ml levamisole added to 100ml veronal acetate buffer and mixed until dissolved. Naphthol AS-BI phosphate (250mg/ml) was dissolved in dimethylformamide (made in a glass container), and 200µl added immediately to the veronal acetate buffer containing fast red and levamisole. The detection solution was filtered and prior to incubating slides for 1 hour at room temperature. The detection buffer was poured off and slides washed in cold water until non-specific staining was reduced. Sections were counterstained in haematoxylin for 30 seconds, and slides rinsed in water for 10 minutes. Finally, sections were air dried for approximately 15 minutes, mounted in Loctite, and glass coverslips bonded using UV irradiation applied for 5 minutes.

5.3.9 Histological Analysis of Morphology and Changes to NP Extracellular Matrix

5.3.9.1 Materials and Reagents

5.3.9.1.1 Materials

Glass coverslips (22x40mm)	Scientific Laboratory Supplies
Shandon consul permanent mountant	Thermo Scientific

5.3.9.1.2 Reagents

Acetic acid	Fisher Scientific
Fast green	Difco
Giemsa reagent	Thermo Fisher
Jenner reagent	TCS Biosciences
Masson trichrome staining kit	Biostain Ready Reagent
Mayer’s haematoxylin	Solmedia
pH 6.4 buffer solution	Merck
Safranin-O	Sigma Aldrich
Weigert’s haematoxylin	TCS Biosciences Ltd

5.3.9.2 Giemsa Staining

Slides were placed into a coplin jar and 0.3% (w/v) Jenner (in 100% methanol) added to half-fill the jar, incubating the slides for 2 minutes. The solution within the coplin jar then filled to the top with pH 6.4 buffer solution and slides incubated for a

further 60 seconds. The Jenner solution was poured off the slides, and 2% (v/v) Giemsa stain (in pH 6.4 buffer solution) applied, and slides incubated for 20 minutes. Following this, Giemsa stain was poured off the slides and slides washed twice using pH 6.4 buffer solution. Slides were placed on a sheet of filter paper, and a second sheet of filter paper applied to the top, gently pressing on the slides to remove excess stain and buffer solution. Slides were mounted in Shandon Consul permanent mountant, and a 22x40mm glass coverslip applied.

5.3.9.3 Masson Trichrome Staining

Wax embedded sections 5µm in thickness were prepared as detailed in 2.3.4 and were dewaxed in xylene for 3 x 5 minutes, followed by rehydration in IMS for 4 x 5 minutes. Weigert's haematoxylin was applied to each slide, and incubated for 10 minutes. Haematoxylin was poured off each slide, and ponceau fuchsin masson applied for 10 minutes. Following this, slides were briefly washed in deionised water, and phosphotungstic acid applied for 10 minutes. Slides were again washed in deionised water and aniline blue applied to each, followed by incubation for 8 minutes. Slides were then drained and 1% (v/v) acetic acid applied. After 5 minutes of incubation, slides were washed in deionised water, dehydrated in IMS for 4 x 1 minute, and cleared in xylene for 3 x 3 minutes. Finally, slides were mounted using Shandon Consul permanent mountant and covered with a 22x40mm glass coverslip.

5.3.9.4 Safranin-O/Fast Green Staining

Wax embedded specimens 5µm in thickness were dewaxed in xylene for 3 x 5 minutes, rehydrated in IMS for 4 x 5 minutes and stained in filtered Weigert's haematoxylin for 3 minutes. Sections were washed in tap water for 10 minutes and stained in 0.2% (w/v) Fast Green for 5 minutes. Slides were washed briefly in 1% acetic acid and the liquid poured off the slides. Sections were then stained in filtered 0.1% (w/v) Safranin-O for 4 minutes. Finally, sections were rinsed in IMS for 1 minute, dehydrated further in IMS for 4 x 3 minutes, cleared in xylene for 3 x 5 minutes and mounted in Shandon Consul permanent mountant and covered with a 22x40mm glass coverslip. All histological analysis was performed as outlined in 2.3.8.

5.4 Results

5.4.1 Size-Based Separation of NP and NC Cells from Bovine Coccygeal Disc Tissue

Haematoxylin and eosin stained sections of fixed bovine IVD tissue provided evidence that NC cell clusters existed within the NP tissue (Figure 5.3B), as well as small chondrocyte-like NP cells, akin to that of the adult human IVD (Figure 5.3A).

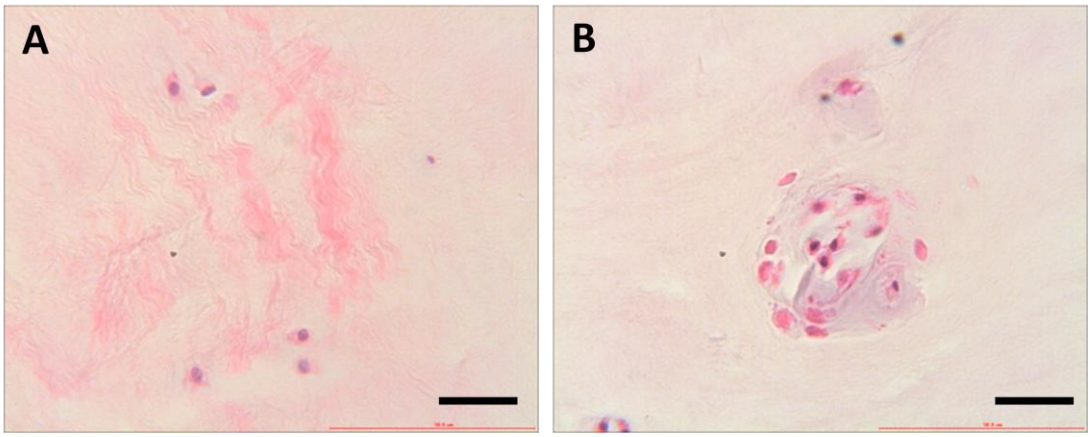

Figure 5.3 Haematoxylin and eosin stained sections of bovine coccygeal NP. Small NP cells (A) and NC cells (B) identified within the tissue sections. Scale bars= 50µm.

Gene expression profiles of isolated NP and NC cells from enzymatically-digested tissue were subsequently compared (Figure 5.4). In terms of the expression of the classic chondrogenic markers, expression of ACAN did not differ significantly between NP and NC cells (p= 0.8417). Expression of both SOX9 and COL2A1 was significantly greater in NP as compared to NC cells (p= 0.0091 and p= 0.0086 respectively), whilst expression of the novel NP cell marker CAXII was not significantly different between the two cell types (p=0.6343). Regarding the expression of novel NP cell negative markers, IBSP expression was comparable between the two cell types (p=0.5344), but expression of FBLN1 was significantly decreased in NC when compared to NP cells (p= 0.0004). Notochordal cell markers T, LGALS3 and CD24 were all detected in bovine NP and NC cells, with both LGALS3 and CD24 significantly more highly expressed in NC as compared to NP cells (p= 0.0391 and p= 0.0095 respectively). Expression of T did not vary significantly between the two cell types (p= 0.7656).

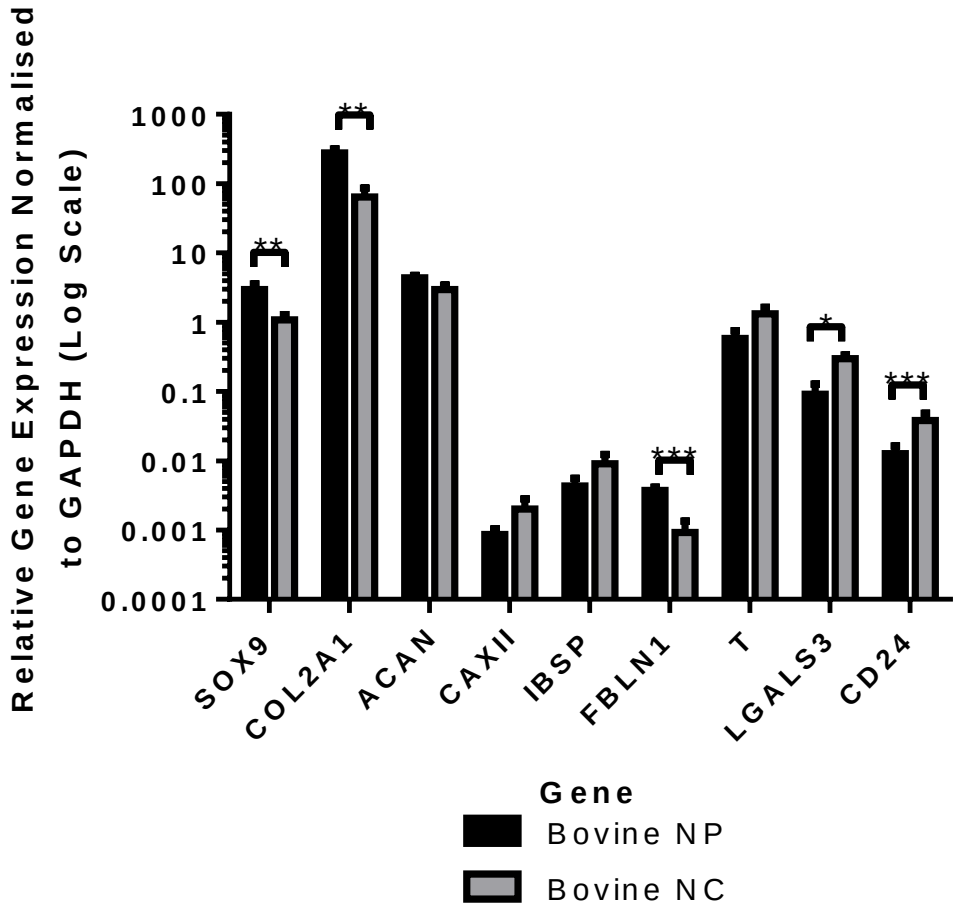

Figure 5.4 Gene expression profiles of isolated bovine NP and NC cells. Bovine small NP cells (<8µm; black bars) and NC cells (>15µm; grey bars) were compared for their gene expression profiles for a genes SOX9, COL2A1, ACAN, CAXII, IBSP, FBLN1, T, LGALS3 and CD24. *p=0.05 **p=0.01 **p=0.001.

Figure 5.5 illustrates the morphology and size of bovine NP cells separated by size-based filtration following cytospinning of the preparation. Both filtrates appeared to contain cells that were similar in terms of size and morphology. The arrows indicate that both separations contained cells that appeared to be vacuolated, like NC cells, but also smaller cells, akin to the adult chondrocyte-like NP cells, indicative of heterogeneous cell populations. Additionally, portions of undigested ECM tissue were apparent in the cell suspension obtained from the 15µm filter, which may have affected the ability of cells to pass through the membrane.

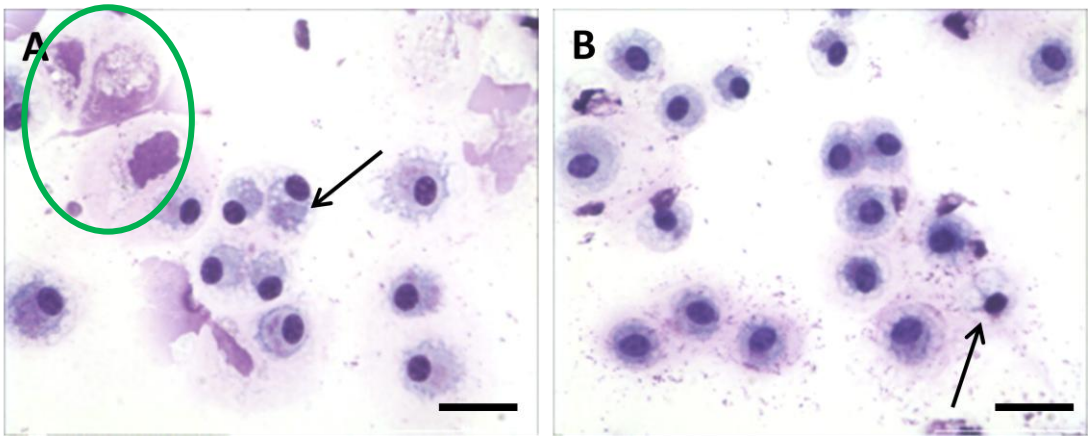

Figure 5.5 Giemsa stained isolated bovine NP and NC cells. Supposed bovine small NP cells (<8µm; A) and NC cells (>15µm; B) were stained with giemsa to compare and confirm isolated cells were distinct in terms of size and morphology. Arrows indicate the presence of NC cells in both populations. Undigested ECM tissue was also apparent in the cell suspension obtained from the 15µm filter (green circle). Scale bar =25µm.

5.4.2 Assessment of the Porcine NC Cell Phenotype as a Suitable Model

Given that the populations of cells isolated by size-based filtration in the bovine model were not distinct in terms of morphology, a porcine NP model was employed as it is comprised primarily of morphologically distinct NC cells. Cells extracted from porcine NP tissue were stained with Giemsa to ensure that they were comprised predominantly of morphologically distinct NC cells (Figure 5.6).

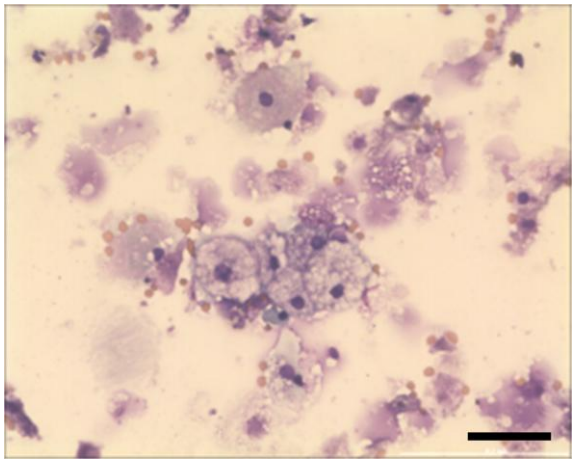

Figure 5.6 Giemsa stained porcine NC cells. Cells isolated from porcine NP tissue were stained with giemsa to ensure that the isolated cells were akin to an NC morphology. Scale bar =50µm.

The gene expression profile of porcine NC cells was investigated (Figure 5.7). Expression of all of the genes analysed (COL1A1, COL2A1, ACAN, KRT8, KRT18, KRT19, CAXII, NOTO, FOXJ1, T, FOXA2 and NOGGIN) was detected in porcine NC cells.

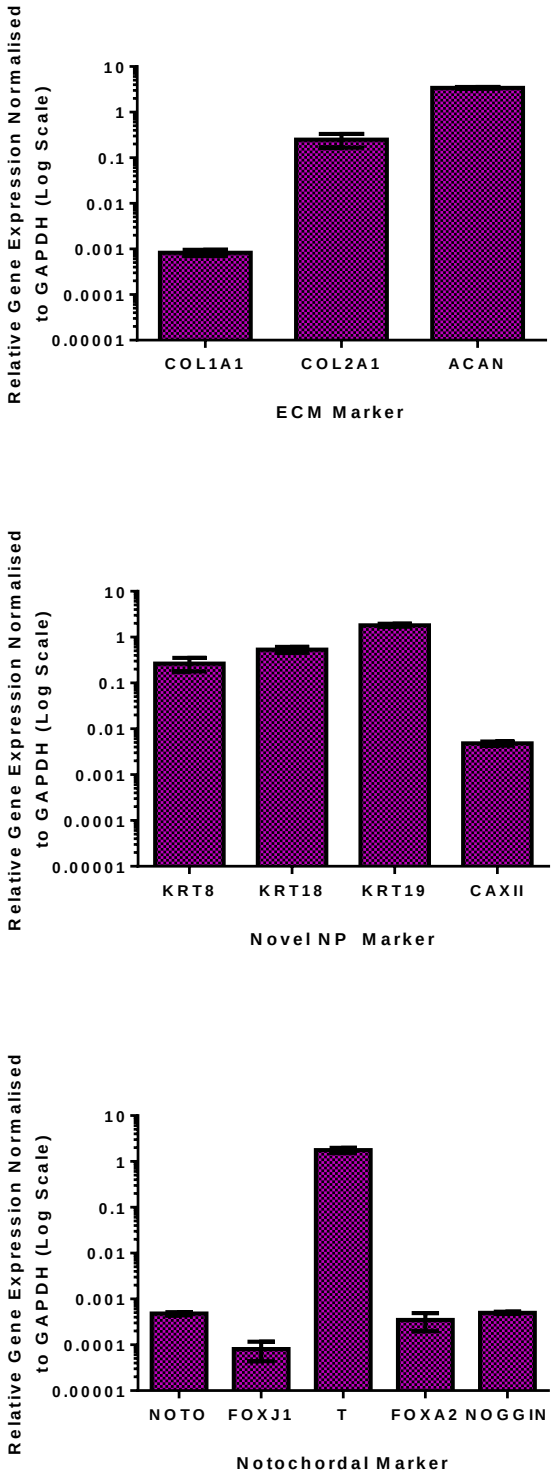

Figure 5.7 Gene expression profile of porcine NC cells. Porcine NC cells were assessed for their expression of the ECM markers COL1A1, COL2A1 and ACAN; novel NP cell markers KRT8, KRT18, KRT19, and CAXII; and notochordal cell markers NOTO, FOXJ1, T, FOXA2 and NOGGIN.

5.4.3 The Effects of the IVD Microenvironment on Porcine NC Cell Phenotype

5.4.3.1 Assessment of Cellular Viability

Porcine NC cell viability following culture was confirmed by *in situ* hybridisation for total message RNA (Figure 5.8). Viable cells were noted in explants cultured under all conditions (Figure 5.8A, 5.8B, 5.8C and 5.8D), as well as explants of NP obtained at day 0 (Figure 5.8E). Negative control sections demonstrated no positivity (Figure 5.8F), confirming that porcine NP explants remain viable following 14 days of *in vitro* culture.

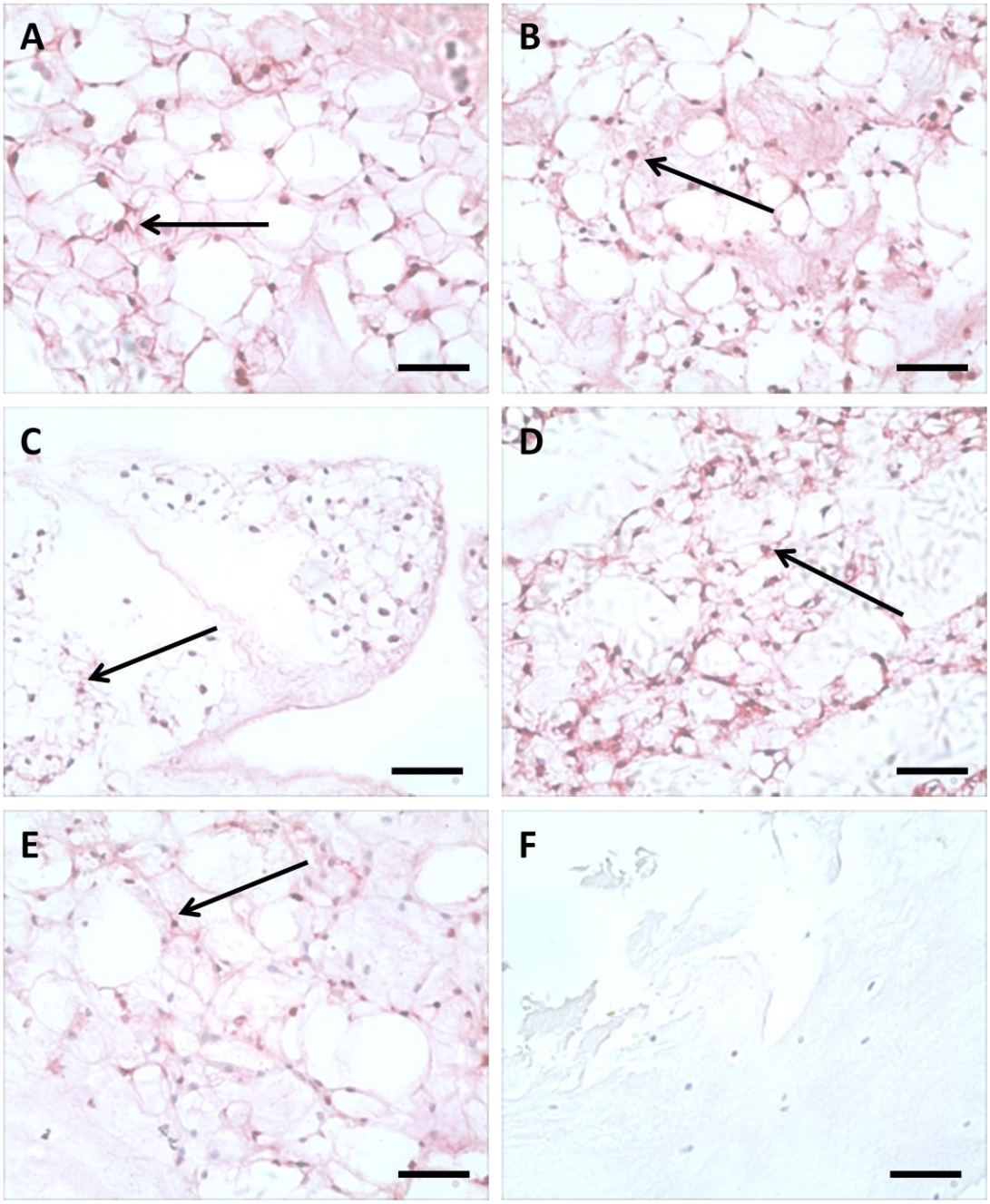

Figure 5.8 *In situ* hybridisation for total message RNA in cultured porcine NP explants. Sections cultured in normoxia (A), normoxia + IL-1β (B), hypoxia (C), hypoxia + IL-1β (D), and day 0 control explants (E) were assessed. Negative control sections of IVD control tissue were tested with the addition of no probe (F). Red stained nuclei indicate viable cells (black arrows). Scale bar =50µm.

5.4.3.2 Gene Expression Analysis

As it had been established that porcine NC cells express markers also expressed by human NC and NP cells, explants of porcine NP tissue were utilised in the assessment of the effect of an IVD-like microenvironment (high IL-1β and hypoxia) on the phenotype of NC cells. Figures 5.9, 5.10 and 5.11 illustrate the gene expression profiles of porcine NP explants when exposed to normoxic culture, normoxic culture and IL-1β challenge, hypoxic culture, or hypoxic culture and IL-1β challenge, when normalised to directly extracted NC cells (no culture).

Regarding the expression of the ECM markers (Figure 5.9), COL1A1 expression was significantly increased under all culture conditions as compared to day 0 controls, whilst COL2A1 and ACAN expression did not differ at all: normoxia ($p = <0.0001$, $p = 0.5636$, $p = 0.3469$ respectively); normoxia + IL-1β ($p = <0.0001$, $p = 0.3469$, $p = 0.6390$ respectively); hypoxia ($p = <0.0001$, $p = 0.5740$, $p = 0.3971$); and hypoxia + IL-1β ($p = <0.0001$, $p = 0.0739$, $p = 0.9688$). COL1A1 expression was significantly decreased in hypoxic compared to normoxic culture ($p = 0.0004$), but COL2A1 and ACAN demonstrated no such variations ($p = 0.1902$ and $p = 0.0776$ respectively). Expression of COL1A1, COL2A1 and ACAN did not differ under normoxia and normoxia with IL-1β ($p = 0.9291$, $p = 0.7123$, and $p = 0.2243$ respectively), or under hypoxia and hypoxia with IL-1β ($p = 0.4317$, $p = 0.4545$, $p = 0.2387$ respectively). Finally, under IL-1β challenge, expression of COL1A1, COL2A1 and ACAN did not differ when cultured in normoxia or hypoxia ($p = 0.0705$, $p = 0.2273$, $p = 0.8451$ respectively).

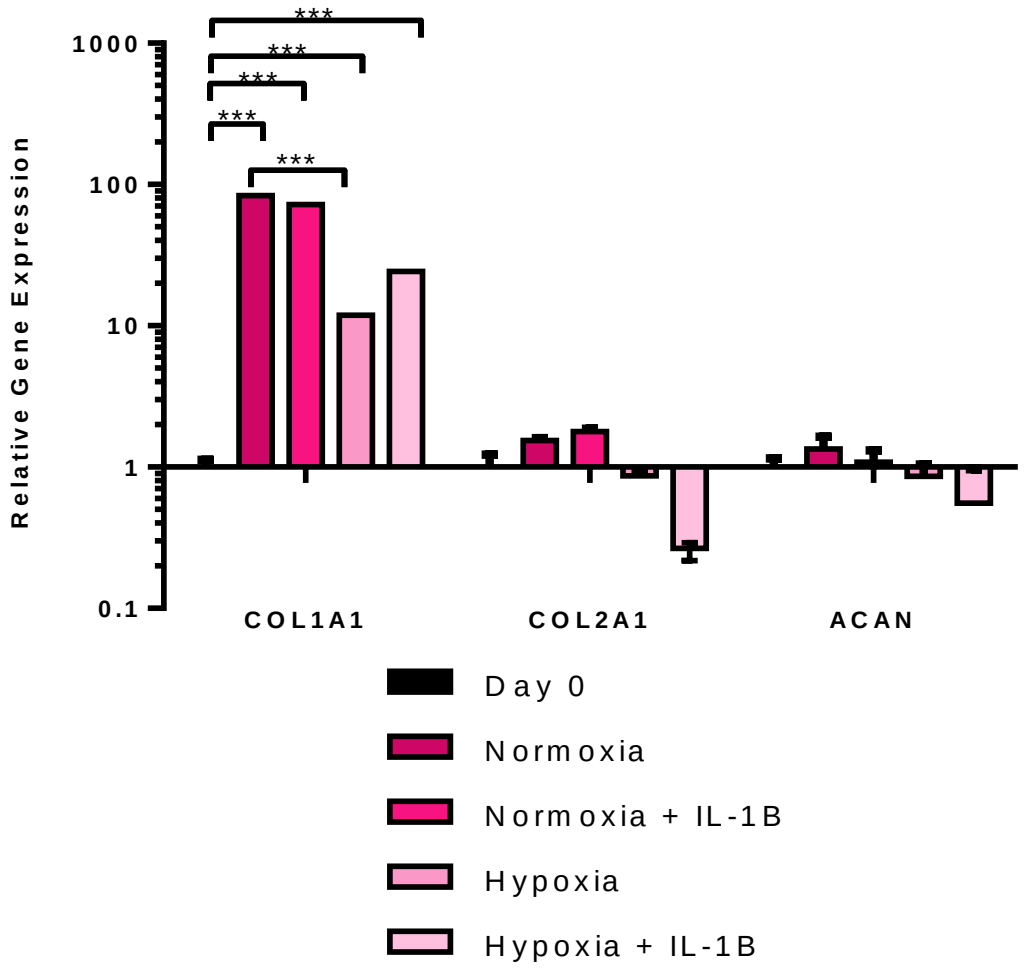

Figure 5.9 The effects of the IVD microenvironment on the expression of ECM markers in porcine NP explants. Expression levels of COL1A1, COL2A1 and ACAN were assessed in NC cells from porcine NP explants when cultured in normoxia, normoxia + IL-1β, hypoxia, and hypoxia + IL-β. Gene expression was normalised to reference gene GAPDH and back to day 0 control levels (2-ΔΔCt method). ***p= 0.001.

With reference to novel NP marker expression (Figure 5.10), generally, significant downregulations in expression were noted under all culture conditions when compared to day 0 control expression levels for KRT8, KRT18, KRT19 and CAXII: normoxia (p= <0.0001, p= <0.0001, p= 0.0298, and p= 0.0081 respectively); normoxia + IL-1β (p= 0.0080, p= <0.0001, p= <0.0001, and p= 0.0238 respectively); hypoxia (p= 0.0105, p= <0.0001, p= 0.0007, and p= <0.0001 respectively); and

hypoxia + IL-1β (p= 0.2526, p= <0.0001, p= 0.0027, and p= 0.2684 respectively), with the exception of CAXII which was significantly upregulated under hypoxia. Regarding variations between normoxic and hypoxic culture, KRT8, KRT18 and KRT19 expression demonstrated no significant differences (p= 0.0680, p= 0.1331, and p= 0.4980 respectively), but CAXII expression was significantly increased in normoxic as compared to hypoxic cultures (p= <0.0001). Addition of IL-1β resulted in some significant variations. Under normoxia, KRT19 expression was significantly decreased in IL-1β culture (p= 0.0410), but expression levels of KRT8, KRT18 and CAXII did not differ (p= 0.0506, p= 0.9538, and p= 0.5162 respectively). In hypoxia, KRT18 was significantly decreased upon addition of IL-1β, whilst CAXII was significantly increased (p= 0.0478 and p= 0.0320 respectively), whilst expression of KRT8 and KRT19 did not alter (p= 0.7492 and p= 0.7627 respectively). Finally, under IL-1β challenge, expression of KRT8 and KRT19 did not vary between normoxic and hypoxic cultures (p= 0.6569 and p= 0.9057 respectively), but significant variations were noted in KRT18 and CAXII expression (p= 0.0245 and p= 0.0191 respectively).

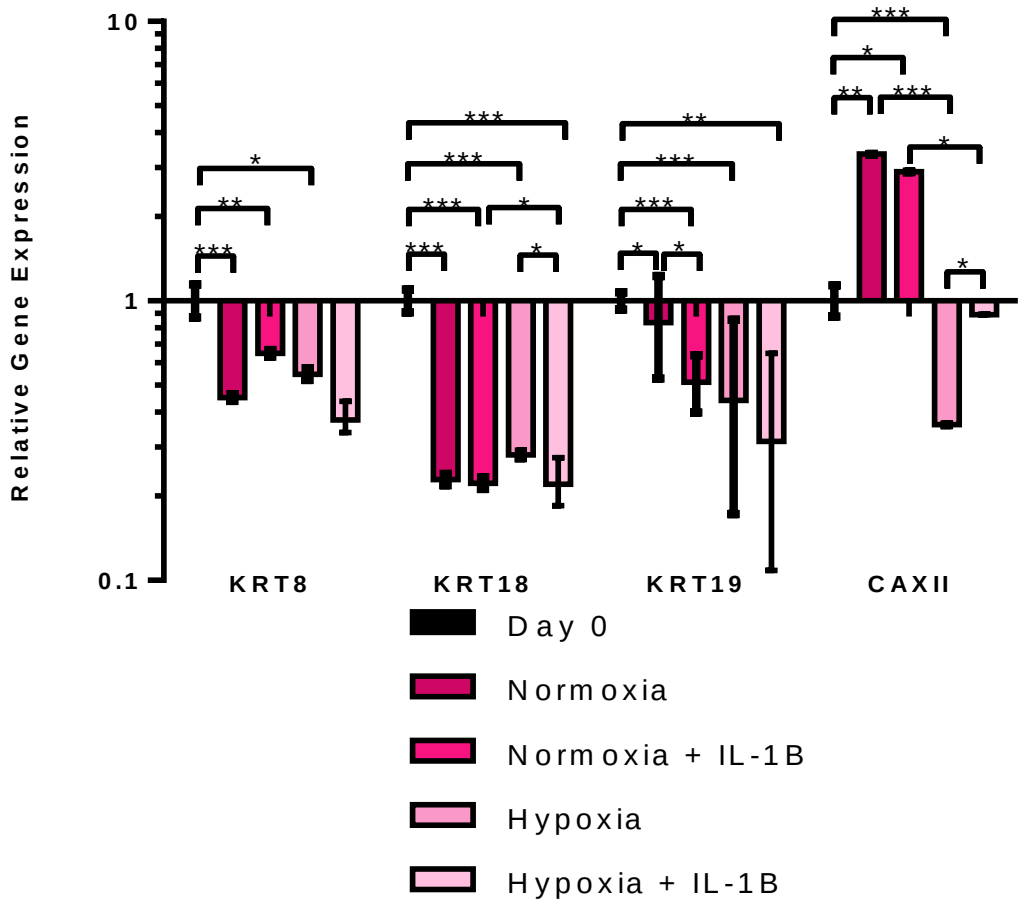

Figure 5.10 The effects of the IVD microenvironment on the expression of novel NP cell markers in porcine NP explants. Expression levels of KRT8, KRT18, KRT19 and CAXII were assessed in NC cells from porcine NP explants when cultured in normoxia, normoxia + IL-1β, hypoxia, and hypoxia + IL-β. Gene expression was normalised to reference gene GAPDH and back to day 0 control levels (2-ΔΔCt method). *p= 0.05 **p= 0.01 ***p= 0.001.

Notochordal cell marker expression was also assessed (Figure 5.11). Again, significant downregulations in expression were largely noted under all culture conditions when compared to day 0 control expression levels for NOTO, FOXJ1, T, FOXA2 and NOGGIN: normoxia (p= <0.0001, p= <0.0001, <0.0001, p= <0.0001 and p= 0.0670 respectively); normoxia + IL-1β (p= <0.0001, p= <0.0001, p= <0.0001, p= <0.0001 and p= 0.0042 respectively); hypoxia (p= <0.0001, p= <0.0001, p= <0.0001, p= 0.0651 and p= <0.0001 respectively); and hypoxia + IL-1β (p= <0.0001, p= <0.0001, p= <0.0001, p= <0.0001 and p= <0.0001 respectively). When expression levels were compared between normoxic and hypoxic cultures, FOXJ1, T and NOGGIN expression was significantly decreased under hypoxia (p=

<0.0001, p= 0.0186 and p= 0.0045 respectively), whilst NOTO and FOXA2 expression demonstrated no variation (p= 0.1251 and p= 0.4838 respectively). Addition of IL-1β in normoxia in fact increased NOTO expression (p= 0.0378), but expression levels of FOXJ1, T, FOXA2 and NOGGIN were unaltered (p= 0.0588, p= 0.2763, p= 0.6893 and p= 0.9755 respectively). Similarly, supplementing culture media with IL-1β in hypoxia did not alter gene expression levels of NOTO, FOXJ1, T, FOXA2, and NOGGIN (p= 0.8938, p= 0.3444, p= 0.1875, p= 0.3693 and p= 0.0845 respectively). Finally, when expression levels of hypoxic and normoxic cultures with IL-1β were compared, NOTO, FOXJ1 and NOGGIN expression was significantly decreased (p= 0.0004, p= 0.0088, and p= 0.0131 respectively), whilst T and FOXA2 expression did not alter significantly (p= 0.4622 and p= 0.7492 respectively).

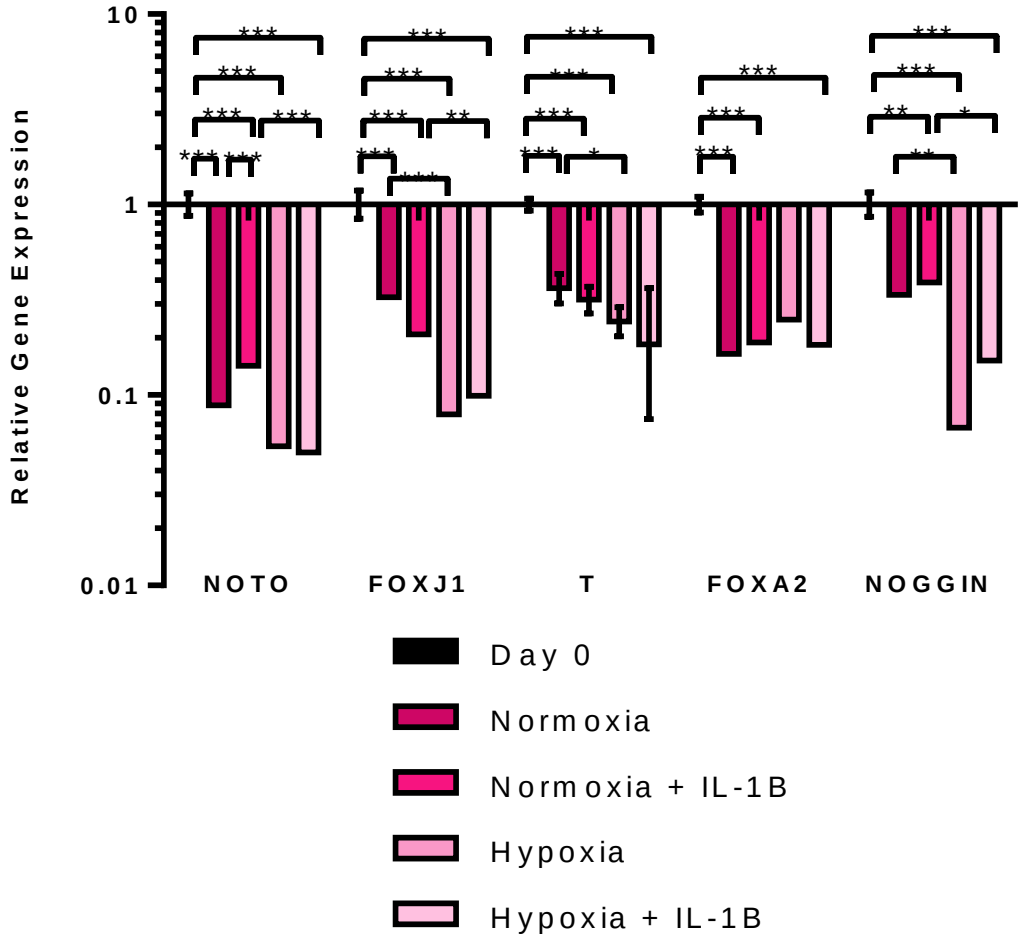

Figure 5.11 The effects of the IVD microenvironment on the expression of notochordal cell markers in porcine NP explants. Expression levels of NOTO, FOXJ1, T, FOXA2 and NOGGIN were assessed in NC cells from porcine NP explants when cultured in normoxia, normoxia + IL-1β, hypoxia, and hypoxia + IL-β. Gene expression was normalised to reference gene GAPDH and back to day 0 control levels (2-ΔΔCt method). *p= 0.05 **p= 0.01 ***p= 0.001.

5.4.3.3 Histological Analysis

Figure 5.12 illustrates the morphology of cells within the NP explants, stained with H&E. In all of the cultures (Figures 5.12A-D), there was loss of collagen within the NP as compared to day 0 controls (Figure 5.12E). Also, a loss in the organisation of the NC network was noted as compared to day 0 controls, particularly in the hypoxic cultures (Figures 5.12C and 5.12D). Interestingly, explants cultured in hypoxia (Figure 5.12C) alone lost much of the PG within the ECM, as noted from the decreased staining of the matrix. Thus, *in vitro* culture resulted in decreased organisation of the cellular network and a loss of collagen/PG within the ECM.

PG content of explants following *in vitro* culture was assessed using Safranin-O and Fast Green histological staining (Figure 5.13). Histological analysis demonstrated that PG content was completely lost following the 14 day *in vitro* culture protocol irrespective of the culture conditions (Figure 5.13A, 5.13B, 5.13C and 5.13D), as compared to day 0 control, which had high levels of PG staining (Figure 5.13E). A small amount of PG was retained in cultures exposed to only normoxia (Figure 5.13A).

Similarly, Masson trichrome staining of cultured explants tissues was performed in order to further investigate alterations to the explant ECM following culture (Figure 5.14). Collagen fibres appear blue or green in this histological stain, and this staining was not present in any of the cultured explants (Figure 5.14A-D), as compared to day 0 controls (Figure 5.14E), which showed high levels of collagen staining. Also, these images serve to confirm the findings presented with the H&E staining of loss of ECM and cellular network organisation following *in vitro* culture.

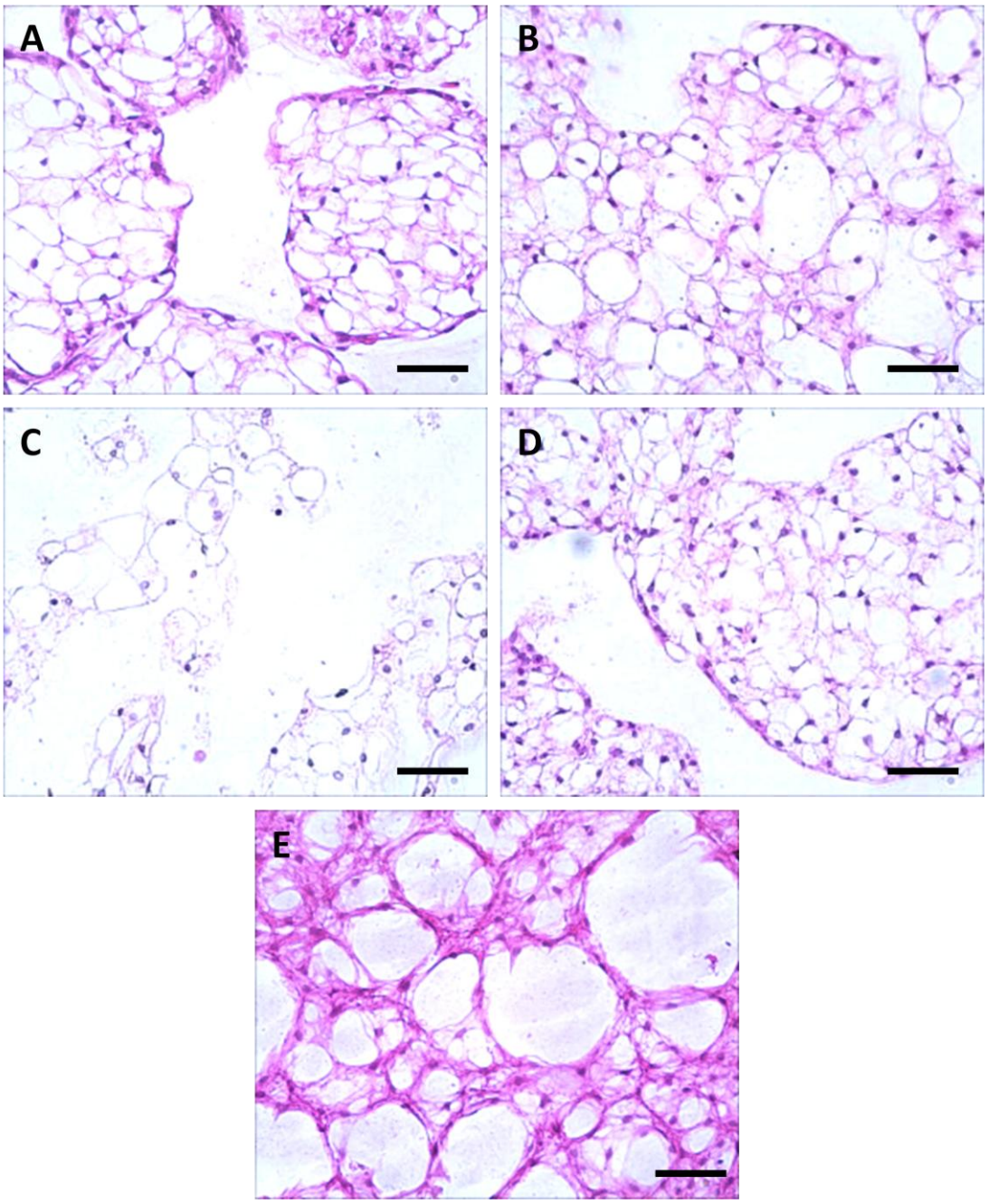

Figure 5.12 Haematoxylin and eosin stained sections of cultured porcine NP explants. Sections cultured in normoxia (A), normoxia + IL-1β (B), hypoxia (C), and hypoxia + IL-1β (D) and day 0 control explants (E) were stained with H&E. Scale bar =50μm.

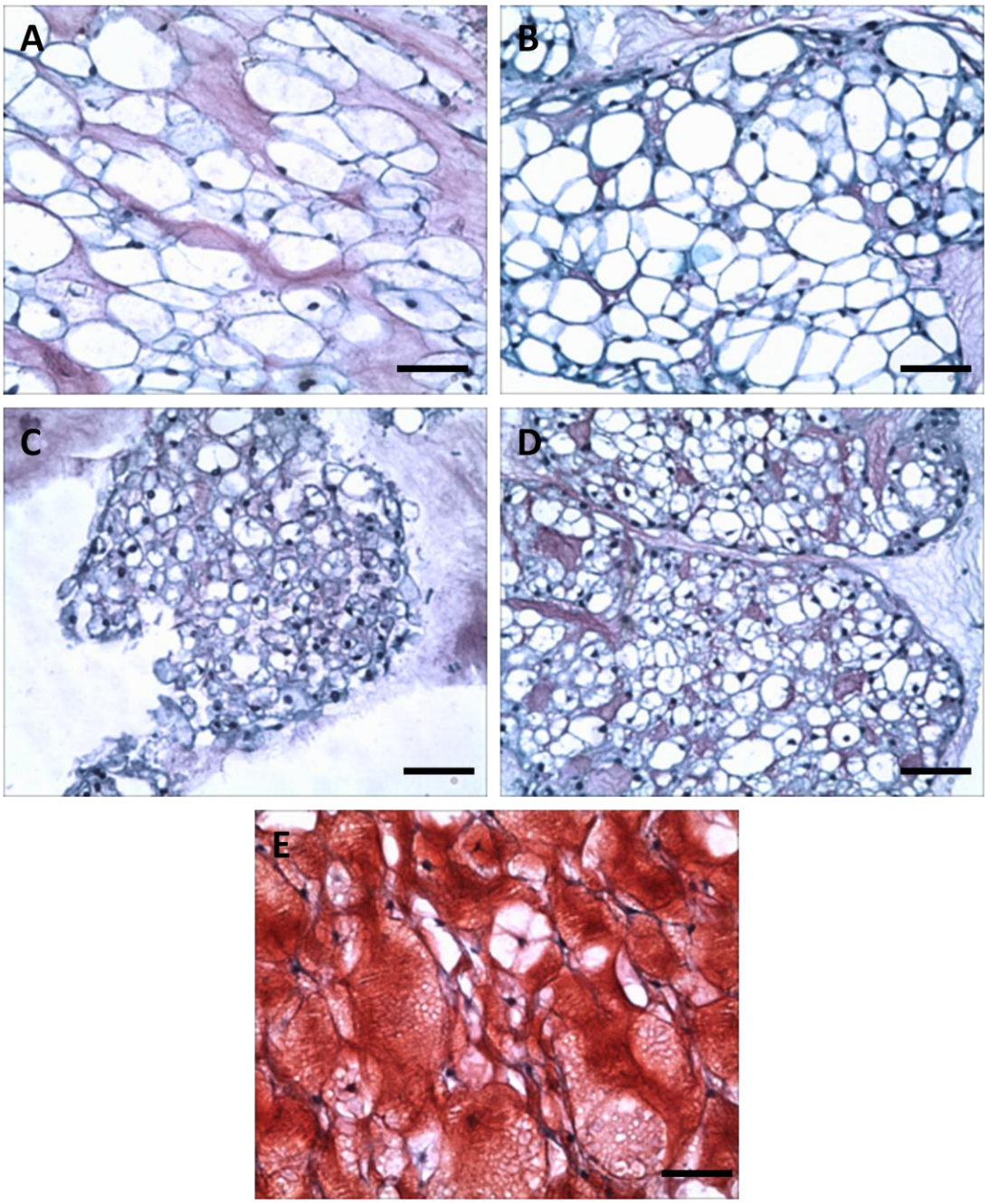

Figure 5.13 Safranin-O and fast green stained sections of cultured porcine NP explants. Sections cultured in normoxia (A), normoxia + IL-1β (B), hypoxia (C), and hypoxia + IL-1β (D) and day 0 control explants (E) were stained with Safranin-O and fast green. Scale bar =50μm.

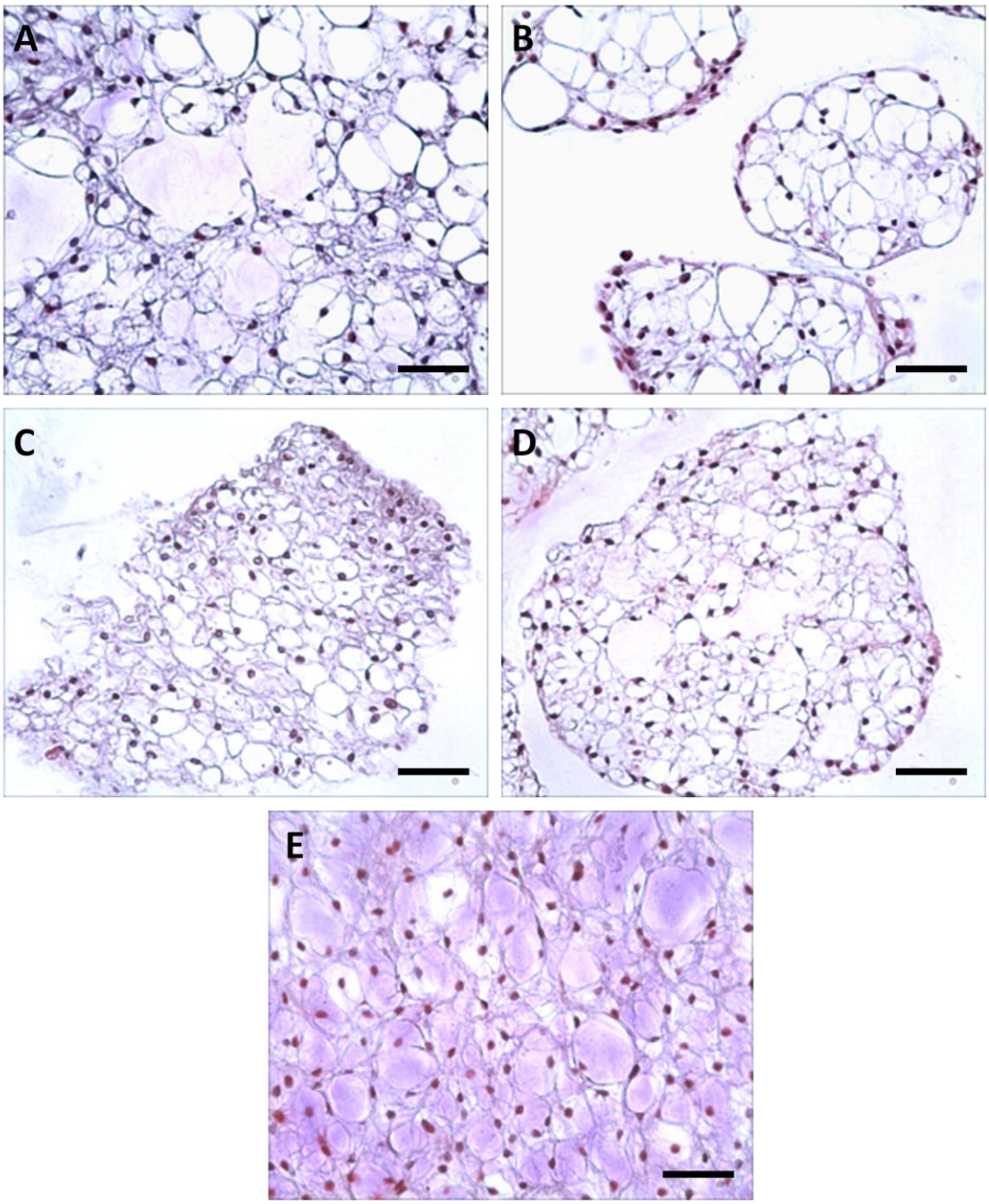

Figure 5.14 Masson trichrome stained sections of cultured porcine NP explants. Sections cultured in normoxia (A), normoxia + IL-1β (B), hypoxia (C), and hypoxia + IL-1β (D) and day 0 control explants (E) were stained with Masson trichrome. Scale bar =50µm.

5.4.4 Testing the Effect of Constraint on Maintenance of NC Cell Phenotype *in vitro*

As 5.4.3 demonstrated that *in vitro* culture alone was detrimental to NC cell phenotype (as observed from decreased expression of several marker genes in normoxic cultures after 14 days), it was hypothesised that a model where the NP remained constrained (akin to constraint by the AF and CEP *in vivo*) would be more appropriate for mimicking the change in cell populations within the NP tissue with maturity. As such, porcine whole motion segments were cultured in normoxia for 7 days and compared to tissue obtained at day 0, to assess the impact of culture on phenotype, viability and morphology.

5.4.4.1 Assessment of Cellular Viability

In situ hybridisation for total message RNA was performed in order to confirm tissue viability within the whole motion segment following the 7 day culture protocol (Figure 5.15). The majority of NC cells within the porcine NP demonstrated staining, although some cells were negatively stained, and these were localised in close proximity to one another.

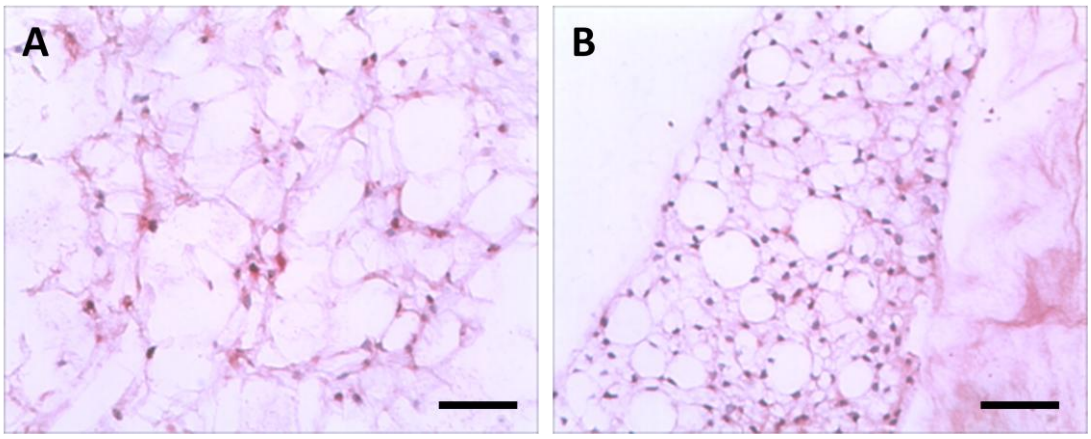

Figure 5.15 *In situ* hybridisation for total message RNA analysis of cultured whole motion segments. Tissue obtained following 7 days *in vitro* normoxic culture (A) and at day 0 (B) were assessed for expression of total message RNA. Scale bars =50μm.

5.4.4.2 Gene Expression Analysis

With regards to the effects of culture on phenotype, comparisons of gene expression levels of ECM markers COL1A1, COL2A1 and ACAN demonstrated no variations between day 0 specimens and samples cultured for 7 days in normoxia (p= 0.4363, p= 0.8633, and p= 0.0503 respectively), as illustrated by Figure 5.16. With regards to novel NP cell marker expression, KRT8 expression was significantly decreased after 7 days *in vitro* culture (p= 0.0464), although expression of KRT18, KRT19 and CAXII did not vary (p= 0.0503, p= 0.0625, and p= 0.4363 respectively). Notochordal cell marker expression was also analysed. FOXJ1 expression was increased following the culture period (p= 0.0142), whilst expression of NOTO, T, FOXA2 and NOGGIN did not differ between controls and cultured samples (p= 0.7304, p= 0.0939, p= 0.969, and p= 0.7062 respectively). Thus, with the exception of KRT8 and FOXJ1, NC cell phenotype was maintained following 7 days *in vitro* culture in normoxia.

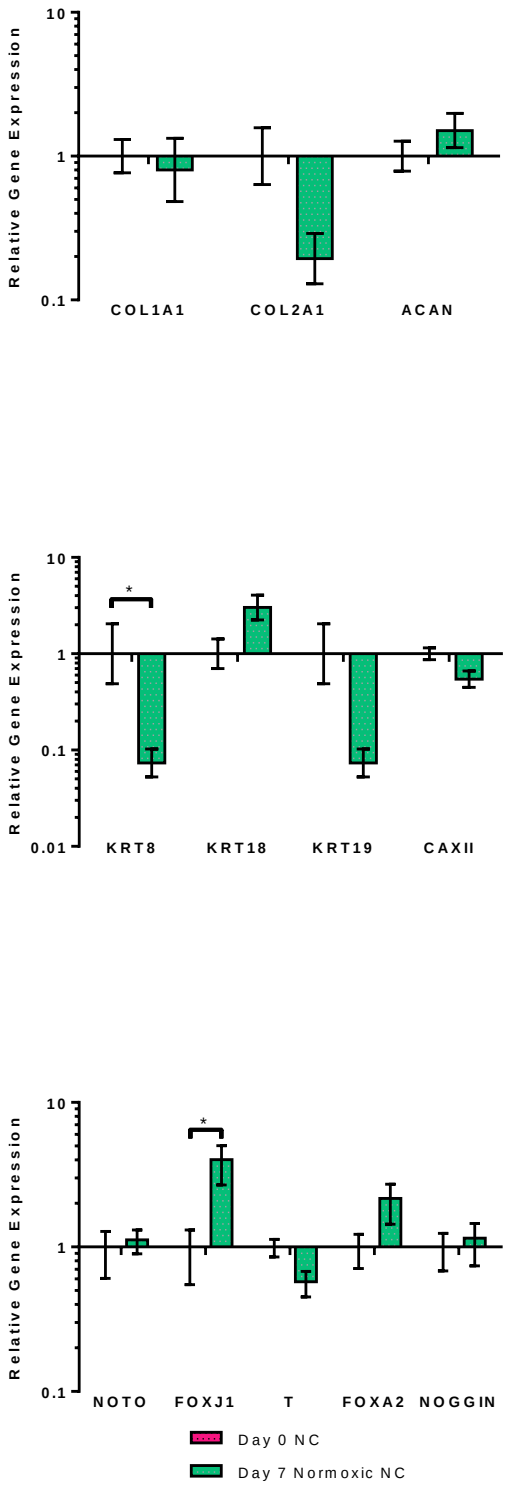

Figure 5.16 The effect of normoxic culture on NC cell phenotype in a constrained model. qPCR analysis of ECM markers (COL1A1, COL2A1 and ACAN), novel NP cell markers (KRT8, KRT18, KRT19 and CAXII) and notochordal cell markers (NOTO, FOXJ1, T, FOXA2 and NOGGIN) for NC cells cultured in whole motion segments for 7 days (green bars). Gene expression was normalised to reference gene GAPDH and back to day 0 controls (ΔΔCt method). *p= <0.05.

5.4.4.3 Histological Analysis

Tissue morphology was assessed by haematoxylin and eosin staining (Figure 5.17). Normoxic culture in a constrained model retained collagen content of the ECM (as highlighted by retention of pink stain in Figure 5.17A), but some loss of the organisation of the cellular network was noted as compared to control tissue (Figure 5.17B).

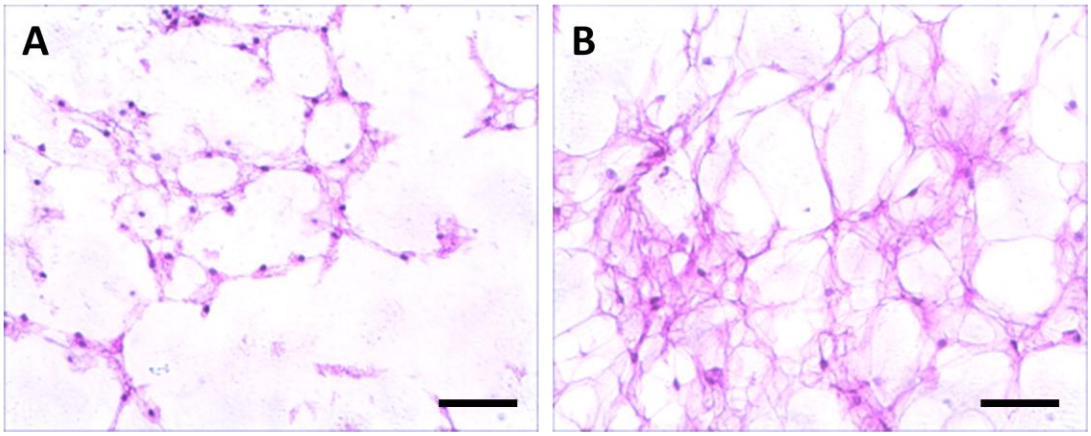

Figure 5.17 Haematoxylin and eosin staining of cultured whole motion segments. Tissue morphology was assessed for specimens obtained following 7 days *in vitro* normoxic culture (A) and at day 0 (B). Scale bars =50µm.

Safranin-O and fast green stains were performed to assess the PG content of NC cell-rich NP tissues following *in vitro* culture (Figure 5.18). PG content was maintained following culture (Figure 5.18A) in a constrained model in comparison with day 0 control (Figure 5.18B). Finally, Masson trichrome staining was performed to assess for maintenance of collagen content within the constrained model following culture (Figure 5.19). Although cellular organisation altered slightly, collagen was demonstrated to be dispersed throughout the ECM following 7 day culture (Figure 5.19A), as well as day 0 (Figure 5.19B).

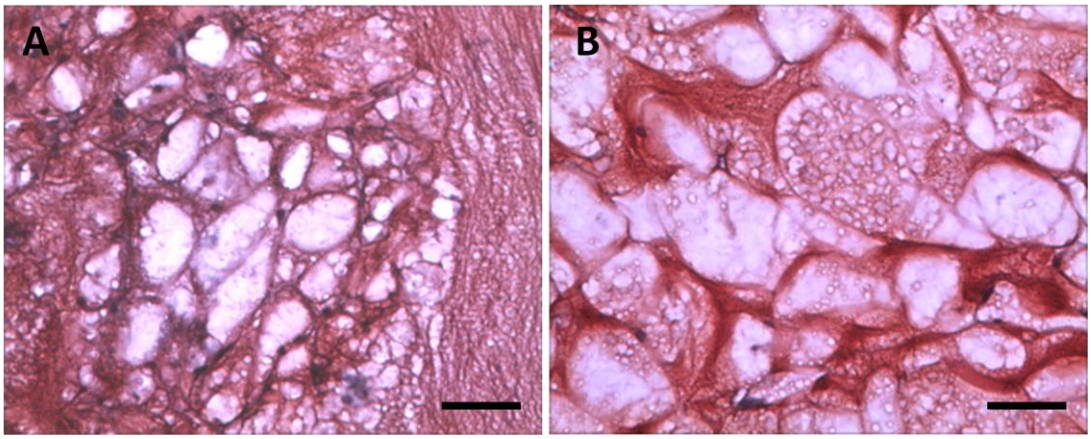

Figure 5.18 Safranin-O and fast green staining of cultured whole motion segments. PG content was assessed for specimens obtained at day 0 (A) and following 7 days *in vitro* normoxic culture (B). Scale bars =50µm.

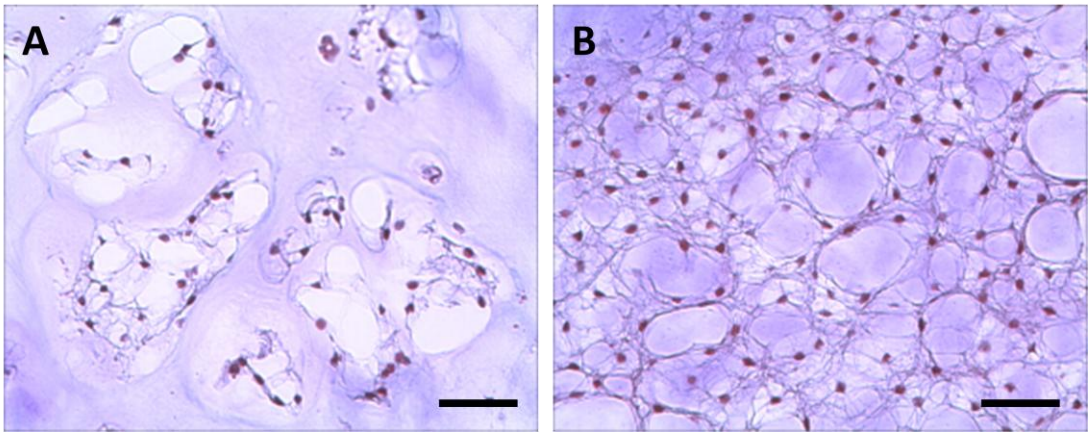

Figure 5.19 Masson trichrome staining of cultured whole motion segments. Collagen content was assessed for specimens obtained at day 0 (A) and following 7 days *in vitro* normoxic culture (B). Scale bare =50µm.

5.4.5 Effect of Hypoxia on Porcine NC Cells in a Constrained Model

As it had been confirmed that the constrained disc model would be appropriate for assessment of NC cell changes in response to microenvironmental factors, the effect of hypoxic culture on porcine NC cell-rich NP tissue was evaluated. Unfortunately, RNA was extracted from these specimens, but samples were of too poor quality to complete analysis by qPCR. Thus, the effect of hypoxic culture was studied in terms of histological variations.

Figure 5.20 illustrates the morphology of specimens cultured for 7 days in normoxia and hypoxia as compared to control samples. Normoxic cultures (Figure 5.20A) appeared to retain the organisation of the NC cell network to a better extent than sections cultured in hypoxia (Figure 5.20B) when compared to specimens at day 0 (Figure 5.20C).

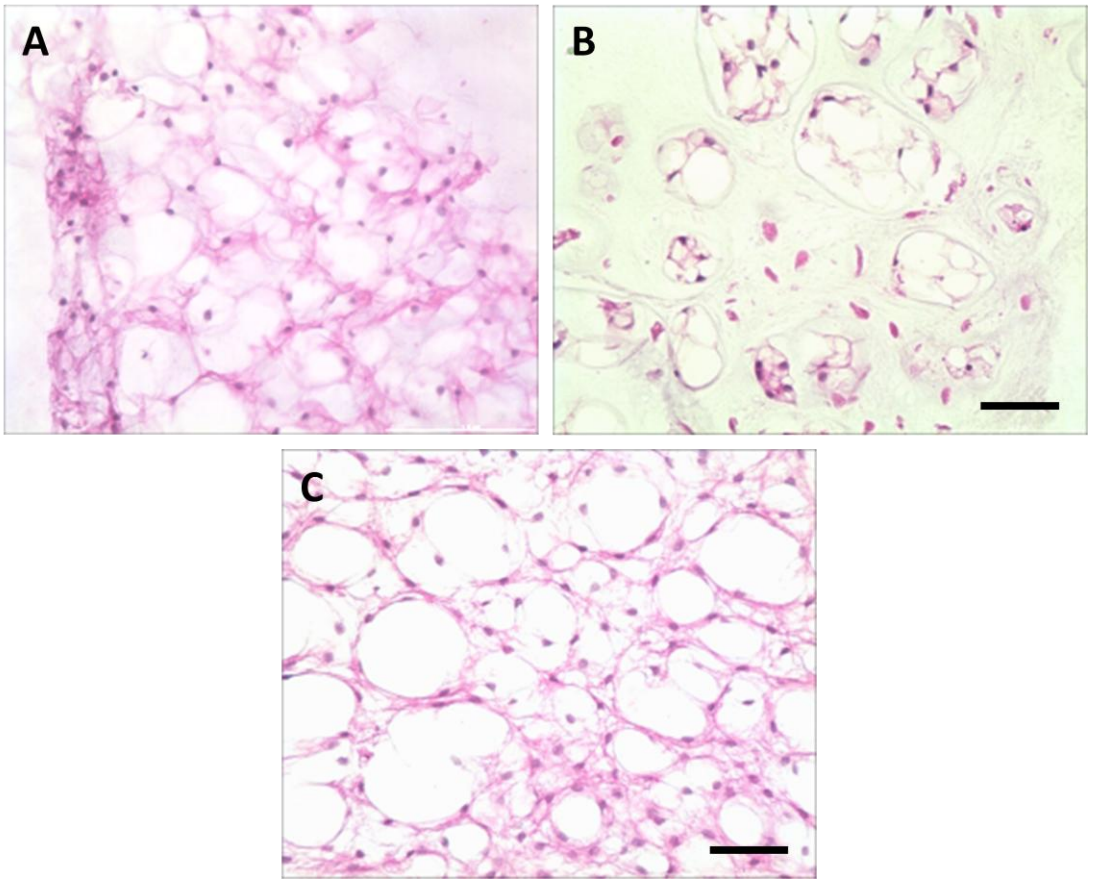

Figure 5.20 Haematoxylin and eosin stained sections of cultured whole motion segments in normoxia and hypoxia. Specimens cultured for 7 days in normoxia (B), hypoxia (C) and day 0 controls (C) were stained with H&E. Scale bars =50µm.

When PG content of the cultured discs was assessed by Safranin-O and fast green staining, distinct differences were noted between staining of hypoxic cultures (Figure 5.21B) and those taken at day 0 (Figure 5.21C) and after 7 days in normoxic culture (Figure 5.21A). These images also highlighted the differences in tissue organisation in the hypoxic specimens noted by the H&E staining. Finally, the collagen content of specimens was assessed by Masson trichrome stain (Figure 5.22). Collagen stain (blue) was noted as dispersed throughout the NP tissue of specimens taken at day 0 (Figure 5.22C), and to a much lesser extent in samples cultured in normoxia (Figure 5.22A). However, specimens cultured in hypoxia (Figure 5.22B) demonstrated little staining, as well as a much less organised cellular network as noted for the H&E and Safranin-O stained sections.

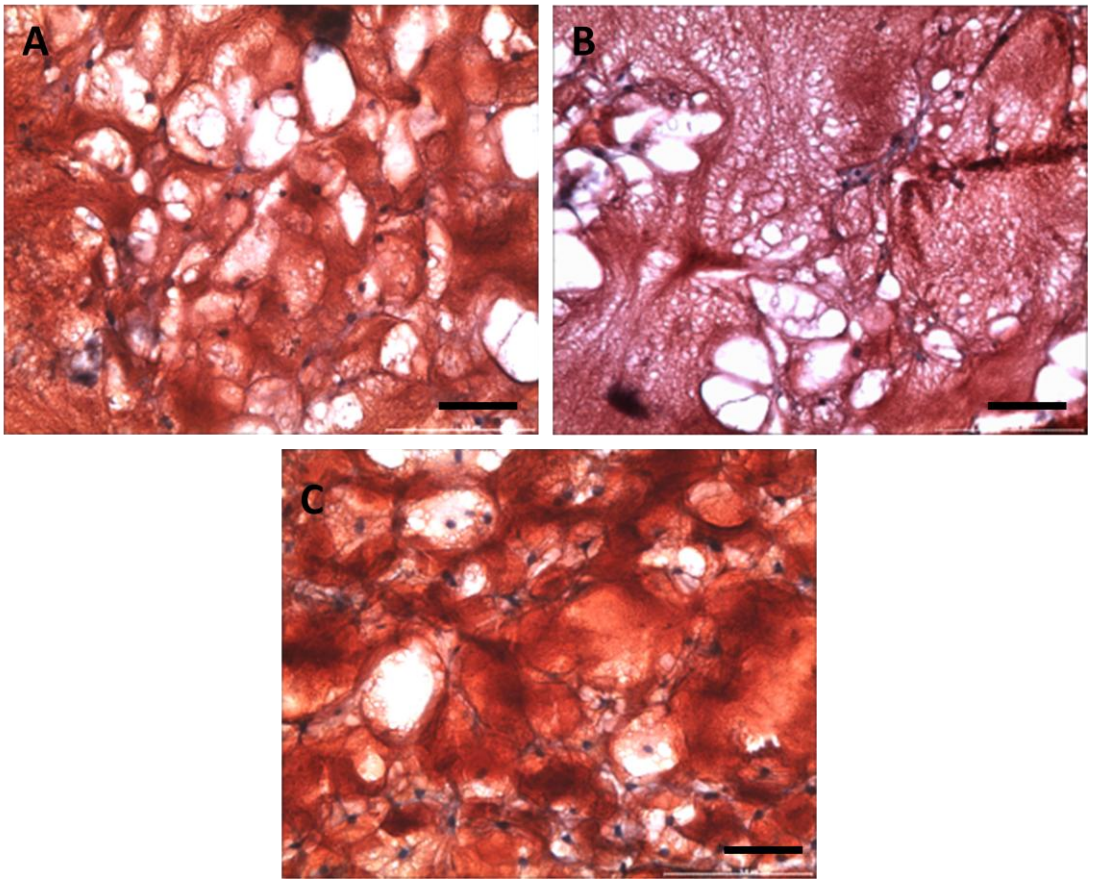

Figure 5.21 Safranin-O and fast green stained sections of cultured whole motion segments in normoxia and hypoxia. Specimens cultured for 7 days in normoxia (B), hypoxia (C) and day 0 controls (C) were stained with Safranin-O and fast green. Scale bars =50µm.

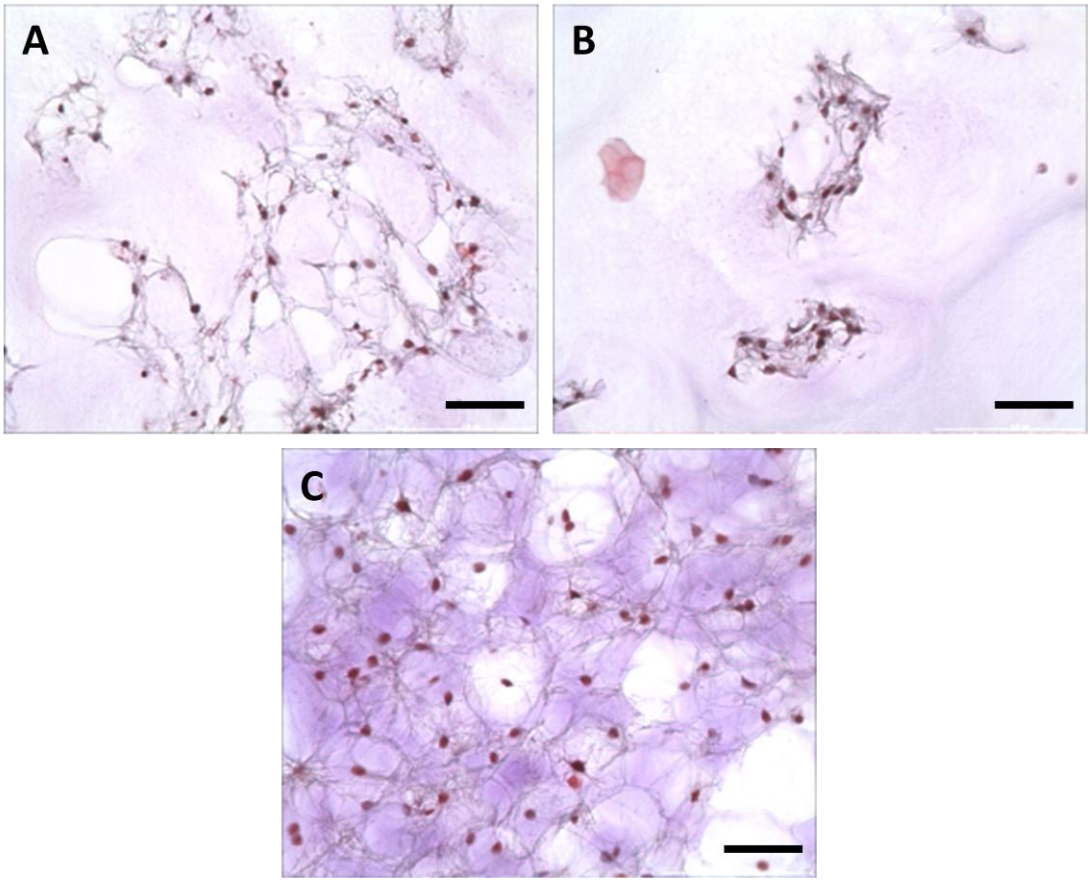

Figure 5.22 Masson trichrome stained sections of cultured whole motion segments in normoxia and hypoxia. Specimens cultured for 7 days in normoxia (B), hypoxia (C) and day 0 controls (C) were stained with Masson trichrome. Scale bars =50µm.

5.5 Discussion

Scientists have hypothesised that during human development and growth, cells of the embryonic notochord give rise to NP cells, and rather than being lost from the tissue, differentiate into cells resembling those that populate the adult human NP both in terms of phenotype and morphology. However, if this is the case, the mechanisms underlying this cellular transformation remain undefined, and thus require investigation. Crucially, a suitable cell culture model for studying such processes first requires development and testing, and was the aim of the current investigation. Additionally, once a suitable model has been identified, the effect of microenvironmental factors on NC cell phenotype could be elucidated. Here, it has been demonstrated that a previously described size-based filtration methodology for the isolation of NC cells from a mixed population did not result in pure isolates, but that an *ex vivo* culture model of porcine whole motion segments shows promise as a novel model in which to test NC cell phenotypic alterations in response to microenvironment.

Initially, a bovine model was employed for analysis as it had previously been demonstrated that remnants of bovine NC cells can be separated from resident NP cell populations using size-based filtration methods (Cappello *et al.*, 2006, Minogue *et al.*, 2010b). Previous investigations however, failed to investigate the purity of isolated cellular populations histologically, and therefore, the histological analysis presented here is the first to demonstrate that size-based filtration methodologies may not be appropriate for investigations as the resultant mixed cell population may skew any phenotypic findings. Silicon membranes such as those utilised in the current investigation have been investigated for efficiency of separation and compared to other sized-based filtration systems (Ji *et al.*, 2008). Clogging of filter pores and deformation of cells have been described as limitations of such techniques. In the current investigation, specimens were passed through a cell sieve prior to membrane filtration to reduce the amount of tissue debris that could potentially clog the membrane, but removal of all matrix debris would not be achieved in this manner, as the cell sieve pore size was 40µm, and any fragments of tissue smaller than this would therefore pass through, as indicated by the presence of tissue debris in the cytospins generated from cells retained on the 15µm membrane. In addition to this, large volumes of tissue debris <40µm potentially clogged the filter, preventing

the proper passing of cells through the filter even if they were <15μm. A vacuum was applied to the apparatus in short intervals to draw the liquid through the filter; however, application of such a force to has the potential to deform the membrane by stretching the fibres, and allowing cells to pass through that may otherwise have been retained. Therefore, separation of NC from NP cells by size-based filtration cannot ensure that homogenous cell populations are obtained, and thus, other methodologies should be investigated. Given that the techniques employed here are exactly the same as that undertaken by Minogue *et al.*, it is unsurprising that overlapping gene expression profiles between supposed NP and NC cell populations were noted here also. One of the limitations of this model is the relatively low number of NC cells present within the tissues (Demers *et al.*, 2004). Bovine specimens are often preferential for use when an animal model closely resembling the adult human IVD is required; however, use of a more NC cell-rich tissue such as rabbit, porcine or rodent NP would yield a more adequate number of cells for investigation.

The porcine NP has been utilised in numerous investigations previously as it is a tissue that is rich in NC cells, which are relatively easy to isolate (Cho *et al.*, 2013, Guehring *et al.*, 2009, Korecki *et al.*, 2010, Mercuri *et al.*, 2013, Purmessur *et al.*, 2012). However, detailed investigation as to the phenotype of porcine NC cells (with regards to NP and NC cell markers) has not been described previously, and thus, this is the first investigation to demonstrate such comprehensive analysis. With regards to the novel NP cell markers, cytokeratin-8 protein expression has previously been utilised for identification of porcine NC cells, but to date, identification of KRT8 gene expression in this species remains undefined, although given the previously demonstrated expression of this protein, the finding of KRT8 gene expression is unsurprising (Omlor *et al.*, 2009). Similarly, KRT18 and NOGGIN expression has been noted in porcine NP cells when tested under hydrostatic loading, but only these two genes were investigated, and therefore is not descriptive of the NC cell phenotype (Purmessur *et al.*, 2012). KRT19 and CAXII expression in porcine NC cells has not been described in any of the previous literature, and thus, the data presented here regarding that is entirely novel. Surprisingly, although the porcine NC is comprised predominantly of NC cells as compared to smaller NP cells, previous literature regarding the expression of NC cell markers by these cells is limited, and

with the exception of the previously mentioned NOGGIN analysis, the NC cell genes analysed here have not been described before. This gene expression analysis therefore confirmed that the porcine NP (which is rich in NC cells) would be suitable for assessment of loss of NC/gain of NP cell phenotypic expression.

An NP-explant model was first chosen for *in vitro* analysis of response to microenvironmental factors because previous literature had demonstrated that NP tissue explants are responsive to different culture environments, whilst maintaining tissue integrity (Purmessur *et al.*, 2012). However, significant decreases were noted in the expression levels of most of the genes analysed in normoxic-cultured samples when compared back to specimens obtained at day 0, suggesting that the standard culture environment is detrimental to the maintenance of NC cell phenotype in this setting. Given that the NP tissue was unconstrained in this set-up, the decreased gene expression levels may be attributed to a loss of constraint akin to that provided by the AF and CEP *in vivo*. An investigation utilising adult human specimens demonstrated that a loss of constraint results in atypical swelling of tissues and loss of PG (Le Maitre *et al.*, 2004b). Additionally, murine analyses of the importance of a notochordal sheath during development showed a scattering of NC cells and loss of integrity in this tissue, under removal of Hedgehog signalling required for formation and maintenance of the NC sheath - a structure that protects and constrains NC tissue during development of the spine (Choi and Harfe, 2011). Therefore, it is possible that removal of the surrounding AF and CEP alters the mechanics of the NP tissue which results in a loss of normal tissue structure and phenotype. When normoxic and hypoxic cultures were compared, a loss of FOXJ1, T and NOGGIN expression was noted in a low-oxygen microenvironment. As the NC cell phenotype is currently undefined in terms of the porcine IVD model, the reasons for variation under hypoxia can only be obtained from studies in other animal models. Hypoxia has been demonstrated to reduce expression of CD24 in a rat model, but the expression levels of no other NC cell genes were investigated (Rastogi *et al.*, 2009). Interestingly, the same study identified that non-enzymatically digested tissues (similar to those used in the current investigation) were influenced detrimentally by oxygen state, and the loss of NC cell marker expression noted here may therefore be a response by the explant tissue to the culture environment. It should also be noted however, that non-enzymatically digested rat NP tissue was disrupted mechanically

prior to combining with alginate to form a gel, and this mechanical disruption may explain the altered response to hypoxia. However, isolation of NC cells by enzymatic digestion was not undertaken in the current investigation as previous literature had shown that this methodology for isolation of NC cells negatively affects cell survival (Hunter *et al.*, 2004).

The loss of virtually all PG content in the unconstrained culture model differs from data published previously utilising an unconstrained *in vitro* culture model (Purmessur *et al.*, 2012), although the previous investigation cultured specimens in plastic culture bags rather than in cell culture inserts as employed here. Safranin-O stains all PGs within a tissue, and therefore will not only stain ACAN (as analysed by qPCR), but also versican, decorin and biglycan – all known to be expressed within the intervertebral disc (Gotz *et al.*, 1997a), and thus through analysis of such staining, one is unable to distinguish between the various proteoglycans within the tissue. However, NC cell-rich discs contain high levels of aggrecan and literature has been presented which suggests that NC cells express smaller PGs at very low levels or not at all (Chen *et al.*, 2006), which indicates that the PG loss noted in the current study is due to loss of aggrecan rather than any other PG.

The data presented here also suggests that culture in the presence of IL-1 generally does not influence expression of NP and NC cell markers by NC cells. NC cells have previously been shown to possess anti-inflammatory properties in a co-culture model with AF cells and macrophages where the presence of NC cells reduced the expression of IL-6, IL-8 and iNOS by AF cells (Kim *et al.*, 2012). However, the effect of the pro-inflammatory mediators secreted by the AF cells on the NC cell phenotype was not assessed, and thus it is unknown whether these molecules induced a shift in the phenotype of NC cells. Interestingly, a previous investigation has suggested that NC cells in fact secrete pro-inflammatory cytokines during standard culture, and the authors conclude that these cells may in fact be able to initiate inflammatory processes *in vivo* (Rand *et al.*, 1997). However, secretion was only noted after induction with lipopolysaccharide (LPS), which is known to induce expression of cytokines including IL-1 (Kim *et al.*, 2013), and thus the initiation of inflammatory cascades noted by Rand *et al.*, may be due to LPS-challenge rather than being a natural process within NC cells. The increase in CAXII expression under hypoxic culture upon supplementation with IL-1β mirrors findings presented

for CAIX in hepatocellular carcinoma cells (Kockar *et al.*, 2012). Like CAXII, CAIX is a membrane-associated carbonic anhydrase, also known to be expressed in the developing IVD (Liao *et al.*, 2009), and therefore this finding presented here that matches that of a previous study is unsurprising.

Thus, the data presented for the unconstrained porcine NP model suggested that the lack of constraint in this model was detrimental to maintenance of phenotype, but that differences existed between normoxic and hypoxic cultures also, prompting investigation using a constrained disc model. The NC cell phenotype was therefore assessed using a model where whole motion segments (including both bony and cartilaginous endplates) were utilised. The data has shown that with the exception of KRT8 and FOXJ1, expression of all ECM, NP and NC cell markers was maintained during normoxic culture. The vascular blood supply of the immature human NP (NC cell-rich) decreases in the growing disc, and NC cell disappearance is thought to coincide with this (Taylor and Twomey, 1986). Thus, given the ample blood supply to the immature NP tissue, it is considered normoxic, and the maintenance of phenotype noted in normoxia here is therefore to be expected. When the model was tested under hypoxic conditions, some disorganisation of the cellular network was noted. Previous literature has not elucidated the effect of hypoxic culture on the organisation of NC cell networks, and the data presented here is therefore novel and crucial, intimating that the shift in oxygen state with growth of the IVD from normoxic to hypoxic, may be a key factor in driving the change in cell type resident within the NP tissue. While preliminary, the changes noted in this model system under hypoxic conditions need to be studied further, looking particularly at alterations to gene expression.

5.5.1 Implications of this Investigation

This investigation has demonstrated that separation of NC and NP cell populations by size-filtration is not adequate to ensure isolation of pure populations, and that a more NC cell-rich tissue (such as porcine) would be more appropriate for studying alterations in NC cell phenotype. An *ex vivo* model has been developed, the results of which, albeit preliminary, have indicated that constraint of NP tissue is essential for maintenance of phenotype during *in vitro* culture, and that hypoxia may alter NC

cell network and tissue organisation, as well as the expression of a number of NP and NC cell markers. Studying the effects of other microenvironmental factors on phenotypic maintenance of NC cells may allow for elucidation of the *in vivo* processes that underlie the loss of morphologically distinct NC cells from the NP with ageing of the human IVD.

Chapter 6:

Conclusions and Future Work

6.1 General Discussion and Conclusions

Over recent years a number of studies have sought to identify novel markers of the NP cell phenotype (Lee *et al.*, 2007, Minogue *et al.*, 2010a, Minogue *et al.*, 2010b, Power *et al.*, 2012, Sakai *et al.*, 2009), and although important for the field of IVD research, these studies have failed to assess gene and protein expression of the markers across a range of ages and levels of tissue degeneration. Thus, the current investigation was undertaken with a view to fully elucidating the phenotype of adult human NP cells utilising a panel of recently described novel NP and NC cell markers. The most pertinent finding of this study was that the adult human NP is comprised of a heterogeneous cell population as illustrated by the highly variable NP and NC cell marker protein expression levels noted by both immunohistochemistry and multi-parametric flow cytometry analysis. The role of these different cell sub-populations was not investigated but it is likely that these cell populations may have differing functions in the disc, whilst their differential phenotype may also represent distinctions in cellular ontogeny, although this requires further investigation. Additionally, it has been shown here that the phenotype of NP cells from different spinal regions is comparable, and thus this vastly increases the number of human specimens available for research. In order to assess whether microenvironmental factors influence the alteration in NC cell phenotype that is postulated to occur with ageing/degeneration (thus explaining the differing expression profiles shown here), an *ex vivo* model system utilising NC cell-rich porcine IVDs has been developed. The preliminary data presented here suggests that an IVD-like microenvironment may influence NC cellular networks and ECM composition. Thus, this evidence has shown that the characterisation of NP cells based on markers determined by microarray analysis of pooled NP cells may not be reflective of the protein expression profile of cell sub-populations, and raises the question as to the roles of these cell populations *in vivo* and their developmental origins.

Key to fully delineating the phenotype of adult human NP cells was the assessment of NP cell marker expression in cells from different IVD regions. Much research regarding the pathology and biology of NP cells has utilised lumbar disc specimens, and as such, it is assumed that the cervical NP cell phenotype mirrors that of the lumbar with regards to chondrogenic and catabolic gene expression. The first aim of this investigation was to identify whether degenerate lumbar and cervical NP cell

specimens are comparable phenotypically in order that surgically-obtained tissue specimens from these disc levels could be used interchangeably in a research setting, and the data presented here confirms that this is the case. In addition to this, the current investigation has identified that histological features of degeneration used previously to grade lumbar specimens for the severity of tissue degeneration, applies also to cervical disc specimens, and that the degenerative scores calculated for these specimens are comparable. Taken together, these findings confirm that NP cells of lumbar and cervical disc specimens are phenotypically comparable across a range of degenerative scores expressing a similar gene expression profile, and thus, specimens can be used interchangeably for *in vitro* research purposes, thereby increasing the number of samples available for study significantly. Moreover, the noted expression of markers previously used to characterise degeneration in the lumbar IVD is suggestive of similarities existing in the molecular pathological processes underlying disc degeneration in tissues from the cervical and lumbar region. Following this, it was then possible to include both cervical and lumbar disc specimens for analysis of the NP cell phenotypic profile. It is imperative that future research involving human IVD specimens utilises not only lumbar specimens but also those taken from the cervical region. This then will enable the development of novel therapeutic techniques for chronic neck pain in addition to LBP.

Elucidation of the cervical and lumbar NP cell phenotype utilising a panel of NP and NC cell marker genes and proteins formed the second aim of this investigation, and this study has demonstrated that the NP marker expression remains largely unaltered by age or degeneration, and is comparable between cells obtained from cervical and lumbar tissues. Interestingly, the findings intimate that NC cell marker genes associated with earlier stages of development were expressed in fewer specimens overall than those associated with latter stages, which may be indicative of NC cells undergoing a transformation or differentiation with ageing in the human disc, rather than being lost from the tissue entirely via apoptosis.

Further investigation through localisation of protein expression indicated that recently identified novel NP and NC cell markers were not expressed by all cells of the adult human NP, and rather, that the adult human NP is comprised of a heterogeneous cell population with regards to phenotype, and such cells may have differing functions. It is unclear as to the role of an NC cell marker expressing cell

sub-population within the adult human NP, although it has been demonstrated previously that factors secreted by NC cells promote GAG production in degenerate human IVD cells (Abbott *et al.*, 2012) and the differentiation of MSCs to NP-like cells, as noted by the increased expression of GAG, SOX9 and type II collagen by cells cultured with NC-conditioned media (Purmessur *et al.*, 2011), suggesting that NC cells may confer a reparative function. Additionally, $Tie2^{+}/GD2^{+}$ cells isolated from murine and human NP tissues are postulated to act as a progenitor cell population that is exhausted with both age and degeneration (Sakai *et al.*, 2012). Furthermore, the progenitor cell population identified in said investigation supports the conclusions of the present study of the adult human NP being comprised of a heterogeneous cell population, and provides evidence that a differential phenotype may represent distinctions in cellular function. Isolation of adult human NP cell sub-populations by techniques such as fluorescence-activated cell sorting (FACS) may enable the study of separate cell populations. Given that previous literature (Purmessur *et al.*, 2011) has indicated that NC-conditioned media contains factors that promote MSC differentiation, ELISA analysis of anabolic, catabolic and cytokine factors in the various NP cell sub-populations may elucidate distinctions in sub-population function.

The finding of non-ubiquitous expression of NP and NC cell markers adult human NP cells also has implications for the understanding of NP cell ontogeny. On the one hand, low levels of NC cell marker expression in the AF may intimate that NP and AF tissues are distinct in terms of ontogeny. However, the data presented here may also be indicative of different developmental origins for cells of the adult human NP. Those with high levels of NC cell marker expression are likely derived from the embryonic notochord, whilst those devoid of all NC cell marker expression could arise as a result of AF/CEP infiltration into the NP, whereby they adopt a NP cell-like morphology. This would then serve to explain the high levels of Pax-1 expression (a mesenchymal marker) noted at both the gene and protein level in cells throughout the NP. Thus, given the high levels of Pax-1 expression demonstrated, it is concluded here that cells of the adult human NP are distinct with regards to ontogeny, although this requires further validation. Crucial to determining if multiple sources do give rise to cells of the adult human NP would be the analysis of AF cell marker expression in these cells. If a sub-population of NP cells were demonstrated

to express AF markers, this would certainly support the theory that the infiltrating AF may populate the NP, and that NC cells are largely lost from the tissue with maturity. However, to date, previous NP cell microarray investigations have focussed on the identification of novel NP-specific or IVD cell markers and thus specific markers of AF cells should be determined.

This study has also highlighted that a greater proportion of NP cells localised in clusters are immunopositive for novel NP and NC cell marker proteins as compared to single NP cells. Thus, in degenerate tissue specimens, NP and NC cell marker expression appears to be retained in NP cells localised in clusters, which may indicate that these resemble a more healthy NP cell phenotype that may function to repair the NP tissue during degeneration. NP cells localised in clusters are noted to increase with progressing degeneration, and are linked to cellular proliferation (Johnson *et al.*, 2001, Pritzker, 1977, Sive *et al.*, 2002). If further analysis of the functionality of NP cells localised in clusters indicates that these function more like healthy NP cells, it could be postulated that their increasing frequency with tissue degeneration is an endogenous attempt at restoration of tissue integrity. This may then have implications for the field of IVD regeneration, where the issue of an optimal cell phenotype for recapitulation remains unanswered.

The final aim of the present study was to develop a model system that would allow for the exposure of NC cells to a range of microenvironmental factors in order that the effects of this on NC cell phenotype could be investigated. Initial investigation using a previously described bovine model demonstrated that size-based separation of pure populations of NP and NC cells could not be obtained using membrane filtration methodologies. The isolation of mixed cell suspensions not only indicated that tissue debris may have affected the proper filtration of cells, but also that a more NC cell-rich tissue (such as porcine NP) would be a more appropriate choice. The current investigation has shown that culture of porcine NP explants in a non-constrained model results in a detrimental loss of phenotypic expression in the absence of microenvironmental factors, and thus, that constraint of porcine NP tissue *in vitro* is fundamental to maintenance of cell phenotype during culture. Preliminary testing of this model system has suggested that microenvironmental factors may influence the alterations to the NP that take it from an NC cell-rich to an NP cell-rich tissue during ageing of the human spine. Although *in vivo* models would mimic

human IVD biology and function more completely, no animal model is able to accurately replicate the loading regime applied to the normal human spine, and thus, an *ex vivo* model such as that utilised here is most appropriate. Following this, explants can be tested using a loading rig, and the effects of load on NC cell phenotype investigated.

In conclusion, the current study has described in-depth the phenotype of adult human NP cells. It has been demonstrated that phenotypic similarities exist between cells of the adult human lumbar and cervical NP but that crucially, the adult human NP is comprised of a heterogeneous cell population that expresses differential levels of both NP and NC cell markers. Expression of NP and NC cell markers at both the gene and protein level demonstrates some variation with ageing and degeneration, but expression is largely constitutive in degenerate specimens. Elucidation of the functions of these cell sub-populations *in vivo* and of factors that influence the loss of distinct NC cells in adult human specimens is essential to understanding these subsets of cells, and may provide evidence that the distinctions in cell phenotype noted here arise as a consequence of cells differing with regards to ontogeny. A novel porcine *ex vivo* model system will allow for assessment of NC cell phenotypic response to microenvironmental factors, as the preliminary data presented here indicates that hypoxia may be important.

6.2 Future Work

Although this investigation has provided a detailed description of the adult human NP cell phenotype at the gene and protein level, a number of questions have been raised by this research which still require analysis. Firstly, any future research conducted with human IVD specimens should now look to include testing both lumbar and cervical samples. The data presented here is indicative of a similar phenotypic profile between NP cells derived from the two spinal regions, but a comparison of degenerative and anabolic processes and the capacity for regeneration requires elucidation. It is well documented that NP cells themselves are responsible for the generation of factors (such as inflammatory cytokines and degradative enzymes) that induce tissue degeneration. Here, it has been demonstrated that gene expression levels of most of these molecules is comparable between lumbar and cervical NP cells; however, whether these cells respond in the same way to degeneration-inducing stimuli is yet to be determined. *In vitro* culture of such cells where they are exposed to a varied cytokine milieu akin to that of the degenerate IVD may allow for this comparison. Moreover, specimens used for study were solely obtained from surgery, and are therefore all taken from patients symptomatic of LBP or neck pain. In order that it can be determined whether the phenotypic profile of NP and AF cells (at both the gene and protein level) alters with age or degeneration analysis such as this should be performed using samples from asymptomatic individuals, the presumed source of which will be cadaveric tissue. Additionally, although a large range of ages were investigated, inclusion of infant, paediatric and adolescent tissue will allow for a more full characterisation of the NP cell phenotype with regards to age.

Use of immunohistochemical staining techniques is limited by the fact that only single proteins were stained for at one time. The number of antibodies available for use, meant that multiple proteins could not be assessed simultaneously, thus requiring verification using flow cytometry. However, expression of only 4 proteins could be quantified due to the combinations of directly-conjugated antibodies available for study. Ideally, a panel containing antibodies for all of the marker proteins of interest here would have been investigated. Where possible, cell surface marker proteins would be utilised, as assessment of these would allow for further study using the cells as they will not have been fixed (as is performed for

intracellular protein staining). In terms of practical limitations, immunohistochemistry requires optimisation of multiple parameters before it can be deduced that detected staining is specific and not related to improper processing or non-specific signal. An alternative to the use of immunohistochemistry would be to perform Western blot analysis of protein lysate directly extracted from NP specimens. Quantification of protein expression levels would be noted and the technique may also be able to indicate if different isoforms are present, information which again cannot be obtained from immunohistochemistry. If the various cell populations were pre-sorted by FACS analysis, Western blot would allow for quantification of protein levels within specific cell sub-populations. However, such techniques would provide a global view of marker expression and not be cell-specific, thus limiting the potential of such assays.

The identification of NP cell sub-populations and differential levels of NC cell marker expression within NP specimens intimates one of two possible explanations. Firstly, that NC cells are not lost from the tissue with ageing, but are rather differentiated into cells that resemble chondrocyte-like NP cells in terms of morphology, but are distinct with regards to phenotype, or secondly, that cells within the adult human IVD differ with regards to ontogeny, which is reflected in the differential gene and protein expression profiles. Isolation of these cell sub-populations by FACS would allow for separate study of their degenerative and regenerative potentials, and may elucidate the functions of the various cell sub-populations. Moreover, in order to address the hypothesis presented here that the adult human NP contains cells derived from different tissues, it is essential that NP cell differentiation is monitored across all stages of development and maturity of the tissue, with animal models being the most obvious choice for study. However, most common laboratory animal models are limited by the fact that the NP cellular composition is largely notochordal (even in adult animals) and is therefore not representative of the human NP cell population. Thus, either a species where IVDs contain both NC cell and small chondrocyte-like cells (such as bovine and chondrodystrophic canine breeds) should be utilised, or human notochordal cells could also be used. However, little is currently known about the adult NC cell phenotype and the cells themselves are difficult to culture *in vitro*, which may limit their potential for this. Culture of NC cells in a 3D environment may enable their

study *in vitro*, and allow for them to be exposed to microenvironmental conditions mirroring that of the adult human IVD (such as high load, hypoxia and low pH) in order to ascertain whether this induces cell differentiation.

If further *in vitro* work can determine whether certain NP cell sub-populations have a greater potential for maintaining IVD health, it is essential that this is confirmed *in vivo*. *In vivo* investigations are scarcely undertaken in the field of IVD research, with investigators often preferring to assess outcome using *ex vivo* model systems. However, if it is shown that a certain phenotypic profile denotes preferential regenerative capabilities of NP cells, isolation of these cells (by FACS) and injection of them into a degenerate disc model (presumably chondrodystrophic canine breeds) and assessment of their potential *in vivo* would lead the way in a methodology frequently ignored in this field. Similarly, as it can be presumed that the numbers of cells isolated from particular NP cell sub-populations for further investigation would be low (as the NP is a hypocellular tissue), it should be investigated whether cells can be forced to express desired marker proteins by means of virus-mediated cellular transduction. Thus as long as transduced cells were found to function in a manner akin to phenotypically-identical native cells, a method for generating greater quantities of distinct NP cell populations would have been developed for use both *in vitro* and *in vivo*.

Additionally, the mechanisms that underlie the loss of NC cells with ageing in the human NP require definition. Evidence exists which suggest that NC cells are influenced by microenvironmental factors including pH, load, nutrient supply and oxygen state (Grunhagen *et al.*, 2006, Guehring *et al.*, 2010, Guehring *et al.*, 2009, Park and Park, 2013a, Park and Park, 2013b, Purmessur *et al.*, 2012), but analysis of the influence of these factors, particularly on the phenotype of NC cells has yet to be performed. A novel *ex vivo* system has been developed here which would permit such investigations, although whether such specimens can be tested under load, low glucose, or low pH has not been investigated. Further development of this model to assess this will determine whether alterations are required to the model as it stands in order to provide a low pH, low glucose, loaded culture environment.

With regards to clinical translation of this work, after further investigation of adult human NP cell sub-population functionality and the degenerative/regenerative

potential of these, isolation of optimal cell sub-populations from autologous tissue and implantation into degenerate discs may be considered for the treatment of IVD degeneration. However, isolation of healthy autologous NP tissue for acquisition of cells is limited by the potential to induce degeneration at the donor disc level. Additionally, the numbers of cells isolated will be few, and thus, allogeneic tissues (from e.g. cadaveric specimens) may be considered, although these too have associated limitations, predominantly surrounding immune reactivity to donor cells. Thus, an alternative source of cells may be considered. Autologous adipose tissue can be easily sampled in the clinic, and thus (once more fully investigated), it could be assessed whether adipose-derived stem cells can differentiate to the phenotype of an NP cell sub-population. However, the mesodermal ontogeny of MSCs is not reflective of the notochordal origin of the NP, and thus, it should be considered whether embryonic stem cells are a more appropriate cell source, as these have previously been demonstrated as capable of differentiation to a notochordal cell phenotype (Winzi *et al.*, 2011).

Chapter 7:

References

7.0 References

ABBOTT, R. D., PURMESSUR, D., MONSEY, R. D. & IATRIDIS, J. C. (2012) Regenerative potential of TGFbeta3 + Dex and notochordal cell conditioned media on degenerated human intervertebral disc cells. *J Orthop Res,* 30**,** 482-8.

ABDELKHALEK, H. B., BECKERS, A., SCHUSTER-GOSSLER, K., PAVLOVA, M. N., BURKHARDT, H., LICKERT, H., ROSSANT, J., REINHARDT, R., SCHALKWYK, L. C., MULLER, I., HERRMANN, B. G., CEOLIN, M., RIVERA-POMAR, R. & GOSSLER, A. (2004) The mouse homeobox gene Not is required for caudal notochord development and affected by the truncate mutation. *Genes Dev,* 18**,** 1725-36.

ADAMS, M. A. & DOLAN, P. (1991) A technique for quantifying the bending moment acting on the lumbar spine in vivo. *J Biomech,* 24**,** 117-26.

ADAMS, M. A., MCNALLY, D. S. & DOLAN, P. (1996) 'Stress' distributions inside intervertebral discs. The effects of age and degeneration. *J Bone Joint Surg Br,* 78**,** 965-72.

ADAMS, M. A. & ROUGHLEY, P. J. (2006) What is intervertebral disc degeneration, and what causes it? *Spine (Phila Pa 1976),* 31**,** 2151-61.

AGUIAR, D. J., JOHNSON, S. L. & OEGEMA, T. R. (1999) Notochordal cells interact with nucleus pulposus cells: regulation of proteoglycan synthesis. *Exp Cell Res,* 246**,** 129-37.

AKMAL, M., KESANI, A., ANAND, B., SINGH, A., WISEMAN, M. & GOODSHIP, A. (2004) Effect of nicotine on spinal disc cells: a cellular mechanism for disc degeneration. *Spine (Phila Pa 1976),* 29**,** 568-75.

ALI, R., LE MAITRE, C. L., RICHARDSON, S. M., HOYLAND, J. A. & FREEMONT, A. J. (2008) Connective tissue growth factor expression in human intervertebral disc: implications for angiogenesis in intervertebral disc degeneration. *Biotech Histochem,* 83**,** 239-45.

ALVAREZ, L. & ORTIZ, A. (1999) The study of apoptosis in spine pathology. *Spine (Phila Pa 1976),* 24**,** 500.

ANDERSSON, G. B. (1999) Epidemiological features of chronic low-back pain. *Lancet,* 354**,** 581-5.

ANNUNEN, S., PAASSILTA, P., LOHINIVA, J., PERALA, M., PIHLAJAMAA, T., KARPPINEN, J., TERVONEN, O., KROGER, H., LAHDE, S., VANHARANTA, H., RYHANEN, L., GORING, H. H., OTT, J., PROCKOP, D. J. & ALA-KOKKO, L. (1999) An allele of COL9A2 associated with intervertebral disc disease. *Science,* 285**,** 409-12.

ANTONIOU, J., STEFFEN, T., NELSON, F., WINTERBOTTOM, N., HOLLANDER, A. P., POOLE, R. A., AEBI, M. & ALINI, M. (1996) The human lumbar intervertebral disc: evidence for changes in the biosynthesis and denaturation

of the extracellular matrix with growth, maturation, ageing, and degeneration. *J Clin Invest,* 98**,** 996-1003.

ARIGA, K., YONENOBU, K., NAKASE, T., KANEKO, M., OKUDA, S., UCHIYAMA, Y. & YOSHIKAWA, H. (2001) Localization of cathepsins D, K, and L in degenerated human intervertebral discs. *Spine (Phila Pa 1976),* 26**,** 2666-72.

ASZODI, A., CHAN, D., HUNZIKER, E., BATEMAN, J. F. & FASSLER, R. (1998) Collagen II is essential for the removal of the notochord and the formation of intervertebral discs. *J Cell Biol,* 143**,** 1399-412.

BABA, H., MAEZAWA, Y., FURUSAWA, N., FUKUDA, M., UCHIDA, K., KOKUBO, Y. & IMURA, S. (1997) Herniated cervical intervertebral discs: histological and immunohistochemical characteristics. *Eur J Histochem,* 41**,** 261-70.

BACHMEIER, B. E., NERLICH, A., MITTERMAIER, N., WEILER, C., LUMENTA, C., WUERTZ, K. & BOOS, N. (2009) Matrix metalloproteinase expression levels suggest distinct enzyme roles during lumbar disc herniation and degeneration. *Eur Spine J,* 18**,** 1573-86.

BAFFI, M. O., SLATTERY, E., SOHN, P., MOSES, H. L., CHYTIL, A. & SERRA, R. (2004) Conditional deletion of the TGF-beta type II receptor in Col2a expressing cells results in defects in the axial skeleton without alterations in chondrocyte differentiation or embryonic development of long bones. *Dev Biol,* 276**,** 124-42.

BARRIONUEVO, F., TAKETO, M. M., SCHERER, G. & KISPERT, A. (2006) Sox9 is required for notochord maintenance in mice. *Dev Biol,* 295**,** 128-40.

BARRY, F. P., NEAME, P. J., SASSE, J. & PEARSON, D. (1994) Length variation in the keratan sulfate domain of mammalian aggrecan. *Matrix Biol,* 14**,** 323-8.

BARTELS, E. M., FAIRBANK, J. C., WINLOVE, C. P. & URBAN, J. P. (1998) Oxygen and lactate concentrations measured in vivo in the intervertebral discs of patients with scoliosis and back pain. *Spine (Phila Pa 1976),* 23**,** 1-7; discussion 8.

BATTIE, M. C., HAYNOR, D. R., FISHER, L. D., GILL, K., GIBBONS, L. E. & VIDEMAN, T. (1995a) Similarities in degenerative findings on magnetic resonance images of the lumbar spines of identical twins. *J Bone Joint Surg Am,* 77**,** 1662-70.

BATTIE, M. C., VIDEMAN, T., GIBBONS, L. E., FISHER, L. D., MANNINEN, H. & GILL, K. (1995b) 1995 Volvo Award in clinical sciences. Determinants of lumbar disc degeneration. A study relating lifetime exposures and magnetic resonance imaging findings in identical twins. *Spine (Phila Pa 1976),* 20**,** 2601-12.

BATTIE, M. C., VIDEMAN, T., KAPRIO, J., GIBBONS, L. E., GILL, K., MANNINEN, H., SAARELA, J. & PELTONEN, L. (2009) The Twin Spine Study: contributions to a changing view of disc degeneration. *Spine J,* 9**,** 47-59.

BAUMGARTEN, G., KNUEFERMANN, P., KALRA, D., GAO, F., TAFFET, G. E., MICHAEL, L., BLACKSHEAR, P. J., CARBALLO, E., SIVASUBRAMANIAN, N. & MANN, D. L. (2002) Load-dependent and -

independent regulation of proinflammatory cytokine and cytokine receptor gene expression in the adult mammalian heart. *Circulation,* 105**,** 2192-7.

BECKERS, A., ALTEN, L., VIEBAHN, C., ANDRE, P. & GOSSLER, A. (2007) The mouse homeobox gene Noto regulates node morphogenesis, notochordal ciliogenesis, and left right patterning. *Proc Natl Acad Sci U S A,* 104**,** 15765-70.

BENNEKER, L. M., HEINI, P. F., ANDERSON, S. E., ALINI, M. & ITO, K. (2005) Correlation of radiographic and MRI parameters to morphological and biochemical assessment of intervertebral disc degeneration. *Eur Spine J,* 14**,** 27-35.

BERGKNUT, N., RUTGES, J. P., KRANENBURG, H. J., SMOLDERS, L. A., HAGMAN, R., SMIDT, H. J., LAGERSTEDT, A. S., PENNING, L. C., VOORHOUT, G., HAZEWINKEL, H. A., GRINWIS, G. C., CREEMERS, L. B., MEIJ, B. P. & DHERT, W. J. (2012) The dog as an animal model for intervertebral disc degeneration? *Spine (Phila Pa 1976),* 37**,** 351-8.

BERLEMANN, U., GRIES, N. C. & MOORE, R. J. (1998) The relationship between height, shape and histological changes in early degeneration of the lower lumbar discs. *Eur Spine J,* 7**,** 212-7.

BIBBY, S. R., JONES, D. A., LEE, R. B., YU, J. & URBAN, J. P. G. (2001) The pathophysiology of the intervertebral disc. *Joint Bone Spine,* 68**,** 537-42.

BIJKERK, C., HOUWING-DUISTERMAAT, J. J., VALKENBURG, H. A., MEULENBELT, I., HOFMAN, A., BREEDVELD, F. C., POLS, H. A., VAN DUIJN, C. M. & SLAGBOOM, P. E. (1999) Heritabilities of radiologic osteoarthritis in peripheral joints and of disc degeneration of the spine. *Arthritis Rheum,* 42**,** 1729-35.

BISHOP, P. B. & PEARCE, R. H. (1993) The proteoglycans of the cartilaginous end-plate of the human intervertebral disc change after maturity. *J Orthop Res,* 11**,** 324-31.

BLANCO, J. F., GRACIANI, I. F., SANCHEZ-GUIJO, F. M., MUNTION, S., HERNANDEZ-CAMPO, P., SANTAMARIA, C., CARRANCIO, S., BARBADO, M. V., CRUZ, G., GUTIERREZ-COSIO, S., HERRERO, C., SAN MIGUEL, J. F., BRINON, J. G. & DEL CANIZO, M. C. (2010) Isolation and characterization of mesenchymal stromal cells from human degenerated nucleus pulposus: comparison with bone marrow mesenchymal stromal cells from the same subjects. *Spine (Phila Pa 1976),* 35**,** 2259-65.

BODEN, S. D., MCCOWIN, P. R., DAVIS, D. O., DINA, T. S., MARK, A. S. & WIESEL, S. (1990) Abnormal magnetic-resonance scans of the cervical spine in asymptomatic subjects. A prospective investigation. *J Bone Joint Surg Am,* 72**,** 1178-84.

BOGDUK, N. & TWOMEY, L. T. (1987) *Clinical Anatomy of the Lumbar Spine,* Churchill Livingstone.

BOOS, N., NERLICH, A. G., WIEST, I., VON DER MARK, K. & AEBI, M. (1997) Immunolocalization of type X collagen in human lumbar intervertebral discs during ageing and degeneration. *Histochem Cell Biol,* 108**,** 471-80.

BOOS, N., WEISSBACH, S., ROHRBACH, H., WEILER, C., SPRATT, K. F. & NERLICH, A. G. (2002) Classification of age-related changes in lumbar intervertebral discs: 2002 Volvo Award in basic science. *Spine (Phila Pa 1976),* 27**,** 2631-44.

BOZKUS, H., CRAWFORD, N. R., CHAMBERLAIN, R. H., VALENZUELA, T. D., ESPINOZA, A., YUKSEL, Z. & DICKMAN, C. A. (2005) Comparative anatomy of the porcine and human thoracic spines with reference to thoracoscopic surgical techniques. *Surg Endosc,* 19**,** 1652-65.

BRINCKMANN, P., BIGGEMANN, M. & HILWEG, D. (1989) Prediction of the compressive strength of human lumbar vertebrae. *Spine (Phila Pa 1976),* 14**,** 606-10.

BUCKWALTER, J. A. (1995) Aging and degeneration of the human intervertebral disc. *Spine (Phila Pa 1976),* 20**,** 1307-14.

BURKE, J. G., WATSON, R. W., MCCORMACK, D., DOWLING, F. E., WALSH, M. G. & FITZPATRICK, J. M. (2002) Intervertebral discs which cause low back pain secrete high levels of proinflammatory mediators. *J Bone Joint Surg Br,* 84**,** 196-201.

CAMPBELL, C. E., CASEY, G. & GOODRICH, K. (1998) Genomic structure of TBX2 indicates conservation with distantly related T-box genes. *Mamm Genome,* 9**,** 70-3.

CAPPELLO, R., BIRD, J. L., PFEIFFER, D., BAYLISS, M. T. & DUDHIA, J. (2006) Notochordal cell produce and assemble extracellular matrix in a distinct manner, which may be responsible for the maintenance of healthy nucleus pulposus. *Spine (Phila Pa 1976),* 31**,** 873-82; discussion 883.

CATTARUZZA, S., SCHIAPPACASSI, M., KIMATA, K., COLOMBATTI, A. & PERRIS, R. (2004) The globular domains of PG-M/versican modulate the proliferation-apoptosis equilibrium and invasive capabilities of tumor cells. *Faseb J,* 18**,** 779-81.

CHEN, J., YAN, W. & SETTON, L. A. (2006) Molecular phenotypes of notochordal cells purified from immature nucleus pulposus. *Eur Spine J,* 15 Suppl 3**,** S303-11.

CHEUNG, K. M., CHAN, D., KARPPINEN, J., CHEN, Y., JIM, J. J., YIP, S. P., OTT, J., WONG, K. K., SHAM, P., LUK, K. D., CHEAH, K. S., LEONG, J. C. & SONG, Y. Q. (2006) Association of the Taq I allele in vitamin D receptor with degenerative disc disease and disc bulge in a Chinese population. *Spine (Phila Pa 1976),* 31**,** 1143-8.

CHEUNG, K. M., KARPPINEN, J., CHAN, D., HO, D. W., SONG, Y. Q., SHAM, P., CHEAH, K. S., LEONG, J. C. & LUK, K. D. (2009) Prevalence and pattern of lumbar magnetic resonance imaging changes in a population study of one thousand forty-three individuals. *Spine (Phila Pa 1976),* 34**,** 934-40.

CHO, H., LEE, S., PARK, S. H., HUANG, J., HASTY, K. A. & KIM, S. J. (2013) Synergistic effect of combined growth factors in porcine intervertebral disc degeneration. *Connect Tissue Res,* 54**,** 181-6.

CHOI, K. S., COHN, M. J. & HARFE, B. D. (2008) Identification of nucleus pulposus precursor cells and notochordal remnants in the mouse: implications for disk degeneration and chordoma formation. *Dev Dyn,* 237**,** 3953-8.

CHOI, K. S. & HARFE, B. D. (2011) Hedgehog signaling is required for formation of the notochord sheath and patterning of nuclei pulposi within the intervertebral discs. *Proc Natl Acad Sci U S A,* 108**,** 9484-9.

CHRISTE, A., LAUBLI, R., GUZMAN, R., BERLEMANN, U., MOORE, R. J., SCHROTH, G., VOCK, P. & LOVBLAD, K. O. (2005) Degeneration of the cervical disc: histology compared with radiography and magnetic resonance imaging. *Neuroradiology,* 47**,** 721-9.

CLOUET, J., GRIMANDI, G., POT-VAUCEL, M., MASSON, M., FELLAH, H. B., GUIGAND, L., CHEREL, Y., BORD, E., RANNOU, F., WEISS, P., GUICHEUX, J. & VINATIER, C. (2009) Identification of phenotypic discriminating markers for intervertebral disc cells and articular chondrocytes. *Rheumatology (Oxford),* 48**,** 1447-50.

COLOMBINI, A., LOMBARDI, G., CORSI, M. M. & BANFI, G. (2008) Pathophysiology of the human intervertebral disc. *Int J Biochem Cell Biol,* 40**,** 837-42.

COMPER, W. D. (1996) *Extracelluar Matrix,* Harwood Academic Publishers.

DAHIA, C. L., MAHONEY, E. & WYLIE, C. (2012) Shh signaling from the nucleus pulposus is required for the postnatal growth and differentiation of the mouse intervertebral disc. *PLoS One,* 7**,** e35944.

DAHIA, C. L., MAHONEY, E. J., DURRANI, A. A. & WYLIE, C. (2009) Intercellular signaling pathways active during intervertebral disc growth, differentiation, and aging. *Spine (Phila Pa 1976),* 34**,** 456-62.

DATH, R., EBINESAN, A. D., PORTER, K. M. & MILES, A. W. (2007) Anatomical measurements of porcine lumbar vertebrae. *Clin Biomech (Bristol, Avon),* 22**,** 607-13.

DEMERS, C. N., ANTONIOU, J. & MWALE, F. (2004) Value and limitations of using the bovine tail as a model for the human lumbar spine. *Spine (Phila Pa 1976),* 29**,** 2793-9.

DEMIRCAN, M. N., ASIR, A., CETINKAL, A., GEDIK, N., KUTLAY, A. M., COLAK, A., KURTAR, S. & SIMSEK, H. (2007) Is there any relationship between proinflammatory mediator levels in disc material and myelopathy with cervical disc herniation and spondylosis? A non-randomized, prospective clinical study. *Eur Spine J,* 16**,** 983-6.

DEYO, R. A. & BASS, J. E. (1989) Lifestyle and low-back pain. The influence of smoking and obesity. *Spine (Phila Pa 1976),* 14**,** 501-6.

DIAMANT, B., KARLSSON, J. & NACHEMSON, A. (1968) Correlation between lactate levels and pH in discs of patients with lumbar rhizopathies. *Experientia,* 24**,** 1195-1196.

DIPAOLA, C. P., FARMER, J. C., MANOVA, K. & NISWANDER, L. A. (2005) Molecular signaling in intervertebral disk development. *J Orthop Res,* 23**,** 1112-9.

DOEGE, K. J., COULTER, S. N., MEEK, L. M., MASLEN, K. & WOOD, J. G. (1997) A human-specific polymorphism in the coding region of the aggrecan gene. Variable number of tandem repeats produce a range of core protein sizes in the general population. *J Biol Chem,* 272**,** 13974-9.

EHLEN, H. W., BUELENS, L. A. & VORTKAMP, A. (2006) Hedgehog signaling in skeletal development. *Birth Defects Res C Embryo Today,* 78**,** 267-79.

ELFERING, A., SEMMER, N., BIRKHOFER, D., ZANETTI, M., HODLER, J. & BOOS, N. (2002) Risk factors for lumbar disc degeneration: a 5-year prospective MRI study in asymptomatic individuals. *Spine (Phila Pa 1976),* 27**,** 125-34.

ERNST, E. (1993) Smoking, a cause of back trouble? *Br J Rheumatol,* 32**,** 239-42.

ERWIN, W. M., ASHMAN, K., O'DONNEL, P. & INMAN, R. D. (2006) Nucleus pulposus notochord cells secrete connective tissue growth factor and up-regulate proteoglycan expression by intervertebral disc chondrocytes. *Arthritis Rheum,* 54**,** 3859-67.

ERWIN, W. M. & INMAN, R. D. (2006) Notochord cells regulate intervertebral disc chondrocyte proteoglycan production and cell proliferation. *Spine (Phila Pa 1976),* 31**,** 1094-9.

ERWIN, W. M., ISLAM, D., EFTEKARPOUR, E., INMAN, R. D., KARIM, M. Z. & FEHLINGS, M. G. (2013) Intervertebral disc-derived stem cells: implications for regenerative medicine and neural repair. *Spine (Phila Pa 1976),* 38**,** 211-6.

ERWIN, W. M., ISLAM, D., INMAN, R. D., FEHLINGS, M. G. & TSUI, F. W. (2011) Notochordal cells protect nucleus pulposus cells from degradation and apoptosis: implications for the mechanisms of intervertebral disc degeneration. *Arthritis Res Ther,* 13**,** R215.

ERWIN, W. M., LAS HERAS, F., ISLAM, D., FEHLINGS, M. G. & INMAN, R. D. (2009) The regenerative capacity of the notochordal cell: tissue constructs generated in vitro under hypoxic conditions. *J Neurosurg Spine,* 10**,** 513-21.

ESER, B., CORA, T., ESER, O., KALKAN, E., HAKTANIR, A., ERDOGAN, M. O. & SOLAK, M. (2010) Association of the polymorphisms of vitamin D receptor and aggrecan genes with degenerative disc disease. *Genet Test Mol Biomarkers,* 14**,** 313-7.

FAN, C. M. & TESSIER-LAVIGNE, M. (1994) Patterning of mammalian somites by surface ectoderm and notochord: evidence for sclerotome induction by a hedgehog homolog. *Cell,* 79**,** 1175-86.

FENG, H., DANFELTER, M., STROMQVIST, B. & HEINEGARD, D. (2006) Extracellular matrix in disc degeneration. *J Bone Joint Surg Am,* 88 Suppl 2**,** 25-9.

FERNANDES, R. J., HIROHATA, S., ENGLE, J. M., COLIGE, A., COHN, D. H., EYRE, D. R. & APTE, S. S. (2001) Procollagen II amino propeptide processing by ADAMTS-3. Insights on dermatosparaxis. *J Biol Chem,* 276**,** 31502-9.

FLEMING, A., KEYNES, R. & TANNAHILL, D. (2004) A central role for the notochord in vertebral patterning. *Development,* 131**,** 873-80.

FREEMONT, A. J. (2009) The cellular pathobiology of the degenerate intervertebral disc and discogenic back pain. *Rheumatology (Oxford),* 48**,** 5-10.

FREEMONT, A. J., PEACOCK, T. E., GOUPILLE, P., HOYLAND, J. A., O'BRIEN, J. & JAYSON, M. I. (1997) Nerve ingrowth into diseased intervertebral disc in chronic back pain. *Lancet,* 350**,** 178-81.

FREEMONT, A. J., WATKINS, A., LE MAITRE, C., BAIRD, P., JEZIORSKA, M., KNIGHT, M. T., ROSS, E. R., O'BRIEN, J. P. & HOYLAND, J. A. (2002) Nerve growth factor expression and innervation of the painful intervertebral disc. *J Pathol,* 197**,** 286-92.

FROBIN, W., BRINCKMANN, P., KRAMER, M. & HARTWIG, E. (2001) Height of lumbar discs measured from radiographs compared with degeneration and height classified from MR images. *Eur Radiol,* 11**,** 263-9.

FUJITA, N., MIYAMOTO, T., IMAI, J., HOSOGANE, N., SUZUKI, T., YAGI, M., MORITA, K., NINOMIYA, K., MIYAMOTO, K., TAKAISHI, H., MATSUMOTO, M., MORIOKA, H., YABE, H., CHIBA, K., WATANABE, S., TOYAMA, Y. & SUDA, T. (2005) CD24 is expressed specifically in the nucleus pulposus of intervertebral discs. *Biochem Biophys Res Commun,* 338**,** 1890-6.

FURUSAWA, N., BABA, H., MIYOSHI, N., MAEZAWA, Y., UCHIDA, K., KOKUBO, Y. & FUKUDA, M. (2001) Herniation of cervical intervertebral disc: immunohistochemical examination and measurement of nitric oxide production. *Spine (Phila Pa 1976),* 26**,** 1110-6.

GAO, G., WESTLING, J., THOMPSON, V. P., HOWELL, T. D., GOTTSCHALL, P. E. & SANDY, J. D. (2002) Activation of the proteolytic activity of ADAMTS4 (aggrecanase-1) by C-terminal truncation. *J Biol Chem,* 277**,** 11034-41.

GILSON, A., DREGER, M. & URBAN, J. P. (2010) Differential expression level of cytokeratin 8 in cells of the bovine nucleus pulposus complicates the search for specific intervertebral disc cell markers. *Arthritis Res Ther,* 12**,** R24.

GOTZ, W., BARNERT, S., BERTAGNOLI, R., MIOSGE, N., KRESSE, H. & HERKEN, R. (1997a) Immunohistochemical localization of the small proteoglycans decorin and biglycan in human intervertebral discs. *Cell Tissue Res,* 289**,** 185-90.

GOTZ, W., KASPER, M., FISCHER, G. & HERKEN, R. (1995) Intermediate filament typing of the human embryonic and fetal notochord. *Cell Tissue Res,* 280**,** 455-62.

GOTZ, W., KASPER, M., MIOSGE, N. & HUGHES, R. C. (1997b) Detection and distribution of the carbohydrate binding protein galectin-3 in human notochord, intervertebral disc and chordoma. *Differentiation,* 62**,** 149-57.

GRANDE-ALLEN, K. J., CALABRO, A., GUPTA, V., WIGHT, T. N., HASCALL, V. C. & VESELY, I. (2004) Glycosaminoglycans and proteoglycans in normal mitral valve leaflets and chordae: association with regions of tensile and compressive loading. *Glycobiology,* 14**,** 621-33.

GRIES, N. C., BERLEMANN, U., MOORE, R. J. & VERNON-ROBERTS, B. (2000) Early histologic changes in lower lumbar discs and facet joints and their correlation. *Eur Spine J,* 9**,** 23-9.

GROPPE, J., GREENWALD, J., WIATER, E., RODRIGUEZ-LEON, J., ECONOMIDES, A. N., KWIATKOWSKI, W., AFFOLTER, M., VALE, W. W., IZPISUA BELMONTE, J. C. & CHOE, S. (2002) Structural basis of BMP signalling inhibition by the cystine knot protein Noggin. *Nature,* 420**,** 636-42.

GRUBER, H., HOELSCHER, G., INGRAM, J., NORTON, H. & HANLEY, E., JR. (2013) Increased IL-17 expression in degenerated human discs and increased production in cultured annulus cells exposed to IL-1ss and TNF-alpha. *Biotech Histochem,* 88**,** 302-10.

GRUBER, H. E., INGRAM, J. A. & HANLEY, E. N., JR. (2005) Immunolocalization of MMP-19 in the human intervertebral disc: implications for disc aging and degeneration. *Biotech Histochem,* 80**,** 157-62.

GRUBER, H. E., INGRAM, J. A., HOELSCHER, G. L., ZINCHENKO, N., NORTON, H. J. & HANLEY, E. N., JR. (2009) Matrix metalloproteinase 28, a novel matrix metalloproteinase, is constitutively expressed in human intervertebral disc tissue and is present in matrix of more degenerated discs. *Arthritis Res Ther,* 11**,** R184.

GRUBER, H. E., INGRAM, J. A., HOELSCHER, G. L., ZINCHENKO, N., NORTON, H. J. & HANLEY, E. N., JR. (2011) Constitutive expression of cathepsin K in the human intervertebral disc: new insight into disc extracellular matrix remodeling via cathepsin K and receptor activator of nuclear factor-kappaB ligand. *Arthritis Res Ther,* 13**,** R140.

GRUNHAGEN, T., WILDE, G., SOUKANE, D. M., SHIRAZI-ADL, S. A. & URBAN, J. P. (2006) Nutrient supply and intervertebral disc metabolism. *J Bone Joint Surg Am,* 88 Suppl 2**,** 30-5.

GUEHRING, T., NERLICH, A., KROEBER, M., RICHTER, W. & OMLOR, G. W. (2010) Sensitivity of notochordal disc cells to mechanical loading: an experimental animal study. *Eur Spine J,* 19**,** 113-21.

GUEHRING, T., WILDE, G., SUMNER, M., GRUNHAGEN, T., KARNEY, G. B., TIRLAPUR, U. K. & URBAN, J. P. (2009) Notochordal intervertebral disc cells: sensitivity to nutrient deprivation. *Arthritis Rheum,* 60**,** 1026-34.

GUO, T. M., LIU, M., ZHANG, Y. G., GUO, W. T. & WU, S. X. (2011) Association between Caspase-9 promoter region polymorphisms and discogenic low back pain. *Connect Tissue Res,* 52**,** 133-8.

HAAPASALO, J., HILVO, M., NORDFORS, K., HAAPASALO, H., PARKKILA, S., HYRSKYLUOTO, A., RANTALA, I., WAHEED, A., SLY, W. S., PASTOREKOVA, S., PASTOREK, J. & PARKKILA, A. K. (2008) Identification of an alternatively spliced isoform of carbonic anhydrase XII in diffusely infiltrating astrocytic gliomas. *Neuro Oncol,* 10**,** 131-8.

HARRELSON, Z., KAESTNER, K. H. & EVANS, S. M. (2012) Foxa2 mediates critical functions of prechordal plate in patterning and morphogenesis and is cell autonomously required for early ventral endoderm morphogenesis. *Biol Open,* 1**,** 173-81.

HAYASHI, K., WADANO, Y. & AITA, I. (1997) Disc degeneration in the cervical spine. *Journal of Orthopaedic Science,* 2**,** 131-136.

HAYASHI, S., TAIRA, A., INOUE, G., KOSHI, T., ITO, T., YAMASHITA, M., YAMAUCHI, K., SUZUKI, M., TAKAHASHI, K. & OHTORI, S. (2008) TNF-alpha in nucleus pulposus induces sensory nerve growth: a study of the mechanism of discogenic low back pain using TNF-alpha-deficient mice. *Spine (Phila Pa 1976),* 33**,** 1542-6.

HAYES, A. J., BENJAMIN, M. & RALPHS, J. R. (1999) Role of actin stress fibres in the development of the intervertebral disc: cytoskeletal control of extracellular matrix assembly. *Dev Dyn,* 215**,** 179-89.

HEATHFIELD, S. K., LE MAITRE, C. L. & HOYLAND, J. A. (2008) Caveolin-1 expression and stress-induced premature senescence in human intervertebral disc degeneration. *Arthritis Res Ther,* 10**,** R87.

HELIOVAARA, M., MAKELA, M., KNEKT, P., IMPIVAARA, O. & AROMAA, A. (1991) Determinants of sciatica and low-back pain. *Spine (Phila Pa 1976),* 16**,** 608-14.

HENRIKSSON, H., THORNEMO, M., KARLSSON, C., HAGG, O., JUNEVIK, K., LINDAHL, A. & BRISBY, H. (2009) Identification of cell proliferation zones, progenitor cells and a potential stem cell niche in the intervertebral disc region: a study in four species. *Spine (Phila Pa 1976),* 34**,** 2278-87.

HENRIKSSON, H. B., SVALA, E., SKIOLDEBRAND, E., LINDAHL, A. & BRISBY, H. (2012) Support of concept that migrating progenitor cells from stem cell niches contribute to normal regeneration of the adult mammal intervertebral disc: a descriptive study in the New Zealand white rabbit. *Spine (Phila Pa 1976),* 37**,** 722-32.

HERMANN, B. G. & KISPERT, A. (1994) The T genes in embryogenesis. *Trends in Genetics,* 10**,** 280-286.

HOLM, S., MAROUDAS, A., URBAN, J., SELSTAM, G. & NACHEMSON, A. (1981) Nutrition of the intervertebral disc: solute transport and metabolism. *Connect Tissue Res,* 8**,** 101-119.

HORNER, H. A. & URBAN, J. (2001) Effect of nutrient supply on the viability of cells from the nucleus pulposus of the intervertebral disc. *Spine (Phila Pa 1976),* 26**,** 2543-2549.

HUANG, B., LIU, L. T., LI, C. Q., ZHUANG, Y., LUO, G., HU, S. Y. & ZHOU, Y. (2012) Study to determine the presence of progenitor cells in the degenerated human cartilage endplates. *Eur Spine J,* 21**,** 613-22.

HUMZAH, M. D. & SOAMES, R. W. (1988) Human intervertebral disc: structure and function. *Anat Rec,* 220**,** 337-56.

HUNTER, C. J. (2005) The notochordal cell in the postnatal intervertebral disc. *Eur Cell Mater,* 10**,** 15.

HUNTER, C. J., MATYAS, J. R. & DUNCAN, N. A. (2003a) The notochordal cell in the nucleus pulposus: a review in the context of tissue engineering. *Tissue Eng,* 9**,** 667-77.

HUNTER, C. J., MATYAS, J. R. & DUNCAN, N. A. (2003b) The three-dimensional architecture of the notochordal nucleus pulposus: novel observations on cell structures in the canine intervertebral disc. *J Anat,* 202**,** 279-91.

HUNTER, C. J., MATYAS, J. R. & DUNCAN, N. A. (2004) The functional significance of cell clusters in the notochordal nucleus pulposus: survival and signaling in the canine intervertebral disc. *Spine (Phila Pa 1976),* 29**,** 1099-104.

HUTTON, W. C. & ADAMS, M. A. (1982) Can the lumbar spine be crushed in heavy lifting? *Spine (Phila Pa 1976),* 7**,** 586-90.

ILLMAN, S. A., KESKI-OJA, J., PARKS, W. C. & LOHI, J. (2003) The mouse matrix metalloproteinase, epilysin (MMP-28), is alternatively spliced and processed by a furin-like proprotein convertase. *Biochem J,* 375**,** 191-7.

IMAI, K., YOKOHAMA, Y., NAKANISHI, I., OHUCHI, E., FUJII, Y., NAKAI, N. & OKADA, Y. (1995) Matrix metalloproteinase 7 (matrilysin) from human rectal carcinoma cells. Activation of the precursor, interaction with other matrix metalloproteinases and enzymic properties. *J Biol Chem,* 270**,** 6691-7.

INKINEN, R. I., LAMMI, M. J., LEHMONEN, S., PUUSTJARVI, K., KAAPA, E. & TAMMI, M. I. (1998) Relative increase of biglycan and decorin and altered chondroitin sulfate epitopes in the degenerating human intervertebral disc. *J Rheumatol,* 25**,** 506-14.

ISHIHARA, H., MCNALLY, D. S., URBAN, J. P. & HALL, A. C. (1996) Effects of hydrostatic pressure on matrix synthesis in different regions of the intervertebral disk. *J Appl Physiol,* 80**,** 839-46.

ISHII, Y., THOMAS, A. O., GUO, X. E., HUNG, C. T. & CHEN, F. H. (2006) Localization and distribution of cartilage oligomeric matrix protein in the rat intervertebral disc. *Spine (Phila Pa 1976),* 31**,** 1539-46.

JI, H. M., SAMPER, V., CHEN, Y., HENG, C. K., LIM, T. M. & YOBAS, L. (2008) Silicon-based microfilters for whole blood cell separation. *Biomed Microdevices,* 10**,** 251-7.

JIM, J. J., NOPONEN-HIETALA, N., CHEUNG, K. M., OTT, J., KARPPINEN, J., SAHRARAVAND, A., LUK, K. D., YIP, S. P., SHAM, P. C., SONG, Y. Q., LEONG, J. C., CHEAH, K. S., ALA-KOKKO, L. & CHAN, D. (2005) The TRP2 allele of COL9A2 is an age-dependent risk factor for the development and severity of intervertebral disc degeneration. *Spine (Phila Pa 1976),* 30**,** 2735-42.

JIMBO, K., PARK, J. S., YOKOSUKA, K., SATO, K. & NAGATA, K. (2005) Positive feedback loop of interleukin-1beta upregulating production of inflammatory mediators in human intervertebral disc cells in vitro. *J Neurosurg Spine,* 2**,** 589-95.

JOHNSON, W. E., CATERSON, B., EISENSTEIN, S. M., HYNDS, D. L., SNOW, D. M. & ROBERTS, S. (2002) Human intervertebral disc aggrecan inhibits nerve growth in vitro. *Arthritis Rheum,* 46**,** 2658-64.

JOHNSON, W. E., EISENSTEIN, S. M. & ROBERTS, S. (2001) Cell cluster formation in degenerate lumbar intervertebral discs is associated with increased disc cell proliferation. *Connect Tissue Res,* 42**,** 197-207.

JOHNSON, W. E. & ROBERTS, S. (2007) 'Rumours of my death may have been greatly exaggerated': a brief review of cell death in human intervertebral disc disease and implications for cell transplantation therapy. *Biochem Soc Trans,* 35**,** 680-2.

KALINICHENKO, V. V., ZHOU, Y., BHATTACHARYYA, D., KIM, W., SHIN, B., BAMBAL, K. & COSTA, R. H. (2002) Haploinsufficiency of the mouse Forkhead Box f1 gene causes defects in gall bladder development. *J Biol Chem,* 277**,** 12369-74.

KANEMOTO, M., HUKUDA, S., KOMIYA, Y., KATSUURA, A. & NISHIOKA, J. (1996) Immunohistochemical study of matrix metalloproteinase-3 and tissue inhibitor of metalloproteinase-1 human intervertebral discs. *Spine (Phila Pa 1976),* 21**,** 1-8.

KANG, J. D., GEORGESCU, H. I., MCINTYRE-LARKIN, L., STEFANOVIC-RACIC, M., DONALDSON, W. F., 3RD & EVANS, C. H. (1996) Herniated lumbar intervertebral discs spontaneously produce matrix metalloproteinases, nitric oxide, interleukin-6, and prostaglandin E2. *Spine (Phila Pa 1976),* 21**,** 271-7.

KANG, T., NAGASE, H. & PEI, D. (2002) Activation of membrane-type matrix metalloproteinase 3 zymogen by the proprotein convertase furin in the trans-Golgi network. *Cancer Res,* 62**,** 675-81.

KAPLAN, K. M., SPIVAK, J. M. & BENDO, J. A. (2005) Embryology of the spine and associated congenital abnormalities. *Spine J,* 5**,** 564-76.

KARANTZA, V. (2011) Keratins in health and cancer: more than mere epithelial cell markers. *Oncogene,* 30**,** 127-38.

KAWAGUCHI, Y., KANAMORI, M., ISHIHARA, H., OHMORI, K., MATSUI, H. & KIMURA, T. (2002) The association of lumbar disc disease with vitamin-D receptor gene polymorphism. *J Bone Joint Surg Am,* 84-A**,** 2022-8.

KAWAGUCHI, Y., OSADA, R., KANAMORI, M., ISHIHARA, H., OHMORI, K., MATSUI, H. & KIMURA, T. (1999) Association between an aggrecan gene polymorphism and lumbar disc degeneration. *Spine (Phila Pa 1976),* 24**,** 2456-60.

KELSEY, J. L., GITHENS, P. B., O'CONNER, T., WEIL, U., CALOGERO, J. A., HOLFORD, T. R., WHITE, A. A., 3RD, WALTER, S. D., OSTFELD, A. M. & SOUTHWICK, W. O. (1984) Acute prolapsed lumbar intervertebral disc. An epidemiologic study with special reference to driving automobiles and cigarette smoking. *Spine (Phila Pa 1976),* 9**,** 608-13.

KELSEY, J. L., MUNDT, D. J. & GOLDEN, A. L. (1992) *Epidemiology of low back pain,* Churchill Livingstone.

KEPLER, C. K., PONNAPPAN, R. K., TANNOURY, C. A., RISBUD, M. V. & ANDERSON, D. G. (2013) The molecular basis of intervertebral disc degeneration. *Spine J,* 13**,** 318-30.

KIM, J. H., DEASY, B. M., SEO, H. Y., STUDER, R. K., VO, N. V., GEORGESCU, H. I., SOWA, G. A. & KANG, J. D. (2009) Differentiation of intervertebral notochordal cells through live automated cell imaging system in vitro. *Spine (Phila Pa 1976),* 34**,** 2486-93.

KIM, J. H., MOON, H. J., LEE, J. H., KIM, J. H., KWON, T. H. & PARK, Y. K. (2012) Rabbit notochordal cells modulate the expression of inflammatory mediators by human annulus fibrosus cells cocultured with activated macrophage-like THP-1 cells. *Spine (Phila Pa 1976),* 37**,** 1856-64.

KIM, J. S., ELLMAN, M. B., YAN, D., AN, H. S., KC, R., LI, X., CHEN, D., XIAO, G., CS-SZABO, G., HOSKIN, D. W., BUECHTER, D. D., VAN WIJNEN, A. J. & IM, H. J. (2013) Lactoferricin mediates anti-inflammatory and anti-catabolic effects via inhibition of IL-1 and LPS activity in the intervertebral disc. *J Cell Physiol,* 228**,** 1884-96.

KNAUPER, V., WILL, H., LOPEZ-OTIN, C., SMITH, B., ATKINSON, S. J., STANTON, H., HEMBRY, R. M. & MURPHY, G. (1996) Cellular mechanisms for human procollagenase-3 (MMP-13) activation. Evidence that MT1-MMP (MMP-14) and gelatinase a (MMP-2) are able to generate active enzyme. *J Biol Chem,* 271**,** 17124-31.

KOCKAR, F., YILDRIM, H., SAGKAN, R. I., HAGEMANN, C., SOYSAL, Y., ANACKER, J., HAMZA, A. A., VORDERMARK, D., FLENTJE, M. & SAID, H.

M. (2012) Hypoxia and cytokines regulate carbonic anhydrase 9 expression in hepatocellular carcinoma cells in vitro. *World J Clin Oncol,* 3**,** 82-91.

KOKUBO, Y., UCHIDA, K., KOBAYASHI, S., YAYAMA, T., SATO, R., NAKAJIMA, H., TAKAMURA, T., MWAKA, E., ORWOTHO, N., BANGIRANA, A. & BABA, H. (2008) Herniated and spondylotic intervertebral discs of the human cervical spine: histological and immunohistological findings in 500 en bloc surgical samples. Laboratory investigation. *J Neurosurg Spine,* 9**,** 285-95.

KOKUBUN, S., SAKURAI, M. & TANAKA, Y. (1996) Cartilaginous endplate in cervical disc herniation. *Spine (Phila Pa 1976),* 21**,** 190-5.

KOLSTAD, F., MYHR, G., KVISTAD, K. A., NYGAARD, O. P. & LEIVSETH, G. (2005) Degeneration and height of cervical discs classified from MRI compared with precise height measurements from radiographs. *Eur J Radiol,* 55**,** 415-20.

KONTTINEN, Y. T., KAAPA, E., HUKKANEN, M., GU, X. H., TAKAGI, M., SANTAVIRTA, S., ALARANTA, H., LI, T. F. & SUDA, A. (1999) Cathepsin G in degenerating and healthy discal tissue. *Clin Exp Rheumatol,* 17**,** 197-204.

KORECKI, C. L., TABOAS, J. M., TUAN, R. S. & IATRIDIS, J. C. (2010) Notochordal cell conditioned medium stimulates mesenchymal stem cell differentiation toward a young nucleus pulposus phenotype. *Stem Cell Res Ther,* 1**,** 18.

KOSEKI, H., WALLIN, J., WILTING, J., MIZUTANI, Y., KISPERT, A., EBENSPERGER, C., HERRMANN, B. G., CHRIST, B. & BALLING, R. (1993) A role for Pax-1 as a mediator of notochordal signals during the dorsoventral specification of vertebrae. *Development,* 119**,** 649-60.

KULESH, D. A., CECENA, G., DARMON, Y. M., VASSEUR, M. & OSHIMA, R. G. (1989) Posttranslational regulation of keratins: degradation of mouse and human keratins 18 and 8. *Mol Cell Biol,* 9**,** 1553-65.

KUMAR, A., VARGHESE, M., MOHAN, D., MAHAJAN, P., GULATI, P. & KALE, S. (1999) Effect of whole-body vibration on the low back. A study of tractor-driving farmers in north India. *Spine (Phila Pa 1976),* 24**,** 2506-15.

LAMMI, P., INKINEN, R. I., VON DER MARK, K., PUUSTJARVI, K., AROKOSKI, J., HYTTINEN, M. M. & LAMMI, M. J. (1998) Localization of type X collagen in the intervertebral disc of mature beagle dogs. *Matrix Biol,* 17**,** 449-53.

LANDOLT, R. M., VAUGHAN, L., WINTERHALTER, K. H. & ZIMMERMANN, D. R. (1995) Versican is selectively expressed in embryonic tissues that act as barriers to neural crest cell migration and axon outgrowth. *Development,* 121**,** 2303-12.

LE MAITRE, C. L., FOTHERINGHAM, A. P., FREEMONT, A. J. & HOYLAND, J. A. (2009) Development of an in vitro model to test the efficacy of novel therapies for IVD degeneration. *J Tissue Eng Regen Med,* 3**,** 461-9.

LE MAITRE, C. L., FREEMONT, A. J. & HOYLAND, J. A. (2004a) Localization of degradative enzymes and their inhibitors in the degenerate human intervertebral disc. *J Pathol,* 204**,** 47-54.

LE MAITRE, C. L., FREEMONT, A. J. & HOYLAND, J. A. (2005) The role of interleukin-1 in the pathogenesis of human intervertebral disc degeneration. *Arthritis Res Ther,* 7**,** R732-45.

LE MAITRE, C. L., FREEMONT, A. J. & HOYLAND, J. A. (2006) Human disc degeneration is associated with increased MMP 7 expression. *Biotech Histochem,* 81**,** 125-31.

LE MAITRE, C. L., FREEMONT, A. J. & HOYLAND, J. A. (2007a) Accelerated cellular senescence in degenerate intervertebral discs: a possible role in the pathogenesis of intervertebral disc degeneration. *Arthritis Res Ther,* 9**,** R45.

LE MAITRE, C. L., HOYLAND, J. A. & FREEMONT, A. J. (2004b) Studies of human intervertebral disc cell function in a constrained in vitro tissue culture system. *Spine (Phila Pa 1976),* 29**,** 1187-95.

LE MAITRE, C. L., HOYLAND, J. A. & FREEMONT, A. J. (2007b) Catabolic cytokine expression in degenerate and herniated human intervertebral discs: IL-1beta and TNFalpha expression profile. *Arthritis Res Ther,* 9**,** R77.

LE MAITRE, C. L., POCKERT, A., BUTTLE, D. J., FREEMONT, A. J. & HOYLAND, J. A. (2007c) Matrix synthesis and degradation in human intervertebral disc degeneration. *Biochem Soc Trans,* 35**,** 652-5.

LEE, C. R., GRAD, S., MACLEAN, J. J., IATRIDIS, J. C. & ALINI, M. (2005) Effect of mechanical loading on mRNA levels of common endogenous controls in articular chondrocytes and intervertebral disk. *Anal Biochem,* 341**,** 372-5.

LEE, C. R., SAKAI, D., NAKAI, T., TOYAMA, K., MOCHIDA, J., ALINI, M. & GRAD, S. (2007) A phenotypic comparison of intervertebral disc and articular cartilage cells in the rat. *Eur Spine J,* 16**,** 2174-85.

LEE, J. M., SONG, J. Y., BAEK, M., JUNG, H. Y., KANG, H., HAN, I. B., KWON, Y. D. & SHIN, D. E. (2011) Interleukin-1beta induces angiogenesis and innervation in human intervertebral disc degeneration. *J Orthop Res,* 29**,** 265-9.

LIANG, Q. Q., CUI, X. J., XI, Z. J., BIAN, Q., HOU, W., ZHAO, Y. J., SHI, Q. & WANG, Y. J. (2011) Prolonged upright posture induces degenerative changes in intervertebral discs of rat cervical spine. *Spine (Phila Pa 1976),* 36**,** E14-9.

LIAO, S. Y., LERMAN, M. I. & STANBRIDGE, E. J. (2009) Expression of transmembrane carbonic anhydrases, CAIX and CAXII, in human development. *BMC Dev Biol,* 9**,** 22.

LIEBSCHER, T., HAEFELI, M., WUERTZ, K., NERLICH, A. G. & BOOS, N. (2011) Age-related variation in cell density of human lumbar intervertebral disc. *Spine (Phila Pa 1976),* 36**,** 153-9.

LINDSKOG, S. (1997) Structure and mechanism of carbonic anhydrase. *Pharmacol Ther,* 74**,** 1-20.

LIU, L. T., HUANG, B., LI, C. Q., ZHUANG, Y., WANG, J. & ZHOU, Y. (2011) Characteristics of stem cells derived from the degenerated human intervertebral disc cartilage endplate. *PLoS One,* 6**,** e26285.

LIVAK, K. J. & SCHMITTGEN, T. D. (2001) Analysis of relative gene expression data using real-time quantitative PCR and the 2(-Delta Delta C(T)) Method. *Methods,* 25**,** 402-8.

LONGO, U. G., RIPALDA, P., DENARO, V. & FORRIOL, F. (2006) Morphologic comparison of cervical, thoracic, lumbar intervertebral discs of cynomolgus monkey (Macaca fascicularis). *Eur Spine J,* 15**,** 1845-51.

LOUMAN-GARDINER, K. M., COOMBE, D. & HUNTER, C. J. (2011) Computation models simulating notochordal cell extinction during early ageing of an intervertebral disc. *Comput Methods Biomech Biomed Engin,* 14**,** 1071-7.

MA, F., ZHANG, L. & WESTLUND, K. N. (2009) Reactive oxygen species mediate TNFR1 increase after TRPV1 activation in mouse DRG neurons. *Mol Pain,* 5**,** 31.

MAHLAPUU, M., ORMESTAD, M., ENERBACK, S. & CARLSSON, P. (2001) The forkhead transcription factor Foxf1 is required for differentiation of extra-embryonic and lateral plate mesoderm. *Development,* 128**,** 155-66.

MAIER, J. A., LO, Y. & HARFE, B. D. (2013) Foxa1 and Foxa2 are required for formation of the intervertebral discs. *PLoS One,* 8**,** e55528.

MAKELA, M., HELIOVAARA, M., SIEVERS, K., IMPIVAARA, O., KNEKT, P. & AROMAA, A. (1991) Prevalence, determinants, and consequences of chronic neck pain in Finland. *Am J Epidemiol,* 134**,** 1356-67.

MANIADAKIS, N. & GRAY, A. (2000) The economic burden of back pain in the UK. *Pain,* 84**,** 95-103.

MARCHAND, F. & AHMED, A. M. (1990) Investigation of the laminate structure of lumbar disc anulus fibrosus. *Spine (Phila Pa 1976),* 15**,** 402-10.

MAROUDAS, A., STOCKWELL, R. A., NACHEMSON, A. & URBAN, J. (1975) Factors involved in the nutrition of the human lumbar intervertebral disc: cellularity and diffusion of glucose in vitro. *J Anat,* 120**,** 113-30.

MARTIN, B. I., DEYO, R. A., MIRZA, S. K., TURNER, J. A., COMSTOCK, B. A., HOLLINGWORTH, W. & SULLIVAN, S. D. (2008) Expenditures and health status among adults with back and neck problems. *Jama,* 299**,** 656-64.

MASHAYEKHI, F., SHAFIEE, G., KAZEMI, M. & DOLATI, P. (2010) Lumbar disk degeneration disease and aggrecan gene polymorphism in northern Iran. *Biochem Genet,* 48**,** 684-9.

MATSUI, H., KANAMORI, M., ISHIHARA, H., YUDOH, K., NARUSE, Y. & TSUJI, H. (1998) Familial predisposition for lumbar degenerative disc disease. A case-control study. *Spine (Phila Pa 1976),* 23**,** 1029-34.

MATSUMOTO, M., FUJIMURA, Y., SUZUKI, N., NISHI, Y., NAKAMURA, M., YABE, Y. & SHIGA, H. (1998) MRI of cervical intervertebral discs in asymptomatic subjects. *J Bone Joint Surg Br,* 80**,** 19-24.

MATSUMOTO, M., OKADA, E., TOYAMA, Y., FUJIWARA, H., MOMOSHIMA, S. & TAKAHATA, T. (2012) Tandem age-related lumbar and cervical intervertebral disc changes in asymptomatic subjects. *Eur Spine J,* 22**,** 708-13.

MCCANN, M. R., PATEL, P., BEAUCAGE, K. L., XIAO, Y., BACHER, C., SIQUEIRA, W. L., HOLDSWORTH, D. W., DIXON, S. J. & SEGUIN, C. A. (2013) Acute vibration induces transient expression of anabolic genes in the murine intervertebral disc. *Arthritis Rheum,* 65**,** 1853-64.

MCCANN, M. R., TAMPLIN, O. J., ROSSANT, J. & SEGUIN, C. A. (2012) Tracing notochord-derived cells using a Noto-cre mouse: implications for intervertebral disc development. *Dis Model Mech,* 5**,** 73-82.

MCGAUGHRAN, J. M., OATES, A., DONNAI, D., READ, A. P. & TASSABEHJI, M. (2003) Mutations in PAX1 may be associated with Klippel-Feil syndrome. *Eur J Hum Genet,* 11**,** 468-74.

MCMAHON, J. A., TAKADA, S., ZIMMERMAN, L. B., FAN, C. M., HARLAND, R. M. & MCMAHON, A. P. (1998) Noggin-mediated antagonism of BMP signaling is required for growth and patterning of the neural tube and somite. *Genes Dev,* 12**,** 1438-52.

MELROSE, J., SMITH, S., GHOSH, P. & TAYLOR, T. K. (2001) Differential expression of proteoglycan epitopes and growth characteristics of intervertebral disc cells grown in alginate bead culture. *Cells Tissues Organs,* 168**,** 137-46.

MELROSE, J., SMITH, S. M., APPLEYARD, R. C. & LITTLE, C. B. (2008) Aggrecan, versican and type VI collagen are components of annular translamellar crossbridges in the intervertebral disc. *Eur Spine J,* 17**,** 314-24.

MERCER, S. & BOGDUK, N. (1999) The ligaments and annulus fibrosus of human adult cervical intervertebral discs. *Spine (Phila Pa 1976),* 24**,** 619-26; discussion 627-8.

MERCURI, J. J., PATNAIK, S., DION, G., GILL, S. S., LIAO, J. & SIMIONESCU, D. T. (2013) Regenerative potential of decellularized porcine nucleus pulposus hydrogel scaffolds: stem cell differentiation, matrix remodeling, and biocompatibility studies. *Tissue Eng Part A,* 19**,** 952-66.

MILLER, V. M., CLOUSE, W. D., TONNESSEN, B. H., BOSTON, U. S., SEVERSON, S. R., BONDE, S., RUD, K. S. & HURT, R. D. (2000) Time and dose effect of transdermal nicotine on endothelial function. *Am J Physiol Heart Circ Physiol,* 279**,** H1913-21.

MILLWARD-SADLER, S. J., COSTELLO, P. W., FREEMONT, A. J. & HOYLAND, J. A. (2009) Regulation of catabolic gene expression in normal and degenerate human intervertebral disc cells: implications for the pathogenesis of intervertebral disc degeneration. *Arthritis Res Ther,* 11**,** R65.

MINOGUE, B. M., RICHARDSON, S. M., ZEEF, L. A., FREEMONT, A. J. & HOYLAND, J. A. (2010a) Characterization of the human nucleus pulposus cell phenotype and evaluation of novel marker gene expression to define adult stem cell differentiation. *Arthritis Rheum,* 62**,** 3695-705.

MINOGUE, B. M., RICHARDSON, S. M., ZEEF, L. A., FREEMONT, A. J. & HOYLAND, J. A. (2010b) Transcriptional profiling of bovine intervertebral disc cells: implications for identification of normal and degenerate human intervertebral disc cell phenotypes. *Arthritis Res Ther,* 12**,** R22.

MIYAGI, M., ISHIKAWA, T., KAMODA, H., SUZUKI, M., MURAKAMI, K., SHIBAYAMA, M., ORITA, S., EGUCHI, Y., ARAI, G., SAKUMA, Y., KUBOTA, G., OIKAWA, Y., OZAWA, T., AOKI, Y., TOYONE, T., TAKAHASHI, K., INOUE, G., KAWAKAMI, M. & OHTORI, S. (2012) ISSLS prize winner: disc dynamic compression in rats produces long-lasting increases in inflammatory mediators in discs and induces long-lasting nerve injury and regeneration of the afferent fibers innervating discs: a pathomechanism for chronic discogenic low back pain. *Spine (Phila Pa 1976),* 37**,** 1810-8.

MIYAZAKI, T., KOBAYASHI, S., TAKENO, K., MEIR, A., URBAN, J. & BABA, H. (2009) A phenotypic comparison of proteoglycan production of intervertebral disc cells isolated from rats, rabbits, and bovine tails; which animal model is most suitable to study tissue engineering and biological repair of human disc disorders? *Tissue Eng Part A,* 15**,** 3835-46.

MOORE, R. J. (2006) The vertebral endplate: disc degeneration, disc regeneration. *Eur Spine J,* 15**,** S333-S337.

MURPHY, G., STANTON, H., COWELL, S., BUTLER, G., KNAUPER, V., ATKINSON, S. & GAVRILOVIC, J. (1999) Mechanisms for pro matrix metalloproteinase activation. *Apmis,* 107**,** 38-44.

MWALE, F., MASUDA, K., PICHIKA, R., EPURE, L. M., YOSHIKAWA, T., HEMMAD, A., ROUGHLEY, P. J. & ANTONIOU, J. (2011) The efficacy of Link N as a mediator of repair in a rabbit model of intervertebral disc degeneration. *Arthritis Res Ther,* 13**,** R120.

MWALE, F., ROUGHLEY, P. & ANTONIOU, J. (2004) Distinction between the extracellular matrix of the nucleus pulposus and hyaline cartilage: a requisite for tissue engineering of intervertebral disc. *Eur Cell Mater,* 8**,** 58-63; discussion 63-4.

N.I.C.E. (2009) Low back pain costing report. IN N.I.C.E. (Ed.).

NAKA, T., IWAMOTO, Y., SHINOHARA, N., CHUMAN, H., FUKUI, M. & TSUNEYOSHI, M. (1997) Cytokeratin subtyping in chordomas and the fetal

notochord: an immunohistochemical analysis of aberrant expression. *Mod Pathol,* 10**,** 545-51.

NEIDLINGER-WILKE, C., MIETSCH, A., RINKLER, C., WILKE, H. J., IGNATIUS, A. & URBAN, J. (2012) Interactions of environmental conditions and mechanical loads have influence on matrix turnover by nucleus pulposus cells. *J Orthop Res,* 30**,** 112-121.

NERLICH, A. G., SCHLEICHER, E. D. & BOOS, N. (1997) 1997 Volvo Award winner in basic science studies. Immunohistologic markers for age-related changes of human lumbar intervertebral discs. *Spine (Phila Pa 1976),* 22**,** 2781-95.

ODA, J., TANAKA, H. & TSUZUKI, N. (1988) Intervertebral disc changes with aging of human cervical vertebra. From the neonate to the eighties. *Spine (Phila Pa 1976),* 13**,** 1205-11.

OGUZ, E., TSAI, T. T., DI MARTINO, A., GUTTAPALLI, A., ALBERT, T. J., SHAPIRO, I. M. & RISBUD, M. V. (2007) Galectin-3 expression in the intervertebral disc: a useful marker of the notochord phenotype? *Spine (Phila Pa 1976),* 32**,** 9-16.

OHSHIMA, H. & URBAN, J. (1992) The effect of lactate and pH on proteoglycan and protein synthesis rates in the intervertebral disc. *Spine (Phila Pa 1976),* 17**,** 1079-1082.

OKADA, Y., MORODOMI, T., ENGHILD, J. J., SUZUKI, K., YASUI, A., NAKANISHI, I., SALVESEN, G. & NAGASE, H. (1990) Matrix metalloproteinase 2 from human rheumatoid synovial fibroblasts. Purification and activation of the precursor and enzymic properties. *Eur J Biochem,* 194**,** 721-30.

OMLOR, G. W., NERLICH, A. G., WILKE, H. J., PFEIFFER, M., LORENZ, H., SCHAAF-KEIM, M., BERTRAM, H., RICHTER, W., CARSTENS, C. & GUEHRING, T. (2009) A new porcine in vivo animal model of disc degeneration: response of anulus fibrosus cells, chondrocyte-like nucleus pulposus cells, and notochordal nucleus pulposus cells to partial nucleotomy. *Spine (Phila Pa 1976),* 34**,** 2730-9.

ORMESTAD, M., ASTORGA, J., LANDGREN, H., WANG, T., JOHANSSON, B. R., MIURA, N. & CARLSSON, P. (2006) Foxf1 and Foxf2 control murine gut development by limiting mesenchymal Wnt signaling and promoting extracellular matrix production. *Development,* 133**,** 833-43.

ORTOLANI, F., RASPANTI, M., FRANCHI, M. & MARCHINI, M. (1988) Localization of different alcian blue-proteoglycan particles in the intervertebral disc. *Basic Appl Histochem,* 32**,** 443-53.

OSHIMA, H., ISHIHARA, H., URBAN, J. P. & TSUJI, H. (1993) The use of coccygeal discs to study intervertebral disc metabolism. *J Orthop Res,* 11**,** 332-8.

OSHIMA, R. G. (2002) Apoptosis and keratin intermediate filaments. *Cell Death Differ,* 9**,** 486-92.

PAASSILTA, P., LOHINIVA, J., GORING, H. H., PERALA, M., RAINA, S. S., KARPPINEN, J., HAKALA, M., PALM, T., KROGER, H., KAITILA, I., VANHARANTA, H., OTT, J. & ALA-KOKKO, L. (2001) Identification of a novel common genetic risk factor for lumbar disk disease. *Jama,* 285**,** 1843-9.

PANKOV, R., SIMCHA, I., ZOLLER, M., OSHIMA, R. G. & BEN-ZE'EV, A. (1997) Contrasting effects of K8 and K18 on stabilizing K19 expression, cell motility and tumorigenicity in the BSp73 adenocarcinoma. *J Cell Sci,* 110 (Pt 8)**,** 965-74.

PARK, E. Y. & PARK, J. B. (2013a) Dose- and time-dependent effect of high glucose concentration on viability of notochordal cells and expression of matrix degrading and fibrotic enzymes. *Int Orthop,* 37**,** 1179-86.

PARK, E. Y. & PARK, J. B. (2013b) High glucose-induced oxidative stress promotes autophagy through mitochondrial damage in rat notochordal cells. *Int Orthop***,** E-pub (not yet in print).

PARK, J. Y., YOON, Y. S., PARK, H. S. & KUH, S. U. (2013) Molecular response of human cervical and lumbar nucleus pulposus cells from degenerated discs following cytokine treatment. *Genet Mol Res,* 12**,** 838-51.

PAZZAGLIA, U. E., SALISBURY, J. R. & BYERS, P. D. (1989) Development and involution of the notochord in the human spine. *J R Soc Med,* 82**,** 413-5.

PEACOCK, A. (1951) Observations on the prenatal development of the intervertebral disc in man. *J Anat,* 85**,** 260-74.

PELTON, R. W., DICKINSON, M. E., MOSES, H. L. & HOGAN, B. L. (1990) In situ hybridization analysis of TGF beta 3 RNA expression during mouse development: comparative studies with TGF beta 1 and beta 2. *Development,* 110**,** 609-20.

PENG, B., WU, W., HOU, S., LI, P., ZHANG, C. & YANG, Y. (2005) The pathogenesis of discogenic low back pain. *J Bone Joint Surg Br,* 87**,** 62-7.

PETERS, H., WILM, B., SAKAI, N., IMAI, K., MAAS, R. & BALLING, R. (1999) Pax1 and Pax9 synergistically regulate vertebral column development. *Development,* 126**,** 5399-408.

PFIRRMANN, C. W., METZDORF, A., ZANETTI, M., HODLER, J. & BOOS, N. (2001) Magnetic resonance classification of lumbar intervertebral disc degeneration. *Spine (Phila Pa 1976),* 26**,** 1873-8.

PLUIJM, S. M., VAN ESSEN, H. W., BRAVENBOER, N., UITTERLINDEN, A. G., SMIT, J. H., POLS, H. A. & LIPS, P. (2004) Collagen type I alpha1 Sp1 polymorphism, osteoporosis, and intervertebral disc degeneration in older men and women. *Ann Rheum Dis,* 63**,** 71-7.

POCKERT, A. J., RICHARDSON, S. M., LE MAITRE, C. L., LYON, M., DEAKIN, J. A., BUTTLE, D. J., FREEMONT, A. J. & HOYLAND, J. A. (2009) Modified expression of the ADAMTS enzymes and tissue inhibitor of

metalloproteinases 3 during human intervertebral disc degeneration. *Arthritis Rheum,* 60**,** 482-91.

POIRAUDEAU, S., MONTEIRO, I., ANRACT, P., BLANCHARD, O., REVEL, M. & CORVOL, M. T. (1999) Phenotypic characteristics of rabbit intervertebral disc cells. Comparison with cartilage cells from the same animals. *Spine (Phila Pa 1976),* 24**,** 837-44.

POONI, J. S., HUKINS, D. W., HARRIS, P. F., HILTON, R. C. & DAVIES, K. E. (1986) Comparison of the structure of human intervertebral discs in the cervical, thoracic and lumbar regions of the spine. *Surg Radiol Anat,* 8**,** 175-82.

POSTACCHINI, F., LAMI, R. & PUGLIESE, O. (1988) Familial predisposition to discogenic low-back pain. An epidemiologic and immunogenetic study. *Spine (Phila Pa 1976),* 13**,** 1403-6.

POWER, K. A., GRAD, S., RUTGES, J. P., CREEMERS, L. B., VAN RIJEN, M. H., O'GAORA, P., WALL, J. G., ALINI, M., PANDIT, A. & GALLAGHER, W. M. (2012) Identification of cell surface-specific markers to target human nucleus pulposus cells: expression of carbonic anhydrase XII varies with age and degeneration. *Arthritis Rheum,* 63**,** 3876-86.

PRITZKER, K. P. (1977) Aging and degeneration in the lumbar intervertebral disc. *Orthop Clin North Am,* 8**,** 66-77.

PRZYBYLA, A. S., SKRZYPIEC, D., POLLINTINE, P., DOLAN, P. & ADAMS, M. A. (2007) Strength of the cervical spine in compression and bending. *Spine (Phila Pa 1976),* 32**,** 1612-20.

PURMESSUR, D., FREEMONT, A. J. & HOYLAND, J. A. (2008) Expression and regulation of neurotrophins in the nondegenerate and degenerate human intervertebral disc. *Arthritis Res Ther,* 10**,** R99.

PURMESSUR, D., GUTERL, C., CORNEJO, M. C., ABBOT, R. A., CHO, S. K., LAUDIER, D. & IATRIDIS, J. C. (2012) Hydrostatic pressure enhances notochordal cell phenotype and metabolic activity with increased proteoglycan accumulation. *ORS 2012 Annual Meeting***,** Paper 0035.

PURMESSUR, D., SCHEK, R. M., ABBOTT, R. D., BALLIF, B. A., GODBURN, K. E. & IATRIDIS, J. C. (2011) Notochordal conditioned media from tissue increases proteoglycan accumulation and promotes a healthy nucleus pulposus phenotype in human mesenchymal stem cells. *Arthritis Res Ther,* 13**,** R81.

PYE, S. R., REID, D. M., ADAMS, J. E., SILMAN, A. J. & O'NEILL, T. W. (2007) Influence of weight, body mass index and lifestyle factors on radiographic features of lumbar disc degeneration. *Ann Rheum Dis,* 66**,** 426-7.

RAJ, P. P. (2008) Intervertebral disc: anatomy-physiology-pathophysiology-treatment. *Pain Pract,* 8**,** 18-44.

RAMOS-DESIMONE, N., HAHN-DANTONA, E., SIPLEY, J., NAGASE, H., FRENCH, D. L. & QUIGLEY, J. P. (1999) Activation of matrix metalloproteinase-9

(MMP-9) via a converging plasmin/stromelysin-1 cascade enhances tumor cell invasion. *J Biol Chem,* 274**,** 13066-76.

RAND, N., REICHERT, F., FLOMAN, Y. & ROTSHENKER, S. (1997) Murine nucleus pulposus-derived cells secrete interleukins-1-beta, -6, and -10 and granulocyte-macrophage colony-stimulating factor in cell culture. *Spine (Phila Pa 1976),* 22**,** 2598-601; discussion 2602.

RASTOGI, A., THAKORE, P., LEUNG, A., BENAVIDES, M., MACHADO, M., MORSCHAUSER, M. A. & HSIEH, A. H. (2009) Environmental regulation of notochordal gene expression in nucleus pulposus cells. *J Cell Physiol,* 220**,** 698-705.

RAWLS, A. & FISHER, R. E. (2010) *Developmental and functional anatomy of the spine.,* Springer Publishers.

REINEMER, P., GRAMS, F., HUBER, R., KLEINE, T., SCHNIERER, S., PIPER, M., TSCHESCHE, H. & BODE, W. (1994) Structural implications for the role of the N terminus in the 'superactivation' of collagenases. A crystallographic study. *FEBS Lett,* 338**,** 227-33.

RICHARDSON, S. M., DOYLE, P., MINOGUE, B. M., GNANALINGHAM, K. & HOYLAND, J. A. (2009) Increased expression of matrix metalloproteinase-10, nerve growth factor and substance P in the painful degenerate intervertebral disc. *Arthritis Res Ther,* 11**,** R126.

RISBUD, M. V., GUTTAPALLI, A., STOKES, D. G., HAWKINS, D., DANIELSON, K. G., SCHAER, T. P., ALBERT, T. J. & SHAPIRO, I. M. (2006) Nucleus pulposus cells express HIF-1 alpha under normoxic culture conditions: a metabolic adaptation to the intervertebral disc microenvironment. *J Cell Biochem,* 98**,** 152-9.

RISBUD, M. V., GUTTAPALLI, A., TSAI, T. T., LEE, J. Y., DANIELSON, K. G., VACCARO, A. R., ALBERT, T. J., GAZIT, Z., GAZIT, D. & SHAPIRO, I. M. (2007) Evidence for skeletal progenitor cells in the degenerate human intervertebral disc. *Spine (Phila Pa 1976),* 32**,** 2537-44.

RISBUD, M. V., SCHAER, T. P. & SHAPIRO, I. M. (2010) Toward an understanding of the role of notochordal cells in the adult intervertebral disc: from discord to accord. *Dev Dyn,* 239**,** 2141-8.

ROBBINS, J. R., EVANKO, S. P. & VOGEL, K. G. (1997) Mechanical loading and TGF-beta regulate proteoglycan synthesis in tendon. *Arch Biochem Biophys,* 342**,** 203-11.

ROBERTS, S., MENAGE, J. & URBAN, J. P. (1989) Biochemical and structural properties of the cartilage end-plate and its relation to the intervertebral disc. *Spine (Phila Pa 1976),* 14**,** 166-74.

RODRIGUEZ, A. G., RODRIGUEZ-SOTO, A. E., BURGHARDT, A. J., BERVEN, S., MAJUMDAR, S. & LOTZ, J. C. (2012) Morphology of the human vertebral endplate. *J Orthop Res,* 30**,** 280-7.

RUFAI, A., BENJAMIN, M. & RALPHS, J. R. (1995) The development of fibrocartilage in the rat intervertebral disc. *Anat Embryol (Berl),* 192**,** 53-62.

RUTGES, J., CREEMERS, L. B., DHERT, W., MILZ, S., SAKAI, D., MOCHIDA, J., ALINI, M. & GRAD, S. (2010) Variations in gene and protein expression in human nucleus pulposus in comparison with annulus fibrosus and cartilage cells: potential associations with aging and degeneration. *Osteoarthritis Cartilage,* 18**,** 416-23.

RUTGES, J. P., KUMMER, J. A., ONER, F. C., VERBOUT, A. J., CASTELEIN, R. J., ROESTENBURG, H. J., DHERT, W. J. & CREEMERS, L. B. (2008) Increased MMP-2 activity during intervertebral disc degeneration is correlated to MMP-14 levels. *J Pathol,* 214**,** 523-30.

SAKAI, D., NAKAI, T., MOCHIDA, J., ALINI, M. & GRAD, S. (2009) Differential phenotype of intervertebral disc cells: microarray and immunohistochemical analysis of canine nucleus pulposus and anulus fibrosus. *Spine (Phila Pa 1976),* 34**,** 1448-56.

SAKAI, D., NAKAMURA, Y., NAKAI, T., MISHIMA, T., KATO, S., GRAD, S., ALINI, M., RISBUD, M. V., CHAN, D., CHEAH, K. S., YAMAMURA, K., MASUDA, K., OKANO, H., ANDO, K. & MOCHIDA, J. (2012) Exhaustion of nucleus pulposus progenitor cells with ageing and degeneration of the intervertebral disc. *Nat Commun,* 3**,** 1264.

SANTAMARIA, J. A., ANDRADES, J. A., HERRAEZ, P., FERNANDEZ-LLEBREZ, P. & BECERRA, J. (1994) Perinotochordal connective sheet of gilthead sea bream larvae (Sparus aurata, L.) affected by axial malformations: an histochemical and immunocytochemical study. *Anat Rec,* 240**,** 248-54.

SEGUIN, C. A., PILLIAR, R. M., ROUGHLEY, P. J. & KANDEL, R. A. (2005) Tumor necrosis factor-alpha modulates matrix production and catabolism in nucleus pulposus tissue. *Spine (Phila Pa 1976),* 30**,** 1940-8.

SEKI, S., KAWAGUCHI, Y., CHIBA, K., MIKAMI, Y., KIZAWA, H., OYA, T., MIO, F., MORI, M., MIYAMOTO, Y., MASUDA, I., TSUNODA, T., KAMATA, M., KUBO, T., TOYAMA, Y., KIMURA, T., NAKAMURA, Y. & IKEGAWA, S. (2005) A functional SNP in CILP, encoding cartilage intermediate layer protein, is associated with susceptibility to lumbar disc disease. *Nat Genet,* 37**,** 607-12.

SHEN, B., MELROSE, J., GHOSH, P. & TAYLOR, F. (2003) Induction of matrix metalloproteinase-2 and -3 activity in ovine nucleus pulposus cells grown in three-dimensional agarose gel culture by interleukin-1beta: a potential pathway of disc degeneration. *Eur Spine J,* 12**,** 66-75.

SHENG, S. R., WANG, X. Y., XU, H. Z., ZHU, G. Q. & ZHOU, Y. F. (2010) Anatomy of large animal spines and its comparison to the human spine: a systematic review. *Eur Spine J,* 19**,** 46-56.

SHOWALTER, B. L., BECKSTEIN, J. C., MARTIN, J. T., BEATTIE, E. E., ESPINOZA ORIAS, A. A., SCHAER, T. P., VRESILOVIC, E. J. & ELLIOTT, D.

M. (2012) Comparison of animal discs used in disc research to human lumbar disc: torsion mechanics and collagen content. *Spine (Phila Pa 1976),* 37**,** E900-7.

SINGH, K., MASUDA, K., THONAR, E. J., AN, H. S. & CS-SZABO, G. (2009) Age-related changes in the extracellular matrix of nucleus pulposus and anulus fibrosus of human intervertebral disc. *Spine (Phila Pa 1976),* 34**,** 10-6.

SIVE, J. I., BAIRD, P., JEZIORSK, M., WATKINS, A., HOYLAND, J. A. & FREEMONT, A. J. (2002) Expression of chondrocyte markers by cells of normal and degenerate intervertebral discs. *Mol Pathol,* 55**,** 91-7.

SMITH, L. J., NERURKAR, N. L., CHOI, K. S., HARFE, B. D. & ELLIOTT, D. M. (2011) Degeneration and regeneration of the intervertebral disc: lessons from development. *Dis Model Mech,* 4**,** 31-41.

SMITS, P. & LEFEBVRE, V. (2003) Sox5 and Sox6 are required for notochord extracellular matrix sheath formation, notochord cell survival and development of the nucleus pulposus of intervertebral discs. *Development,* 130**,** 1135-48.

SOHN, P., COX, M., CHEN, D. & SERRA, R. (2010) Molecular profiling of the developing mouse axial skeleton: a role for Tgfbr2 in the development of the intervertebral disc. *BMC Dev Biol,* 10**,** 29.

STUDER, R. K., VO, N., SOWA, G., ONDECK, C. & KANG, J. (2011) Human nucleus pulposus cells react to IL-6: independent actions and amplification of response to IL-1 and TNF-alpha. *Spine (Phila Pa 1976),* 36**,** 593-9.

SUGIMOTO, K., TAKAHASHI, M., YAMAMOTO, Y., SHIMADA, K. & TANZAWA, K. (1999) Identification of aggrecanase activity in medium of cartilage culture. *J Biochem,* 126**,** 449-55.

SUN, Z., GUO, Y. S., YAN, S. J., WAN, Z. Y., GAO, B., WANG, L., LIU, Z. H., GAO, Y., SAMARTZIS, D., LAN, L. F., WANG, H. Q. & LUO, Z. J. (2013a) CK8 phosphorylation induced by compressive loads underlies the downregulation of CK8 in human disc degeneration by activating protein kinase C. *Lab Invest*.

SUN, Z., WANG, H. Q., LIU, Z. H., CHANG, L., CHEN, Y. F., ZHANG, Y. Z., ZHANG, W. L., GAO, Y., WAN, Z. Y., CHE, L., LIU, X., SAMARTZIS, D. & LUO, Z. J. (2013b) Down-Regulated CK8 Expression in Human Intervertebral Disc Degeneration. *Int J Med Sci,* 10**,** 948-56.

SZTROLOVICS, R., GROVER, J., CS-SZABO, G., SHI, S. L., ZHANG, Y., MORT, J. S. & ROUGHLEY, P. J. (2002) The characterization of versican and its message in human articular cartilage and intervertebral disc. *J Orthop Res,* 20**,** 257-66.

TAKAHASHI, M., HARO, H., WAKABAYASHI, Y., KAWA-UCHI, T., KOMORI, H. & SHINOMIYA, K. (2001) The association of degeneration of the intervertebral disc with 5a/6a polymorphism in the promoter of the human matrix metalloproteinase-3 gene. *J Bone Joint Surg Br,* 83**,** 491-5.

TAKIMOTO, A., MOHRI, H., KOKUBU, C., HIRAKI, Y. & SHUKUNAMI, C. (2013) Pax1 acts as a negative regulator of chondrocyte maturation. *Exp Cell Res,* 319**,** 3128-39.

TANG, X., JING, L. & CHEN, J. (2012) Changes in the molecular phenotype of nucleus pulposus cells with intervertebral disc aging. *PLoS One,* 7**,** e52020.

TARDIF, G., PELLETIER, J. P., HUM, D., BOILEAU, C., DUVAL, N. & MARTEL-PELLETIER, J. (2006) Differential regulation of the bone morphogenic protein antagonist chordin in human normal and osteoarthritic chondrocytes. *Ann Rheum Dis,* 65**,** 261-4.

TAYLOR, J. R. (1975) Growth of human intervertebral discs and vertebral bodies. *J Anat,* 120**,** 49-68.

TAYLOR, J. R. & TWOMEY, L. T. (1986) *The role of the notochord and blood vessels in vertebral column development and in the aetiology of Schmorl's nodes.,* Churchill Livingstone.

TAYLOR, J. R. & TWOMEY, L. T. (1988) *Development of the human intervertebral disc*.

TIAN, Y., YUAN, W., FUJITA, N., WANG, J., WANG, H., SHAPIRO, I. M. & RISBUD, M. V. (2013) Inflammatory cytokines associated with degenerative disc disease control aggrecanase-1 (ADAMTS-4) expression in nucleus pulposus cells through MAPK and NF-kappaB. *Am J Pathol,* 182**,** 2310-21.

TILKERIDIS, C., BEI, T., GARANTZIOTIS, S. & STRATAKIS, C. A. (2005) Association of a COL1A1 polymorphism with lumbar disc disease in young military recruits. *J Med Genet,* 42**,** e44.

TOLOFARI, S. K., RICHARDSON, S. M., FREEMONT, A. J. & HOYLAND, J. A. (2010) Expression of semaphorin 3A and its receptors in the human intervertebral disc: potential role in regulating neural ingrowth in the degenerate intervertebral disc. *Arthritis Res Ther,* 12**,** R1.

TORTORELLA, M. D., PRATTA, M., LIU, R. Q., AUSTIN, J., ROSS, O. H., ABBASZADE, I., BURN, T. & ARNER, E. (2000) Sites of aggrecan cleavage by recombinant human aggrecanase-1 (ADAMTS-4). *J Biol Chem,* 275**,** 18566-73.

TORZILLI, P. A., BHARGAVA, M. & CHEN, C. T. (2011) Mechanical Loading of Articular Cartilage Reduces IL-1-Induced Enzyme Expression. *Cartilage,* 2**,** 364-373.

TROUT, J. J., BUCKWALTER, J. A. & MOORE, K. C. (1982a) Ultrastructure of the human intervertebral disc: II. Cells of the nucleus pulposus. *Anat Rec,* 204**,** 307-14.

TROUT, J. J., BUCKWALTER, J. A., MOORE, K. C. & LANDAS, S. K. (1982b) Ultrastructure of the human intervertebral disc. I. Changes in notochordal cells with age. *Tissue Cell,* 14**,** 359-69.

TWOMEY, L. & TAYLOR, J. (1985) Age changes in lumbar intervertebral discs. *Acta Orthop Scand,* 56**,** 496-9.

UCHIYAMA, Y., CHENG, C. C., DANIELSON, K. G., MOCHIDA, J., ALBERT, T. J., SHAPIRO, I. M. & RISBUD, M. V. (2007) Expression of acid-sensing ion channel 3 (ASIC3) in nucleus pulposus cells of the intervertebral disc is regulated by p75NTR and ERK signalling. *J Bone Miner Res,* 22**,** 1996-2006.

URBAN, J. P. & ROBERTS, S. (1995) Development and degeneration of the intervertebral discs. *Mol Med Today,* 1**,** 329-35.

URBAN, J. P. & ROBERTS, S. (2003) Degeneration of the intervertebral disc. *Arthritis Res Ther,* 5**,** 120-30.

URBAN, M. R., FAIRBANK, J. C., BIBBY, S. R. & URBAN, J. P. (2001) Intervertebral disc composition in neuromuscular scoliosis: changes in cell density and glycosaminoglycan concentration at the curve apex. *Spine (Phila Pa 1976),* 26**,** 610-7.

VAZQUEZ, F., HASTINGS, G., ORTEGA, M. A., LANE, T. F., OIKEMUS, S., LOMBARDO, M. & IRUELA-ARISPE, M. L. (1999) METH-1, a human ortholog of ADAMTS-1, and METH-2 are members of a new family of proteins with angio-inhibitory activity. *J Biol Chem,* 274**,** 23349-57.

VIDEMAN, T., LEPPAVUORI, J., KAPRIO, J., BATTIE, M. C., GIBBONS, L. E., PELTONEN, L. & KOSKENVUO, M. (1998) Intragenic polymorphisms of the vitamin D receptor gene associated with intervertebral disc degeneration. *Spine (Phila Pa 1976),* 23**,** 2477-85.

VIDEMAN, T., NURMINEN, M. & TROUP, J. D. (1990) 1990 Volvo Award in clinical sciences. Lumbar spinal pathology in cadaveric material in relation to history of back pain, occupation, and physical loading. *Spine (Phila Pa 1976),* 15**,** 728-40.

VIDEMAN, T., SAARELA, J., KAPRIO, J., NAKKI, A., LEVALAHTI, E., GILL, K., PELTONEN, L. & BATTIE, M. C. (2009) Associations of 25 structural, degradative, and inflammatory candidate genes with lumbar disc desiccation, bulging, and height narrowing. *Arthritis Rheum,* 60**,** 470-81.

VISSE, R. & NAGASE, H. (2003) Matrix metalloproteinases and tissue inhibitors of metalloproteinases: structure, function, and biochemistry. *Circ Res,* 92**,** 827-39.

VO, N. V., HARTMAN, R. A., YURUBE, T., JACOBS, L. J., SOWA, G. A. & KANG, J. D. (2013) Expression and regulation of metalloproteinases and their inhibitors in intervertebral disc aging and degeneration. *Spine J,* 13**,** 331-41.

VOGEL, C. & MARCOTTE, E. M. (2012) Insights into the regulation of protein abundance from proteomic and transcriptomic analyses. *Nat Rev Genet,* 13**,** 227-32.

VUJOVIC, S., HENDERSON, S., PRESNEAU, N., ODELL, E., JACQUES, T. S., TIRABOSCO, R., BOSHOFF, C. & FLANAGAN, A. M. (2006) Brachyury, a crucial regulator of notochordal development, is a novel biomarker for chordomas. *J Pathol,* 209**,** 157-65.

WADDELL, G. (1996) Low back pain: a twentieth century health care enigma. *Spine (Phila Pa 1976),* 21**,** 2820-5.

WALMSLEY, R. (1953) The development and growth of the intervertebral disc. *Edinb Med J,* 60**,** 341-64.

WALSH, A. J., BRADFORD, D. S. & LOTZ, J. C. (2004) In vivo growth factor treatment of degenerated intervertebral discs. *Spine (Phila Pa 1976),* 29**,** 156-63.

WALTER, B. A., KORECKI, C. L., PURMESSUR, D., ROUGHLEY, P. J., MICHALEK, A. J. & IATRIDIS, J. C. (2011) Complex loading affects intervertebral disc mechanics and biology. *Osteoarthritis Cartilage,* 19**,** 1011-1018.

WANG, D. L., JIANG, S. D. & DAI, L. Y. (2007) Biologic response of the intervertebral disc to static and dynamic compression in vitro. *Spine (Phila Pa 1976),* 32**,** 2521-8.

WANG, W. M., LEE, S., STEIGLITZ, B. M., SCOTT, I. C., LEBARES, C. C., ALLEN, M. L., BRENNER, M. C., TAKAHARA, K. & GREENSPAN, D. S. (2003) Transforming growth factor-beta induces secretion of activated ADAMTS-2. A procollagen III N-proteinase. *J Biol Chem,* 278**,** 19549-57.

WANG, Y. J., SHI, Q., LU, W. W., CHEUNG, K. C., DAROWISH, M., LI, T. F., DONG, Y. F., ZHOU, C. J., ZHOU, Q., HU, Z. J., LIU, M., BIAN, Q., LI, C. G., LUK, K. D. & LEONG, J. C. (2006) Cervical intervertebral disc degeneration induced by unbalanced dynamic and static forces: a novel in vivo rat model. *Spine (Phila Pa 1976),* 31**,** 1532-8.

WEBB, R., BRAMMAH, T., LUNT, M., URWIN, M., ALLISON, T. & SYMMONS, D. (2003) Prevalence and predictors of intense, chronic, and disabling neck and back pain in the UK general population. *Spine (Phila Pa 1976),* 28**,** 1195-202.

WEILER, C., NERLICH, A. G., SCHAAF, R., BACHMEIER, B. E., WUERTZ, K. & BOOS, N. (2010) Immunohistochemical identification of notochordal markers in cells in the aging human lumbar intervertebral disc. *Eur Spine J,* 19**,** 1761-70.

WEINSTEIN, D. C., RUIZ I ALTABA, A., CHEN, W. S., HOODLESS, P., PREZIOSO, V. R., JESSELL, T. M. & DARNELL, J. E., JR. (1994) The winged-helix transcription factor HNF-3 beta is required for notochord development in the mouse embryo. *Cell,* 78**,** 575-88.

WESTLING, J., GOTTSCHALL, P. E., THOMPSON, V. P., COCKBURN, A., PERIDES, G., ZIMMERMANN, D. R. & SANDY, J. D. (2004) ADAMTS4 (aggrecanase-1) cleaves human brain versican V2 at Glu405-Gln406 to generate glial hyaluronate binding protein. *Biochem J,* 377**,** 787-95.

WIBERG, C., HEINEGARD, D., WENGLEN, C., TIMPL, R. & MORGELIN, M. (2002) Biglycan organizes collagen VI into hexagonal-like networks resembling tissue structures. *J Biol Chem,* 277**,** 49120-6.

WILKE, H. J., NEEF, P., CAIMI, M., HOOGLAND, T. & CLAES, L. E. (1999) New in vivo measurements of pressures in the intervertebral disc in daily life. *Spine (Phila Pa 1976),* 24**,** 755-62.

WILKINSON, D. G., BHATT, S. & HERRMANN, B. G. (1990) Expression pattern of the mouse T gene and its role in mesoderm formation. *Nature,* 343**,** 657-9.

WINZI, M. K., HYTTEL, P., DALE, J. K. & SERUP, P. (2011) Isolation and characterization of node/notochord-like cells from mouse embryonic stem cells. *Stem Cells Dev,* 20**,** 1817-27.

WU, Y. J., LA PIERRE, D. P., WU, J., YEE, A. J. & YANG, B. B. (2005) The interaction of versican with its binding partners. *Cell Res,* 15**,** 483-94.

WUERTZ, K., GODBURN, K., MACLEAN, J. J., BARBIR, A., DONNELLY, J. S., ROUGHLEY, P. J., ALINI, M. & IATRIDIS, J. C. (2009) In vivo remodeling of intervertebral discs in response to short- and long-term dynamic compression. *J Orthop Res,* 27**,** 1235-42.

YANG, F., LEUNG, V. Y., LUK, K. D., CHAN, D. & CHEUNG, K. M. (2009) Injury-induced sequential transformation of notochordal nucleus pulposus to chondrogenic and fibrocartilaginous phenotype in the mouse. *J Pathol,* 218**,** 113-21.

YASEN, M., FEI, Q., HUTTON, W. C., ZHANG, J., DONG, J., JIANG, X. & ZHANG, F. (2013) Changes of number of cells expressing proliferation and progenitor cell markers with age in rabbit intervertebral discs. *Acta Biochim Biophys Sin (Shanghai),* 45**,** 368-76.

YASUMA, T., ARAI, K. & YAMAUCHI, Y. (1993) The histology of lumbar intervertebral disc herniation. The significance of small blood vessels in the extruded tissue. *Spine (Phila Pa 1976),* 18**,** 1761-5.

YE, S., WATTS, G. F., MANDALIA, S., HUMPHRIES, S. E. & HENNEY, A. M. (1995) Preliminary report: genetic variation in the human stromelysin promoter is associated with progression of coronary atherosclerosis. *Br Heart J,* 73**,** 209-15.

YU, H. & ZHU, Y. (2011) Expression of ADAMTS-7 and ADAMTS-12 in the nucleus pulposus during degeneration of rat caudal intervetebral disc. *J Vet Med Sci,* 74**,** 9-15.

YU, J., WINLOVE, P. C., ROBERTS, S. & URBAN, J. P. (2002) Elastic fibre organization in the intervertebral discs of the bovine tail. *J Anat,* 201**,** 465-75.

YUAN, W., ZHAO, M. D., YUAN, F. L., CHE, W., DUAN, P. G., LIU, Y. & DONG, J. (2013) Association of endothelin-1 expression and cartilaginous endplate degeneration in humans. *PLoS One,* 8**,** e60062.

ZHANG, Y., CAO, L., KIANI, C. G., YANG, B. L. & YANG, B. B. (1998) The G3 domain of versican inhibits mesenchymal chondrogenesis via the epidermal growth factor-like motifs. *J Biol Chem,* 273**,** 33054-63.

ZHANG, Y. H., ZHAO, C. Q., JIANG, L. S., CHEN, X. D. & DAI, L. Y. (2008) Modic changes: a systematic review of the literature. *Eur Spine J,* 17**,** 1289-99.

ZHAO, C. Q., LIU, D., LI, H., JIANG, L. S. & DAI, L. Y. (2007) Interleukin-1beta enhances the effect of serum deprivation on rat annular cell apoptosis. *Apoptosis,* 12**,** 2155-61.

ZHAO, Q., EBERSPAECHER, H., LEFEBVRE, V. & DE CROMBRUGGHE, B. (1997) Parallel expression of Sox9 and Col2a1 in cells undergoing chondrogenesis. *Dev Dyn,* 209**,** 377-86.

ZIGOURIS, A., ALEXIOU, G. A., BATISTATOU, A., VOULGARIS, S. & KYRITSIS, A. P. (2011) The role of matrix metalloproteinase 9 in intervertebral disc degeneration. *J Clin Neurosci,* 18**,** 1424-5.